Plant Proteases Target Pathogen Outer Membrane Proteins

Alexander Joseph McClelland

Thesis submitted to the University of East Anglia for the Degree of Doctor of Philosophy

October 2024

UEA Registration No.: 100338792

Abstract

Citrus greening disease, or Huanglongbing (HLB), is the most devastating disease of citrus. Florida produces ~10% of the citrus it did before the introduction of HLB, which is caused by the phloem-residing, insect-vectored bacterium *Candidatus* Liberibacter asiaticus (CLas). There is no cure for HLB, and very little is known about how plants mount an immune response against phloem-residing pathogens.

Proteases were previously found to be induced in citrus phloem during CLas infection. CLas deploys an effector protein, SDE1, that inhibits papain-like cysteine protease (PLCP) enzymatic function and contributes to disease progression. This suggests that proteases are important hubs of immunity in the phloem. While proteases are known to regulate plant immunity, identifying relevant substrates of proteases is particularly challenging.

In this work, I identified novel substrates of a citrus PLCP, CsRD21a. CsRD21a interacts with and cleaves beta barrel outer-membrane porin-like proteins (OMPs) from bacteria in the *Liberibacter* genus, including CLasOMP1. CLasOMP1 is highly expressed and may have an essential role in bacterial survival and/or host colonization, making it an attractive target for host defense. Cleaved products of CLasOMP1 are detected in infected citrus and resemble CsRD21a-generated cleavage products detected using a semi-*in vitro* cleavage assay. Further, CsRD21a overexpression enhances tolerance to CLas in transgenic citrus. CLasOMP1 also interacts with two serine carboxypeptidases from citrus and therefore may be a substrate of many classes of host proteases. Lastly, cell surface-exposed beta barrel OMPs are found in all Gram-negative bacteria and might be common targets of proteases in other pathosystems.

As strategies to mitigate the spread of phloem-residing pathogens are limited, engineering proteases in the phloem may be an effective strategy to achieve resistance against economically destructive pathogens, including Liberibacters and Phytoplasmas. Together, this work has shed mechanistic insight into the defense functions of plant proteases.

Table of Contents

Abstract **2**

Table of Contents **2**

List of Figures **6**

List of Tables **8**

Abbreviations **9**

Acknowledgements **11**

Chapter 1: General Introduction **13**

An Overview of Plant Immunity *13*

PTI and ETI are Hallmarks of Plant Immunity 13

Effector Secretion and Function 16

Proteases at the Interface of Hosts and Pathogens 18

Chasing Down Protease Substrates 20

Engineering Defense with Proteases 21

A Unique Agricultural Challenge: Phloem-Limited Pathogens *22*

Phloem Biology 22

Phloem Pathogen Case Studies: *Candidatus* Liberibacter spp. and *Candidatus* Phytoplasma spp. 24

Ca. Liberibacter and *Ca.* Phytoplasma Effectors 25

Resistance Strategies in the Phloem 29

Promising New Tools for Combatting Phloem Pathogens in the Field 31

Chapter 2: Citrus Papain-Like Cysteine Proteases Target CLas Outer Membrane Proteins **33**

Introduction *33*

SDE1 from *Candidatus* Liberibacter asiaticus Contributes to Virulence in Citrus 33

SDE1 Implicates Papain-Like Cysteine Proteases in Phloem Immunity 34

Results *36*

CLasOMP1 Interacts with Two Citrus PLCPs 36

CsRD21a Associates with the N-terminus of CLasOMP1 39
CLasOMP1 is Cleaved by CsRD21a in a semi-*in vitro* assay 39
CLasOMP1 is Cleaved in HLB-Infected Citrus 42
CsRD21a Contributes to Defense in Transgenic Citrus 43
OMP1 Homologs Interact with CsRD21a 45
LcrOMP1 is a Weaker Substrate of CsRD21a than CLasOMP1 50
C14 and Papain Cleave OMP1 Proteins 52
CsRD21a Interacts with CLasOMP1 but not other CLas OMPs 56
Identifying the PLCP cleavage site in CLasOMP1: an Open Question 56
Papain does not Affect Membrane Integrity or Bacterial Growth 58

Conclusions and Discussion *61*

Chapter 3: Two Citrus Serine Carboxypeptidases Target CLasOMP1 67

Introduction *67*

Results *69*
CSPs 10909 and 8175 Interact with OMP1 Homologs in *Liberibacter* 69
An Open Question: Do CSPs 10909 and 8175 cleave CLasOMP1? 71
CSPs 10909 and 8175 are likely not Acyltransferases 72
CSP 10909 and 8175 Expression in Transgenic Arabidopsis Induces Stunting but does not Contribute to Defense Against *P. syringae* 74
Structural Predictions of CSPs Reveal Potential Processing Dynamics 76

Conclusions and Discussion *79*

Chapter 4: Identifying Pathogen Inhibitors and Substrates of Plant Proteases *In Silico*. 81

Introduction *81*

Results *83*
OMPs are Widespread in Gram-negative Bacterial Pathogens 83
OmpA Proteins Have Diverged and Exhibit Extracellular Loop Diversification 85
CLso Encodes Several Candidate PLCP-Inhibiting Secreted Proteins 90
AY-WB Phytoplasma Encodes Six Candidate PLCP-Inhibiting SAPs 94

Conclusions and Discussion *98*

Chapter 5: General Discussion 101

The First Bacterial Substrate of a Plant PLCP 101
Do Proteases Converge on CLasOMP1? 102
Engineering Defense to Combat HLB 103
Open Questions Concerning OMP1-SDE1-PLCP Dynamics 105
Proteases and OMPs in the Future of Molecular Plant-Microbe Interactions 106

Chapter 6: Materials and Methods 109

Aphid Stylectomy 109
Yeast Two Hybrid 109
Plant Material and Protein Expression Analyses 112
Apoplastic Fluid Extraction 113
Membrane Isolation for Enrichment of OMPs 115
Protease Cleavage Assays 116
Activity-Based Protein Profiling 116
OMP1 Expression in Citrus Seed Coat Vasculatures 116
AlphaFold Structure Visualization 117
Bioinformatic Analyses of OMPs 117
AlphaFold Multimer Screening 117

Appendix 119

References 159

List of Figures

Figure 1.1. Black Citrus Aphid stylectomy on Rough Lemon seedlings. 23
Figure 2.1. CLasOMP1 is a cell surface-exposed beta barrel OMP. 37
Figure 2.2. CLasOMP1 interacts with citrus PLCPs in yeast. 37
Figure 2.3. The N-terminus of CLasOMP1 interacts with CsRD21a in yeast. 38
Figure 2.4. Schematic depicting the CsRD21a protease cleavage assay. 40
Figure 2.5. CsRD21a cleaves CLasOMP1. 41
Figure 2.6. CsRD21a is processed and activated *in planta*. 43
Figure 2.7. CsRD21a contributes to HLB tolerance in citrus. 44
Figure 2.8. Clustering of Liberibacter OMPs reveals distinct subfamilies. 46
Figure 2.9. OMP1 homologs in Liberibacter interact with CsRD21a. 49
Figure 2.10. *In vitro* expression of housekeeping and OMP genes in *L. crescens* 50
Figure 2.11. LcrOMP1 is weakly cleaved by CsRD21a. 51
Figure 2.12. C14 and papain cleave CLas and LcrOMP1. 53
Figure 2.13. The enzymatic domains of CsRD21a, C14, and papain are structurally conserved. 54
Figure 2.14. CsRD21a specifically interacts with CLasOMP1. 55
Figure 2.15. Targeted mutagenesis of a hydrophobic residue in CLasOMP1 does not change CsRD21a cleavage. 58
Figure 2.16. EcOmpA is a cell surface-exposed barrel OMP. 60
Figure 2.17. Working model of the citrus-CLas molecular arms race. 61
Figure 2.18. CLasOMP1 is a putative channel protein. 63
Figure 3.1. CSPs 10909 and 8175 interact with the N-terminus of CLasOMP1 and OMP1 homologs. 70
Figure 3.2. CSPs 10909 and 8175 are induced in HLB-infected citrus phloem and specifically interact with CLasOMP1. 71
Figure 3.3. CSPs 10909 and 8175 do not cluster with SCPL acyltransferases. 72
Figure 3.4. CSPs 10909 and 8175 do not contain the SCPL acyltransferase catalytic serine motif. 73
Figure 3.5. CSP10909 is proteolytically processed and induces stunting in *A. thaliana*. 75
Figure 3.6. CSP8175 induces stunting in *A. thaliana*. 75
Figure 3.7. Structural and sequence analyses of CSP10909. 77
Figure 3.8. Structural and sequence analyses of CSP8175. 78

Figure 4.1. OMP profiling in using HMMs.....85
Figure 4.2. Overview of the number of beta strands predicted by DeepTMHMM in the OMP dataset. 87
Figure 4.3. Phylogenetic tree of eight-stranded OMPs.....88
Figure 4.4. Sequence alignment of Enterobacterales OmpA proteins.....89
Figure 4.5. Sequence alignment of Xanthomonas spp. OmpA proteins. 89
Figure 4.6. AlphaFold2 multimer predicts HPE2 as a putative tomato C14-inhibiting effector. 93
Figure 4.7. A CLso OmpA-like secreted protein structurally aligns with the C-terminal peptidoglycan-binding domain of *E. coli* OmpA. 94
Figure 4.8. Summary of the AlphaFold2 multimer screening of six SAP effectors against 31 Arabidopsis PLCPs.....97

List of Tables

Table 2.1. Summary of predicted Liberibacter OMPs. 48
Table 4.1. Bacterial proteomes included in the OMP analysis.....82
Table 4.2. Summary of OMPs predicted in each tested bacterium. 84
Table 4.3. Summary of putative C14-inhibiting CLso ZC1 secreted proteins that scored 0.8ipTM + 0.2pTM ≥ 0.75 in the AlphaFold2 multimer screening.....91
Table 4.4. Summary of putative AtRD21a-inhibiting AY-WB SAPs that scored 0.8ipTM + 0.2pTM ≥ 0.75 in the AlphaFold2 multimer screening.....95
Table 6.1. Yeast-two-hybrid vectors used in this study. 112
Table 6.2. Tag-free vectors used for transient expression of PLCPs in *N. benthamiana*. 115
Table 6.3. Tag-free vectors used for OMP isolation in *E. coli*.....115
Appendix Table 1. 964 OMPs identified in Chapter IV via the HMM screening method. 119

Abbreviations

ab1/2	CLasOMP1-specific antibody 1/2
ab3	LcrOMP1-specific antibody
ABPP	activity-based protein profiling
ACP	Asian citrus psyllid
AF	apoplastic fluid
ATP	adenosine triphosphate
AVR	avirulence
AY-WB	Aster Yellows Witches' Broom
BAK1	BRI1-associated receptor kinase 1
BAM	beta-barrel assembly machinery
cat	catalytic mutant
CLaf	*Candidatus* Liberibacter africanus
CLam	*Candidatus* Liberibacter americanus
CLas	*Candidatus* Liberibacter asiaticus
CLso	*Candidatus* Liberibacter solanacearum
CPRG	chlorophenol red-ß-D-galactopyranoside
Cs	*Citrus sinensis*
CSP	citrus serine protease
CWDE	cell wall degrading enzyme
DAMP	damage-associated molecular pattern
Dex	dexamethasone
DNA	deoxyribonucleic acid
Ec	*Escherichia coli*
ET	ethylene
ETI	effector-triggered immunity
ETS	effector-triggered susceptibility
HLB	Huanglongbing
HMM	hidden Markov model
HPE	hypothetical protein effectors
HR	hypersensitive response
HRP	horseradish peroxidase
IDR	intrinsically disordered region
IM	inner membrane
JA	jasmonic acid
Lcr	*Liberibacter crescens*
LPS	lipopolysaccharide
LptD	LPS-assembly protein
LRR	leucine-rich repeat
M domain	membrane-bound domain
NHP	*N*-hydroxyl-pipecolic acid
NE	neutrophil elastase

NLR	nucleotide-binding LRR receptors
O domain	outside (extracellular) domain
OE	overexpression
OM	outer membrane
OMP	outer membrane protein
P domain	periplasmic domain
PAMP	pathogen-associated molecular pattern
PCR	polymerase chain reaction
PG	polygalacturonase
PGIP	PG-inhibiting protein
PLCP	papain-like cysteine protease
PR gene	pathogenesis-related gene
PRR	pattern recognition receptor
PTI	PAMP-triggered immunity
R gene	resistance gene
RD21a	responsive to desiccation 21a
RLCK	receptor-like cytoplasmic kinase
RLK	receptor-like kinase
RLP	receptor-like protein
RNA	ribonucleic acid
RNAseq	RNA sequencing
ROS	reactive oxygen species
SA	salicylic acid
SAG	senescence-associated gene
SAMP	stable antimicrobial peptide
SAP	secreted AY-WB protein
SAR	systemic acquired resistence
SCP	serine carboxypeptidase
SCPL	serine carboxypeptidase-like
SDE	Sec-delivered effector
Sec	general secretory pathway
SEM	scanning electron microscopy
STP	serine-tyrosine phosphatase
T3SS	type-III secretion system
TAL effector	transcription activator-like effector
TIR	Toll/Interleukin-1 receptor
TM	transmembrane
UF CREC	University of Florida Citrus Research and Education Center
WT	wildtype

Acknowledgements

First, I would like to thank my supervisor, Dr. Wenbo Ma, for her support and guidance through this PhD. It is not an ideal situation for your supervisor to move in the middle of your PhD, but it afforded me the wonderful, unforgettable opportunity to move to the UK and work at The Sainsbury Laboratory. Thank you, Wenbo, for guiding me when I need guidance and simultaneously encouraging me to grow as an independent scientist.

Thank you, Dr. Saskia Hogenhout, for serving as my secondary supervisor and providing me valuable guidance and feedback. Thank you to Dr. Jacob Malone for serving as my Internal Assessor for my PhD probation. Thank you to Dr. Núria Sánchez Coll and Dr. Jonathan Jones for serving as my viva examiners. I hope you enjoy this reading this thesis.

I would like to thank Dr. Walter Gassmann, Dr. Blake Meyers, and Dr. Sang-Hee Kim for their valuable mentorship, training, and guidance. Without their encouragement, I likely would never have pursued a PhD.

Thank you to Dr. Amit Levy, Dr. Chunxia Wang, Dr. Yosvanis Acanda Artiga, Dr. Nian Wang, and Dr. Zhiqian Pang at the UF CREC for their helpful guidance, collaboration, and experimental support. Thank you Dr. Qiang Xu, Dr. Yuantao Xu, and Bin Hu at Huazhong Agricultural University for sharing your findings on RD21a overexpression in citrus. A big thanks to Dr. Jiorgos Kourelis, Dr. Renier van der Hoorn, Dr. Adam Bentham, and Dr. Yinghong Gu, who have been particularly helpful in helping me troubleshoot the biochemistry in this thesis.

I would like to thank the many, many members of the Ma Lab that I've had the pleasure of working with over the last six years at both the University of California-Riverside and The Sainsbury Laboratory. Thank you to Dr. Agustina de Francesco, Dr. Amelia Lovelace, Dr. Kelley Clark, Dr. Simon Schwizer, Dr. Eva Hawara, Dr. Nicola Atkinson, and Dr. Morgan Halane for their direct contributions to the work in this thesis as well as their mentorship and friendship. Thank you to Dr. Yingnan Hou, Dr. Hui Li, Dr. Michelle Hulin, Dr. Alexandre Leary, Dr. Xiaodong Fang, Dr. Li Feng, Dr. Min Wang, Dr. Danxia He, and Dr. Bozeng Tang for being amazing postdoc allies and role models in the Ma Lab. Thank you Dr. Jessica Trinh, Shuang Yang, Rita Archibong, Dr. Min Qiu, Dr. Ariel Kuan, Renzo Villena-Gaspar, Jennie Yank, and more for being helpful and kind lab mates. It was a pleasure to train two bright young scientists, Priya Desikan and Amanda Chai, who helped immensely with laboratory tasks. Thank you all.

The TSL student and postdoc community has made this PhD worth it. From bowling to running (shoutout TMMRC) to karaoke and Hong Kong Fusion, I've had such a blast. A massive thank you to the Room 200 Ma Lab and Kamoun Lab students for providing me many welcome scientific discussions, distractions, laughs, and Cork Cup Ball wins. May CCBL live forever. To Dr. Sara Dorhmi, Yufei Li, Josh Bennett, Attilio Pascucci, Lena Knorr, AmirAli Toghani, Andy Posbeyikian, Yori Dolaptchiev, Markus Dräger, Camilla Molinari, Dr. Diana Gómez de la Cruz, and Dr. Daniel Lüdke: you are rockstars. Thank you for sharing your support and fun-loving personalities with me.

A massive thanks to Amelia, Yuantao, AmirAli, and Yufei for providing helpful feedback for the rough drafts of this thesis!

Thank you to everyone at TSL for sharing this lovely community with me and providing me valuable feedback and support. A special thanks to the Media Services, Insectary, SynBio, Horticultural Services, Tissue Culture, and Proteomics support teams who have kept my PhD research afloat. Thank you.

Thank you to The Figs, ZWB, and DJ James Naughty for your musical support and collaboration.

Thank you to my dear friends back home for laughing with me and keeping me rooted: Jacob Barger, Mark Vance, Randy James, Tyler Cano, Emily Aiken, Kyle Roberts, and Nathan Hoffman.

Thank you to my sister and brother-in-law, Kirsten and Greg Hackett, for their continuous love and support and for producing my favorite nephew, Grayson.

Thank you to Michael, Mona, the Alberts, the Gooches, and the Smiths for always cheering me on.

A huge thank you to my grandma, Dauna, for her unconditional love and support.

Mom, thank you for encouraging my academic journey.

Dad, thank you for being my favorite collaborator. I look forward to many more travels and making music together.

Dana Smith, thank you for being my best friend and number one cheerleader. I am so pleased with the life we have built together, and I can't wait to marry you.

Chapter 1: General Introduction

An Overview of Plant Immunity

Plant diseases pose a constant and urgent threat to agriculture and food security. Climate change is bringing about changes in temperature, carbon dioxide levels, water availability, and humidity, all of which can shift the balance in the disease triangle that exists between plants, pathogens, and the environment (Singh et al., 2023, Roussin-Léveillée et al., 2024). According to the Food and Agriculture Organization of the United Nations, these diseases cost $220 billion USD globally in lost crops each year (fao.org). The major focus of this thesis, citrus greening disease alone costs the global citrus industry roughly $1 billion every year, resulting in thousands of lost jobs (Court, 2017). Compacted by a growing population and the high economic costs of plant diseases, developing sustainable solutions to combat plant pathogens is of the utmost importance. Core to this effort is gaining detailed mechanistic insights into pathogen perception and immune signaling to expedite the development of crops with enhanced traits. First, this introduction will provide a broad overview of our current understanding of these molecular processes and largely focus on the immune system in regard to bacterial, fungal, oomycete, and viral plant pathogens.

PTI and ETI are Hallmarks of Plant Immunity

The evolutionary dynamics of molecular plant-microbe interactions have been summarized as a "zigzag" model (Jones and Dangl, 2006, Ngou et al., 2022a). Briefly, this model explains a scenario in which plants have evolved pattern recognition receptors (PRRs) on the cell surface to detect non-self, molecular signals that are indicative of pathogen invasion in the extracellular space. These signals are referred to as pathogen-associated molecular patterns (PAMPs). Upon this recognition, a kinase-mediated signaling cascade is activated that results in an immune response called PAMP-triggered immunity (PTI). However, successful pathogens overcome this immune response via suppression of PTI via the deployment of proteins called effectors, causing effector-triggered susceptibility (ETS). These effectors are secreted into the host cell and manipulate host processes to promote virulence and cause disease. As a counter-virulence strategy, plants deploy intracellular receptors which directly or indirectly detect

effectors and trigger a defense response known as effector-triggered immunity (ETI). Highlighting an extensive evolutionary arms race, pathogens utilize effectors to suppress ETI, contributing to pathogen colonization and ETS.

Together, extracellular and intracellular receptors functioning in PTI and ETI are historically referred to as resistance or R genes (Kourelis and Van Der Hoorn, 2018). Hundreds of R genes have been cloned and characterized, contributing to a diverse array of immune functions that reflect hundreds of millions of years of co-evolution with pathogens (Kourelis et al., 2021, Adachi et al., 2023, Chia et al., 2024). Some of the diverse functions of these R genes and how they contribute to dynamic plant-pathogen interactions are highlighted below.

PTI is characterized by an influx of calcium, the accumulation of reaction oxygen species (ROS), callose deposition at the cell wall, defense gene expression, and defense hormone production (Dodds et al., 2024, Wan et al., 2019, Jones et al., 2024). PRRs, including receptor-like proteins (RLPs) and receptor-like kinases (RLKs), contain an extracellular ligand-binding domain and a transmembrane (TM) domain, while RLKs contain an additional cytoplasmic kinase domain. Ligand-binding domains of these receptors can be leucine-rich repeats (LRRs), lysin motifs, lectin domains, or epidermal growth factors. Depending on the ligand-binding domain, the PRR can bind proteins or small peptides, polysaccharides, or lipids. LRR-containing RLPs and RLKs bind PAMPs and recruit RLK co-receptors, such as BRI1-associated receptor kinase 1 (BAK1), activating an intracellular phosphorylation cascade mediated by receptor-like cytoplasmic kinases (RLCKs). The RLCKs phosphorylate many downstream targets, which include: RBOHD, which mediates the ROS burst; channel proteins that transport calcium into the cell; and mitogen-activated protein kinases (MAPKs), which trigger defense gene regulation via activation of WRKY transcription factors. While ROS and calcium act as secondary messengers to activate downstream defense signaling (Marcec et al., 2019), the deposition of callose directly reinforces the plant cell wall to prevent pathogen invasion and limits the cell-to-cell movement of pathogens through cell-to-cell channels, called plasmodesmata (Wang et al., 2021b). Defense hormones such as salicylic acid (SA), jasmonic acid (JA), and ethylene (ET) are produced as an output of defense signaling cascades. While there is much interplay between plant defense hormone signaling, generally SA functions in defense against biotrophic and hemi-biotrophic pathogens and in the activation of systemic acquired resistance (SAR) via activating the expression of pathogenesis related (PR) genes (Bari and Jones, 2009).

JA and ET, on the other hand, generally function in defense against herbivorous insects and necrotrophic pathogens.

Well-characterized bacterial PAMPs include the conserved epitopes flg22, a 22-amino acid peptide derived from flagellin; elf18, an acetylated 18-amino acid peptide derived from elongation factor Tu; and csp22, a 22-amino acid peptide derived from cold shock protein (Dodds et al., 2024, Wan et al., 2019, Jones et al., 2024). These conserved peptides are essential to bacterial survival and exhibit limited variability between pathogens, making them attractive targets for host innate immunity. For instance, variation in the amino acid sequence of flg22 can result in reduced immune activation at the cost of bacterial mobility (Sanguankiattichai et al., 2022). Yet bacterial pathogens can overcome this constraint via alternative mechanisms. For example, bacteria have been found to deploy alternate glycan modifications in their flagella or secrete inhibitor molecules that render the flagella insensitive to host glycosidases, which release the flg22 PAMP (Buscaill et al., 2019).

Some PRRs recognize endogenous signals, known as damage-associated molecular patterns (DAMPs) that are indicative of pathogen invasion (Tanaka and Heil, 2021). Cell wall- and cuticle-derived molecules are known DAMPs, given that pathogens must overcome these physical barriers to successfully infect their hosts. As such, products of pathogen-derived cutinases and cell wall-degrading enzymes (CWDEs) are perceived as DAMPs by PRRs and induce PTI. Similarly, phytocytokines are peptides that are induced under stress, such as wounding or infection, and are released from precursor propeptides by endogenous proteases (Gust et al., 2017).

Successful pathogens overcome PTI in large part due to their effector protein repertoires (Jones and Dangl, 2006). However, these effector proteins can be recognized by intracellular immune receptors, namely nucleotide-binding LRR receptors (NLRs), and are therefore considered avirulent (AVR) effectors. NLRs mediate ETI upon AVR perception and trigger localized cell death, known as the hypersensitive response. This is the basis of the gene-for-gene model in which a single pathogen AVR is recognized by a single NLR (Flor, 1971). However, the evolutionary pressure inherent to this model means that pathogen AVRs and NLRs are constantly diversifying to evade and recognize one other, respectively, resulting in variable domain structures and activation mechanisms (Contreras et al., 2023). While some NLRs directly bind their effector targets to trigger HR, many NLRs can also indirectly perceive effector proteins by monitoring the effector host target or decoys of the host target. This is the basis for the guard model whereby the R proteins monitor host proteins for changes caused by

effectors. For example, *P. syringae* AvrPphb is a cysteine protease that cleaves *Arabidopsis thaliana* RLCKs; however, cleavage of the RLCK PBS1 activates ETI via the NLR RPS5 (Ade et al., 2007, Pottinger and Innes, 2020). Similarly, *P. syringae* AvrRpt2 is a cysteine protease that cleaves Arabidopsis RIN4, which is monitored by the NLR RPS2 (Mackey et al., 2003, Axtell et al., 2003, Axtell and Staskawicz, 2003, Coaker et al., 2005). Further, RPS2 guards RIN4 via sensing its phosphorylation status which is manipulated by *P. syringae* effectors AvrRpm1 and AvrB (Mackey et al., 2002, Liu et al., 2011). Direct detection of pathogen effectors often occurs through the LRR domain, similarly to PRRs, but some NLRs contain integrated domains that mimic effector targets, such as transcription factors and kinases (Marchal et al., 2022).

ETI, like PTI, contributes to the biosynthesis of SA and *N*-hydroxyl-pipecolic acid (NHP), which together regulate the SAR phenomenon (Ngou et al., 2022b). Upon the perception of the SA defense hormone, SA receptors, such as NPR1, bind transcription factors to regulate defense gene expression and induce NHP biosynthesis. NHP functions as a SAR-inducing, mobile signal in uninfected tissues (Chen et al., 2018). The extensive crosstalk between ETI, PTI, and SAR both induces and suppresses defense to achieve a robust and sufficient, yet balanced immune response (Ngou et al., 2021, Ngou et al., 2022b). Indeed, there is a trade-off between defense and growth that plants must tightly regulate to achieve immunity without compromising development (Van Wersch et al., 2016). This is a core principle that must be taken into consideration during the breeding and development of crops with enhanced traits.

Effector Secretion and Function

In most cases, pathogens must overcome PTI and ETI to cause disease with the help of their effector proteins. Hogenhout et al. (2009) defined effectors broadly as “all pathogen proteins and small molecules that alter host-cell structure and function.” Typically, effector proteins from both prokaryotic and eukaryotic pathogens contain N-terminal motifs that direct their secretion out of the pathogen (Lovelace et al., 2023). In Gram-negative bacterial pathogens, several protein secretion systems have been identified (Chang et al., 2014). Effectors from Gram-negative pathogens must cross both an inner membrane (IM) and outer membrane (OM), as well as the periplasm, the space between the two membranes in order to be completely secreted out of the cell. The Type III secretion system (T3SS) contains a basal body structure that crosses both the IM and OM. From the basal body, unfolded effector proteins are channeled through

a needle-like structure that protrudes outside of the bacterial cell and forms a pore on the cell surface of the host (Izoré et al., 2011). Therefore, the T3SS allows the effective translocation of effectors from the bacterial cytosol to the host cytosol. The general secretory (Sec) pathway, on the other hand, consists of a chaperone SecB that directs unfolded, full-length effector preproteins to SecA, which hydrolyzes ATP, permitting the effector to enter the periplasm via the SecYEG channel protein complex (Lycklama a Nijeholt and Driessen, 2012). In the periplasm, the N-terminal secretion signal is removed by a signal peptidase enzyme, producing a mature effector protein. Passage through the OM by Sec-translocated effectors can be mediated by several mechanisms (Kostakioti et al., 2005). This can be achieved via the effector's own beta-barrel translocator domain (such effectors are referred to as autotransporters or the Type V secretion system); a two-partner system involving the OM channel protein TpsB; or periplasmic chaperone and OM usher proteins. Outer membrane vesicles may also be a route for effector export from the periplasm (Wang et al., 2017). Intracellular pathogens commonly utilize the Sec system because Sec-secreted effectors are transported directly to the host cytosol, thereby making a needle-like delivery system unnecessary.

Depending on the pathogen in question, effectors may function within the host cells or extracellularly in the apoplast, often targeting PTI and ETI signaling components (Hogenhout et al., 2009, Zhou and Chai, 2008). Typically, effectors contribute to virulence via their inherent enzymatic functions and/or via disrupting host enzymatic functions. For example, the *P. syringae* effector HopBY possesses an enzymatic Toll/Interleukin-1 receptor (TIR)-like domain which hydrolyzes an important small molecule, NAD, in plants to contribute to virulence (Hulin et al., 2023). Intriguingly, the TIR domain-containing NLR RPS4 also hydrolyzes NAD into the same product molecule produced by HopBY, called 2'cADPR (Yu et al., 2024). Yet, the NADase activities of RPS4 and HopBY result in defense activation and virulence, respectively, highlighting small molecules as important components of both sides of the plant-pathogen arms race. In another example, the oomycete pathogen *Phytophthora sojae* effector PSR2 is a modular RNA silencing-suppressing effector that hijacks a host phosphatase enzyme to contribute to virulence in plants (Li et al., 2023, He et al., 2019, Hou et al., 2019, Qiao et al., 2013, Xiong et al., 2014). In this case, the effector itself has no known enzymatic function but functions as a regulatory subunit of the host phosphatase complex. Conversely, plants can hijack pathogen enzymes as a counter-virulence strategy. For example, the CWDE polygalacturonase (PG) from *Fusarium phyllophilum* is a virulence

factor that is modulated by a host PG-inhibiting protein (PGIP), thus promoting the production of DAMPs that activate defense (Xiao et al., 2024). Indeed, CWDEs and their inhibitors are widespread in pathogens and plants, respectively, and represent exciting targets for engineering resistance in agriculture (Juge, 2006, Di Matteo et al., 2006, Federici et al., 2006, Kalunke et al., 2015, Lagaert et al., 2009, Sun et al., 2022, Wei et al., 2022, McClelland and Ma, 2024).

Another effective virulence strategy for pathogens is to directly regulate host gene expression. *P. syringae* AvrRPS4 targets and disrupts defense-associated WRKY transcription factors to modulate gene expression; however, as a counter-virulence strategy, the NLR RRS1 contains an integrated decoy WRKY domain to activate immunity together with the NLR RPS4 (Nguyen et al., 2024, Sarris et al., 2015). On the contrary, transcription activator-like (TAL) effectors directly bind host DNA to regulate gene expression and contribute to virulence of pathogenic *Xanthomonas* bacteria; however, they can also be recognized by host immune receptors (Schornack et al., 2013). Together, the examples highlighted in this section represent just a limited overview of the extensive roles and delivery mechanisms of pathogen effector proteins in the host-pathogen arms race.

Proteases at the Interface of Hosts and Pathogens

Proteases, enzymes which cleave other proteins, are another common target of pathogen effectors. Godson and van der Hoorn (2021) conducted a study analyzing 46 plant proteases with published immune functions. These represent aspartic, cysteine, metallo-, and serine proteases and are named as such based on the mechanisms of their catalytic activity. They found that 76 percent of these proteases are known to be secreted into the apoplast; 37 percent are required genetically for immunity; 83 percent are induced during infection; and 24 percent are targeted and inhibited by pathogens. As such, host- and pathogen-derived proteases are at the forefront of molecular-plant microbe interactions, and they can regulate immunity through several mechanisms:

(1) Proteases can release DAMPs from precursor peptides to activate defense. For example, papain-like cysteine proteases (PLCPs) from maize have been shown to cleave an endogenous protein, ProZip1 to release Zip1, a DAMP that activates defense (Ziemann et al., 2018).

(2) Proteases can act as co-receptors of immune receptors. A host RLP Cf-2 guards the tomato PLCP Rcr3 in the apoplast and triggers HR upon Rcr3 inhibition by the effector Avr2 from the fungus *Cladosporium fulvum* (Dixon et al., 2000, Kruger et al., 2002, Rooney et al., 2005, Kourelis et al., 2020).

(3) Proteases can activate other proteases with roles in defense. Apoplastic subtilase proteases, including tomato P69B and *Nicotiana benthamiana* SBT5.2, cleave and activate Rcr3. This activation is required for Avr2/Cf-2-mediated defense (Paulus et al., 2020). Intriguingly, the *P. infestans* effector EPI1 inhibits P69B activation of Rcr3. In this case, multiple proteases are involved in achieving resistance, and pathogen effectors have evolved to inhibit them, suggesting that modulating protease activity is a critical component of the host-pathogen arms race.

(4) Proteases can directly target and cleave pathogen substrates as an antimicrobial strategy, sometimes releasing immune-eliciting PAMPs in the process. An *Arabidopsis thaliana* secreted aspartic protease SAP1 targets and cleaves the conserved *P. syringae* protein, MucD, thus inhibiting its growth *in vitro* and *in planta* (Wang et al., 2019). Similarly, subtilases, including P69B, cleave and release immunogenic peptides from the *P. infestans* effector PC2 (Wang et al., 2021a). *P. infestans*, in turn, blocks P69B activity via secreted protease inhibitors EPI1, EPI4, and EPI10.

(5) Proteases regulate cell death. Such proteases include PLCPs, vacuolar processing enzymes (VPEs), serine proteases, and threonine proteases (Salguero-Linares and Coll, 2019). Some proteases implicated in HR also contribute to senescence, a developmental process by which aging plant cells recycle and mobilize their nutrients, ultimately resulting in cell death (Buono et al., 2019). For example, Arabidopsis CathB PLCPs redundantly contribute to basal resistance against *P. syringae* as well as the development of HR and senescence (McLellan et al., 2009). Further, senescence-associated gene 12 (SAG12), which encodes a PLCP, from rice was reported to negatively regulate both senescence and bacteria-induced cell death (Singh et al., 2013). Lastly, not unlike caspases in animals which antagonistically regulate innate immunity in animals, *A. thaliana* metacaspases AtMC1 and AtMC2 of the cysteine protease superfamily positively and negatively regulate HR, respectively (Coll et al., 2010). AtMC1

specifically functions in clearing protein aggregates during proteotoxic stress and regulating senescence (Ruiz-Solaní et al., 2023).

(6) Proteases negatively regulate defense to prevent over-activation of immune responses. The *N. benthamiana* subtilase SBT5.2 cleaves and inactivates both the flg22 and csp22 PAMPs from *P. syringae*, suppressing ROS production (Chen et al., 2024, Buscaill et al., 2024).

(7) Pathogen-derived effector proteases target host substrates to suppress immunity. For example, *P. syringae* HopB1 cleaves BAK1 to block its function in PTI signaling (Li et al., 2016). The soybean cyst nematode deploys the cysteine protease effector CPR1 to target and cleave the mitochondrial BCAT1 protein, contributing to virulence in soybean roots (Margets et al., 2024). As previously mentioned, cysteine protease effectors AvrPphb and AvrRpt2 from *P. syringae* target regulators of defense in *A. thaliana* as a virulence strategy; however, their targets are guarded by NLRs, which subsequently activate defense (Ade et al., 2007, Coaker et al., 2005, Liu et al., 2011, Mackey et al., 2003, Mackey et al., 2002, Axtell et al., 2003, Axtell and Staskawicz, 2003).

(8) Pathogen effector proteases cleave PAMPs to suppress PTI. Not unlike SBT5.2, many commensal microbes encode a subtilase IssA to cleave flg22 and suppress defense (Eastman et al., 2024). Further, the metalloprotease AprA is conserved in animal and plant bacterial pathogens, cleaving flagellin to avoid host innate immunity (Bardoel et al., 2011, Pel et al., 2014).

Chasing Down Protease Substrates

Finding biologically-significant protease substrates and determining their cut site specificity remains a major challenge in the field (Godson and van der Hoorn, 2021). Many immune proteases are promiscuous in nature, targeting many substrates with little specificity. While identifying protease substrates can be a challenge, it is likely their promiscuity that makes them adaptable to combat ever-evolving pathogen substrates while retaining their enzymatic activity. For example, despite several identified substrates of SBT5.2, no clear cleavage site specificity for SBT5.2 has been determined to date (Buscaill et al., 2024, Chen et al., 2024, Paulus et al., 2020). As such, synthetic substrates have demonstrated the ability of SBT5.2 to cleave peptide sequences derived from pathogen elicitors *in vitro*.

Proteomics-based tools are promising in the identification of protease substrate specificities (Demir et al., 2018). Mass spectrometry can be used to identify substrates either using quantitative analyses (i.e., directly measuring the abundance of proteins with and without a specific protease or with activated and inactivated proteases), using protease-treated peptide libraries (such as the PICS assay), and via chemical labeling of protease-generated N-termini. Alternatively, running protein samples via gel electrophoresis and extracting gel slices of different molecular weights for subsequent proteomics analyses has proven successful in identifying proteins that undergo proteolytic processing *in planta* (Zheng et al., 2024). Yet, overall, there is still much to be uncovered regarding how proteases use their catalytic activity to regulate biological processes.

Engineering Defense with Proteases

Proteases and their engineered derivates have broad-spectrum applications in medicine, industry, and research (Dyer and Weiss, 2022). Given their demonstrated importance in the field of plant immunity, proteases are also enticing targets for engineering defense in crops. For example, mutating a single residue in eggplant Rcr3 rescues its ability to trigger Avr2/Cf-2-mediated defense, providing a framework for engineering PLCPs to trigger HR upon pathogen inhibitor perception (Kourelis et al., 2024). Additionally, the introduction of AlphaFold has accelerated our ability to identify novel pathogen-derived protease inhibitors and carry out structure-guided engineering of proteases. AlphaFold is a machine learning tool that utilizes multiple sequence analyses, protein structure databases, and amino acid pair representations to produce protein structural models and has improved to predict higher order protein complexes through what is called AlphaFold multimer (Abramson et al., 2024, Bryant et al., 2022, Evans et al., 2021, Jumper et al., 2021). As such, AlphaFold multimer-based protein interaction screenings are gaining attraction as a tool to predict novel protein-protein interactions in plant-microbe biology. For example, a multimer screening between 11,274 pairs of tomato proteases and secreted pathogen proteins uncovered novel protease-inhibiting virulence factors from bacterial, oomycete, and fungal pathogens (Homma et al., 2023). The predicted structures of these protease/inhibitor complexes can then guide the engineering of inhibitor-insensitive proteases. For example, the AlphaFold-predicted structure of the PLCP tomato Pip1 in complex with the *P. infestans* PLCP-inhibitor EpiC2B guided the engineering of ePip1 which is insensitive to EpiC2B

while retaining its function in defense (Schuster et al., 2024). In conjunction with improved transformation and gene editing tools, such approaches provide a powerful avenue for engineering resistance in crops.

A Unique Agricultural Challenge: Phloem-Limited Pathogens

Much of what we know about plant immunity to date has been uncovered through studies of leaf apoplast-residing pathogens. However, several economically important diseases originate from intracellular, phloem-residing pathogens, where host defense and pathogen virulence strategies are far less understood. Understanding how and if the above outlined principles of the perception of and response to pathogens applies in the phloem is key to developing strategies to combat these diseases in agricultural settings. This section will present an overview of our current understanding of phloem biology and how it relates to and challenges our understanding of plant immunity.

Phloem Biology

Plants utilize the phloem as a nutrient highway, moving photosynthesis-derived sugars from leaf "source" tissues to various "sink" tissues, such as new leaves, roots, and fruits. It is host to many molecules including important signaling proteins, RNAs, and hormones that have been implicated in plant-wide defense responses, such as SAR and systemic wound response (Bendix and Lewis, 2018, Lewis et al., 2022, Knoblauch et al., 2018, Turgeon and Wolf, 2009). The conducting cells of the phloem are called sieve elements, which degrade the majority of their organelles upon maturation, only retaining some mitochondria, plastids, and a smooth endoplasmic reticulum. This makes it difficult to understand the specific contents of the phloem given that the degraded sieve element components may contaminate the mature sieve element cells and thus any analyzed phloem sap. Further, collecting pure phloem sap is no easy task given the tremendous phloem osmotic pressure and its propensity to clog upon wounding. Even the best sampling techniques likely contain contaminants from neighboring cells. Minimal contamination from these neighboring cells may be obtained via insect stylectomy, by which the mouthpart, or stylet, of a phloem feeding insect is manually severed upon its insertion into the phloem, generating a tap through which phloem sap is exuded and can

be collected (Figure 1.1). However, aphid feeding induces host defense responses and introduces aphid-derived molecules that may distort downstream analyses. While some plants, such as cucurbits, castor bean, and legumes readily "bleed" out phloem upon wounding, the presence of contamination from nearby cells is still debated (Turgeon and Wolf, 2009). Isotope labeling in source tissues, such as leaves, can be helpful in determining what compounds are mobile, if the labeled compound is found in the downstream sink tissues.

Figure 1.1. Black Citrus Aphid stylectomy on Rough Lemon seedlings. A) Image of the Black Citrus Aphid (*Toxoptera citricida*) colony feeding of Rough Lemon seedlings. B) Image of a single microcauterized aphid stylet, presumably exuding phloem sap.

Sieve elements rely largely on adjacent cells to supply them with metabolites and macromolecules. The dependence of sieve elements on these cells, called companion cells, has been referred to as "the comatose patient and the hyperactive nurse", whereby the companion cell is the metabolically hyperactive nurse supplying its comatose patient, the sieve element, with any necessary metabolites and macromolecules (van Bel et al., 2002). The sieve elements and companion cells are connected to one another via specialized pore-plasmodesmata which permit the cell-to-cell trafficking of molecules and proteins (Lewis et al., 2022). Sugars may be transported via this network down its concentration gradient from mesophyll cells to companion cells and, ultimately, the sieve element. This is referred to as symplastic loading, where apoplastic loading requires that sugars are secreted into the apoplast from mesophyll cells via SWEET transporters and subsequently actively transported via the SUC2 sucrose transporter into the phloem against a concentration gradient (Zhang and Turgeon, 2018).

The sugar- and metabolite-rich nature of the phloem makes it an attractive niche for pathogens. The following sections of this introduction will highlight two important phloem pathogens and how they challenge our understanding of plant immunity.

Phloem Pathogen Case Studies: *Candidatus* Liberibacter spp. and *Candidatus* Phytoplasma spp.

Citrus Greening Disease, also known as Huanglongbing (HLB), is the most devastating disease of citrus and is caused by an insect-vectored, phloem-residing Gram-negative bacterium. HLB has spread globally to nearly all major citrus producing nations, infecting all commercial citrus varieties and causing massive yield losses (Alquézar et al., 2022). The citrus industry in Florida has been particularly hurt by both HLB and natural disasters, producing roughly 92 percent less citrus than it did before HLB was first detected in the state (USDA-ERS, 2024). Globally, a three-pronged approach has been implemented with moderate success: removal of infected trees, planting of certified disease-free trees, and treating groves with insecticides. Unaffected areas such as the European Union, Australia, and New Zealand are on high alert to keep HLB out of important citrus growing areas, and there is a dire need for long-term, sustainable solutions to this disease in areas where it is already present.

HLB-associated bacteria have been identified as *Candidatus* Liberibacter species in the Rhizobiaceae family, including *Ca.* L. asiaticus (CLas), *Ca.* L. africanus (CLaf), and *Ca.* L. americanus (CLam) (Alquézar et al., 2022, Thapa et al., 2020). CLas is now the dominant HLB-causing bacterium worldwide, having outcompeted CLam in the Americas, while CLaf is less damaging and primarily limited to Africa. These Gram-negative, obligate bacteria reside in the citrus phloem, where they are transmitted by phloem-feeding insect hosts. Specifically, CLas and CLam are vectored by the Asian Citrus Psyllid (ACP), *Diaphorina citri*, and CLaf is vectored by the African Citrus Psyllid, *Trioza erytreae* (Wang et al., 2017). Closely related to these citrus-infecting bacteria, *Ca.* L. solanacearum (CLso) has a wide host range, causing Zebra chip disease of potato and other diseases in pepper, tomato, carrot, and celery (Trkulja et al., 2023). CLas, CLaf, CLam, and CLso are unculturable in artificial media, earning them the '*Candidatus*' moniker and making functional studies of these bacteria challenging. However, *Liberibacter crescens* (Lcr), a culturable relative of *Ca.* L. species, has emerged as a critical tool for the functional study of this genus. While Lcr was isolated from papaya phloem sap (Davis et al., 2008), it is proposed to be non-pathogenic.

Characteristic HLB symptoms originate from the blockage of phloem brought on by CLas colonization. These symptoms include asymmetrical leaf mottling, underdeveloped fruits, reduced canopies, root loss, and ultimately tree death (Wang et al., 2017). Microscopy has revealed that CLas cells can move between sieve elements

through sieve pores (Achor et al., 2020). It has been observed that phloem blockage due to overaccumulation of callose at sieve pores and companion cell-SE plasmodesmata largely occurs in the leaf tissues where the bacterium is not as abundant; in contrast, large amounts of bacteria are present in the phloem-rich tissue of seed coats, which are apparently void of callose altogether. Whether this dynamic, tissue-specific deposition of callose in HLB-infected citrus is the result of a tug-of-war of resistance and virulence strategies is unknown.

Candidatus Phytoplasma spp. are also bacterial phloem-colonizing bacteria causing major diseases in a wide range of crops, such as wheat, rice, sesame, peanut, maize, soybean, strawberry, grape, sugarcane, pear, apple, citrus, potato, tomato, pepper, sweet potato, carrot, lettuce, jujube, olive, coconut, olive, elm, palm, and mulberry (Wang et al., 2024b, Sugio et al., 2011b). They are mycoplasma-like bacteria, meaning they contain one cell membrane and lack the structural cell wall component peptidoglycan found in Gram-negative and Gram-positive bacteria. While many Phytoplasmas are vectored by planthoppers, leafhoppers, and psyllids, others can be transmitted via dodder parasitic plants, graft inoculation, and seed propagation (Wang et al., 2024b). Symptoms vary by host and Phytoplasma species but can include yellowing, dwarfing, Witches' broom (induced stem and branch formation), leaf mottling, incomplete fruit ripening, fruit shedding, small leaves, necrosis, phyllody (development of leafy structures rather than flowers), and death.

Liberibacters and Phytoplasmas enter their insect vectors via their mouthparts, called stylets, during feeding on the phloem sap. From there, they enter the insect midgut and hemolymph, from which they circulate throughout the insect body, including the salivary gland, thus facilitating future transmission to host plants (Sarkar et al., 2023). Phytoplasmas pack into and reproduce within vesicles inside the intestinal cells, where Liberibacters have been found in the insect endoplasmic reticulum and in vacuoles. While CLas enhances the reproduction of the ACP but may negatively affect development and survival, Phytoplasmas are generally considered to increase vector longevity and reproduction.

Ca. Liberibacter and *Ca.* Phytoplasma Effectors

Despite the unculturable nature of these phloem-residing pathogens, several "omics" approaches have been deployed to increase our understanding of their intracellular lifestyles. Genomic studies have revealed that Liberibacter bacteria have

reduced genomes, with predicted gene numbers ranging from 948 (CLam strain PW_SP) to 1,433 (Lcr strain BT-1) (Wang et al., 2017). Thapa et al (2020) identified just 345 orthologous genes across all Liberibacter species and only one gene encoding a methyltransferase that is unique to the citrus-infecting species. Interestingly, while CLas, CLaf, and CLso have retained genes encoding for the type I secretion system, these have been lost in CLam (Thapa et al., 2020). However, while the T3SS is absent in all Liberibacter species, each of their genomes encode for the components of the Sec pathway (Thapa et al., 2020, Fagen et al., 2014), which it presumably uses to secrete virulence factors, called Sec-delivered effectors (SDEs). Similarly, Phytoplasmas lack the T3SS and also deploy SDEs to contribute to virulence (Sugio et al., 2011b).

Crucial to interrogating virulence strategies of these pathogens is to understand the function of these SDEs and how they are deployed in their hosts. To this end, De Francesco et al. (2022) utilized a bacterial enrichment strategy followed by RNAseq from HLB-infected citrus to obtain a transcriptome of CLas *in planta*. They found that genes encoding porins, transporters, chaperones, lysozymes, and a ferritin enzyme were among the highest expressed CLas genes in citrus. When compared to the CLas transcriptome in ACP, many putative CLas genes, including SDEs, were significantly upregulated in citrus compared to ACP, while others were more highly expressed in ACP than in citrus. While CLas appears to undergo more transcription and translation overall in citrus compared to ACP, CLas genes involved in metabolism are induced in ACP compared to citrus. This demonstrates the adaptability of CLas to both of its hosts.

From 21 CLas isolate genomes, a total of 31 SDEs have been previously predicted, of which 27 were determined to be “core” SDEs shared amongst all CLas isolates (Thapa et al., 2020). While mechanistic studies are difficult in the HLB pathosystem, the virulence functions of several CLas proteins have been demonstrated:

(1) CLIBASIA_05315, or SDE1, is a PLCP-inhibiting effector that contributes to HLB disease progression (Clark et al., 2018, Clark, 2019, Clark et al., 2020, Pitino et al., 2018, Pitino et al., 2016). SDE1 function will be further discussed in detail in Chapter 2.
(2) CLIBASIA_03230, referred to as SDE2 by Clark (2019), is the most highly expressed SDE in both citrus and ACP (De Francesco et al., 2022). SDE2 interacts with a calcium-dependent protein kinase, blocking its autophosphorylation and defense functions (Zhang et al., 2024a). Remarkably, SDE2 and nine other SDEs share a LuxR transcription factor binding motif in

their promoters, suggesting that this transcription factor may regulate virulence in CLas (Lovelace et al., 2024).

(3) CLIBASIA_00420, or SDE3, has been reported to contribute to CLas virulence via interaction with a negative regulator of autophagy, specifically cytosolic glyceraldehyde-3-phophate dehydrogenases (Shi et al., 2023).

(4) CLIBASIA_04025, or SDE15, was found to promote susceptibility of Duncan grapefruit to CLas and *Xanthomonas citri* via targeting of the accelerated cell death 2 protein (Pang et al., 2020).

(5) CLIBASIA_00460 is a nuclear localized SDE that induces chlorosis and necrosis or suppresses cell death depending on the delivery mechanism in *N. benthamiana* (Liu et al., 2019, Oh et al., 2022).

(6) While not a secreted effector, CLIBASIA_00255, a SA hydroxylase (SahA), is a virulence factor that degrades the defense hormone SA, thus suppressing host immunity (Li et al., 2017).

(7) CLIBASIA_05590, a prophage-encoded, nonclassical secreted peroxidase in CLas, likely delays the onset of HLB disease symptoms by scavenging ROS (Jain et al., 2015). Both CLIBASIA_05590 and an SDE, CLIBASIA_04410, were shown to suppress bacteria-induced deposition of callose when expressed in *N. benthamiana* (Lovelace et al., 2024).

(8) A non-classically secreted peroxiredoxin, LasBCP, contributes to oxidative stress when expressed in *L. crescens* and suppresses PTI in tobacco upon transient expression (Jain et al., 2018).

Similarly, Phytoplasmas deploy mobile SDEs that migrate from the phloem into various cell types through plasmodesmata (Sugio et al., 2011b). Some SDEs contain nuclear localization signals, which allow them to be trafficked into host nuclei, where they manipulate transcription factors, resulting in gene expression changes and phenotypes that make the plants more attractive to their insect vectors (Bertaccini et al., 2019). Indeed, targeting specific classes of host transcription factors that regulate plant development is a strategy of several Phytoplasma effectors, revealing that phloem-residing pathogens may manipulate transcription factors more extensively than pathogens that colonize different tissues (Correa Marrero et al., 2024). Many of these studies have been carried out using the *Ca.* Phytoplasma asteris strain Aster Yellows Witches' Broom (AY-WB) on the model plant *Arabidopsis thaliana*.

Like CLas effectors, secreted AY-WB protein (SAP) effectors display host-specific effector expression. For example, the AY-WB effector SAP54 is more highly expressed in *A. thaliana* than the leaf hopper *Macrosteles quadrilineatus* and interacts with RAD23 proteins to facilitate the 26s proteasome degradation of MADS-domain transcription factors, contributing to the phyllody phenotype and increasing plant attractiveness to its leafhopper insect vector (MacLean et al., 2014, MacLean et al., 2011). Further, SAP54-mediated degradation of SVP, a MADS-domain transcription factor, is required for female leafhopper attraction to and egg laying on male leafhopper-exposed plants (Orlovskis et al., 2024). Intriguingly, the CLas effector CLIBASIA_00460 and its CLso homolog HPE1 interact with RAD23 and may also facilitate the targeted degradation of host proteins, suggesting phloem-residing bacteria may hijack the host proteasome complex to degrade host targets as a common virulence strategy (Oh et al., 2022, Kan et al., 2021).

Similarly, AY-WB effectors SAP05 and SAP11 also exhibit higher expression *in planta* than in leafhoppers (MacLean et al., 2011) and target host transcription factors for degradation. SAP05 mediates the degradation of SPL and GATA transcription factors, acting as a scaffold between the transcription factor and the ubiquitin receptor RP10, resulting in ubiquitin-independent, proteasome-mediated degradation of the transcription factors (Huang et al., 2021b, Zhang et al., 2024b, Liu et al., 2023). SAP05 induces the "zombie-like" witches' broom phenotype when expressed in *A. thaliana*, resulting in increased lifespan and sterility, providing a suitable environment for Phytoplasmas and their vectors to proliferate. Indeed, SAP05 expression enhances reproduction of leafhoppers on *A. thaliana*, which requires the RPN10-mediated degradation of SPL transcription factors (Huang and Hogenhout, 2022). SAP11, on the other hand, targets TCP transcription factors, reducing JA synthesis, inducing leaf crinkling, and enhancing vector proliferation (Sugio et al., 2011a, Sugio et al., 2014, Tan et al., 2016). SAP11 is also found in the Phytoplasma responsible for Witches' Broom Disease of Lime and interacts with citrus TCPs (Al-Subhi et al., 2021).

Lastly, the mobile Phytoplasma effector TENGU induces dwarfism and sterility *in planta* via suppressing auxin and JA; yet, whether this is due to targeted disruption of transcription factors is unclear (Hoshi et al., 2009, Minato et al., 2014). Further studies of SDEs and their targets will reveal mechanistic insight into phloem pathogen virulence strategies, which in turn can be leveraged to engineer genetic resistance in plants.

Resistance Strategies in the Phloem

While immune activation via pathogen perception by intracellular and extracellular receptors has been widely observed with apoplast-residing pathogens, how and if these receptors function in the phloem is unknown. It has been hypothesized that CLas may activate immunity in the phloem, and it is this immune response that is the cause of HLB symptoms. Phloem sieve elements are connected to one another via large pores and can be clogged upon damage by phloem proteins, plastids, and ER. Plants are thought to then generate new sieve elements to bridge the healthy phloem across the restricted phloem (Lewis et al., 2022). Microscopy has revealed that CLas infection induces tissue-specific changes throughout the plant. For example, phloem blockage via callose deposition and phloem protein largely occurs when CLas is absent in the leaves while larger titers of CLas are found in seed coat tissues where phloem sieve pores are void of callose (Achor et al., 2020, Achor et al., 2010, Bernardini et al., 2024). The root sieve elements, on the other hand, are blocked by dark deposits of unknown composition and contain little CLas. Ultimately, plugged sieve pores block the flow of sugars, resulting in the accumulation of starch and sucrose in infected leaves (Kim et al., 2009). Starch packing in chloroplasts of infected leaf cells results in inner membrane collapse, explaining the characteristic HLB asymmetrical leaf chlorosis phenotype (Achor et al., 2010). Intriguingly, tolerant citrus varieties “Sugar Belle” mandarin and “Bearss” lemon exhibit less starch accumulation and the generation of more replacement phloem compared to susceptible varieties, such as Valencia sweet orange (Deng et al., 2019). While the susceptible varieties also generated some replacement phloem, the new phloem exhibited more necrosis than those of the tolerant varieties.

The induction of ROS, callose, phloem blockage, and even cell death contributes to the persisting model that HLB is an immune-triggered disease (Ma et al., 2022). Indeed, treatment of these infected trees with the immunoregulating growth hormone, gibberellin, results in decreased ROS and disease symptoms. Yet, the role of gibberellin in HLB tolerance remains elusive as transcriptomic analyses comparing citrus responses to CLas infection indicated that downregulation of gibberellin synthesis genes and a concomitant upregulation of gibberellin degradation genes was associated with HLB tolerance (Curtolo et al., 2020). However, the unpredictable progression of CLas in these varieties makes direct comparisons complicated, and CLas was not detected after infection in resistant hybrids of the susceptible *Citrus sunki* and resistant *Poncirus trifoliata*.

In support of HLB being an immune-mediated disease, it has been observed in infected sweet orange trees that there are higher levels of defense hormones and lower levels of auxin when compared to healthy plants (Neupane et al., 2023). This suggests that the overactive immune response is negatively impacting growth, as evidenced by decreased plant height, shoot development, leaf size, and overall leaf cell numbers. Perhaps CLas overcomes hyper-stimulated immune activity by directly or indirectly scavenging callose and phloem protein to clear its cell-to-cell passage through the phloem and ultimately to a dead-end in the phloem: the seed coat. SahA, CLIBASIA_05590, LasBCP, and/or SDEs, such as CLIBASIA_04410 could contribute to this callose depletion in the immediate vicinity of the bacteria, facilitating its movement through the phloem.

How phloem-residing pathogens “trip the wire” and activate defense remains a big question. Yet, a couple of PTI-inducing molecules from phloem feeding insects have been identified, and their modes of defense activation may be similar to phloem bacteria-derived PAMPs. For example, Aphid-derived CathB3 derived from green peach aphid saliva can trigger ROS production in the phloem of tobacco via interaction of its prodomain with the cytoplasmic EDR1, a serine/threonine-protein kinase MAPKKK, suggesting that PTI activation in the phloem may be mediated via direct, intracellular interaction of PAMPs with host kinases (Guo et al., 2020). Similarly, the potato aphid harbors a bacterium, *Buchnera aphidicola,* that produces a conserved, PTI-inducing chaperonin protein, GroEL, that is present in aphid saliva (Chaudhary et al., 2014). GroEL activates PTI when delivered into host cells via the T3SS of an engineered *Pseudomonas fluorescence* strain, when expressed in transgenic plants, or when purified GroEL protein was infiltrated into the extracellular space. This suggests that it may be recognized extracellularly and intracellularly, but this has not yet been determined.

Due to the induction of ROS and callose in infected citrus, it is reasonable to suggest that PTI is triggered by CLas. Notable PAMPs of bacterial pathogens include epitopes derived from flagella (flg22) and cold shock protein (csp22). Citrus, along with other members of the Rutaceae family, exhibit wide variation in their ability to trigger ROS production upon perception of flg22 and csp22 (Trinh et al., 2023). Interestingly, csp22 derived from CLas differs from the canonical csp22, and some members of the Rutaceae family are responsive to the canonical but not the CLas csp22. Yet, perception of CLas csp22 is not directly correlated with HLB tolerance. Ultimately, CLas is an intracellular pathogen, where csp22 and flg22 receptors recognize apoplastic PAMPs

via their extracellular domains. Further, CLas expresses flagellin in psyllids but not *in planta*, suggesting that it may not be required for movement in the phloem and is likely not a source of flagellin-derived PAMPs during HLB (Andrade et al., 2020).

Therefore, it is currently unknown whether CLas may trigger PTI from within the phloem sieve elements via intracellular receptors or whether CLas-derived PAMPs may somehow escape into the apoplast and trigger cell surface receptor-dependent PTI.

Promising New Tools for Combatting Phloem Pathogens in the Field

The mechanisms underlying HLB disease progression are slowly emerging, and this can inform strategies to develop targeted, long-term solutions to fighting CLas proliferation *in planta*. In tandem, genetically modifying well-characterized immune regulators guided by fundamental research in model organisms is also a promising approach. For example, overexpressing Arabidopsis NPR1 in citrus was found to reduce CLas-induced callose and ROS and contribute to HLB tolerance (Sarkar et al., 2024, Dutt et al., 2015). Similarly, silencing citrus NPR3, a homolog of negative regulators of immunity in *Arabidopsis*, also reduces callose and ROS.

Yet, genetic modification in citrus is particularly laborious. While transgenic or gene-edited seedlings may exhibit HLB tolerance, observing how the modifications will affect long-term growth and fruit development can take decades. Therefore, mitigating the disease in growers' fields now is a major priority. Antibiotic treatments via trunk injections have shown some efficacy in treating HLB (Hu et al., 2018, Li et al., 2019), but these methods can select for more resistant bacteria while disrupting beneficial host microbiota. Recently, a stable antimicrobial peptide (SAMP) was identified in HLB-tolerant varieties that is found in phloem-rich tissue. This SAMP induces host defense gene expression and inhibits CLas infection, presumably through disruption of its outer membrane (Huang et al., 2021a). While the heat-stable, quick-killing SAMP is speculated to decrease incidences of bacterial resistance due to killing α-proteobacteria at low concentrations, this may come at the cost of shifts in the microbiome.

While exploiting the immune strategies of citrus is an exciting avenue to develop natural tools to fight HLB in the field, as with SAMP, generating synthetic tools to inhibit or disrupt Liberibacter growth or virulence in a targeted fashion is a promising, sustainable approach. Recently, a CLas serine-tyrosine phosphatase (STP) that is unique to, but conserved within Liberibacter species, was demonstrated to perturb HR in *N. benthamiana* (Wang et al., 2024a). Homology modeling and *in silico* docking

analyses of STP led to the discovery of chemical ligands that interact with and inhibit STP phosphatase activity *in vitro* and block STP-mediated HR suppression *in planta*. Further, infiltration of these compounds in citrus and potato reduced CLas and CLso titers, respectively.

Likely the best solution to combatting diseases in the field is through a combinatorial approach, perhaps by using a combination of transgenic or gene edited crops and the direct application of targeted, pathogen-killing compounds. However, the most effective solutions to plant diseases will be those that are thoroughly studied and rooted in fundamental research, thus minimizing off-target effects and maintaining important agronomic traits. As such, phloem-residing pathogens represent a unique challenge in agriculture because very little is known about the molecular interplay between such pathogens and their hosts. Therefore, more knowledge in this area is paramount to the development of sustainable tools to tackle these diseases in the field.

Chapter 2: Citrus Papain-Like Cysteine Proteases Target CLas Outer Membrane Proteins

Introduction

SDE1 from *Candidatus* Liberibacter asiaticus Contributes to Virulence in Citrus

The molecular events underpinning plant defense against phloem pathogens are largely unknown. Therefore, studying effectors of phloem pathogens and their host targets is a promising avenue to uncover novel defense strategies in the phloem. In the case of citrus greening disease, the best-characterized effector of CLas is CLIBASIA_05315, or SDE1. SDE1 is a conserved effector protein across all sequenced isolates of CLas (Thapa et al., 2020). PCR- and antibody-based detection methods have revealed that SDE1 can be found in both asymptomatic and symptomatic infected citrus, suggesting that it may have a role in early infection of citrus, and making it a promising detection marker for citrus greening disease (Pagliaccia et al., 2017, Tran et al., 2020). Further, SDE1 is expressed significantly higher in citrus relative to psyllids, meaning that it may have a specific role in facilitating CLas colonization of plants (Pagliaccia et al., 2017, Thapa et al., 2020, De Francesco et al., 2022).

In one study, it was found that transgenic Duncan grapefruit citrus plants expressing SDE1 under the constitutive 35s promoter were hypersusceptible to CLas infection, exhibiting higher bacterial titers and more severe disease symptoms earlier than wildtype plants (Clark et al., 2020). While SDE1 expression in the absence of CLas infection did not trigger any developmental phenotypes in citrus, inducible expression of SDE1 in *Arabidopsis thaliana* revealed a yellowing phenotype in mature leaves, but not seedlings, that was reminiscent of greening disease symptoms. *AtSEN1*, a gene marker for senescence, exhibited enhanced expression upon Dex-induction, which was accompanied by the accumulation of ROS. Similarly, SDE1-expressing Duncan grapefruit plants exhibited increased expression of senescence-associated genes (*SAG*s) only after CLas infection. Another group reported that expression of SDE1 in *N. benthamiana* triggers chlorosis, cell death, callose deposition, and ROS, while a truncated form of SDE1 induces starch accumulation and reduces chlorophyl levels (Pitino et al., 2018, Pitino et al., 2016). These phenotypes are consistent with

senescence and typical HLB symptoms. The same group reported that SDE1 interacts with RNA helicase protein DDX3 and suppresses its expression *in planta*, contributing to chlorosis**.** Together, this suggests that SDE1 is an effector protein that promotes CLas virulence and characteristic leaf yellowing seen during citrus greening, likely by modulating senescence. However, whether these observations are due to SDE1 functions in the phloem, where CLas is limited, would require the generation and analysis of transgenic lines expressing SDE1 under a phloem-specific promoter.

SDE1 Implicates Papain-Like Cysteine Proteases in Phloem Immunity

Intriguingly, one *SAG* that was induced by SDE1 expression in citrus, *CsSAG12-1*, encodes a PLCP that was found to interact with SDE1 via a yeast-two-hybrid screening assay (Clark et al., 2018). Indeed, SDE1 interacts with several citrus PLCPs from distinct subfamilies, as demonstrated by pairwise yeast-two-hybrid. The protease domains of the representative PLCPs, which contain the catalytic active sites, were sufficient to pulldown SDE1 *in vitro* in some—but not all—cases, suggesting that SDE1 may specifically target the conserved protease domain. Further, SDE1 can inhibit the enzymatic activities of papaya-derived papain as well as a citrus PLCP, CsRD21a, *in vitro*, and PLCP activity is overall reduced in SDE1-overexpressing transgenic Duncan grapefruit plants. These results suggest that SDE1 is a PLCP-inhibiting effector. As such, while CsSAG12 proteases are induced in both infected and salicylic acid-treated *Citrus sinensis* plants, their activity levels do not increase during infection, suggesting that their enzymatic functions are compromised, likely by SDE1 inhibition. Therefore, SDE1 appears to inhibit the defense functions of PLCPs to promote disease. Yet many questions remain. To what extent do proteases regulate defense against CLas and are they functioning intracellularly in the phloem? Are SDE1-PLCP interactions taking place within the sieve element? If so, how are the PLCPs transported into the sieve elements?

A proteomics analysis on the phloem sap of CLas-infected and healthy Washington navel sweet orange plants further implicated PLCPs and other proteases in citrus greening disease (Franco et al., 2020). The phloem sap, which was collected via centrifugation of citrus inner bark, revealed that while proteins associated with growth and development were repressed, receptor-like proteins, peroxidases, and proteases were induced in infected samples. Specifically, four major classes of proteases were identified in the sap: aspartic, metallo-, serine, and papain-like cysteine proteases (PLCPs). The majority of these were significantly higher in infected samples than healthy

samples. Concomitantly, inhibitors of aspartic, cysteine, and serine proteases were also either significantly induced or repressed during CLas infection. The dynamic regulation of proteases and other hydrolases at the host-pathogen interface has also been demonstrated using activity-based protein profiling (ABPP) during *P. syringae* infection of the *N. benthamiana* apoplast (Sueldo et al., 2024), suggesting that overcoming the functions of these enzymes is crucial to pathogen infection. Intriguingly, the PLCPs AALP and RD19 exhibit higher gene expression levels upon CLas infection in the tolerant Sugar Belle variety but are repressed in the susceptible Pineapple sweet orange (Robledo et al., 2024), further implicating them in defense against CLas. While PLCP repression in Pineapple sweet orange is inconsistent with the phloem sap proteomics analysis performed by Franco et al. on Washington navel sweet orange, it is possible that there are variety-specific mechanisms regulating PLCP gene expression or protein stability (perhaps via post-translational modifications or processing by other proteases) upon CLas infection.

Together, the regulation of proteases and their inhibitors in the phloem during HLB infection—plus the inhibition of PLCPs by SDE1—suggests a crucial role of these proteolytic enzymes in phloem defense responses. The known roles of proteases in plant defense were outlined in Chapter 1. In setting out to investigate the roles of citrus PLCPs in HLB, I hypothesized that PLCPs target CLas proteins to promote defense. This defense could be achieved via antimicrobial activity against CLas, perhaps by cleaving CLas substrates that are crucial to its virulence. Additionally, a cleaved CLas protein may release PAMPs that activate defense. To investigate this further, I sought to identify a CLas protein that is targeted by citrus PLCPs.

Results

CLasOMP1 Interacts with Two Citrus PLCPs

I hypothesized that cell surface-exposed membrane proteins of CLas may be targeted by proteases in the citrus phloem. It was previously demonstrated that *CLIBASIA_02425*, a gene annotated as outer membrane protein L, is one of the most highly expressed CLas genes in citrus midribs, suggesting that it is important for CLas colonization in the phloem (De Francesco et al., 2022). To confirm its annotation, I utilized the deep learning transmembrane domain prediction software DeepTMHMM to compare its topology to *Escherichia coli* OmpL (Hallgren et al., 2022). This revealed that OmpL and CLIBASIA_02425 contain different numbers of transmembrane beta strands, 12 and 8, respectively. To eliminate any confusion, I decided to refer to CLIBASIA_02425 as CLas outer membrane protein 1 (OMP1), or CLasOMP1. DeepTMHMM predicts that CLasOMP1 contains four extracellular loops, eight transmembrane beta strands, three periplasmic loops, and an extended periplasmic N-terminus. AlphaFold3 structural modeling of the mature protein (with the signal peptide removed) supports this prediction, demonstrating the formation of high-confidence, eight-stranded beta-barrel (Figure 2.1) (Abramson et al., 2024). The extracellular and periplasmic domains, however, appear disordered with low pLDDT scores.

As a highly expressed, cell surface-exposed CLas protein, I hypothesized that CLasOMP1 extracellular loops may interact with citrus proteases in the phloem. To test if CLasOMP1 could interact with citrus proteases, I performed a yeast-two-hybrid screening of the mature CLasOMP1 protein in the bait vector (pGBKT7) against *Citrus sinensis* PLCPs CsSAG12 and CsRD21a in the prey vector (pGADT7) using empty vectors of each as negative controls. These constructs were generated sourced from Clark et al. (2018). I found that, like SDE1, CLasOMP1 interacts via yeast-two-hybrid with both PLCPs tested, and no auto-activity was detected with the empty vectors (Figure 2.2).

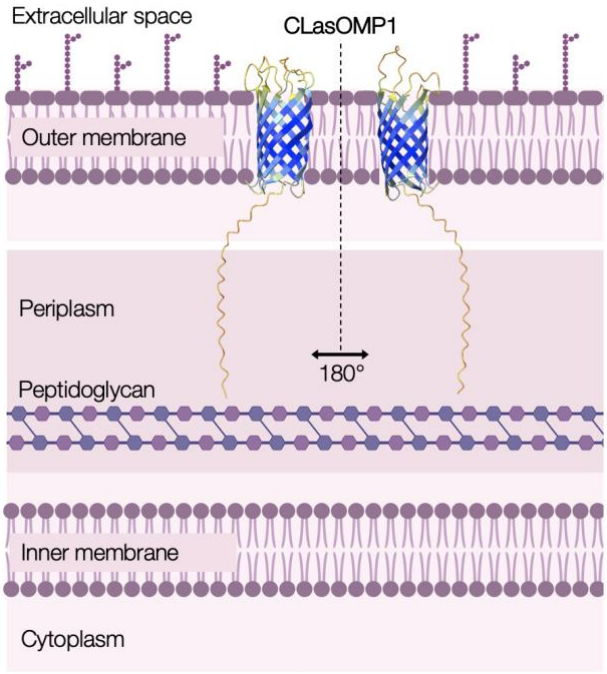

Figure 2.1. CLasOMP1 is a cell surface-exposed beta barrel OMP. AlphaFold3 model of CLasOMP1 colored by pLDDT confidence. High-confidence (pLDDT > 90) regions are dark blue; confident (pLDDT between 70 and 90) regions are light blue; low-confidence (pLDDT between 50 and 70) regions are yellow; and very-low confidence (pLDDT lower than 50) are orange. The AlphaFold3-predicted model was visualized using ChimeraX (Goddard et al., 2018, Meng et al., 2023, Pettersen et al., 2021). The model was then appended to the "Gram-negative bacteria cell wall" template by BioRender.com (2024).

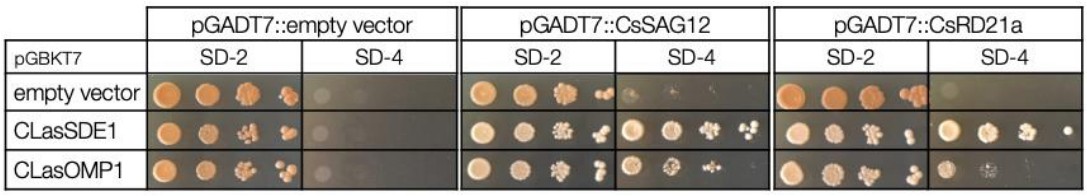

Figure 2.2. CLasOMP1 interacts with citrus PLCPs in yeast. Yeast-two-hybrid between citrus PLCPs CsSAG12 (XM_006495158) and CsRD21a (XM_006473212) in the prey vector (pGADT7) and CLasSDE1 and CLasOMP1 in the bait vector (pGBKT7) with empty vector negative controls. SD-2 medium lacks leucine and tryptophan and was used to select the co-transformed colonies. One colony was serially diluted and plated for each co-transformation in yeast on both SD-2 and the selective SD-4, which lacks leucine, tryptophan, adenine, and histidine. Growth on SD-4 indicates interaction of the proteins in the prey and bait vectors.

OMPs are produced in the cytoplasm, translocated into the periplasm via the Sec pathway upon removal of their N-terminal signal peptide, and are imbedded into the outer membrane via the beta-barrel assembly machinery (BAM) complex (Rollauer et al., 2015). OMPs with eight beta strands function as channel proteins and adhesin/invasins, while some contain domains with deacylase, palmitoyltransferase, or phospholipase activity (Fairman et al., 2011). While CLasOMP1 does not have any predicted enzymatic domains, it may function in adhesion, cell membrane integrity, and/or transportation of metabolites and ions. Due to these diverse functions and their cell surface-exposed nature, OMPs may be attractive substrates for host proteases. Further, CsSAG12 and CsRD21a are both induced in the phloem extract of HLB-infected citrus (Franco et al., 2020). It is plausible that these PLCPs are deployed directly into the phloem sieve elements from the companion cells to hydrolyze microbial substrates, such as CLasOMP1, as the basis of an immune response. While the specific mechanism of PLCP trafficking was not studied here, I decided to investigate CLasOMP1-PLCP interactions further.

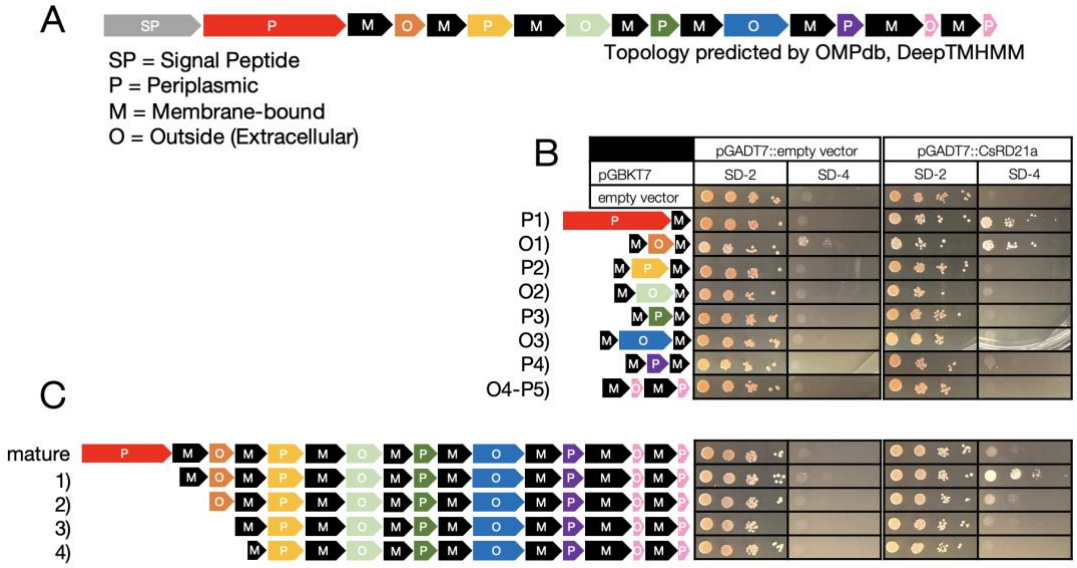

Figure 2.3. The N-terminus of CLasOMP1 interacts with CsRD21a in yeast. A) The domain structure of CLasOMP1 as predicted by OMPdb and DeepTMHMM. B+C) Truncations of CLasOMP1 cloned into the bait vector (pGBKT7) were screened for interaction against CsRD21a (pGADT7) in the prey vector with empty vector negative controls. SD-2 medium lacks leucine and tryptophan and was used to select the co-transformed colonies. One colony was serially diluted and plated for each co-transformation in yeast on both SD-2 and the selective SD-4, which lacks leucine, tryptophan, adenine, and histidine. Growth on SD-4 indicates interaction of the proteins in the prey and bait vectors.

CsRD21a Associates with the N-terminus of CLasOMP1

Given their predicted exposure on the CLas cell surface to proteases in the phloem, I hypothesized that CLasOMP1 extracellular loops facilitate interaction with CsRD21a. To test this, I first generated a domain structure of CLasOMP1 using OMPdb (Roumia et al., 2021) and DeepTMHMM (Hallgren et al., 2022) topology predictions as a guide (Figure 2.3A). After the N-terminal signal peptide, OMP1 contains repeats of periplasmic "P", membrane-bound "M", and outside (extracellular) "O" domains. I used this domain structure as a guide to generate truncations of OMP1 to determine which regions of the protein are targeted by CsRD21a. Cutting at each of the first seven "M" regions, eight total truncations were designed and cloned into the bait vector. Truncations P1 and O1, containing the first "P" and "O" domains, respectively, individually interacted with CsRD21a after co-transformation in yeast, demonstrating that these N-terminal domains are important for CsRD21a association (Figure 2.3B). Given that there was some autoactivation of O1, (i.e., growth of yeast co-transformed with O1 and empty vector on SD-4), I decided to further confirm this finding by generating a series of N-terminal truncations. I found that each N-terminal truncation of CLasOMP1 interacted with CsRD21a, and it was not until truncation 4, where the "O" domain and five amino acids of the following "M" domain were removed, that interaction with CsRD21a was completely abolished (Figure 2.3C). Together, these findings show that the N-terminus of CLasOMP1, including an extracellular domain, mediates interaction with CsRD21a in yeast.

CLasOMP1 is Cleaved by CsRD21a in a semi-*in vitro* assay

As the "O" loop that contributes to CsRD21a interaction is predicted to be directly exposed on the surface of the cell, it is plausible that this region of the protein might be cleaved by citrus PLCPs. To test this, I designed a semi-*in vitro* proteolytic assay (Figure 2.4). In brief, CsRD21a was transiently expressed in *N. benthamiana* via agroinfiltration. CsRD21a has a native N-terminal secretion signal peptide which directs its secretion to the apoplast. As such, at three days post-inoculation, the CsRD21a-containing apoplastic fluid (AF) of *N. benthamiana* leaves was extracted, concentrated, and subjected to ABPP or incubated with CLasOMP1. CLasOMP1 was expressed in *E. coli* with its signal peptide replaced with that from *E. coli* OmpA to increase the chances of its secretion to the periplasm. Then the membrane fraction was isolated from these

cells via sonication, centrifugation, and ultracentrifugation. The waxy membrane pellets were then resuspended and incubated with the CsRD21a collected from the AF for three hours.

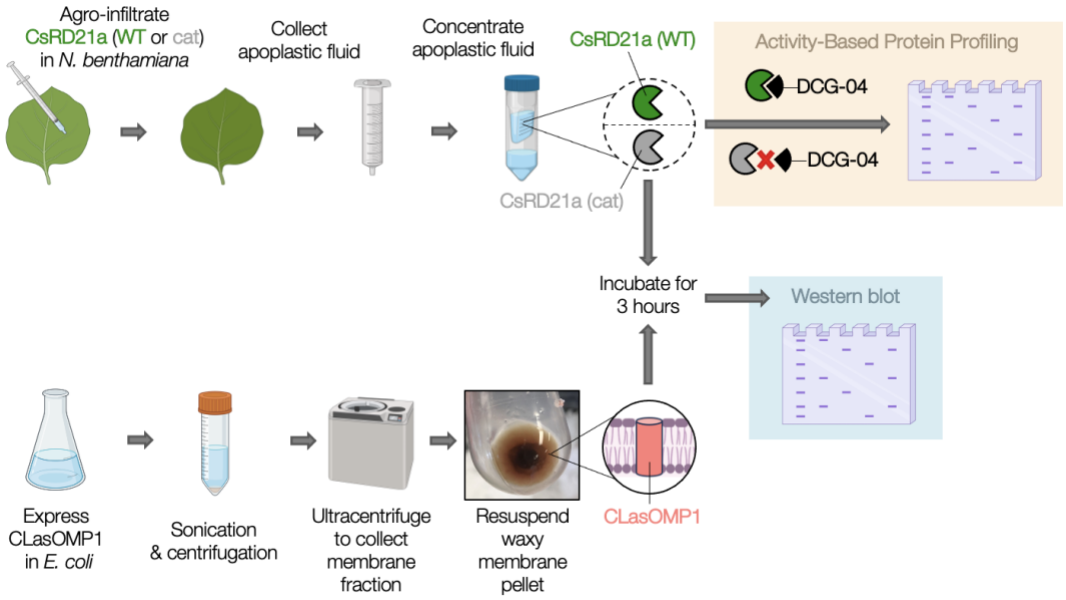

Figure 2.4. Schematic depicting the CsRD21a protease cleavage assay. WT = wildtype, cat = catalytic mutant.

To confirm that CsRD21a is indeed active in the *N. benthamiana* AF, I subjected it to ABPP in the form of a modified, biotinylated substrate DCG-04, which irreversibly binds active PLCPs (van der Hoorn et al., 2004) (Figure 2.4). Detection of the probe by streptavidin-HRP revealed three bands between 20 and 35 kDa which increase in intensity as the concentration of the cysteine protease inhibitor E-64 is decreased (Figure 2.5A). RD21-like proteases undergo significant processing *in planta* (Gu et al., 2012). Its signal peptide is first removed from preproRD21a during secretion to make proRD21a, which is inactive. Then the autoinhibitory prodomain is removed, exposing the catalytic triad and producing iRD21a, which is an active enzyme. The exposure of the catalytic residues in iRD21a is apparent in the AlphaFold modeling of CsRD21a (Figure. 2.6). Finally, the granulin domain of unknown function is removed, leaving just the protease domain, called mRD21a, which is also active. Therefore, the smallest band (~23 kDa) is likely mRD21a while the largest band (~35 kDa) is likely iRD21a, and the middle band (~30 kDa) may be an additional active intermediate. Together, these results demonstrate that CsRD21a is active in *N. benthamiana* AF. To generate a catalytic mutant, I replaced each of the three catalytic residues in the catalytic triad with alanine. The positioning of the catalytic residues (C163, H299, and N319) was predicted by

InterProScan (Jones et al., 2014). The catalytic mutant of CsRD21a, in which all three catalytic residues are replaced with alanine, cannot bind DCG-04, and therefore was not detected via using streptavidin-HRP, regardless of E-64 concentration (Figure 2.5A).

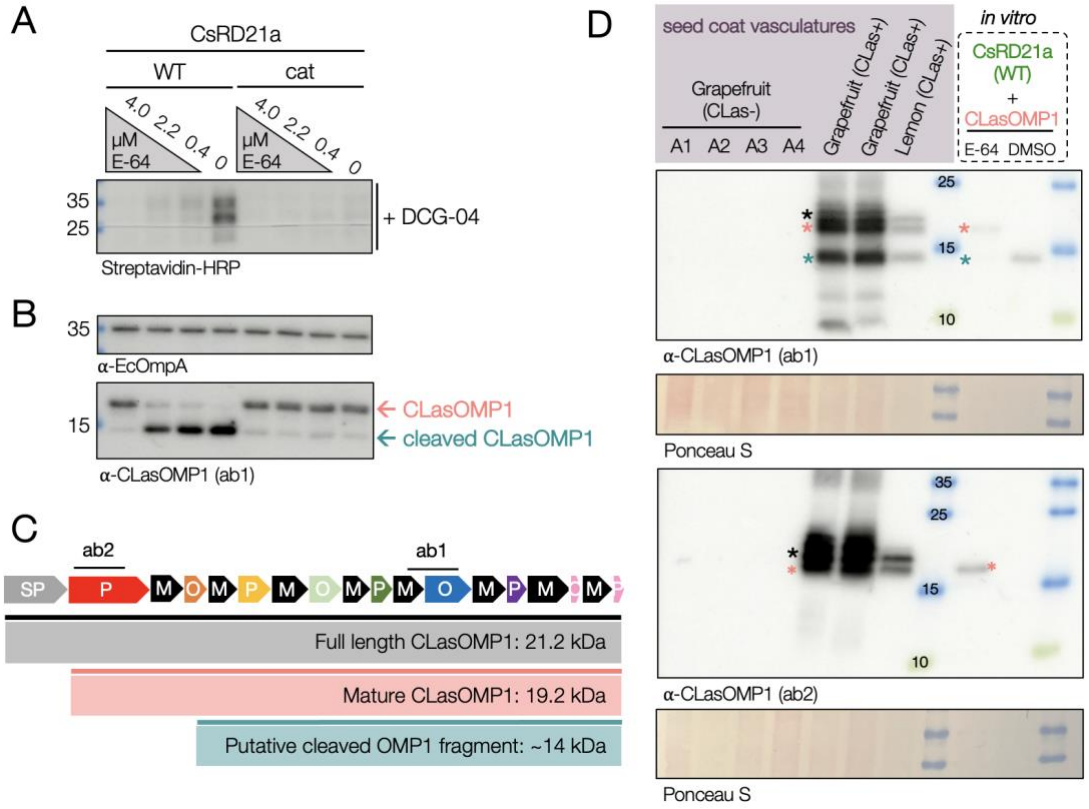

Figure 2.5. CsRD21a cleaves CLasOMP1. A) Western blot detection of active CsRD21a in apoplastic fluid using ABPP. A concentration gradient of E-64 (a cysteine protease inhibitor) in DMSO was incubated with the AF prior to DCG-04 labeling. B) Degradation assay of CLasOMP1 by CsRD21a. The same AF from panel A was incubated with CLasOMP1 from the *E. coli* membrane fraction, and EcOmpA was used as a loading control. The mature CLasOMP1 protein was fused to the N-terminal signal peptide from *E. coli* OmpA, or *Ec*OmpA(sp). C) Domain structure and size of cleaved CLasOMP1 products. D) Western blot showing CLasOMP1 cleaved products detected semi-*in vitro* and infected citrus. The asterisk color (black, pink, and sea-green) corresponds to cleaved CLasOMP1 products in C. CLas+ = infected citrus, CLas- = healthy citrus, WT = wildtype, cat = catalytic mutant, ab1 and ab2 = CLasOMP1-specific antibodies. CLas+ grapefruit samples are duplicates of the same sample. Molecular weights on Western blots are represented in kDa using protein ladder.

When the resuspended waxy pellets isolated from CLasOMP1-expressing *E. coli* were incubated with 4.0 μM E-64-treated *N. benthamiana* AF from CsRD21a-expressing leaves, CLasOMP1 appeared in its mature form without a signal peptide at ~19 kDa using an OMP1-specific antibody (ab1) (Figure 2.5B,C). As the concentration of E-64 was decreased, the signal from the ~19 kDa band decreased, and a smaller band at

~14 kDa increased. As a loading control, the signal from *E. coli* OmpA (detected using an EcOmpA-specific antibody) remained unchanged (Figure 2.5B). Further, the ~19 kDa CLasOMP1 band remained unchanged when incubated with the CsRD21a cat mutant, regardless of E-64 concentration. This suggests that CsRD21a cleaves CLasOMP1, and this is dependent on its catalytic activity. Intriguingly, if CLasOMP1 is cleaved in the middle of its first extracellular "O" domain, this would produce a ~14 kDa C-terminal product that could be detected by ab1 (Figure 2.5C); however, the specific cleavage site(s) have not yet been determined.

CLasOMP1 is Cleaved in HLB-Infected Citrus

CsRD21a cleaves CLasOMP1 in the semi-*in vitro* system, so I hypothesized that this cleavage may also occur in infected citrus. To test if CLasOMP1 is cleaved *in planta*, I used two purified CLasOMP1-specific antibodies, ab1 and ab2, which were generated in rabbits against synthesized CLasOMP1 peptides (courtesy of Pacific Immunology). These peptides corresponded to two different regions of CLasOMP1 highlighted in Figure 2.5C. Specifically, I used these antibodies to detect CLasOMP1 in infected grapefruit and lemon seed coat vasculature tissues, which have been reported to contain higher titers of CLas (Achor et al., 2020). To my surprise, three major CLasOMP1 bands were detected in both infected grapefruit and lemon samples using ab1, corresponding roughly to the full length (21.2 kDa), mature (19.2 kDa), and putative cleaved OMP1 fragment (~14 kDa) (Figure 2.5C,D). These bands were completely absent in the healthy grapefruit samples, while the mature and cleaved bands were the same size as those identified in the semi-*in vitro* assay, with E-64- and DMSO-treated CsRD21a, respectively (Figure 2.5D). Using ab2, which recognizes the N-terminal periplasmic domain of CLasOMP1, only two major bands were identified in the infected samples, corresponding to the full length and mature proteins while no cleavage product was clearly detected (Figure 2.5D). As with ab1, no bands were detected in the healthy samples using ab2. Similarly, the mature band could be detected with ab2 when CLasOMP1 was incubated with E-64-treated CsRD21a, but no bands were detected when CLasOMP1 was incubated with DMSO-treated CsRD21a. Given that ab2 recognizes the N-terminus of CLasOMP1, perhaps the cleaved peptide is too small to detect via Western blot or perhaps the ab2 recognition sequence is cleaved. Together, this suggests that CLasOMP1 is cleaved in citrus in the same manner that CsRD21a cleaves it in the semi-*in vitro* assay. Intriguingly, smaller cleavage products under 10

kDa were observed using ab1 in the infected grapefruits, suggesting that CLasOMP1 may be further processed *in planta* by other proteases.

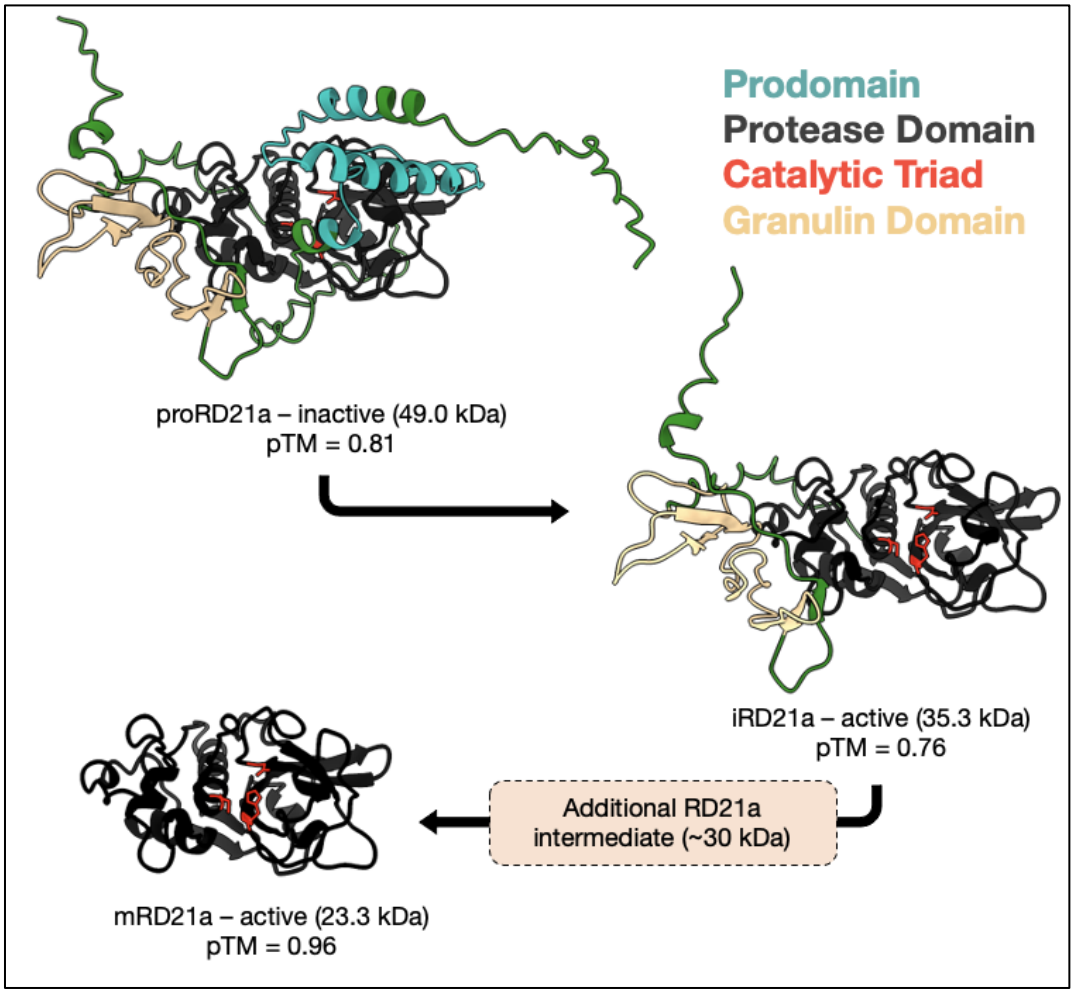

Figure 2.6. CsRD21a is processed and activated *in planta*. Structures were predicted with AlphaFold3 (Abramson et al., 2024) and visualized using ChimeraX (Goddard et al., 2018, Meng et al., 2023, Pettersen et al., 2021). Their molecular weights (in kDa) and confidence scores (in pTM) are shown.

CsRD21a Contributes to Defense in Transgenic Citrus

Given that CsRD21a cleaves CLasOMP1 in the semi-*in vitro* assay and this same cleavage appears in infected citrus, it stands to reason that CsRD21a may contribute to defense against HLB via CLasOMP1 cleavage. If CLasOMP1 is essential to bacterial survival, its degradation by CsRD21a may reduce CLas fitness. Additionally, cleavage products produced from CLasOMP1 may function as immune-eliciting PAMPs. To test if CsRD21a contributes to HLB tolerance, our collaborators at the National Key Laboratory for Germplasm Innovation & Utilization of Horticultural Crops at Huazhong

Agricultural University in Wuhan, China, overexpressed it in citrus and subjected the transgenic plants to CLas infection. They utilized a graft inoculation strategy by which transgenic explants were grafted onto HLB-infected sweet orange seedlings (Figure 2.7A). Non-transgenic explants were used as wildtype (WT) controls and grafted onto the same infected seedlings. They then examined CLas titers in the transgenic and WT scions via reverse transcription quantitative polymerase chain reaction (RT-qPCR). CLas was detected (Ct < 35) in the WT scions three months earlier than the CsRD21a overexpression lines, as the CsRD21a scions had significantly lower CLas titers than WT scions (Figure 2.7B). Further, infected CsRD21a-overexpressing scions exhibit less HLB symptoms compared to the WT infected scions (Figure 2.7C). These results suggest that CsRD21a contributes to defense against CLas *in vivo*, making PLCP engineering an exciting new avenue to combat CLas infection.

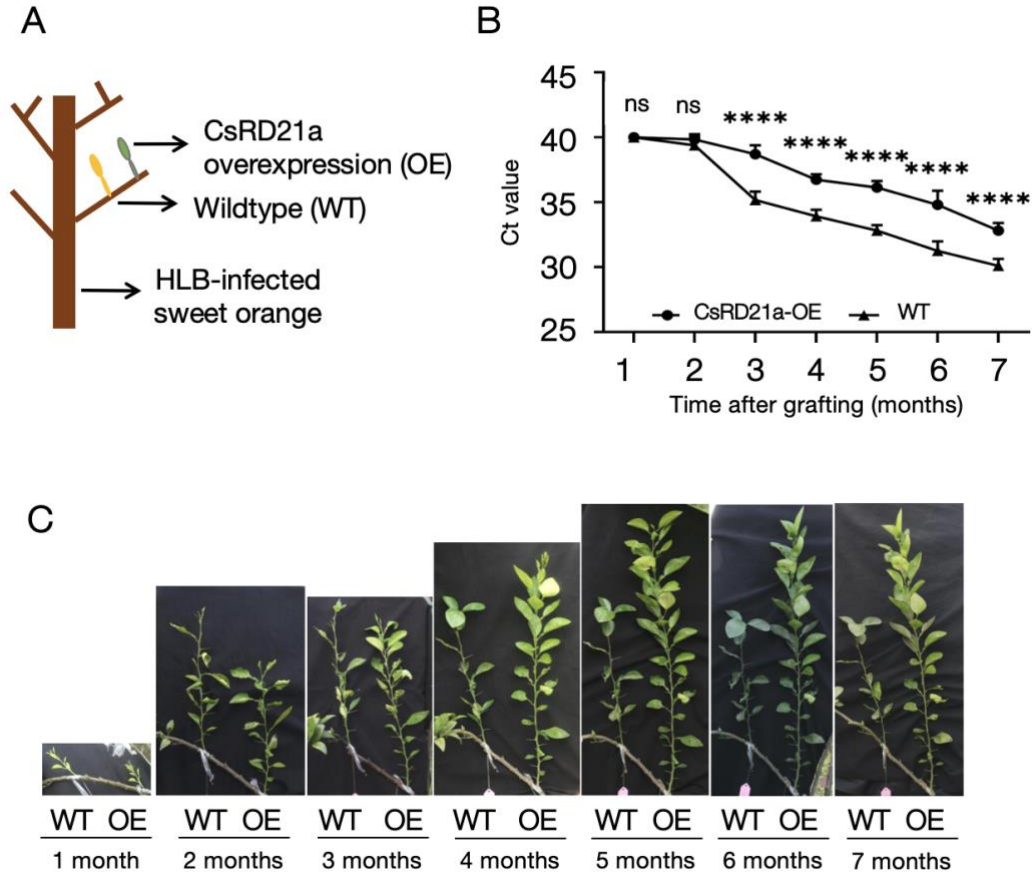

Figure 2.7. CsRD21a contributes to HLB tolerance in citrus. A) Schematic of the transgenic citrus graft inoculation strategy. B) RT-qPCR of CLas in CsRD21a overexpression (OE) or wildtype (WT) scions after graft inoculation on infected *Citrus sinensis* seedlings. Statistical significance was determined by one-way ANOVA (ns = not significant, **** = $p < 0.001$). C) Images of WT and OE scions on infected *Citrus sinensis.* The experiments were performed by Bin Hu and Dr. Yuantao Xu in the laboratory of Prof. Qiang Xu at the National Key Laboratory for Germplasm Innovation & Utilization of Horticultural Crops at Huazhong Agricultural University in Wuhan, China.

OMP1 Homologs Interact with CsRD21a

OMPs are widespread among Gram-negative bacteria and may represent a large class of putative protease targets in plant pathogens. OMP profiling in plant pathogens will be discussed in Chapter 4 of this thesis. I hypothesized that OMPs from other Liberibacters may be targeted by CsRD21a. Using hmmbuild, I developed a Hidden Markov Model (HMM) based on beta-barrel OMP PFAM alignments (clan CL0193). I used this HMM to search (via hmmsearch) for beta-barrel OMPs in representative strains of CLas (strain psy62), CLaf (strain PTSAPSY), CLso (strain ISR100), CLam (strain PW_SP), and Lcr (strain BT-1). I then screened the positive hits against DeepTMHMM, keeping only the hits that were identified as membrane proteins by both programs. The result was a list of 31 Liberibacter OMPs (Table 2.1). A MAFFT v7.490 amino acid sequence alignment of the OMPs was then used for subsequent clustering analysis using a maximum likelihood model in FastTree v2.1.11 (Price et al., 2010, Price et al., 2009, Katoh and Standley, 2013). In total, six clusters of OMPs were present in the dataset (Figure 2.8). Based off their NCBI protein annotations, each Liberibacter encodes one “OMP assembly factor BamA” protein, one “porin” protein, and one “LPS assembly protein LptD”. Each of these protein families formed distinct clusters. Another three clusters appeared, and their annotations varied from “beta-barrel OMP” to “porin family protein” and “hypothetical protein”. Among these proteins was CLasOMP1, and its clade was therefore designated as the “OMP1” clade. The remaining two clades were designated as “OMP2” and “OMP3”.

Each of the Liberibacter species encodes a single protein in the “OMP1” clade, except for Lcr, which encodes four (Figure 2.9A). The Alphafold2-predicted structural models of these OMPs revealed the presence of eight-stranded beta-barrels and disordered N-terminal periplasmic domains, similar to CLasOMP1. While the OMP1 homologs are structurally conserved, their extracellular loops vary in length and structure (Figure 2.9B). Sequence alignment of the OMP1 homologs demonstrates that the membrane-bound beta strands exhibit a much higher degree of conservation than the extracellular loops (Figure 2.9C), suggesting that the extracellular loops may be under selective pressure.

Despite low overall sequence similarity between OMP1 homologs, each interacted with CsRD21a via yeast-two-hybrid with varying interaction strengths (Figure 2.9D). This suggests that the conserved membrane-bound regions of OMP1 may contribute to interaction with CsRD21a, or CsRD21a can bind a wide range of

sequence-diverse but structurally similar OMP1-like proteins. Like CLasOMP1, OMP1 homologs in Lcr are highly expressed *in vitro*, suggesting they play important housekeeping functions (Figure 2.10). It is possible that the expansion of OMP1 proteins in Lcr may be partially responsible for its ability to be cultured *in vitro*, and it could also contribute to redundancy to overcome protease cleavage.

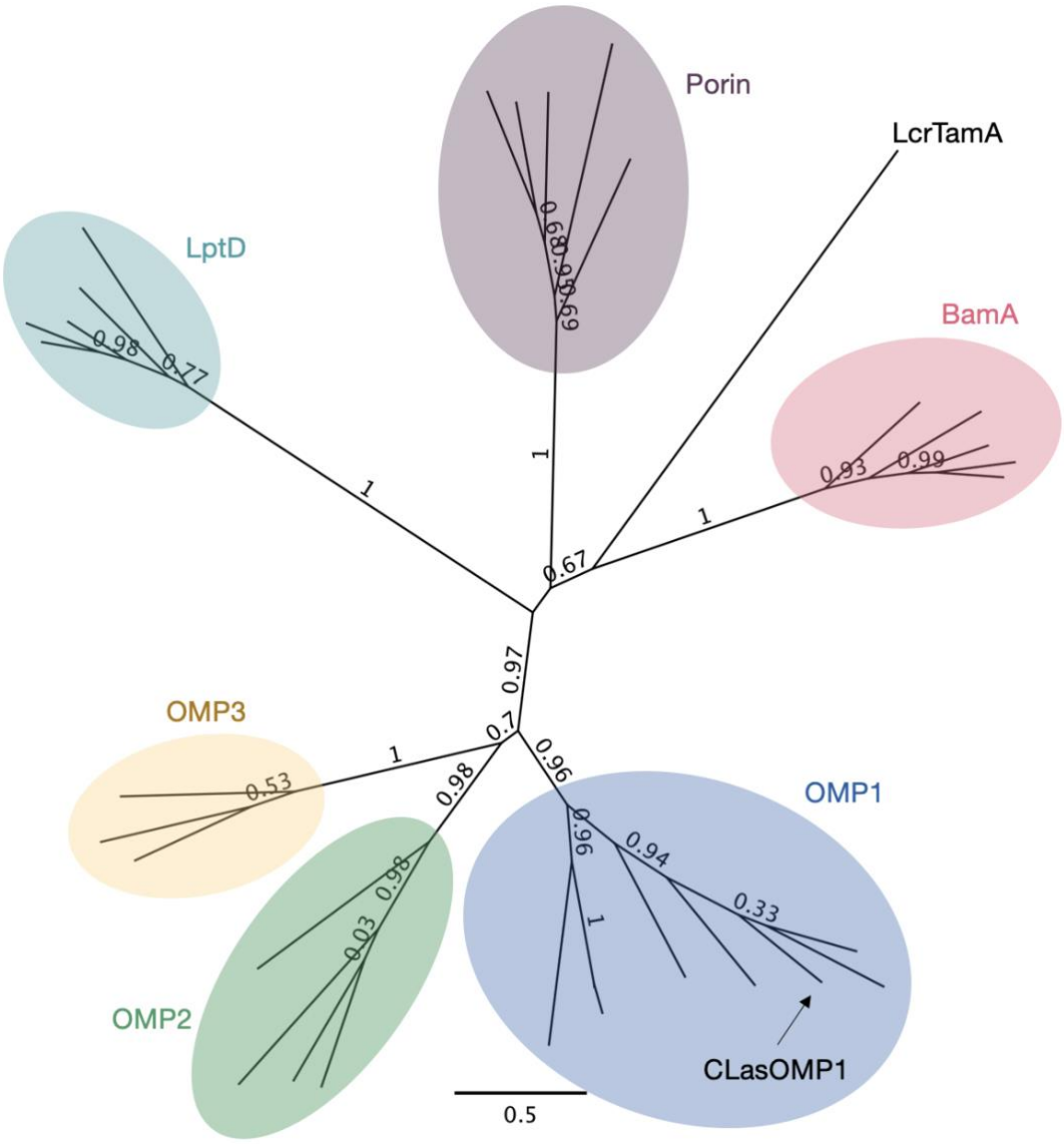

Figure 2.8. Clustering of Liberibacter OMPs reveals distinct subfamilies. Unrooted maximum likelihood FastTree v2.1.11-generated tree (Price et al., 2010, Price et al., 2009) depicting six clusters of 31 predicted OMPs in Liberibacter as identified by both the beta-barrel OMP HMM and DeepTMHMM. A MAFFT amino acid sequence alignment (Katoh and Standley, 2013) was used to generate the phylogeny. FastTree support values are indicated at each node. Tree visualized using Geneious Prime.

Protein ID	Bacteria	Cluster Name	OMP Description
WP_047264148.1	*Ca.* L. africanus	BamA	outer membrane protein assembly factor BamA species
WP_007556730.1	*Ca.* L. americanus	BamA	outer membrane protein assembly factor BamA species
WP_015452389.1	*Ca.* L. asiaticus	BamA	outer membrane protein assembly factor BamA species
WP_013461646.1	*Ca.* L. solanacearum	BamA	outer membrane protein assembly factor BamA species
WP_015272467.1	*L. crescens*	BamA	outer membrane protein assembly factor BamA species
WP_244464434.1	*Ca.* L. africanus	LptD	LPS assembly protein LptD species
WP_007556927.1	*Ca.* L. americanus	LptD	LPS assembly protein LptD species
WP_012778614.1	*Ca.* L. asiaticus	LptD	LPS assembly protein LptD species
WP_244391984.1	*Ca.* L. solanacearum	LptD	LPS assembly protein LptD species
WP_015272661.1	*L. crescens*	LptD	LPS-assembly protein LptD species
WP_047264709.1	*Ca.* L. africanus	OMP1	porin family protein species
WP_007556586.1	*Ca.* L. americanus	OMP1	outer membrane beta-barrel protein species
WP_015452561.1	*Ca.* L. asiaticus	OMP1	outer membrane beta-barrel protein species
WP_013461455.1	*Ca.* L. solanacearum	OMP1	outer membrane beta-barrel protein species
WP_015272991.1	*L. crescens*	OMP1-b	outer membrane beta-barrel protein species
WP_015273041.1	*L. crescens*	OMP1-c	porin family protein species

WP_015273568.1	*L. crescens*	OMP1	porin family protein species
WP_244422703.1	*L. crescens*	OMP1-a	porin family protein species
WP_047264568.1	*Ca.* L. africanus	OMP2	hypothetical protein species
WP_007557366.1	*Ca.* L. americanus	OMP2	outer membrane beta-barrel protein species
WP_015452909.1	*Ca.* L. asiaticus	OMP2	outer membrane beta-barrel protein species
WP_013462120.1	*Ca.* L. solanacearum	OMP2	outer membrane beta-barrel protein species
WP_007557438.1	*Ca.* L. americanus	OMP3	outer membrane beta-barrel protein species
WP_238556157.1	*Ca.* L. asiaticus	OMP3	hypothetical protein species
WP_013462180.1	*Ca.* L. solanacearum	OMP3	hypothetical protein species
WP_047263948.1	*Ca.* L. africanus	Porin	porin species
WP_007556998.1	*Ca.* L. americanus	Porin	porin species
WP_012778533.1	*Ca.* L. asiaticus	Porin	porin species
WP_013461918.1	*Ca.* L. solanacearum	Porin	porin species
WP_015273477.1	*L. crescens*	Porin	porin species
WP_172792750.1	*L. crescens*	TamA	autotransporter assembly complex protein TamA species

Table 2.1. Summary of predicted Liberibacter OMPs. Beta barrel OMPs predicted by hmmsearch and DeepTMHMM in representative Liberibacter strains: CLas (strain psy62), CLaf (strain PTSAPSY), CLso (strain ISR100), CLam (strain PW_SP), and Lcr (strain BT-1). Annotations are derived from NCBI reference genomes for each strain, and clustering is colored based on Figure 2.8.

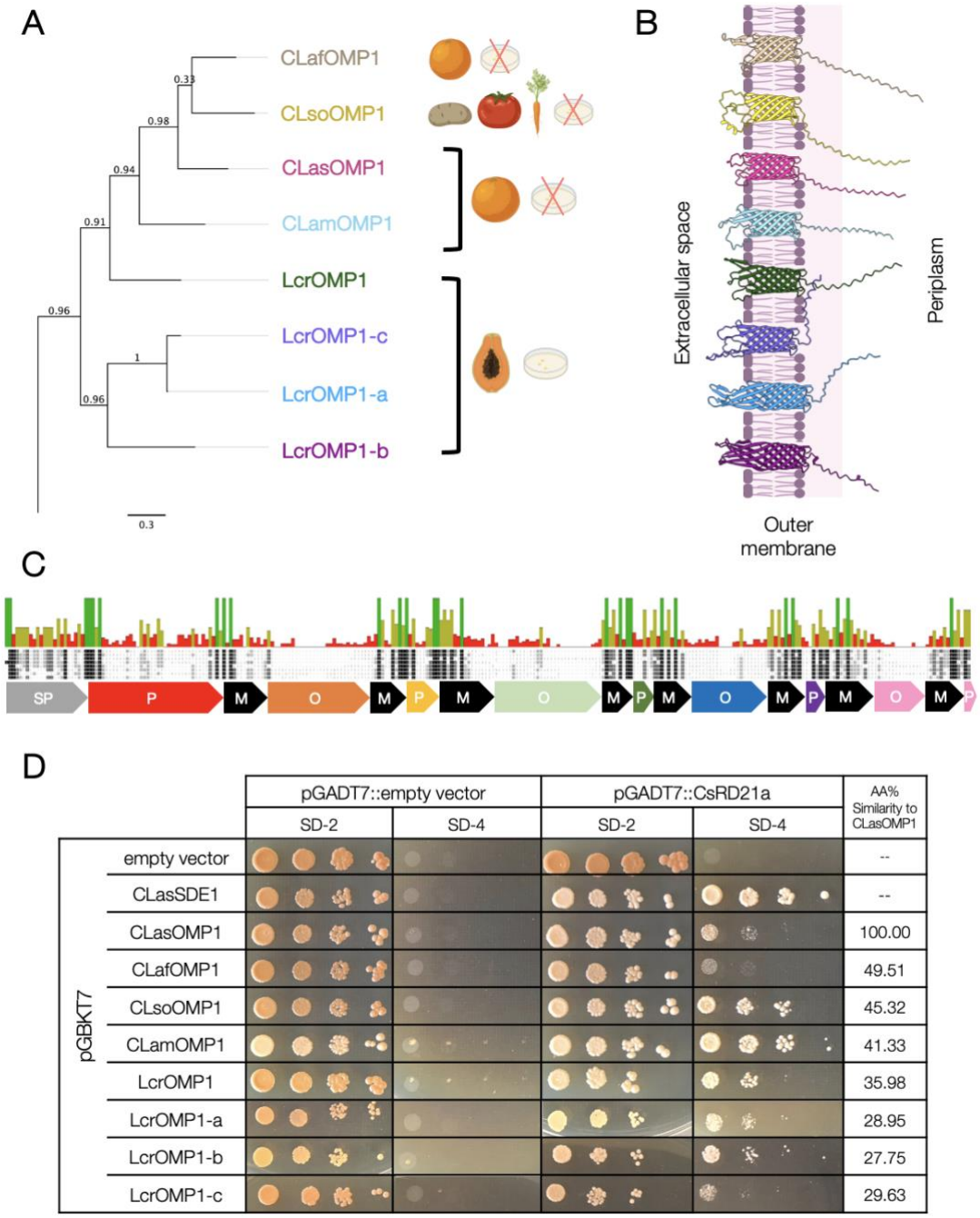

Figure 2.9. OMP1 homologs in Liberibacter interact with CsRD21a. A) The OMP1 cluster extracted from the Figure 2.8. Plant hosts and culturable status of each bacterium are displayed beside the tree. B) AlphaFold3 structural models for each OMP1 homolog. All pTM scores for the models are between 0.65 and 0.73. C) MUSCLE alignment (Edgar, 2004) of OMP1 homologs and the domain structure of CLasOMP1. Conservation levels are displayed for each amino acid (green = 100% conserved, green-brown = 30-99% conserved, red = 0-29% conserved). D) OMP1 homologs were cloned into the bait vector (pGBKT7) and screened against CsRD21a in the prey vector (pGADT7) via yeast-two-hybrid with empty vector negative controls. SD-2 medium lacks leucine and tryptophan and was used to select the co-transformed colonies. One colony was serially diluted and plated for each co-transformation in yeast on both SD-2 and the selective SD-4, which lacks leucine, tryptophan, adenine, and histidine. Growth on SD-4 indicates interaction of the proteins in the prey and bait vectors. The percentages of shared amino

acids between each OMP and CLasOMP1 are also displayed. The co-transformants of CLasSDE1 and CLasOMP1 with empty vector and CsRD21a are the same images shown in Figure 2.2.

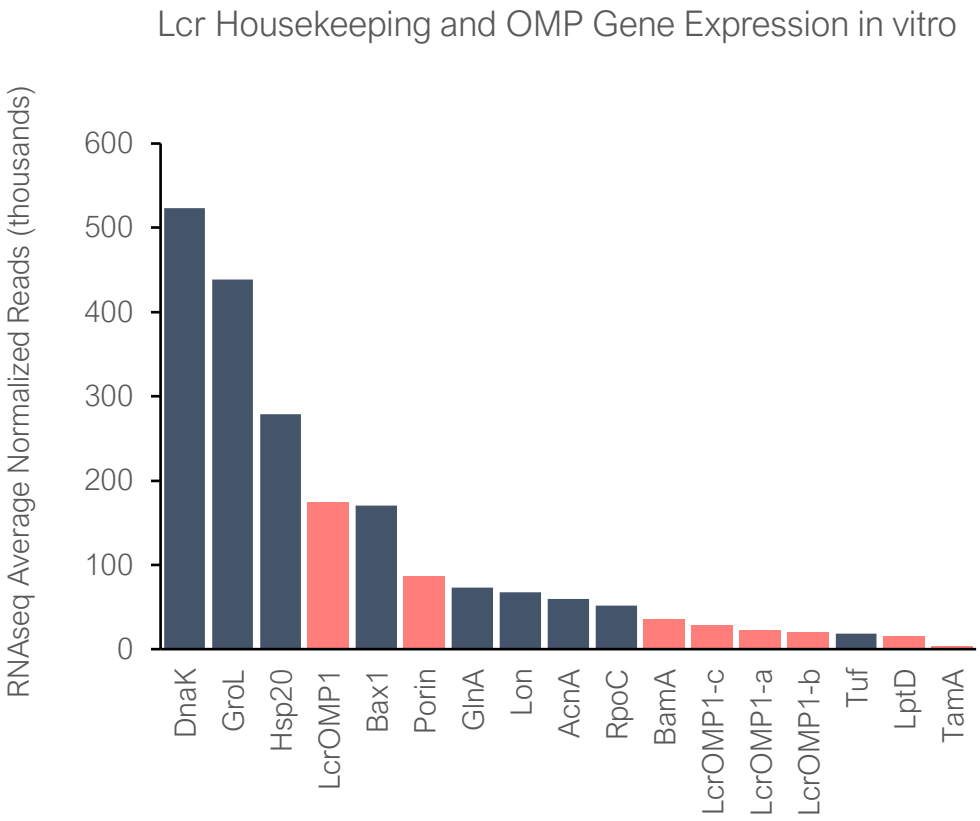

Figure 2.10. ***In vitro*** **expression of housekeeping and OMP genes in** ***L. crescens.*** Graph shows average normalized reads (two replicates) as determined by RNAseq. Lcr genes identified as OMPs in this thesis are highlighted in pink-red. All genes shown here, except for TamA, are in the top 17% of highest expressed genes in the dataset. Unpublished data courtesy of Dr. Amelia Lovelace and Dr. Eva Hawara.

LcrOMP1 is a Weaker Substrate of CsRD21a than CLasOMP1

While OMP1 homologs interact with CsRD21a in yeast, whether this interaction equates to proteolytic cleavage is unknown. To demonstrate CsRD21a cleavage of CLasOMP1, I had detected CLasOMP1 using ab1 and ab2. This allowed me to express the protein without having to fuse it to a tag. In other experiments, I found that C-terminally tagging OMP1 homologs resulted in additional and non-specific Western blot bands that made it difficult to discern which bands corresponded to the full length, mature, or cleaved proteins (data not shown). As such, I decided to generate an LcrOMP1-specific antibody to test tag-free LcrOMP1 cleavage by CsRD21a. The

purified LcrOMP1-specific antibody (ab3, courtesy of Pacific Immunology) was generated against a synthesized peptide that corresponds to a region near the C-terminus of LcrOMP1 (Figure 2.11A). I then subjected the tag-free LcrOMP1 protein to the same assay that was outlined in Figure 2.4 using the same apoplastic fluid used in Figure 2.5A/B. One major band between 15 and 25 kDa, presumably corresponding to the secreted, mature LcrOMP1 protein, was not affected with any amount of E-64-treated CsRD21a or the catalytic mutant (Figure 2.11B). Instead, a cleaved product appeared only when the wildtype CsRD21a was incubated without any E-64, suggesting that LcrOMP1 can also be cleaved by CsRD21a. Unlike LcrOMP1, CLasOMP1 can still be cleaved with as much as 2.2 μM E-64 present using the same apoplastic fluid (Fig 2.5B), suggesting that CLasOMP1 is cleaved more efficiently than LcrOMP1 by CsRD21a. These results suggest that sequence diversification in OMP1 may be, in some cases, sufficient to reduce the efficiency of CsRD21a proteolytic cleavage.

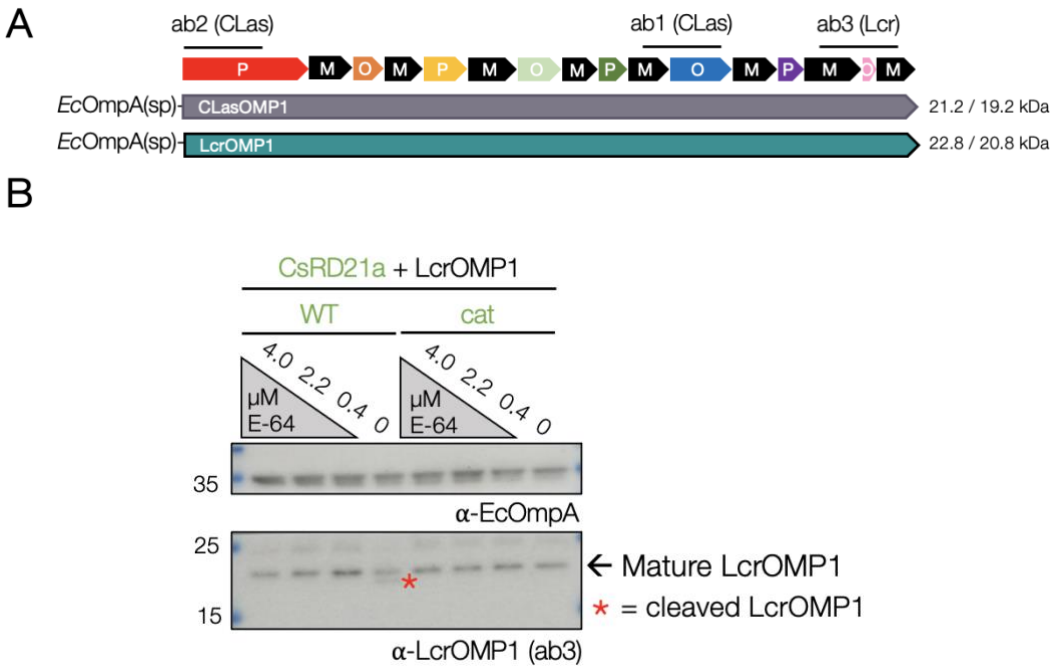

Figure 2.11. LcrOMP1 is weakly cleaved by CsRD21a. A) Schematic depicting Lcr and CLas OMP1 domain structures as well as their protein-specific antibody recognition sites. The mature OMP1 proteins were fused to the N-terminal signal peptide from *E. coli* OmpA, or *Ec*OmpA(sp). The molecular weights (kDa) of the full length and mature proteins, respectively, are shown at the right. B) LcrOMP1 was expressed in *E. coli,* and the resulting membrane fractions were incubated with the same CsRD21a-containing *N. benthamiana* apoplastic fluid used in Figure 2.5A/B. These samples were analyzed via Western blot using the LcrOMP1-specific antibody and, as a control, an EcOmpA-specific antibody. WT = wildtype, cat = catalytic mutant, ab1 and ab2 = CLasOMP1-specific antibodies, ab3 = LcrOMP1-specific antibody. Molecular weights on Western blots are represented in kDa using protein ladder.

C14 and Papain Cleave OMP1 Proteins

PLCPs are widespread in plants (Richau et al., 2012). It has been previously shown that a homolog of CsRD21a, C14 in tomato and potato, is a major player in the host-pathogen arms race with the oomycete *Phytophthora infestans* (Kaschani et al., 2010). C14 is inhibited by *P. infestans* EPIC effectors, and silencing it enhances host susceptibility during infection. Further, the purified papaya-derived enzyme papain is commercially available for purchase, and SDE1 was previously found to inhibit its enzymatic activity *in vitro* (Clark et al., 2018). I therefore decided to further investigate the catalytic activity of these enzymes against CLas and LcrOMP1.

As with CsRD21a, after transient expression in *N. benthamiana*, the tomato C14 is an active protease in apoplastic fluid, as determined by ABPP (Figure 2.12A). When incubated with CLasOMP1 and LcrOMP1, cleavage of these proteins by C14 is clearly observed in an E-64 dosage-dependent manner (Figure 2.12B). Where CsRD21a cannot cleave LcrOMP1 in the presence of 0.4 μM E-64 (Figure 2.11B), C14 has activity against LcrOMP1 at this concentration of E-64, producing a cleavage product that is roughly the same size of the CsRD21a-produced LcrOMP1 cleavage product when no E-64 is present (Figure 2.11B,2.12B). However, these proteins would need to be run side-by-side on a protein gel to confirm this observation. In the absence of E-64, C14 further processes LcrOMP1, producing a cleavage product that is not produced by CsRD21a (Figure 2.11B,2.12B). This demonstrates that, like CsRD21a, C14 can cleave CLasOMP1 and LcrOMP1 in the semi-*in vitro* assay, yet C14 appears to be more active than CsRD21a against LcrOMP1. This could be, in part, because *N. benthamiana* is a closer host to tomato than it is to citrus, perhaps making it more suitable environment for its enzymatic activation.

The transient expression system in *N. benthamiana* makes it difficult to obtain consistent concentrations of PLCPs in the apoplastic fluid between experiments, whereas the concentration of purified protease can be controlled *in vitro*. Therefore, I next tested whether purified papain could cleave CLasOMP1. Papain exhibits a clear increase in activity as the concentration of the enzyme increases, as determined by ABPP (Figure 2.12C). Further, it cleaves LcrOMP1 and CLasOMP1 in a concentration-dependent manner (Figure 2.12D). The cleavage pattern of CLasOMP1 upon papain treatment resembles what was observed with C14 and CsRD21a, where one cleaved band between 11 and 17 kDa appears at higher enzyme concentrations. Yet, like C14, papain produces multiple cleavage products from LcrOMP1. As Lcr was previously

isolated from mountain babaco papaya phloem sap (Davis et al., 2008), it is an intriguing finding that LcrOMP1 can be cleaved by papaya papain *in vitro*, suggesting that this bacterium may also have to overcome papain or PLCP cleavage *in planta*. It may overcome this cleavage via redundant functions of LcrOMP1a/b/c homologs, for example.

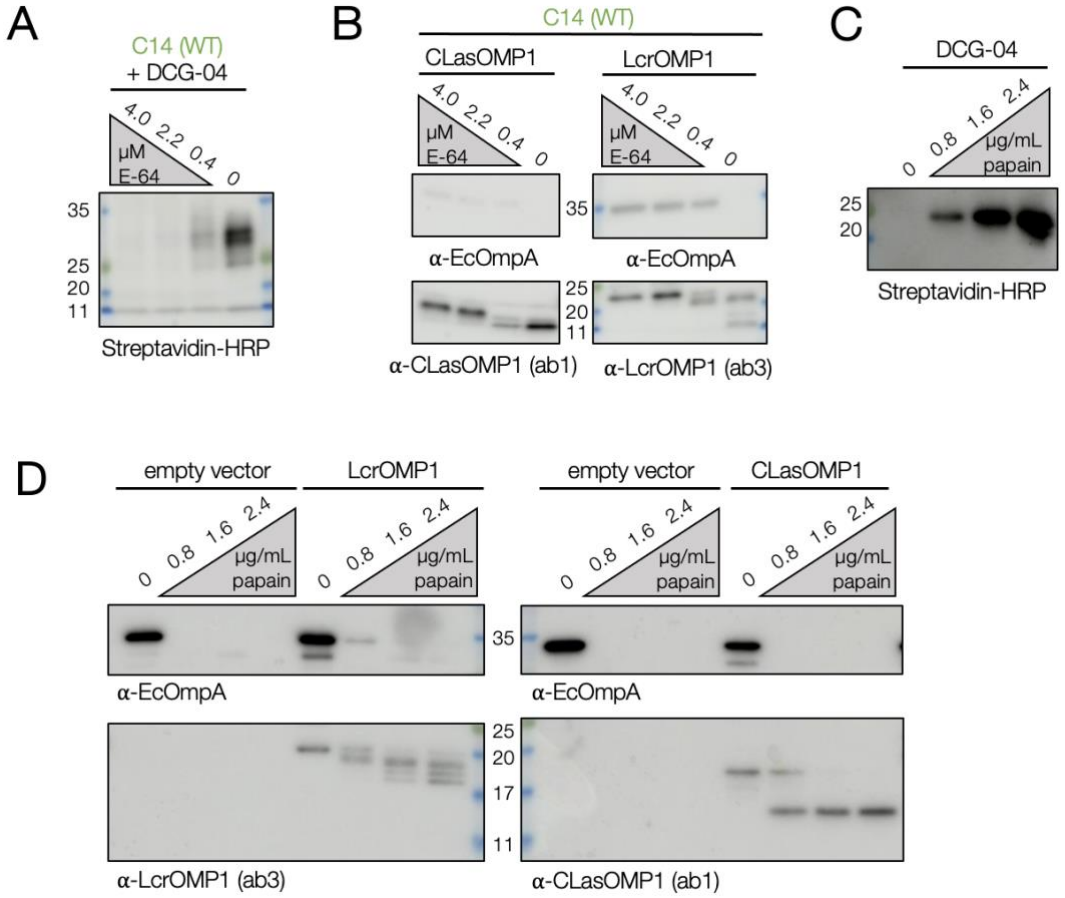

Figure 2.12. C14 and papain cleave CLas and LcrOMP1. A+C) Western blot depicting ABPP of (A) apoplastic fluid from C14-expressing *N. benthamiana* or (C) purified papain using the DCG-04 probe. B+D) CLas and Lcr OMP1 proteins were expressed in *E. coli* and the resulting membrane fractions were incubated with (B) C14-containing *N. benthamiana* apoplastic fluid or (C) purified papain. Cleaved OMPs were detected via Western blot and EcOmpA was used as a loading control. WT = wildtype. Molecular weights on Western blots are represented in kDa using protein ladder.

That CsRD21a, C14, and papain all cleave CLasOMP1 and LcrOMP1 in the semi-*in vitro* assays and produce similar sized cleavage products suggests that they are similar, conserved enzymes. However, C14 and papain generate more cleavage products than CsRD21a from LcrOMP1. This could reflect differences between the sequences or structures of these enzymes. To assess their similarity to one another, I utilized AlphaFold3 to compare the predicted structures of their protease domains. The

three structures were predicted with high confidence, each producing pTM scores of 0.96. Using ChimeraX matchmaker, I found that the three protease domains overlay with one another almost perfectly, including their catalytic residues (Figure 2.13A). The RMSD values of this overlay are very strong, with C14 and papain producing structures within 0.547 and 1.222 Å, respectively, of CsRD21a (Figure 2.13B). However, despite this high predicted structural conservation, the amino acid sequences between these proteins vary. For example, CsRD21a shares 73.4 and 47.0% sequences identity with C14 and papain, respectively (Figure 2.13C). This suggests that despite evolutionary distance and sequence diversification, PLCPs protease domain structures are constrained to retain their enzymatic functions. This may account for why they produce similar cleavage products from CLasOMP1 and LcrOMP1. Yet, enough sequence variation exists to suggest why CsRD21a has less activity against LcrOMP1. This may reflect variations in CsRD21a substrate-binding residues, but this has not yet been investigated. Alternatively, CsRD21a may have citrus-specific adaptations or post-translational modifications that limit its activity against LcrOMP1 using the *N. benthamiana* transient expression system.

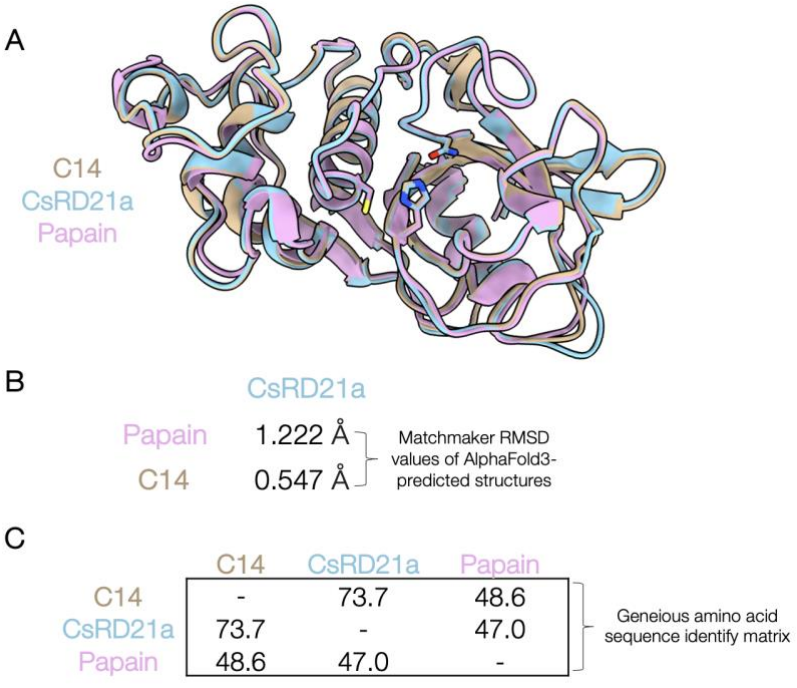

Figure 2.13. The enzymatic domains of CsRD21a, C14, and papain are structurally conserved. A) Structural alignment AlphaFold3-predicted structures of C14 (tan), CsRD21a (light blue), and papain (pink) visualized by ChimeraX (Goddard et al., 2018, Meng et al., 2023, Pettersen et al., 2021). Each structural model gave a pTM score of 0.96. The catalytic residues are highlighted in blue, red, and yellow. B) RMSD values of the predicted structures as determined by ChimeraX matchmaker structural alignment. C) Amino acid sequence similarity matrix of the protease domains of the three proteases.

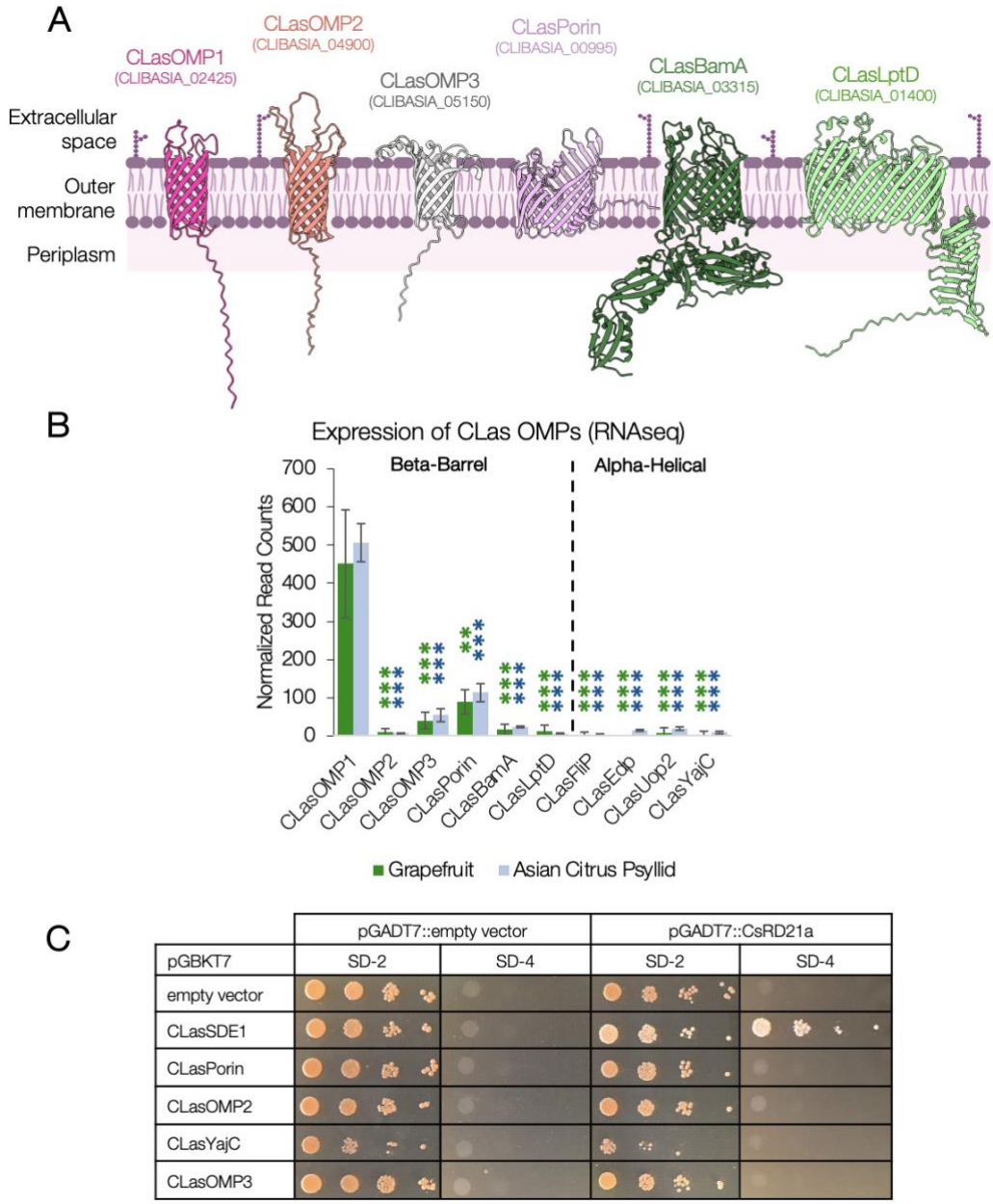

Figure 2.14. CsRD21a specifically interacts with CLasOMP1. A) AlphaFold3 structural models of CLas membrane proteins selected from clusters in Figure 2.8. All models exhibit pTM scores between 0.65 and 0.84. B) Expression of CLas membrane proteins in infected grapefruit midribs (n=6) and the Asian citrus psyllid (n=4) represented by normalized read counts. Error bars indicate standard deviation. Asterisks (*) represent degrees of significance as determined by two-tailed, type-three T-test between each gene and CLasOMP1, where ** signifies $p < 0.01$ and *** signifies $p < 0.001$. Green and blue asterisks represent significance for the grapefruit and Asian citrus psyllid samples, respectively. Data courtesy of Lovelace et al. (2024). C) Yeast-two-hybrid screening between CsRD21a (pGADT7-prey) and CLas membrane proteins (pGBKT7-bait). SD-2 medium lacks leucine and tryptophan and was used to select the co-transformed colonies. One colony was serially diluted and plated for each co-transformation in yeast on both SD-2 and the selective SD-4, which lacks leucine, tryptophan, adenine, and histidine. Growth on SD-4 indicates interaction of the proteins in the prey and bait vectors.

CsRD21a Interacts with CLasOMP1 but not other CLas OMPs

Given that CsRD21a, C14, and papain can cleave two OMP1 homologs, I aimed to further understand the substrate specificity of CsRD21a. To do this, I extracted each of the six total CLas OMPs identified by both the beta barrel OMP HMM and DeepTMHMM, as described previously. CLas encodes one protein from each of the six clusters identified in Figure 2.8, and these proteins were named according to their respective clusters: CLasBamA, CLasLptD, CLasPorin, CLasOMP1, CLasOMP2, and CLasOMP3. I next analyzed the AlphaFold2 structural models of these proteins (Figure 2.14A), which revealed the conserved beta barrel transmembrane domain, extracellular loops, and periplasmic loops/domains. Additionally, DeepTMHMM predicted four alpha-helical membrane proteins, including: a flagellar pore FliP protein (CLasFliP), an EAL domain-containing protein (CLasEdp), a ubiquinol oxidase II (CLasUop2), and a preprotein translocase YajC (CLasYajC). CLasOMP1 is by far the most highly expressed of beta-barrel and alpha-helical membrane proteins with similar levels of normalized read counts in both infected grapefruit and ACP (data courtesy of Dr. Amelia Lovelace) (Figure 2.14B). CLasPorin and CLasOMP3 were expressed to slightly higher levels in both grapefruit and the ACP compared to the other membrane proteins.

I next sought to clone each of the CLas membrane proteins into the pGBKT7 bait yeast-two-hybrid vector to test if CsRD21a interaction with CLasOMP1 is specific. Of the nine membrane proteins (not including CLasOMP1), I successfully cloned only CLasOMP2, CLasOMP3, CLasPorin, and alpha-helical CLasYajC from infected citrus cDNA sourced from Dr. Amelia Lovelace. Unlike CLasOMP1, none of these OMPs interacted with CsRD21a in yeast (Figure 2.14C), but whether this lack of interaction equates to a lack of proteolytic cleavage remains unknown. CLasOMP2, CLasOMP3, and CLasPorin were all tested for proteolytic cleavage by CsRD21a using the C-terminal FLAG tag system. However, the results from this method were inconclusive for the reasons previously indicated.

Identifying the PLCP cleavage site in CLasOMP1: an Open Question

That CsRD21a interacts with OMP1 homologs but not the other CLas OMPs tested suggests that it does not target OMPs broadly. While PLCPs are generally considered to be promiscuous enzymes, it has been demonstrated that PLCPs in plants prefer hydrophobic residues in the P2 position (two amino acids away from the cut site)

of their substrates (Kourelis et al., 2024, Richau et al., 2012). Intriguingly, the outside extracellular loop that contributes to CsRD21a interaction in yeast contains a hydrophobic phenylalanine residue at the 68th residue in the protein. I tested whether mutation of this phenylalanine may reduce CsRD21a cleavage. The F68 residue is located at a predicted membrane-outside loop junction, where the preceding residue is a membrane-bound serine. To avoid replacing the phenylalanine with a residue that may disrupt membrane incorporation, I replaced it with residues found at the remaining three membrane-outside loop junctions in CLasOMP1. In addition to phenylalanine, these resides (valine, alanine, and glutamine) coincidentally represent a gradient of hydrophobicity, where phenylalanine is the most hydrophobic and glutamine is the most hydrophilic (Figure 2.15A). I therefore generated three CLasOMP1 mutants (F68A, F68Q, and F68V) to test for their cleavage by CsRD21a. First, I predicted the AlphaFold2 structures of these mutants to ensure that they did not disrupt the OMP1 beta-barrel structure. Indeed, these mutations did not disrupt the overall predicted structure of CLasOMP1 (Figure 2.15B). Next, I cloned these mutants and subjected them to the CsRD21a cleavage assay. However, each mutant displayed a similar cleavage pattern to the wildtype CLasOMP1, demonstrating that mutating this phenylalanine residue does not abolish CLasOMP1 cleavage by CsRD21a (Figure 2.15C). To determine if the efficiency of cleavage is reduced in these mutants, they should be subjected to a concentration gradient of E-64 as with previous experiments in this chapter, and equal loading should be assessed using the EcOmpA-specific antibody.

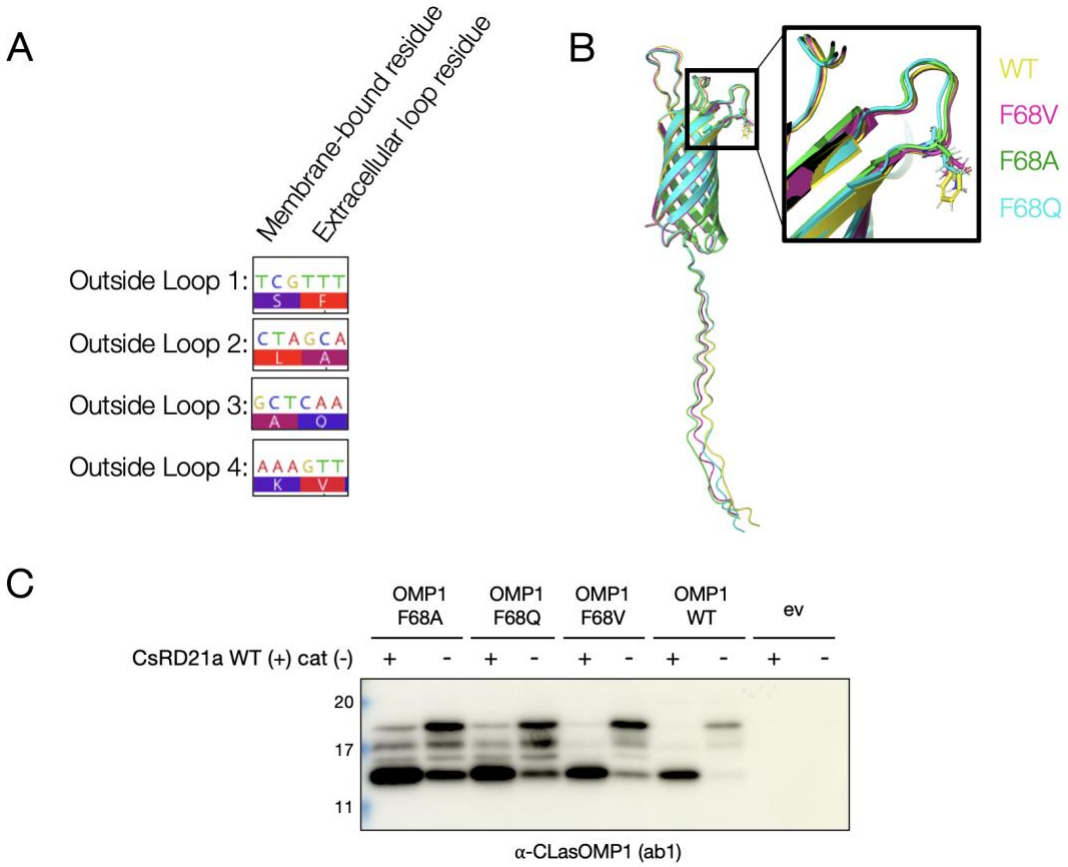

Figure 2.15. Targeted mutagenesis of a hydrophobic residue in CLasOMP1 does not change CsRD21a cleavage. A) Nucleotide and amino acid sequence of membrane-extracellular loop junctions in CLasOMP1. Amino acids are colored by hydrophobicity, where red is the most hydrophobic and blue is the most hydrophilic. B) AlphaFold2 protein structural alignment of CLasOMP1 and CLasOMP1 F68 mutants using ChimeraX matchmaker. C) Western blot depicting wildtype (WT) or F68 mutants of CLasOMP1 incubated with CsRD21a WT or the CsRD21a catalytic (cat) mutant with empty vector (ev) as a negative control.

Papain does not Affect Membrane Integrity or Bacterial Growth

Papain may inhibit Lcr growth given that it cleaves LcrOMP1. To test this, our collaborators Dr. Chunxia Wang and Dr. Amit Levy at UF CREC monitored the effect of papain on Lcr growth *in vitro* but found no evidence of antimicrobial activity (data not shown). One plausible explanation for this is that Lcr encodes its own PLCP inhibitors or overcomes LcrOMP1 cleavage via OMP1 homolog redundancy, but this has not yet been investigated.

Curiously, when EcOmpA was used as a loading control for protease assays containing C14 and papain, but not CsRD21a, a clear reduction of signal corresponding to EcOmpA was observed when E-64 concentrations or papain concentrations were

decreased or increased, respectively (Figure 2.12B,D). The AlphaFold3-predicted structure of EcOmpA forms a similar eight-stranded beta-barrel structure but encodes an additional peptidoglycan-binding periplasmic domain that is absent in OMP1 homologs (Figure 2.16) (Samsudin et al., 2016). It has been previously reported that serine protease-mediated cleavage of EcOmpA leads to a destabilized membrane and causes a wrinkled morphological phenotype when observed with scanning electron microscopy (SEM), ultimately resulting in bacterial death (Belaaouaj et al., 2000). Therefore, I hypothesized that papain and C14 may lead to bacterial cell wall destabilization and, ultimately, death. In collaboration with Kim Findlay at the John Innes Centre BioImaging facility, we subjected BSA- and papain-treated *E. coli* to SEM; however, no obvious morphological changes were observed with papain treatment compared with BSA treatment, and no growth inhibition effect was observed *in vitro* (data not shown). To test if some bacterial cell wall weakening was first required for papain-mediated cell wall destabilization, I pre-treated the *E. coli* cells with a gradient (0-25 µg/mL) of ampicillin which interferes with cell wall synthesis (DrugBank). While ampicillin reduced *E. coli* growth in a concentration-dependent manner *in vitro*, papain (50 µg/mL) did not further inhibit bacterial growth or induce SEM-detectable membrane destabilization as compared to the BSA-treated cells (data not shown).

Using an alternative strategy, I employed a membrane integrity assay that utilizes chlorophenol red-ß-D-galactopyranoside (CPRG), a substrate of LacZ that cannot enter the cell during normal growth conditions. When the *E. coli* membrane is compromised, CPRG enters the cell and is converted to CPR by LacZ, giving the damaged bacteria a purple-pink color (Paradis-Bleau et al., 2014). Using this method, it has been previously demonstrated that single knockouts of OmpA, OmpC, and OmpF in *E. coli* reduce membrane integrity (Choi and Lee, 2019). I hypothesized that expressing OMP1 proteins in these knockout mutants could rescue the compromised membrane phenotype. If OMP1 rescues the knockout mutant phenotype, then perhaps it could be reversed by the addition of PLCPs. However, I found that both overexpression (Bentham et al., 2021) and arabinose-inducible expression (Milnes et al., 2023) of EcOmpA, CLasOMP1, LcrOMP1, CLamOMP1, and CLafOMP1 in these knockout mutants induced further membrane instability, even at the lowest concentrations of arabinose tested (0.001%) (data not shown). The OmpA/C/F knockouts provided by Choi and Lee (2019) were in the MG1655 strain. However, some *E. coli* strains better tolerate the over-expression of OMPs compared to MG1655, such as the C41 strain used for CLasOMP1 and LcrOMP1 expression in this chapter (McIlwain and Kermani, 2020). As

such, further investigation into OMP1 functions may be best conducted with OMP1 complementation of OMP knockouts in the C41 background. Additionally, the native OmpA promoter may be a better alternative to over- or inducible expression systems. As such, no evidence of an effect of papain or PLCPs on bacterial growth or membrane stability has been observed to date.

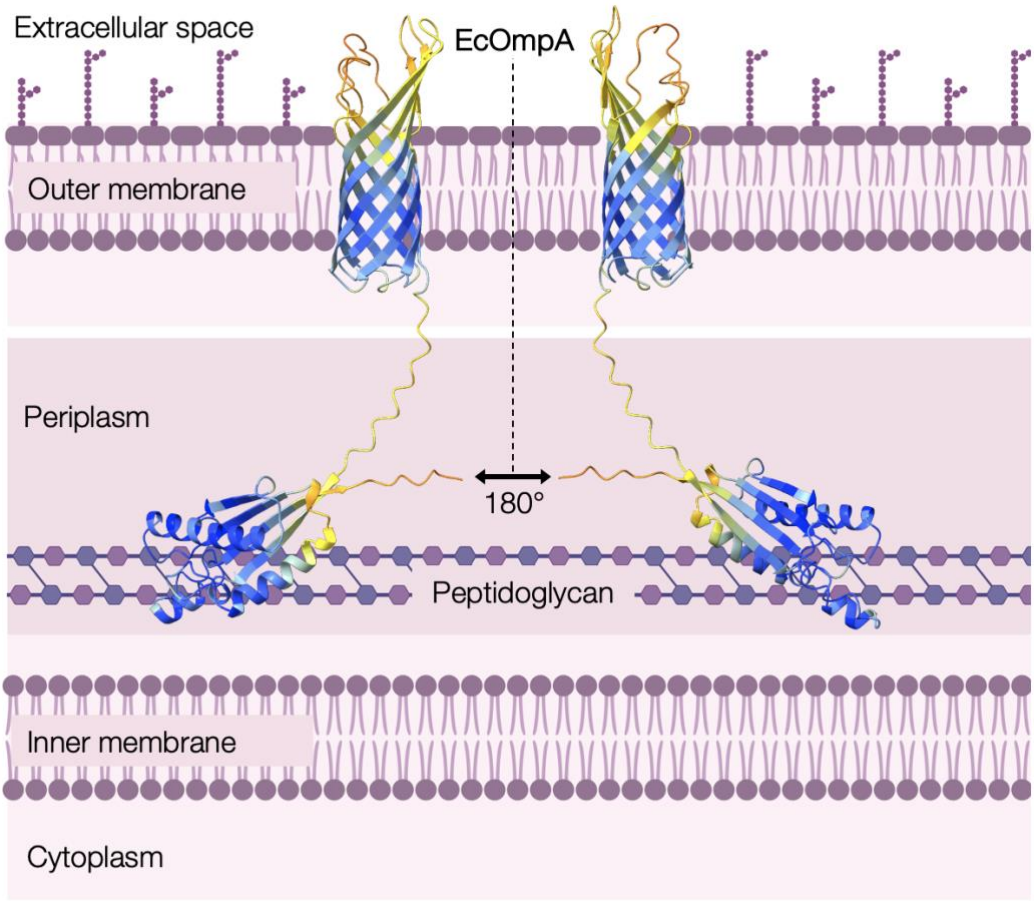

Figure 2.16. EcOmpA is a cell surface-exposed barrel OMP. AlphaFold3 model of EcOmpA colored by pLDDT confidence. High-confidence (pLDDT > 90) regions are dark blue; confident (pLDDT between 70 and 90) regions are light blue; low-confidence (pLDDT between 50 and 70) regions are yellow; and very-low confidence (pLDDT lower than 50) are orange. The AlphaFold3-predicted model was visualized using ChimeraX (Goddard et al., 2018, Meng et al., 2023, Pettersen et al., 2021). The model was then appended to the "Gram-negative bacteria cell wall" template by BioRender.com (2024).

Conclusions and Discussion

SDE1, a CLas effector protein, contributes to CLas virulence and inhibits citrus PLCPs (Clark et al., 2018, Clark, 2019, Clark et al., 2020). This begs the question of the roles of citrus PLCPs in defense against the HLB pathogen. In this chapter, I identified a CLas-derived substrate of citrus PLCPs: a cell surface-exposed, highly expressed OMP called CLasOMP1. As such, this is the first bacterial-derived substrate of a PLCP that has been identified to date. Furthermore, with the help of our collaborators, we have established that CsRD21a, an SDE1-inhibited citrus PLCP, contributes to HLB tolerance. Therefore, this work establishes an evolutionary arms race between CLas in citrus, in which citrus PLCPs contribute to defense via cleaving CLas substrates, and, as a counter-defense, CLas deploys a PLCP-inhibiting effector, SDE1, to suppress defense (Figure 2.17).

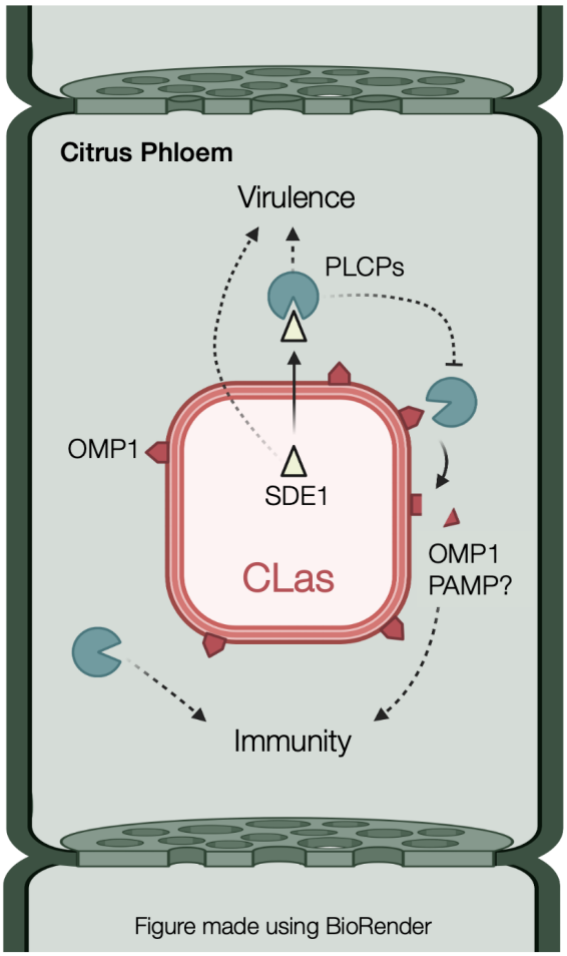

Figure 2.17. Working model of the citrus-CLas molecular arms race.

Despite this advancement in our understanding of citrus-CLas molecular interactions, several open questions remain. CLasOMP1 interacts with two citrus PLCPs, CsRD21a and CsSAG12, via yeast-two-hybrid, and is cleaved by CsRD21a. How do these proteases reach the phloem? Are these proteases trafficked into the cell during infection from companion cells? Further, CsRD21a and CsSAG12 are derived from sweet orange citrus, a susceptible citrus variety. Therefore, it would be particularly interesting to investigate the functions and expression levels of PLCPs from tolerant citrus varieties. Do they exhibit enhanced activity towards CLasOMP1 and other CLas proteins? Are they also inhibited by SDE1? As previously mentioned, at least two PLCPs are induced in tolerant Sugar Belle citrus (Robledo et al., 2024). Upregulation of proteases as a defense response may also be partially responsible for higher concentrations of free amino acids in the phloem of some tolerant citrus varieties, such as *Poncirus trifoliata* and *Severinia buxifolia*, as compared to susceptible varieties, such as Valencia sweet orange and Duncan grapefruit (Killiny and Hijaz, 2016). However, this is purely speculative.

While beta-barrel OMPs are widespread across all Gram-negative bacteria, mitochondria, and chloroplasts (Fairman et al., 2011), their functions remain elusive within the context of plant immunity. Conversely, OMPs have been extensively studied in animal pathogens. For example, OmpA proteins of various human-infecting pathogens are involved in adhesion to host tissues, are crucial for virulence, and are common targets of the innate and adaptive immune systems (Confer and Ayalew, 2013). As previously mentioned, *E. coli* OmpA is cleaved by a serine endopeptidase, called neutrophil elastase (NE), reducing bacterial cell membrane integrity, shriveling the normally rod-like morphology of the bacterium, and ultimately killing it (Belaaouaj et al., 2000). OmpA cleavage by NE was also observed in the Gram-negative bacterium *Klebsiella pneumoniae*. Further, disruption of NE in mice leads to enhanced susceptibility to *E. coli* and *K. pneumoniae* but not Gram-positive *Staphylococcus aureus*, which lacks an outer membrane (Belaaouaj et al., 1998). Like NE, I found that C14 and papain also cleave *E. coli* OmpA. Therefore, I hypothesized that C14 and papain may also affect *E. coli* viability and cell morphology, yet we observed no antimicrobial activity or membrane destabilization via SEM when *E. coli* cells were treated with purified papain. Further, the CPRG-based membrane integrity assay requires further optimization to characterize the role of OMP1 in cell morphology.

CLasOMP1 forms a porin-like channel and may function in passing ions in and out of the CLas cell. As such, I found that the AlphaFold3-predicted structure of

CLasOMP1 produces a channel with a hydrophilic, negatively charged interior (Figure 2.18). Therefore, CLasOMP1 may import and/or export positively charged ions. The extracellular loops contain both positively and negatively charged amino acids and may function in interacting with host and/or bacterial-derived proteins. Indeed, extracellular loops of OMPs in Gram-negative bacterial pathogens regulate virulence via adhesion in mammalian hosts (McClean, 2012). In the future, identifying a specific substrate and/or interacting proteins of this channel protein would provide more mechanistic insight into its function in bacterial survival and pathogenesis.

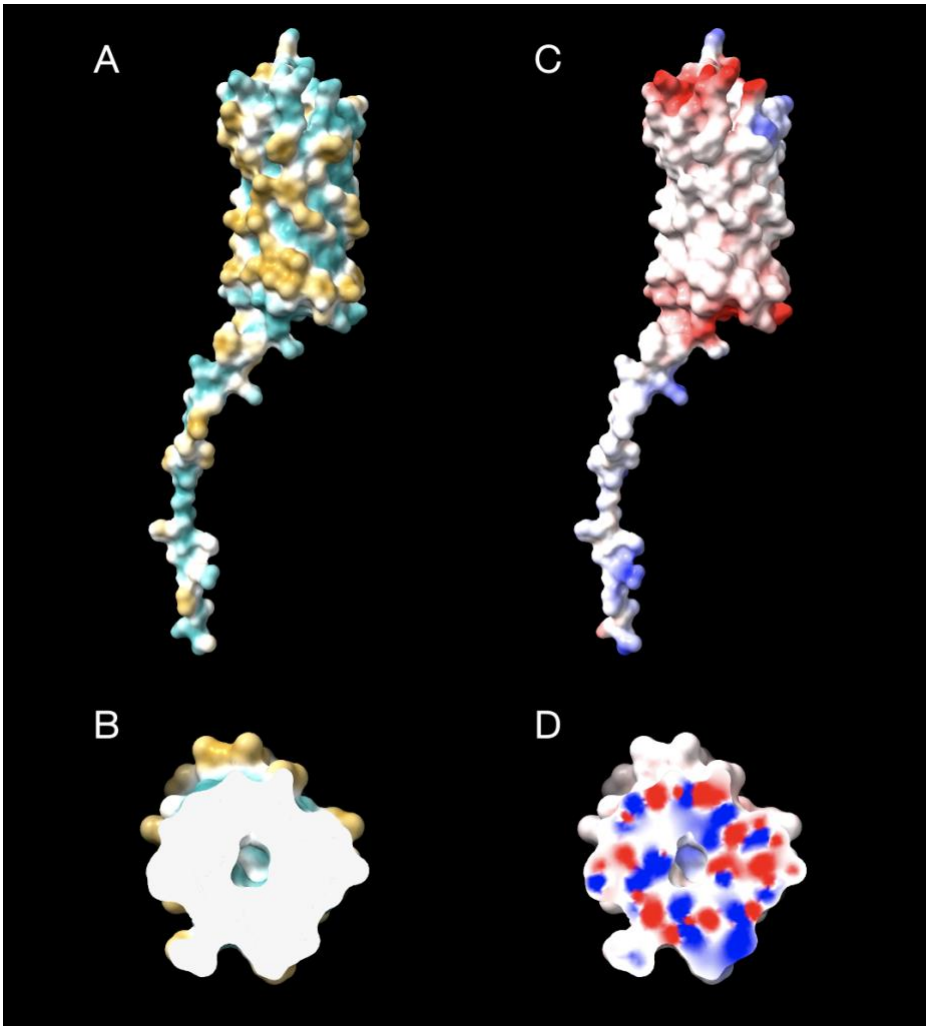

Figure 2.18. CLasOMP1 is a putative channel protein. AlphaFold3 model of CLasOMP1 visualized using ChimeraX (Goddard et al., 2018, Meng et al., 2023, Pettersen et al., 2021). Panels B and D represent top view cross-sections of A and C, respectively. A+B) CLasOMP1 surface residues are colored by hydrophobicity, where gold represents the most lipophilic residues, cyan represents the most hydrophilic residues, and white represents neutral residues. C+D) CLasOMP1 residues are colored by Coulombic electrostatic potential, where red represents negative charge, blue represents positive charge, and white represents neutral charge.

Overexpression of CsRD21a in citrus results in lower CLas titers and healthier plants when compared to wildtype samples, suggesting that CsRD21a contributes to defense against CLas *in planta*. Given difficulties in obtaining transgenic citrus explants, the CsRD21a-overexpressing citrus scions were compared to wildtype citrus scions that went through the same transformation protocol but did not contain the CsRD21a transgene. Further, I was unable to detect CLasOMP1 or its cleavage products in the transgenic or wildtype lines, which may be a result of the low titers and/or unequal distribution of the bacteria *in planta*. Therefore, many questions remain as to the specific role of CsRD21a and its cleavage of CLasOMP1 in citrus defense. Further investigation of the CsRD21a-mediated tolerance phenotype should include a better negative control, ideally the CsRD21a catalytic mutant. Additionally, future work will specifically study the defense functions of CsRD21a in the citrus phloem using the SUC2 phloem-specific promoter through collaborations with Dr. Nian Wang's group at UF CREC.

Whether CLasOMP1 is required for CsRD21a-mediated defense remains unknown. One possibility is that OMP1 peptides released by CsRD21a cleavage may trigger immune responses. For example, maize PLCPs release the endogenous DAMP ZIP1 which elicits SA but not PTI (Ziemann et al., 2018). Therefore, SA accumulation and PR gene expression could be assessed upon treatment of citrus leaves with PLCP-produced, CLasOMP1-derived peptides. Such peptides may also trigger PTI. Infiltrating citrus leaves with CLasOMP1 cleavage products and measuring the accumulation of ROS could reveal if CLasOMP1 cleavage releases PAMPs. Previously, I employed this method by measuring ROS in leaf disks from Australian finger lime, sweet orange, and Duncan grapefruit citrus seedlings. However, ROS induction was inconsistent between biological replicates, perhaps due to difficulties of the peptides to enter the citrus leaf disks (data not shown).

Identifying the CsRD21a cleavage site in CLasOMP1 remains a challenge. Identifying and confirming a specific cleavage site via mutations to block PLCP cleavage would further enhance this mechanistic study. By screening a series of CLasOMP1 truncations for interaction with CsRD21a via yeast-two-hybrid, I narrowed down that this interaction is facilitated by the N-terminus of CLasOMP1, which includes a disordered periplasmic domain, an extracellular loop, and portions of two membrane-bound beta-sheets. Furthermore, the size of the ab1-detected CLasOMP1 cleavage products suggests that this cleavage occurs near N-terminal extracellular loop. However, the yeast-two-hybrid system has its shortcomings in characterizing protease-substrate interactions. For example, these interactions could be transient and result in substrate

destabilization. Indeed, when the N-terminal periplasmic domain was removed from CLasOMP1 (truncation A), the interaction with CsRD21a appears stronger than with the mature CLasOMP1 protein (Figure 2.3C). This could be the result of CsRD21a cleavage of the periplasmic domain in yeast, but the periplasmic domain by itself (truncation 1) interacts strongly with CsRD21a (Figure 2.3B), making it difficult to make such claims. When I tested further truncated forms of CLasOMP1, the interaction becomes weaker again (similar to the mature CLasOMP1) and is not fully abolished until an extracellular loop is removed along with some amino acids in an adjacent membrane-bound beta sheet (Figure 2.3C). Therefore, while I conclude that the N-terminus of CLasOMP1 interacts with CsRD21a, further resolution of this interaction using yeast-two-hybrid is difficult to obtain. Screening the catalytic mutant of CsRD21a could further resolve the protease-substrate interaction interface, but this may also prove difficult if the catalytic triad contributes extensively to CLasOMP1 binding.

With the help of The Sainsbury Laboratory Proteomics team, we attempted to identify the cleavage site by performing N-terminal labeling followed by mass spectrometry of CLasOMP1 after CsRD21a or papain cleavage. This strategy was employed using two separate methods, dimethylation and tandem mass tag (TMT) labeling (Wang et al., 2023); however, no N-terminally labeled peptides were consistently identified in the protease-treated samples that were absent in untreated samples. Yet, efforts to determine the CsRD21a cleavage site using this method were not exhausted, and this method still represents a promising strategy. For example, the analyzed CLasOMP1 samples were not purified protein but CLasOMP1-containing membrane fractions from *E. coli*. Therefore, future strategies could involve further optimizing the purification of CLasOMP1 prior to papain or PLCP cleavage and subsequent N-terminal labeling.

LcrOMP1 appears to be a weaker substrate of CsRD21a than CLasOMP1, and this may explain why LcrOMP1 appears to interact with CsRD21a more strongly in yeast than CLasOMP1. C14 and papain cleave both CLasOMP1 and LcrOMP1 efficiently, further demonstrating that OMPs may be targeted by PLCPs in different hosts. Future work will examine chimeras of CLasOMP1 and LcrOMP1 to determine which regions of CLasOMP1 are targeted by CsRD21a. Further, engineering and testing additional PLCPs, such as Rcr3, against other destructive phloem pathogens, such as CLso, may be an exciting research avenue.

The results in this chapter do not exclude the possibility that CsRD21a contributes to defense in citrus in a CLasOMP1-independent manner. One hypothesis

is that upon SDE1 binding of PLCPs, the resulting protein complex could bind a receptor and activate defense. However, this would likely occur via a Cf-2-independent mechanism given that, unlike Avr2, SDE1 cannot inhibit Rcr3 or cause cell death in tomato (Clark et al., 2018). Further, CLas is an intracellular bacterium and membrane-bound receptor-like proteins, such as Cf-2, are located on the outside of the cell. Alternatively, intracellular NLRs could activate defense if they recognize the PLCP-SDE1 complex. Yet, SDE1 transgenic grapefruit seedlings are susceptible to CLas, suggesting that there is no such NLR in grapefruit. Developing a designer intracellular receptor with Cf-2 guarding-like functions might be an exciting avenue for tackling citrus HLB.

Engineering SDE1-insensitive proteases could also be an exciting application of this mechanistic research. Unfortunately, investigations into the structure of SDE1 have proven unsuccessful in my hands. SDE1 is comprised of 21.3 percent serine residues, contributing to an overall disordered structure as predicted by ANCHOR2 and IUPred2, programs designed to predicted intrinsically disordered regions (IDRs) of proteins (Erdős and Dosztányi, 2020, Mészáros et al., 2018). As such, AlphaFold predictions of SDE1 produce structures with very low confidence scores, and predicting the structure of SDE1 in complex with CsRD21a does not enhance this confidence. Additionally, my attempts to purify SDE1 for further structural and functional analyses were unsuccessful. I enriched His-tagged SDE1 from *E. coli* using immobilized metal affinity chromatography, but separation of SDE1 from the 3C protease-removed His tag was unsuccessful, as SDE1 by itself appears to bind the nickel column. Further, in a trial experiment, I was able to enrich tag-free SDE1 from *E. coli* lysates using anti-His nickel beads, suggesting that SDE1 alone can bind nickel. Indeed, IonCom, a metal ion binding residue prediction website predicts numerous metal ion-binding sites throughout the protein (Hu et al., 2016). Intriguingly, metal ions have been shown to inhibit PLCP activities (Novinec et al., 2022). Therefore, it would be interesting to investigate the role of metal ions in SDE1 inhibition of PLCPs.

Together, the findings in this chapter shed light into the mechanisms of citrus-CLas co-evolution and present exciting new questions and engineering opportunities in the citrus HLB pathosystem. Consequently, now that a conserved bacterial substrate of a plant PLCP has been identified, questions arise regarding the distribution of OMPs in plant pathogens and the extent of OMP targeting by other classes of host proteases. As such, the following chapters will elucidate these concepts.

Chapter 3: Two Citrus Serine Carboxypeptidases Target CLasOMP1

Introduction

In the previous chapter, it was demonstrated that CsRD21a, a citrus PLCP, cleaves an outer membrane protein from CLas and contributes to tolerance against HLB. Yet, PLCPs are not the only class of proteases that respond to CLas infection. Indeed, several classes of proteases are induced in the phloem sap of CLas-infected trees compared to healthy trees (Franco et al., 2020). A total of 22 serine proteases were identified in citrus phloem sap, twelve of which exhibit significant differences in abundance between the healthy and infected samples. The largest class of these differentially accumulating serine proteases belongs to the S10 serine carboxypeptidase (SCP) family, of which seven were induced and one was repressed. Using ABPP, Franco et al. found that CLas infection both induces and represses the activity of serine proteases of various molecular weights. These findings suggest that both the abundance and activity of serine proteases are dynamically regulated during HLB infection.

SCPs, as the name indicates, cleave and release C-terminal amino acids from their substrates (Breddam, 1986). It has been postulated that this may be due to a dead-end substrate binding pocket that can only accommodate one amino acid at a time. However, not all SCP-like (SCPL) proteins exhibit protease activity. Indeed, many SCPL proteins have acyltransferase activity despite carrying a carboxypeptidase alpha-beta hydrolase fold and serine-histidine-aspartic acid catalytic triad characteristic of SCPs (Milkowski and Strack, 2004, Mugford and Milkowski, 2012). Clustering analyses have revealed that SCPL acyltransferases form a distinct clade (Clade I) separate from carboxypeptidases (Clade II) (Mugford et al., 2009, Fraser et al., 2005). SCPL carboxypeptidases and acyltransferases can be further distinguished via a pentapeptide sequence at their catalytic serine (Stehle et al., 2009). This pentapeptide sequence is GESYA in the carboxypeptidases, while it is GDSYS in SCPL acyltransferases.

Many SCPLs are processed into functional heterodimers *in planta.* Processing of SCPLs in *N. benthamiana* into large and small subunits appears to be correlated with the length of the linker peptide located between the two subunits (Zheng et al., 2024). BRS1, a clade II SCPL from *A. thaliana*, is processed into a functional heterodimer *in*

planta and exhibits carboxypeptidase activity against synthetic dipeptides *in vitro* (Zhou and Li, 2005).) BRS1 regulates brassinosteroid signaling mediated by the RLK BRI1, as well as both abiotic and biotic stress responses (Li et al., 2001, Zhang et al., 2021). Similarly, SCPL1 in oat is processed *in planta* but instead functions as an acyltransferase in the synthesis of acylated antimicrobial compounds (Mugford et al., 2009).

Overall, few SCPL proteins have been functionally characterized in plant immunity. In one example, overexpression of a rice SCPL protein, OsBISCPL1, in *A. thaliana* results in defense and oxidative stress-related gene induction, enhanced immunity to *P. syringae* and *Alternaria brassicicola*, and oxidative stress tolerance (Liu et al., 2008). OsBISCPL1 is induced by incompatible interaction with *Magnaporthe grisea*, SA, jasmonic acid, and a precursor of the ethylene pathway, and therefore plays a very dynamic role in both development and immunity. Intriguingly, SCPLs may function in the vasculature of plants. CP, a proteolytically processed, wound-inducible SCP from tomato, localizes to both mesophyll and vascular parenchyma vacuoles (Moura et al., 2001, Mehta et al., 1996). Meanwhile, the wheat SCP CPIII is expressed highly in vascular cells undergoing germination-associated programmed cell death (Domínguez et al., 2002). However, substrates of any SCPs *in vivo* remain elusive, making it difficult to understand how these proteases specifically regulate developmental and stress biology.

Given the specific induction of SCPLs in HLB-infected citrus, I was intrigued to determine if they, like PLCPs, target bacterial proteins to contribute to defense. As such, this chapter aims to elucidate the functions of two SCPLs in immunity against CLas.

Results

CSPs 10909 and 8175 Interact with OMP1 Homologs in *Liberibacter*

In a yeast-two-hybrid screening conducted by Dr. Simon Schwizer, five S10 family SCPLs and one S28 family (a lysosomal carboxypeptidase) identified in citrus phloem sap were tested for protein-protein interaction against an incomplete library of eleven putative secreted proteins from CLas (data not shown). The CLas proteins were predicted to have a signal peptide and were cloned into the bait vector (pGBKT7) without their signal peptides. Similarly, the serine proteases were cloned into the prey vector (pGADT7) without their N-terminal signal peptides. From this screening, two S10 family SCPLs, orange1.1g010909m and Ciclev10008175m, hereafter referred to as citrus serine proteases (CSPs) 10909 and 8175, respectively, were found to interact with CLasOMP1 (Figure 3.1A). Using the same CLasOMP1 truncations in the pGBKT7 bait vector that were used in Chapter 2, I identified that both CSPs 10909 and 8175 interact with the N-terminus of CLasOMP1 in a similar fashion as CsRD21a (Figure 3.1B,C). Specifically, truncations P1 and P2 individually interacted with both CSPs, and each N-terminal truncation also interacted with both CSPs, except for truncation 4. In this way, both CSPs tested interact with CLasOMP1 in almost an identical fashion as CsRD21a. This suggests that CSPs may also target a cell surface-exposed, extracellular loop of CLasOMP1 *in vivo*.

To investigate OMP1-CSP dynamics further, I sought to test if CSPs could target Liberibacter OMP1 homologs using yeast-two-hybrid. Indeed, both CSPs interact with CLaf, CLso, CLam, and Lcr OMP1 homologs (Figure 3.1D). These findings further suggest that OMP1 proteins are targeted by at least two distinct families of host proteases. Further, S10 SCPLs comprise a large protein family in citrus, and CSPs 10909 and 8175 cluster separately within the family (Figure 3.2). Additionally, at least three S10 SCPLs tested do not interact with CLasOMP1 in yeast (data from Dr. Schwizer not shown), and these are scattered throughout the phylogeny (Figure 3.2). This suggests that CLasOMP1 targeting is unique to certain CSPs in a clade-independent manner, but it should be noted that identification of protease substrates via yeast-two-hybrid may be complicated due to the inherent instability of their protein complexes. The finding that CLasOMP1 interacts with CSPs may be confirmed by *in vitro* pulldown or

co-immunoprecipitation in the future. This may be best performed with CSP catalytic mutants which may perform a more stable complex with CLasOMP1.

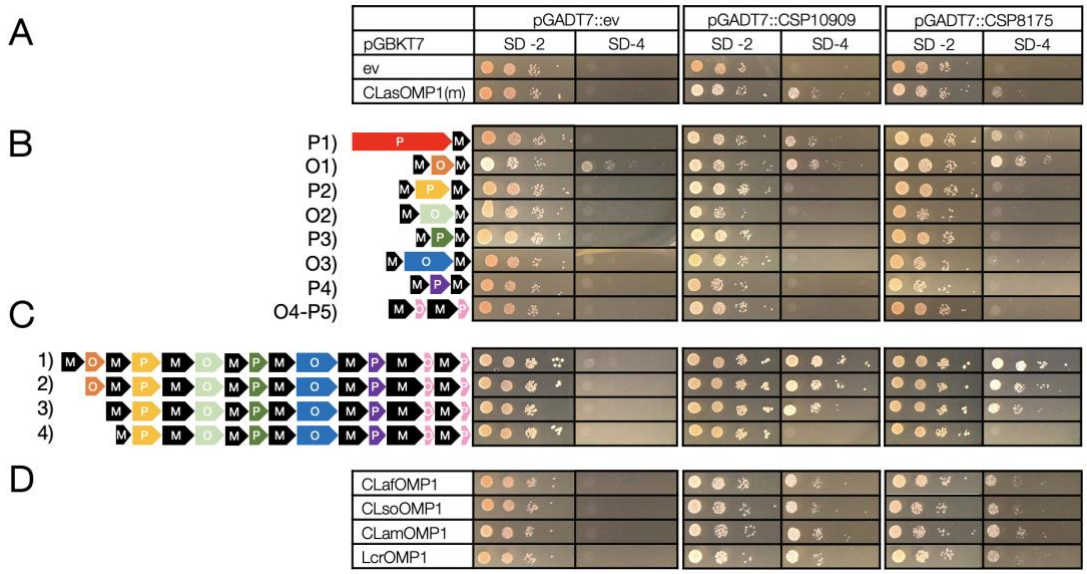

Figure 3.1. CSPs 10909 and 8175 interact with the N-terminus of CLasOMP1 and OMP1 homologs. CSPs 10909 and 8175 in the prey vector (pGADT7) were screened against (A) CLasOMP1, (B,C) CLasOMP1 truncations, and (D) OMP1 homologs in the bait vector (pGBKT7) with empty vector negative controls. SD-2 medium lacks leucine and tryptophan and was used to select the co-transformed colonies. One colony was serially diluted and plated for each co-transformation in yeast on both SD-2 and the selective SD-4, which lacks leucine, tryptophan, adenine, and histidine. Growth on SD-4 indicates interaction of the proteins in the prey and bait vectors.

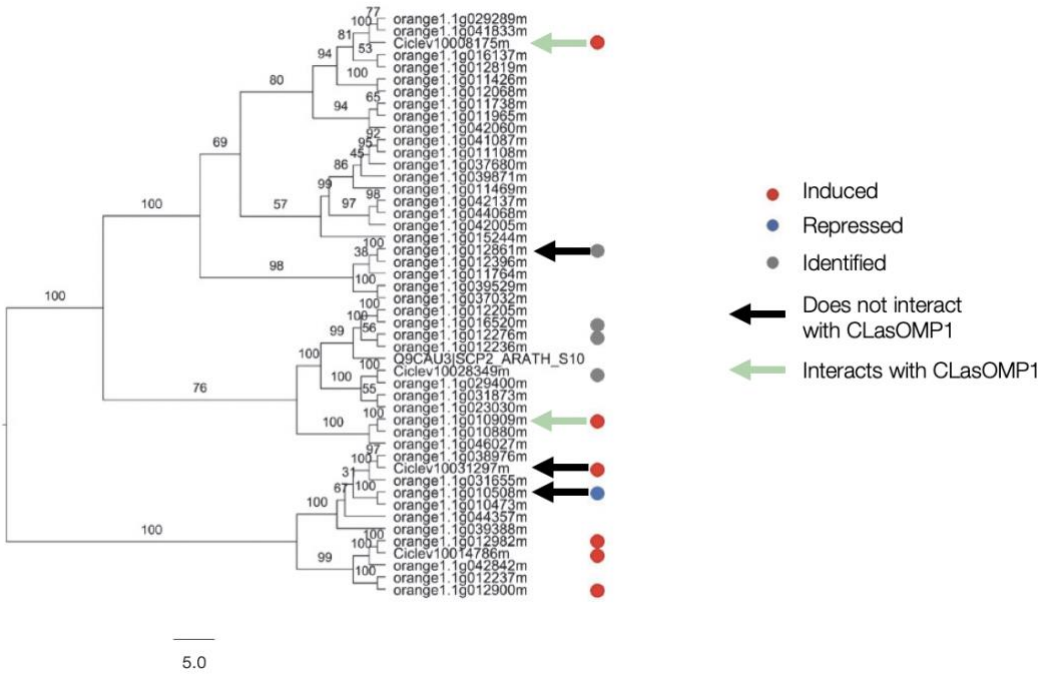

Figure 3.2. CSPs 10909 and 8175 are induced in HLB-infected citrus phloem and specifically interact with CLasOMP1. This phylogeny represents the S10 SCPL family in citrus and was adapted from Franco et al. (2020). SCPLs that were identified or significantly induced or repressed during HLB infection are indicated. The results of Dr. Simon Schwizer's initial yeast-two-hybrid screening are also indicated with arrows, where black and light green arrows indicate no interaction or interaction with CLasOMP1, respectively.

An Open Question: Do CSPs 10909 and 8175 cleave CLasOMP1?

While two CSPs interact with CLasOMP1 in yeast, whether CLasOMP1 is a substrate of these proteases remains unknown. While I troubleshooted techniques to observe degradation of CLasOMP1 by these proteins using a range of C-terminally tagged CSP constructs (HA, GFP, and His), no consistent results were obtained. This included adapting the proteolytic assay in Figure 2.4 or transiently co-expressing CSPs with CLasOMP1 in *N. benthamiana*. Using the ActivX Desthiobiotin-FP serine hydrolase ABPP probe, active CSP was difficult to decouple from background serine hydrolase levels. This suggests that CSPs may not be active upon heterologous expression in *N. benthamiana.* It is possible that C-terminally tagging CSPs affects the proper formation of an active enzyme *in planta*. Therefore, it should not be ruled out that CSPs may cleave CLasOMP1, but further optimization of the proteolytic assay would be required to make such a conclusion.

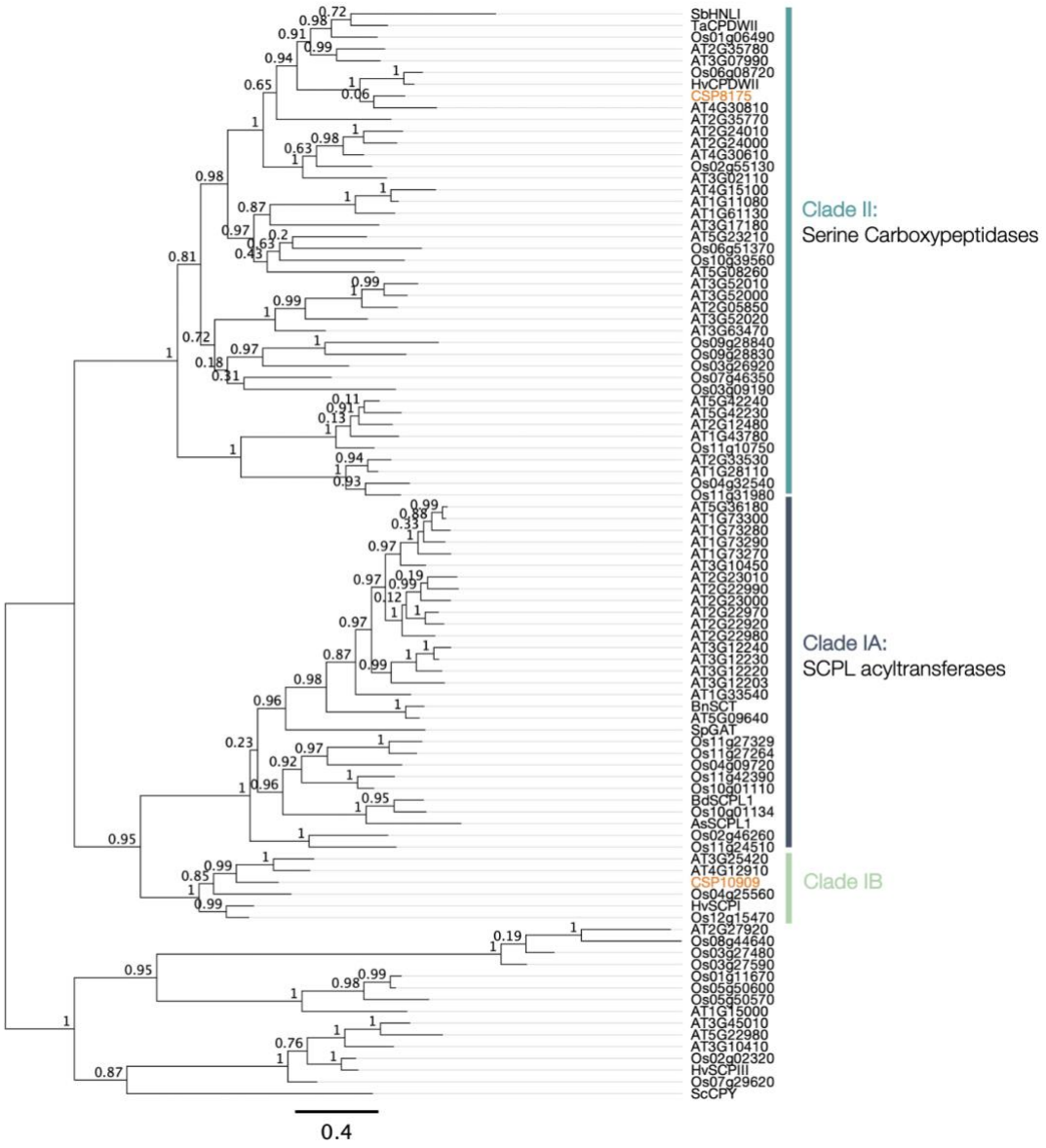

Figure 3.3. CSPs 10909 and 8175 do not cluster with SCPL acyltransferases. 91 SCPL amino acid sequences were sourced from Mugford et al. (2009) and were then used to generate a MAFFT v7.490 (Katoh and Standley, 2013) sequence alignment with CSPs 10909 and 8175 using Geneious Prime. This alignment was then used to cluster the SCPLs using FastTree v2.1.11 (Price et al., 2010, Price et al., 2009). Clusters were labeled as done previously, and the tree was rooted on the uncharacterized SCPL clade (Fraser et al., 2005, Mugford et al., 2009). CSPs 10909 and 8175 are highlighted in orange text. FastTree support values are indicated at each node. Tree visualized using Geneious Prime.

CSPs 10909 and 8175 are likely not Acyltransferases

That CSPs 10909 and 8175 cluster separately in the citrus SCPL phylogeny suggests that one or both enzymes may be acyltransferases and not carboxypeptidases.

This could account for a lack of observed proteolytic cleavage. By appending a dataset of 91 SCPLs generated by Mugford et al. (2009) with the two CSP sequences, I sought to determine if these proteins cluster with acyltransferases or carboxypeptidases. Like the Figure 3.2 phylogeny, CSPs 10909 and 8175 cluster separately from one another among SCPLs from *A. thaliana*, *Brassica napus,* wild tomato, barley, and oat (Figure 3.3). CSP8175 appears as a clade II carboxypeptidase while CSP10909 is a clade IB SCPL, which is distinct from known acyltransferases in clade IA. Therefore, it is plausible that both CSPs analyzed are indeed carboxypeptidases and not acyltransferases.

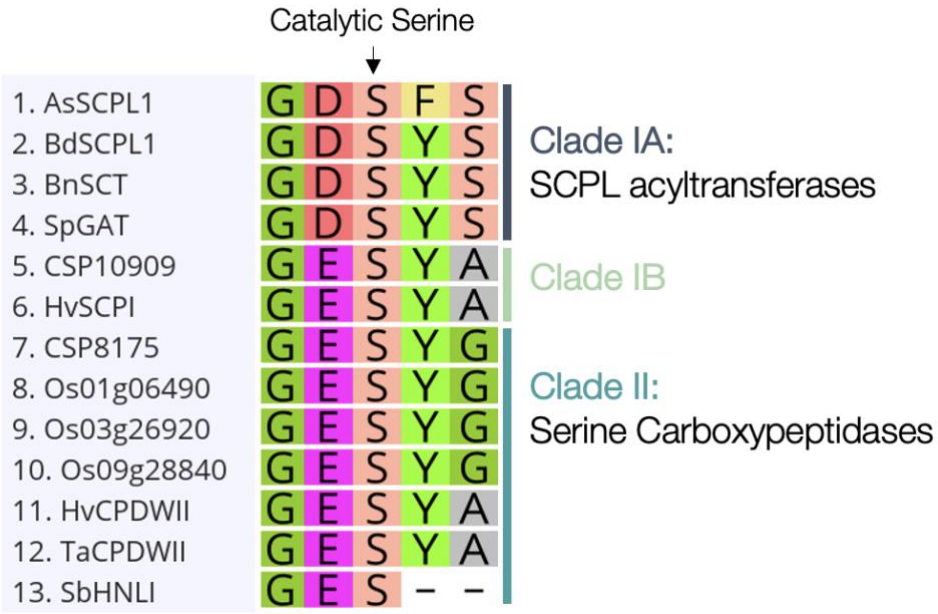

Figure 3.4. CSPs 10909 and 8175 do not contain the SCPL acyltransferase catalytic serine motif. MAFFT v7.490 (Katoh and Standley, 2013) amino acid sequence alignment of the catalytic serine pentapeptide from CSPs 10909 and 8175 with representative SCPLs from clades IA, IB, and II from Mugford et al. (2009).

As SCPL acyltransferases and carboxypeptidases encode unique active serine pentapeptide motifs, I looked specifically at these motifs in CSPs 10909 and 8175. In support of CSP10909 clustering with carboxypeptidases, CSP10909 encodes the characteristic carboxypeptidases GESYA pentapeptide (Figure 3.4). Intriguingly, CSP8175 encodes a unique GESYG pentapeptide sequence found in only three other clade II SCPLs from rice. Yet, these GESYG motif-containing SCPLs are scattered throughout clade II, suggesting that they too have carboxypeptidase activity. Together, phylogenetic and sequence analyses suggest that CSPs 10909 and 8175 are both carboxypeptidases and not acyltransferases.

CSP 10909 and 8175 Expression in Transgenic Arabidopsis Induces Stunting but does not Contribute to Defense Against *P. syringae*

To further investigate CSP functions, stable transgenic lines of CSPs 10909- and 8175-expressing *A. thaliana* were generated by Dr. Morgan Halane under the constitutive Ca35s promoter. In homozygous T3 lines, the CSPs, particularly 10909, exhibited processing *in planta*, as evidenced by extensive banding patterns below their expected molecular weights (Figs. 3.5A, 3.6A). Further, in three independent CSP10909 lines and two independent CSP8175 lines, overexpression of these proteins appeared to induce stunting in some, but not all, seedlings (Figs. 3.5B, 3.6B). It is tempting to suggest that this is due to higher levels of expression in the stunted plants, but this is difficult to ascertain due to variable levels of protein run on the Western blot as demonstrated by Ponceau staining (Figs. 3.5A, 3.6A). Given that stunting in plants can be the result of autoimmune defects, I set to determine if these plants were more resistant to *P. syringae* DC3000. Yet, no significant effects were observed in bacterial growth between the wildtype Col-0 and the CSP transgenic plants in two individual experiments (data not shown).

To determine whether the observed stunting phenotype in CSP transgenic plants requires their enzymatic activity, I generated transgenic *A. thaliana* lines overexpressing CSP catalytic mutants. InterProScan (Jones et al., 2014) predicts the catalytic serine and histidine residues but does not identify the catalytic aspartic acid. Therefore, the catalytic mutants were generated by replacing the serine and histidine, but not the aspartic acid, residues with alanine. However, despite confirming the expression of T2 transgenic lines, I have not yet screened the T3 plants for homozygous lines or stunting phenotypes.

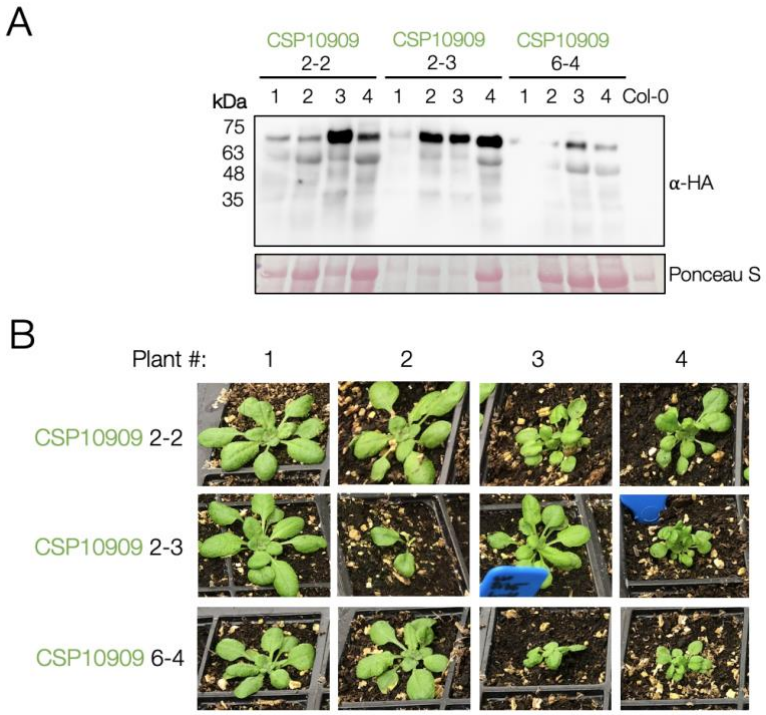

Figure 3.5. CSP10909 is proteolytically processed and induces stunting in *A. thaliana*. A) Western blot depicting CSP10909 expression using an anti-HA antibody in three T3 transgenic *A. thaliana* lines. Numbers 1-4 correspond to individual plants which are shown in (B). Ponceau staining was used as a loading control. B) Photos of individual transgenic lines used for Western blot analysis in (A).

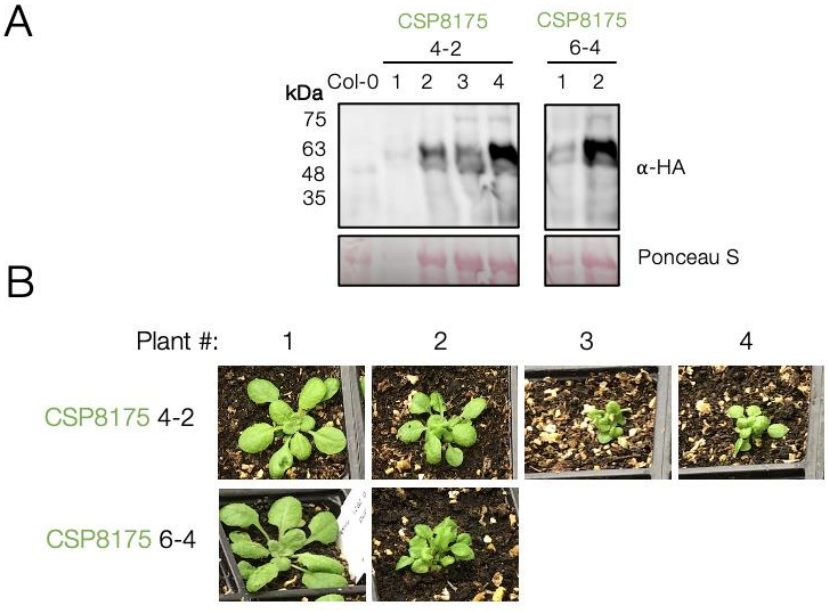

Figure 3.6. CSP8175 induces stunting in *A. thaliana*. A) Western blot depicting CSP8175 expression using an anti-HA antibody in two T3 transgenic *A. thaliana* lines. Numbers 1-4 correspond to individual plants which are shown in (B). Ponceau staining was used as a loading control. B) Photos of individual transgenic lines used for Western blot analysis in (A).

Structural Predictions of CSPs Reveal Potential Processing Dynamics

As previously indicated, CSPs appear to undergo proteolytic processing in transgenic *A. thaliana* plants. While they seem to run higher on the gel than expected in relation to the protein ladder, the HA-tagged CSPs 10909 and 8175 full-length bands are apparent in the Western blot (61.8 and 59.5 kDa, respectively) as well as their mature, secreted sizes (58.9 and 56.6 kDa, respectively) (Figure 3.5A,3.6A). However, distinct, smaller bands appeared for CSP10909 below 48 kDa. Meanwhile, there appears to be smeared bands below 48 kDa for CSP8175. This suggests that these proteins are processed *in planta,* similar to published SCPLs. Given that the CSPs are C-terminally tagged with 3xHA, this processing likely occurs from the N-terminus, after the N-terminal signal peptide.

To further understand the processing of CSPs *in planta*, I further analyzed their domain structures using InterProScan (Jones et al., 2014). This revealed the presence of 43- and 24- residue linker regions following alpha/beta hydrolase domains in both CSPs 10909 and 8175, respectively (Figs. 3.7A, 3.8A). Removal of this linker would produce 16.2 and 17.5 kDa small C-terminal subunits, respectively, but protein products at these molecular weights were not analyzed in the transgenic lines. While the alpha/beta hydrolase domains contain the predicted active serine residues, the predicted histidine active sites are positioned in C-terminal subunits positioned after the linkers (Figs. 3.7A, 3.8A).

The processed nature of the CSPs *in planta* begged the question of how the subunits may come together to form an active enzyme. To gain structural insights into CSP processing, I first generated AlphaFold3 structural models for the mature CSPs. Both CSP models produced highly confident structures (Figure 3.7B, 3.8B). However, the CSP10909 catalytic pocket was buried in the protein, while the catalytic pocket was exposed in the CSP8175 model. To determine if the CSP10909 linker region needs to be removed to expose its active site, I removed the linker from its amino acid sequence, producing two separate subunits. These two subunits were then modeled by AlphaFold3 multimer to observe them in complex, and the resulting model was also predicted with high confidence (Figure 3.7C). Further, this complex clearly exposes the active site pocket and therefore provides structural insight into how removal of the linker region may contribute to its activation *in planta*. Meanwhile, removal of the linker region of CSP8175 also resulted in a confidently predicted AlphaFold3 model which retained the exposed catalytic site, suggesting that this protease may be active regardless of linker

removal *in planta* (Figure 3.8C). Zheng et al. (2024) reported previously that linker regions between 4 and 15 residues are not cleaved in *N. benthamiana* SCPLs, whereas longer linker regions between 32 and 65 are cleaved. The structural predictions of CSPs 10909 and 8175 are consistent with their findings, where the longer linker region of CSP10909, but not the shorter linker region of CSP8175, appears to block the catalytic pocket and needs to be removed for enzymatic activation. This may also account for the more apparent processing of CSP10909 compared to CSP8175 via Western blot (Figs. 3.5A,3.6A).

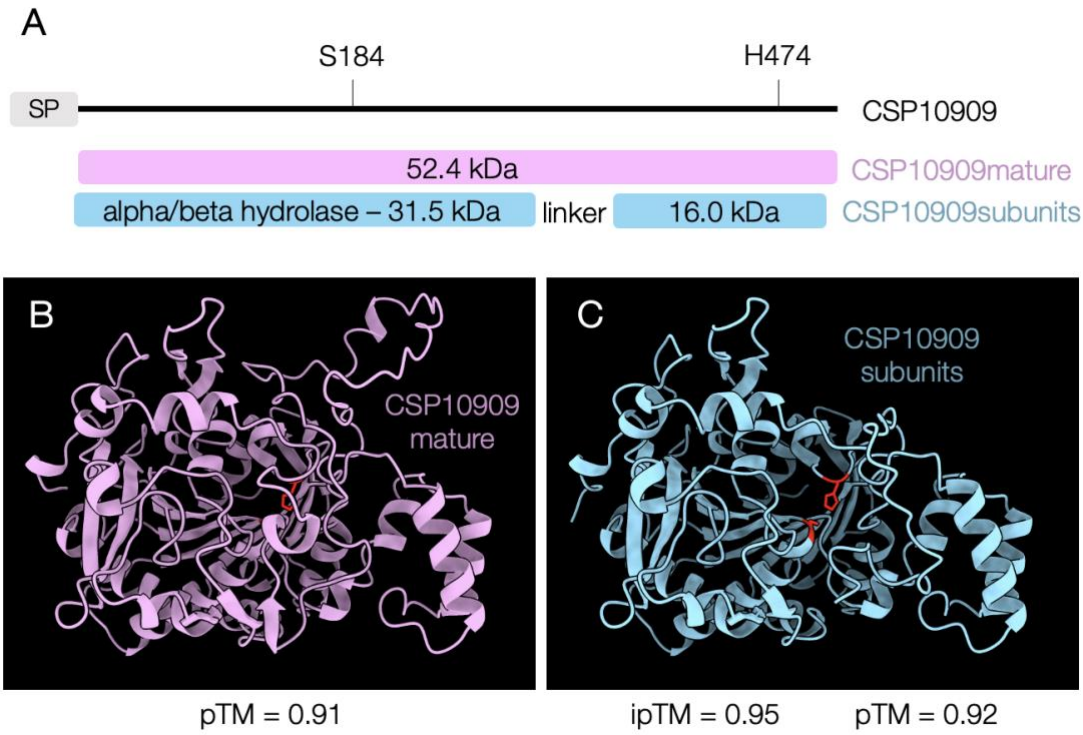

Figure 3.7. Structural and sequence analyses of CSP10909. A) The domain structure of CSP10909 was determined by InterProScan (Jones et al., 2014). The mature protein and processed subunits used for AlphaFold3 prediction are shown. B+C) Models of the mature and subunits, respectively, of CSP10909 as predicted by AlphaFold3 (Abramson et al., 2024).

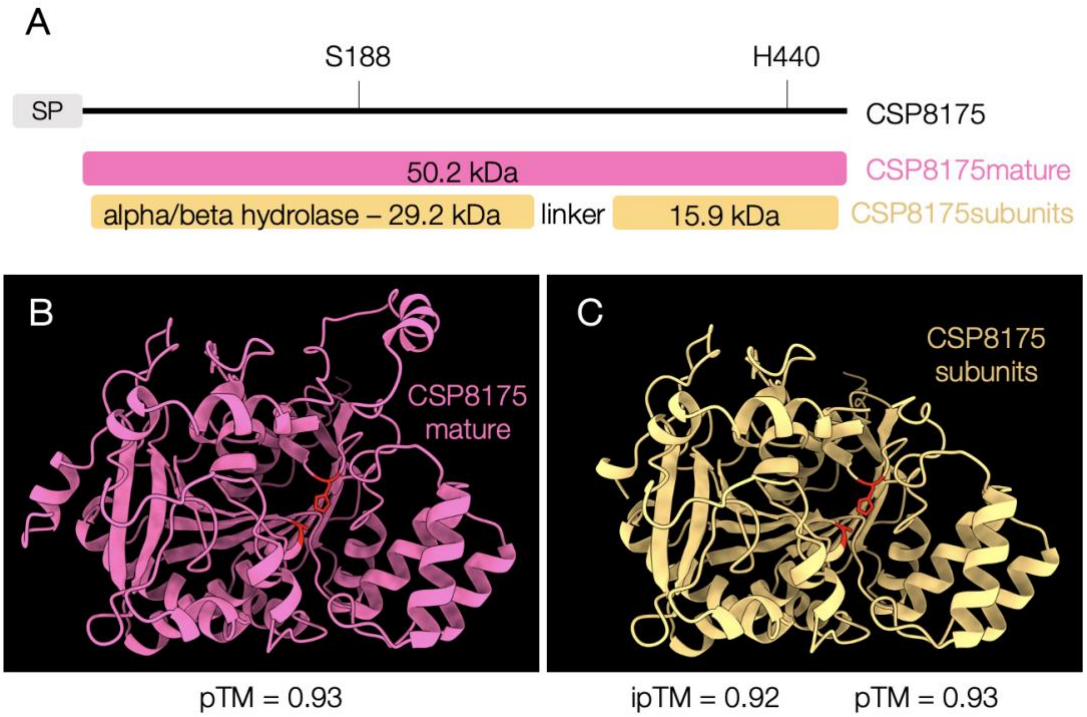

Figure 3.8. Structural and sequence analyses of CSP8175. A) The domain structure of CSP8175 was determined by InterProScan (Jones et al., 2014). The mature protein and processed subunits used for AlphaFold3 prediction are shown. B+C) Models of the mature and subunits, respectively, of CSP8175 as predicted by AlphaFold3 (Abramson et al., 2024).

Conclusions and Discussion

CLasOMP1 interacts with proteases from two distinct families in citrus: PLCPs and SCPLs. While I have uncovered much of the dynamics between CLasOMP1 and the PLCP CsRD21a in Chapter 2, the role of SCPLs in citrus HLB remains elusive. Yet, that two SCPLs, referred to as CSPs 10909 and 8175, interact with CLasOMP1 suggests that multiple families of proteases in citrus individually target CLasOMP1, further implicating it as an important player of CLas virulence. Remarkably, CSPs 10909 and 8175 appear to interact with the same region of CLasOMP1 as CsRD21a, highlighting the potential importance of this region as a target of host defense.

Unlike CsRD21a, I was unable to determine that CSPs 10909 and 8175 cleave CLasOMP1. This may be, in part, due to the nature of carboxypeptidase cleavage, where single amino acids removed from the CLasOMP1 C-terminus may not result in enough of a shift in molecular weight to detect via Western blot. Alternatively, the CSPs may not directly cleave the C-terminus of CLasOMP1. Instead, they may cleave neo-C-termini that are produced by other proteases, such as CsRD21a. In chapter 2, I used the CLasOMP1-specific antibody ab1 to identify a ~14 kDa CsRD21a-generated cleavage product that was detected both in the semi-*in vitro* assay and in CLas-infected grapefruit and lemon tissue (Figure 2.5D). Yet, smaller bands at ~12 and ~10 kDa were also present in the infected grapefruit samples but not the lemon or semi-*in vitro* samples. This suggests that CLasOMP1 may be processed *in planta* by proteases other than CsRD21a, and these may include CSPs 10909 and 8175.

Sequence and phylogenetic analyses in this chapter suggest that CSPs 10909 and 8175 are carboxypeptidases and not acyltransferases. However, the majority of the SCPLs in Figure 3.3 have not been functionally characterized and therefore this analysis should be considered as correlation. While CSP10909 encodes the typical carboxypeptidase pentapeptide motif (GESYA), CSP8175 encodes an atypical (GESYG) motif that has not yet been characterized to my knowledge. Therefore, acyltransferase activity should not be completely ruled out. As such, acyltransferases have been found to regulate plant immunity. For example, the Arabidopsis RLK P2K1 phosphorylates and activates membrane-associated acyltransferases PAT5 and PAT9, which in turn acylate P2K1 to restrict its PTI activation (Chen et al., 2021). Similarly, the RLKs EFR and FLS2 are acylated upon PAMP perception, which positively regulates their immune functions (Hurst et al., 2023). On the other hand, direct acylation of a non-

secreted peptide called ROT4 in Arabidopsis enhances immunity via blocking interaction between the cytoplasmic kinase BSK5 and the receptor kinase PEPR1 (Li et al., 2024). Therefore, acylation can both negatively and positively regulate immunity by direct modification of immune receptors or peptides. One could therefore imagine a scenario in which a putative CLasOMP1-derived PAMP is acylated by SCPLs to activate defense. However, acylation by CSPs 10909 and 8175 has not yet been explored.

Key to our understanding of PLCPs as important nodes of defense in citrus was the finding that they are targeted and inhibited by the CLas effector SDE1. However, to date, no such effector has been identified from CLas that targets SCPLs such as CSPs 10909 and 8175. While the yeast two hybrid screening conducted by Dr. Simon Schwizer included secreted proteins that may have effector functions, this screen was not exhaustive. Therefore, we cannot conclude that there are not SCPL-inhibiting effectors. Further, we do not have CSP 10909 or 8175 overexpression or knockout transgenic lines in citrus and therefore cannot conclude that they have defense functions against CLas. While the CSP-overexpressing *A. thaliana* plants exhibited stunting, this phenotype does not appear to be autoimmune as the plants are not more tolerant against the bacterial pathogen *P. syringae.* However, to conclude that the phenotype is not autoimmune, transcript levels of PR1 between the transgenic and wildtype plants should be assessed.

Together, the findings in this chapter further suggest that cell surface-exposed OMPs may be common targets of host proteases, including PLCPs and SCPLs, yet the roles of SCPLs at the host-pathogen interface in citrus HLB remain elusive and the data presented here should be considered preliminary.

Chapter 4: Identifying Pathogen Inhibitors and Substrates of Plant Proteases *In Silico*

Introduction

Proteases are at the forefront of plant defense and localize in infected tissues, including the apoplast and xylem (Godson and van der Hoorn, 2021). The top 10 bacterial plant pathogens, as determined by votes from bacterial pathologists, were all Gram-negative bacteria that infect the apoplast and/or xylem (Mansfield et al., 2012) and presumably encode numerous OMPs. The previous chapters have demonstrated that at least two classes of citrus proteases target CLasOMP1. Specifically, CsRD21a contributes to defense against CLas, and CLasOMP1 is cleaved in HLB-infected citrus. However, whether proteases broadly target pathogen OMPs is an open question. In one example, a human serine protease cleaves EcOmpA as an antimicrobial strategy, suggesting OMP targeting may be a conserved defense mechanism across domains of life (Belaaouaj, 2002, Belaaouaj et al., 1998, Belaaouaj et al., 2000). If bacterial OMPs are indeed common targets of both animal and plant proteases as a defense strategy, then a comprehensive analysis of OMPs is necessary. As such, the first half of this chapter will focus on curating an OMP dataset to characterize and understand the evolution of OMPs across Gram-negative bacteria, including pathogens of animals and plants.

Whether targeting of OMPs is common in other pathosystems needs to be further dissected. Yet, we do know that many pathogens encode protease-inhibiting effector proteins (Godson and van der Hoorn, 2021, Wang et al., 2020, Wang et al., 2022, Clark et al., 2018, Clark, 2019). This is likely an adaptation to suppress protease-mediated defense, representing an example of the host-pathogen arms race. Further, the results in this thesis suggest that proteases specifically are involved in defense against phloem-residing pathogens, suggesting that engineering proteases in crops may be a successful approach to combatting these pathogens in the field. Computational methods provide a promising avenue for finding new protease inhibitors and engineering proteases to be resistant to pathogen inhibitors (Homma et al., 2023, Schuster et al., 2024, Kourelis et al., 2024). Using similar strategies, I hypothesized that we could identify novel phloem pathogen-derived protease inhibitors. As such, the second half of

this chapter will focus on computationally identifying these candidate inhibitors. Together, this chapter will demonstrate the power of computational and artificial intelligence-based approaches in identifying both protease substrates and inhibitors in the host-pathogen arms race.

Genus species strain (if specified)	Class (-proteobacteria)	Order
Agrobacterium tumefaciens *	Alpha	Hyphomicrobiales
Ca. Liberibacter africanus PTSAPSY	Alpha	Hyphomicrobiales
Ca. Liberibacter americanus SP	Alpha	Hyphomicrobiales
Ca. Liberibacter asiaticus psy62	Alpha	Hyphomicrobiales
Ca. Liberibacter solanacearum ZC1	Alpha	Hyphomicrobiales
Liberibacter crescens BT-1	Alpha	Hyphomicrobiales
Sinorhizobium meliloti	Alpha	Hyphomicrobiales
Ralstonia solanacearum *	Beta	Burkholderiales
Dickeya dadantii 3937 *	Gamma	Enterobacterales
Erwinia amylovora CFBP1430 *	Gamma	Enterobacterales
Escherichia coli K12	Gamma	Enterobacterales
Pectobacterium carotovorum carotovorum *	Gamma	Enterobacterales
Salmonella enterica LT2	Gamma	Enterobacterales
Xanthomonas axonopodis vasculorum *	Gamma	Lysobacterales
Xanthomonas campestris campestris *	Gamma	Lysobacterales
Xanthomonas citri citri	Gamma	Lysobacterales
Xanthomonas oryzae oryzae *	Gamma	Lysobacterales
Xylella fastidiosa Temecula *	Gamma	Lysobacterales
Pseudomonas aeruginosa PAO1	Gamma	Pseudomonadales
Pseudomonas syringae DC3000 *	Gamma	Pseudomonadales

Table 4.1. Bacterial proteomes included in the OMP analysis. Classification information courtesy of NCBI. Asterisks (*) represent pathogens included in the top 10 bacterial pathogens list (Mansfield et al., 2012).

Results

OMPs are Widespread in Gram-negative Bacterial Pathogens

A comprehensive analysis of OMPs in plant pathogens is lacking. To identify putative OMP substrates of plant proteases, I applied the HMM-based pipeline used to identify OMPs in Chapter 2 in Liberibacter to the list of top 10 bacterial plant pathogens, with the addition of several notable human pathogens, including one mutualistic bacterium related to Liberibacter (*Sinorhizobium meliloti*), and the causal agent of citrus canker *Xanthomonas citri* (Table 4.1). Their proteomes were downloaded from NCBI (https://www.ncbi.nlm.nih.gov/). Of 69,739 proteins analyzed from these bacteria, 964 (1.38%) were identified by both hmmsearch (Potter et al., 2018) and DeepTMHMM (Hallgren et al., 2022) to be beta-barrel OMPs (Appendix Table 1). While proteome size differs among the analyzed bacteria (ranging from 962 to 5,967 proteins), the percentage of OMPs identified in each proteome also varies (ranging from 0.42 to 2.69%) (Table 4.2, Figure 4.1A). A MUSCLE amino acid sequence alignment of the 964 total OMPs was then used to generate a phylogenetic tree using FastTree v2.1.11 (Price et al., 2010, Price et al., 2009, Edgar, 2004). I then wrote a combination of bash and python scripts that counted the number of transmembrane beta strands from the DeepTMHMM topology output, and the number of beta strands for each OMP was appended to the tree using ggtree (Yu, 2020) (Figure 4.2). The most prevalent OMPs in this dataset had 22 beta strands and were largely clustered in the tree, nearly all of which are annotated as TonB-dependent receptors and were present in all species except Liberibacter spp. Many of the remaining OMPs are dispersed around the tree, reflecting the large sequence diversity within OMPs regardless of beta strand number.

Looking specifically at eight-stranded OMPs in this dataset may provide insight into the evolution of OMPs, including CLasOMP1 (discussed in Chapters 2 and 3), in Liberibacter. Sequence alignment and tree building of only 8-stranded OMPs from the data set revealed an OMP1 clade that contains proteins of each Rhizobiaceae bacterium tested (Liberibacter spp., *Sinorhizobium meliloti*, and *Agrobacterium tumefaciens*) (Figure 4.3). Just outside of the OMP1 clade are proteins from *Xanthomonas citri* and *Xanthomonas campestris*. Therefore, while OMP1 proteins appear to be Alphaproteobacteria/Hyphomicrobiales/Rhizobiaceae-specific, the proximity of these *Xanthomonas* OMPs to the OMP1 clade suggests that there may be OMP1-like proteins

in Gammaproteobacteria, too. The next closest clade contains CLas4900 (CLasOMP2) and CLas5150 (CLasOMP3) and their respective homologs in CLaf, CLso, and CLam. That these OMPs are not detected in Lcr, *S. meliloti*, or *A. tumefaciens* suggests that these may have evolved to have a specific role in the lifestyle of pathogenic *Ca.* Liberibacters.

	hmm search	Deep TMHMM	total proteins	OMPs (% of proteome)
Agrobacterium tumefaciens	42	39	4939	0.79%
Dickeya dadantii 3937	48	39	4209	0.93%
Erwinia amylovora CFBP1430	42	37	3272	1.13%
Escherichia coli K12	66	57	4298	1.33%
Ca. Liberibacter africanus PTSAPSY	9	5	1006	0.50%
Ca. Liberibacter americanus SP	8	6	962	0.62%
Ca. Liberibacter asiaticus psy62	6	6	1017	0.59%
Liberibacter crescens BT-1	9	8	1243	0.64%
Ca. Liberibacter solanacearum ZC1	7	6	1048	0.57%
Pectobacterium carotovorum carotovorum	61	55	4201	1.31%
Pseudomonas aeruginosa PAO1	108	97	5572	1.74%
Pseudomonas syringae DC3000	79	71	5418	1.31%
Ralstonia solanacearum	67	53	4670	1.13%
Salmonella enterica LT2	79	71	4548	1.56%
Sinorhizobium meliloti	34	25	5967	0.42%
Xanthomonas axonopodis vasculorum	78	70	3526	1.99%
Xanthomonas campestris campestris	114	109	4048	2.69%
Xanthomonas citri citri	126	112	4207	2.66%
Xanthomonas oryzae oryzae	72	68	3486	1.95%
Xylella fastidiosa Temecula	35	30	2102	1.43%
Total	1090	964	69739	1.38%

Table 4.2. Summary of OMPs predicted in each tested bacterium. The number of beta-barrel OMPs predicted by hmmsearch, the number of those proteins also predicted by DeepTMHMM, the total number of proteins in each proteome, and the percentage of total proteins that are predicted OMPs.

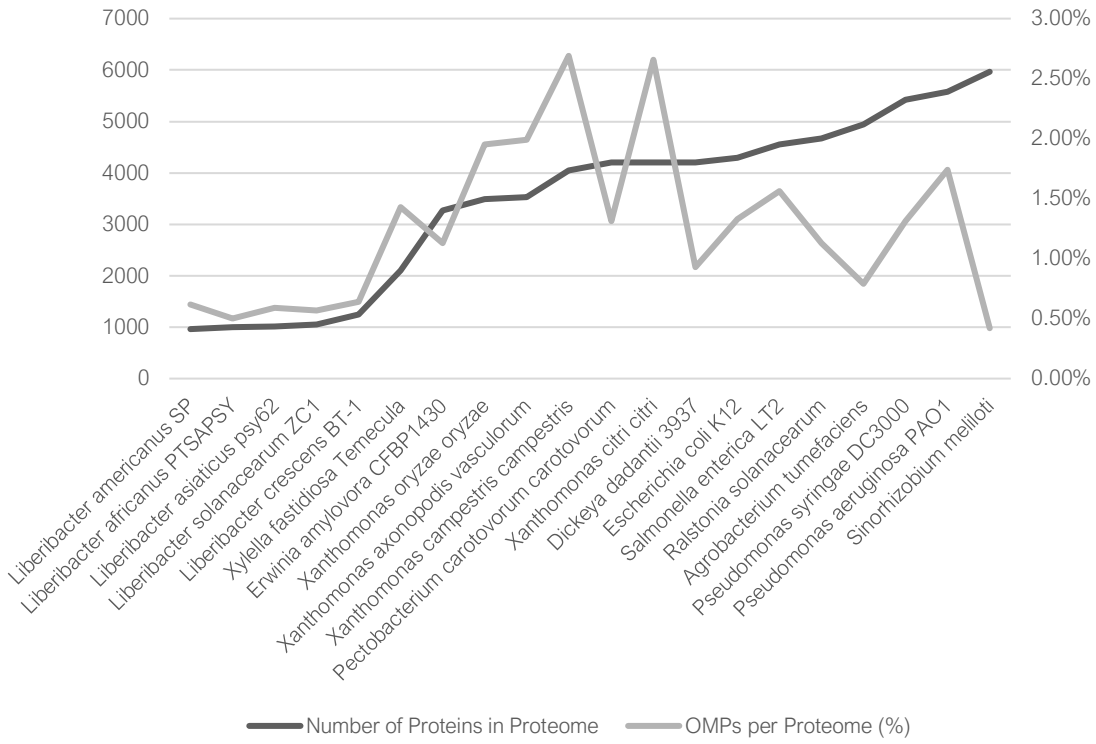

Figure 4.1. OMP profiling in using HMMs. Plotted are the total number of proteins present in each proteome analyzed (on the left y-axis) and the percentage of each proteome that encodes putative OMPs (on the right y-axis). Proteomes are ordered from smallest to largest (left to right).

OmpA Proteins Have Diverged and Exhibit Extracellular Loop Diversification

As previously demonstrated in Chapter 2, OMP1 extracellular loops have diversified, while their membrane bound beta sheets and periplasmic regions are more conserved (Figure 2.9C). It has been previously reported that ompC extracellular loops, but not membrane-bound beta sheets, are under positive selection across *Enterobacter aerogenes* strains, likely reflecting selective pressure applied by the adaptive immune system (Padhi et al., 2009). It was also reported that ompC in *Salmonella* spp. exhibits purifying selection in both exposed and membrane-bound regions, suggesting that OMPs may be subjected to varying selective pressures, perhaps reflecting different lifestyles, hosts, and/or abilities to suppress immunity. As such, analyzing other subfamilies of OMPs in this dataset may reveal similar selective pressures and demonstrate that both adaptive and innate immune systems drive the diversification of pathogen OMPs. Therefore, I sought to analyze the conservation and diversification of extracellular loops in another OMP family.

As previously discussed in Chapter 2, EcOmpA contains a C-terminal peptidoglycan-binding domain that is absent in OMP1 homologs (Figure 2.16), and EcOmpA is cleaved by papain and C14. Therefore, I decided to focus on this family of OMPs and find if they are prevalent in the plant pathogens analyzed in my OMP dataset. I found that OmpA proteins were identified among the extracted eight-stranded OMPs, but they are not ubiquitous among the analyzed bacteria. Two individual clades in Figure 4.3 contain proteins annotated as OmpA. The sequence alignment used to generate the tree in Figure 4.3 revealed that C-terminal domains were only found in the two OmpA clades, which is consistent with their annotations. One cluster consists of OmpA proteins identified in the each of the Lysobacterales and Pseudomonadales bacteria tested, while the other cluster consists solely of Enterobacterales OmpA proteins (Figure 4.3). Notably, these C-terminal domain-containing, eight-stranded beta barrel OMPs are present only in the analyzed Gammaproteobacteria and are absent in the Hyphomicrobiales and Burkholderiales order bacteria analyzed here, which represent the classes Alphaproteobacteria and Betaproteobacteria, respectively. Therefore, these proteins are seemingly not essential for bacterial phytopathogens.

To determine if extracellular loops have also diversified in OmpA proteins, I extracted the OmpA clusters and generated individual sequence alignments for them. Interestingly, the Enterobacterales OmpA cluster proteins are overall quite conserved at the amino acid level (72-93% sequence identity), yet three of their four extracellular loops appear to have undergone extensive diversification compared to the rest of the protein (Figure 4.4). On the other hand, sequence identity between the Lysobacterales and Pseudomonadales OmpA proteins was overall low (~30%). Therefore, I decided to generate a new alignment consisting only of the Lysobacterales OmpA proteins, and these proteins exhibited much higher conservation overall (93-99% amino acid sequence identity). Among these proteins, however, only one extracellular loop specifically appears to have diversified, while the remainder are more conserved (Figure 4.5). This demonstrates that the extracellular loops of OmpA proteins, like OMP1 proteins, are likely under selective pressure applied by both the adaptive and innate immune systems.

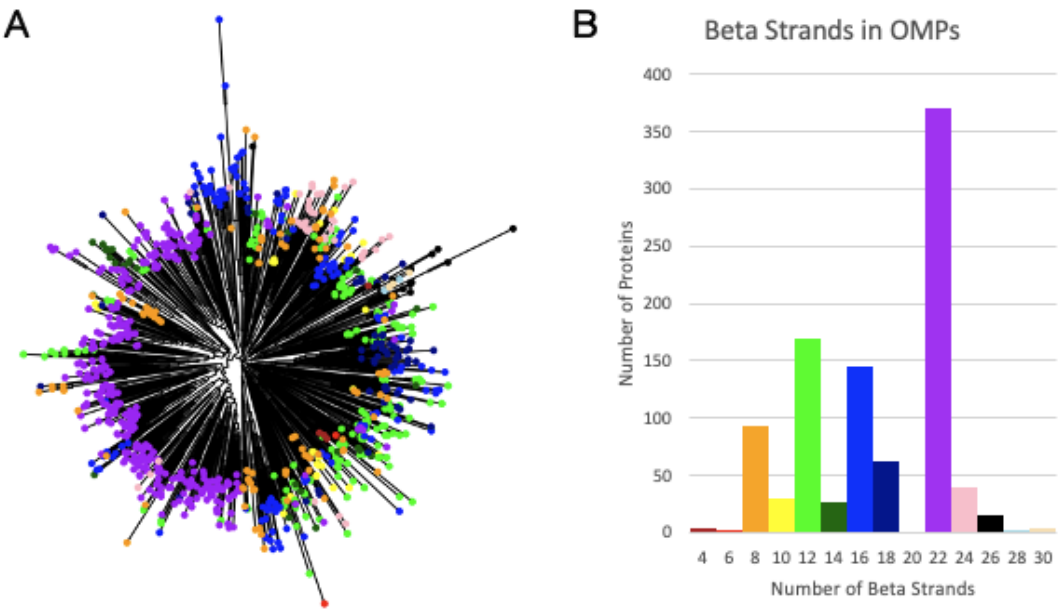

Figure 4.2. Overview of the number of beta strands predicted by DeepTMHMM in the OMP dataset. A) FastTree v2.1.11-generated phylogenetic tree of all HMM-predicted OMPs based on a MUSCLE amino acid sequence alignment (Price et al., 2010, Price et al., 2009, Edgar, 2004). Branch tips are colored by the number of beta strands predicted in the protein using ggtree (Yu, 2020), which are plotted in panel B.

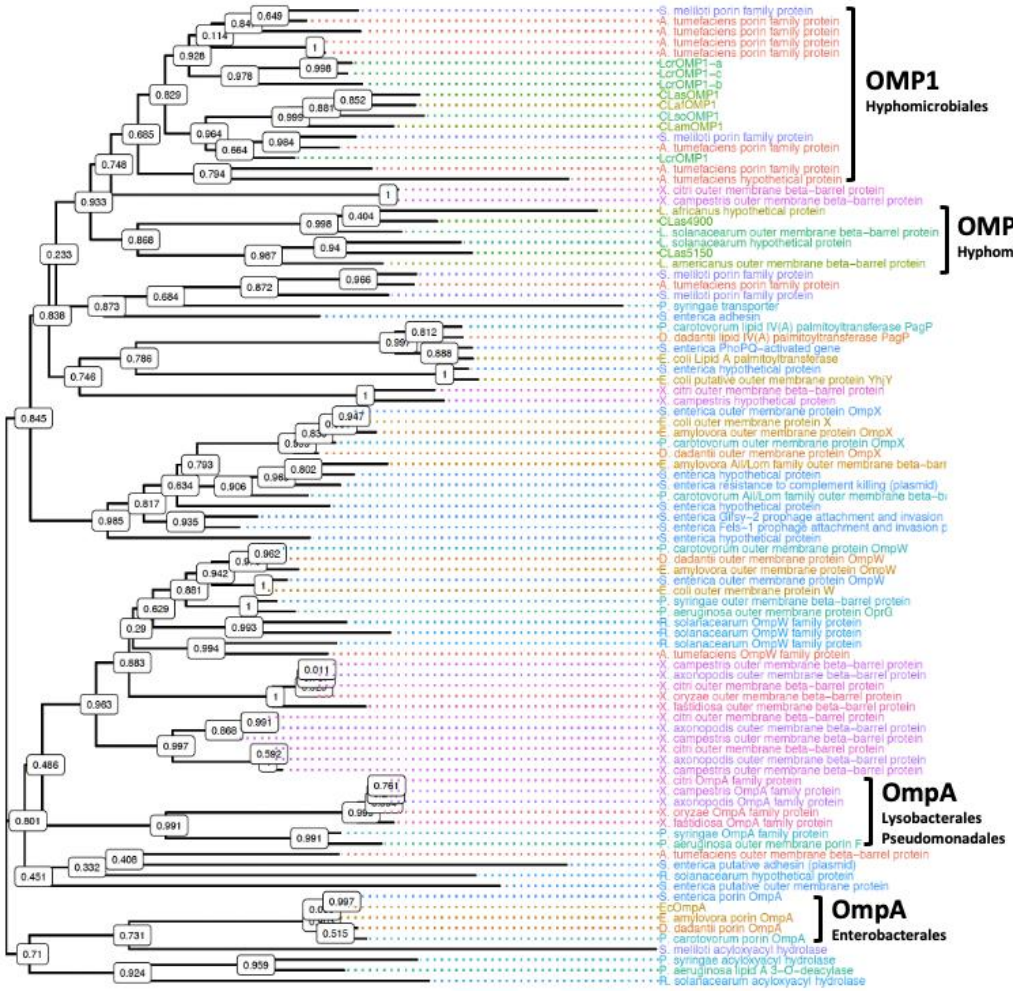

Figure 4.3. Phylogenetic tree of eight-stranded OMPs. Amino acid sequences from eight-stranded OMPs were used to generate a MUSCLE alignment, which was then used to generate a phylogenetic tree using a maximum likelihood model FastTree v2.1.11 (Price et al., 2010, Price et al., 2009, Edgar, 2004). The resulting tree was visualized using ggtree (Yu, 2020). FastTree support values are indicated at each node.

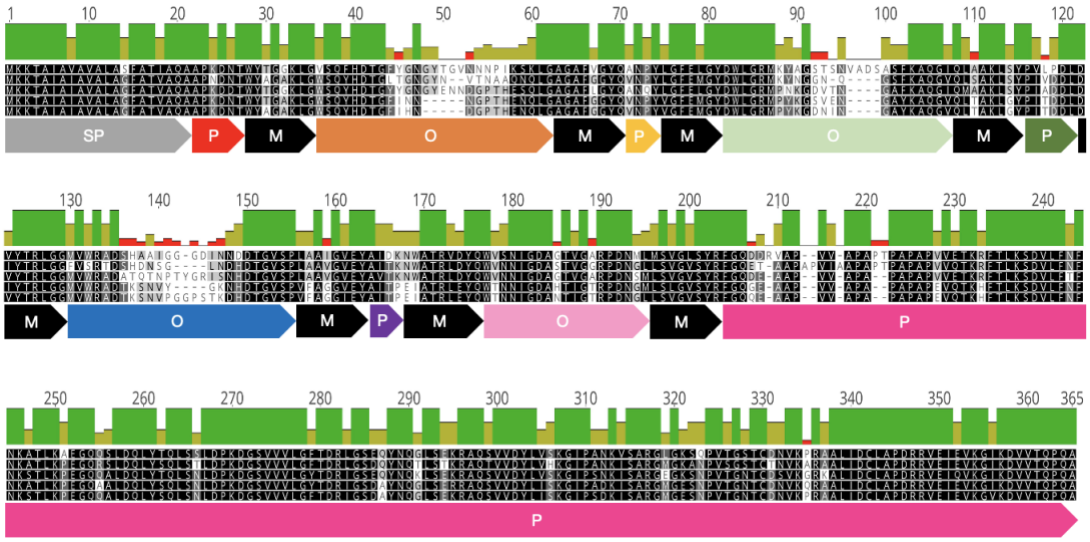

Figure 4.4. Sequence alignment of Enterobacterales OmpA proteins. A MAFFT v7.490 (Katoh and Standley, 2013) amino acid sequence alignment was generated using the Geneious software, and the OMP topology was predicted for EcOmpA using DeepTMHMM. Conservation of amino acids key: green = 100% conserved, green-brown = 30-99% conserved, red = 0-29% conserved. SP = signal peptide, P = periplasmic domain, M = membrane-bound beta sheet, O = extracellular (outside) loop. The OmpA proteins used in the alignment (from top to bottom) are from *P. carotovorum* (WP_010305600.1), *D. dadantii* (WP_013318906.1), *E. amylovora* (WP_004156983.1), *E. coli* (NP_415477.1), and *S. enterica* (NP_460044.1).

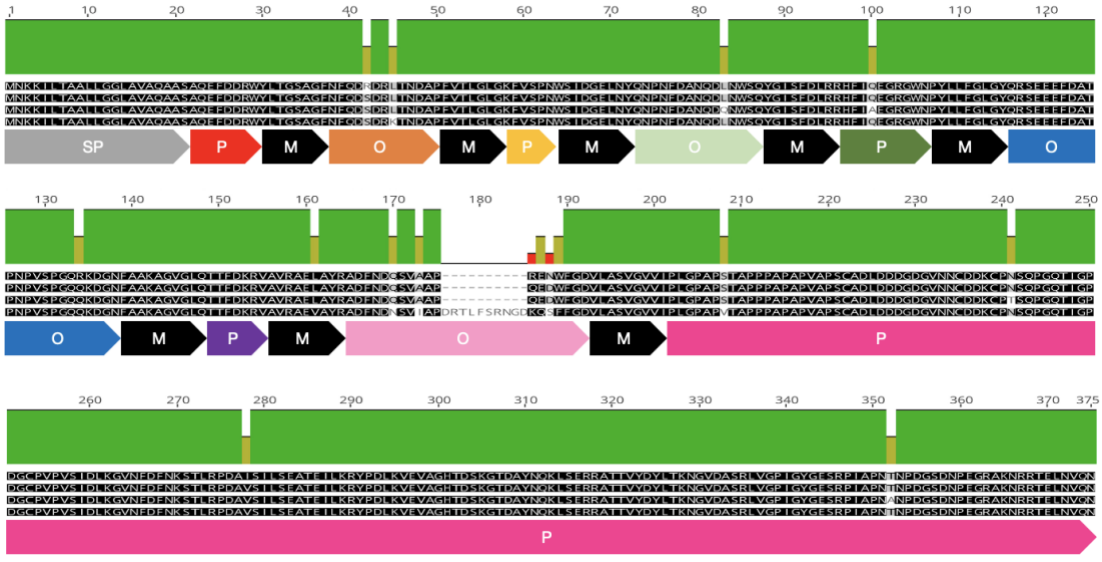

Figure 4.5. Sequence alignment of Xanthomonas spp. OmpA proteins. A MAFFT v7.490 (Katoh and Standley, 2013) amino acid sequence alignment was generated using the Geneious software, and the OMP topology was predicted for *X. citri* OmpA using DeepTMHMM. Conservation of amino acids key: green = 100% conserved, green-brown = 30-99% conserved, red = 0-29% conserved. SP = signal peptide, P = periplasmic domain, M = membrane-bound beta sheet, O = extracellular (outside) loop. The OmpA proteins used in the alignment (from top to bottom) are from *X. oryzae* (WP_014502189.1), *X. citri* (WP_005915855.1), *X. campestris* (WP_011036149.1), and *X. axonopodis* (WP_042823933.1).

CLso Encodes Several Candidate PLCP-Inhibiting Secreted Proteins

In chapter 2, it was demonstrated that the protease CsRD21a contributes to defense against the phloem-residing bacterium, CLas. Further, the tomato homolog of CsRD21a, C14, as well as papain from papaya cleave CLas and Lcr OMP1 proteins, suggesting that proteases from other hosts may cleave cell-surface pathogen proteins as a defense strategy. However, this has not yet been widely investigated. If proteases contribute to defense against other *Ca.* Liberibacter spp., then I hypothesize that those pathogens also encode protease-inhibiting effectors, similar to SDE1.

Knowing that tomato C14 has activity against OMP1 proteins, I decided to look for putative C14-inhibiting effectors of CLso, which infects tomato. First, I predicted every secreted protein in the CLso strain ZC1 proteome using the signal peptide prediction software SignalP 5.0 (Almagro Armenteros et al., 2019). I opted to use this software because it predicts Sec, LIPO, and TET signal peptides, thus providing more potential PLCP-inhibiting candidates. The result was a list of 91 putative secreted CLso proteins. Using AlphaFold2 multimer (Evans et al., 2021), I then predicted the protein structures of each putative, mature secreted protein (without its signal peptide) in complex with the protease domain of tomato C14. AlphaFold2 multimer gives two confidence scores, pTM and ipTM, which summarize the confidence in the structure of a given complex and the confidence in the interaction interface between the chains in a complex, respectively (Evans et al., 2021). A calculation (0.8ipTM + 0.2pTM) that heavily weighs the accuracy of the interaction interface confidence over the complex structure confidence has been used previously to identify novel protease inhibitors (Homma et al., 2023). A score over 0.75 from this calculation is considered a reasonable cutoff for the prediction of a confident protein complex. Using this cutoff, 11 CLso secreted proteins formed confident complexes with tomato C14 (Table 4.3).

Previously, putative SDEs, called hypothetical protein effectors (HPEs) were predicted across CLso haplotypes (Reyes Caldas et al., 2022). Of the 11 putative C14-inhibiting effectors identified in this analysis, five were previously identified as HPEs. Specifically, HPE2 and HPE73 are putative C14-inhibiting effectors and are shared across all CLso haplotypes. Reyes Caldas et al. (2022) analyzed the expression of these effectors using RT-qPCR in CLso-infected tomato and psyllids and found that HPE2 is expressed higher in tomato than in psyllids, where HPE73 is expressed to similar levels in both hosts. Further, they found that HPE2 can significantly suppress ROS triggered

upon chitin treatment. Therefore, HPE2 may have a specific role in CLso virulence by suppressing defense and inhibiting PLCPs, such as C14.

Complex #	Protein ID (NCBI)	0.8ipTM + 0.2pTM =	Name (Haplotypes)	InterProScan Domains	Expression
1	WP_013462424.1	0.87	HPE10 (A,B)		-
4	WP_050780888.1	0.84	HPE43 (A,B,C)	YecR	-
18	WP_013462057.1	0.78	-	Disordered, collagen	-
28	WP_013462515.1	0.78	-	Efflux pump EmrE, 3x transmembrane domains	-
30	WP_013461446.1	0.79	HPE34 (B)	LsoB effector, lipoprotein	-
56	WP_013462162.1	0.77	-	OmpA-like, stator element of flagellar motor	-
65	WP_013462428.1	0.84	HPE73 (A,B,C,D)		insect ≈ plant
66	WP_013461891.1	0.82	-	Periplasmic binding protein-like II_ChoX, OpuAC	-
68	WP_013462221.1	0.76	HPE2 (A,B,C,D)	Disordered	insect < plant
69	WP_013461596.1	0.86	-	Disordered	-
70	WP_244391971.1	0.85	-	Disordered, lipoprotein-like	-

Table 4.3. Summary of putative C14-inhibiting CLso ZC1 secreted proteins that scored 0.8ipTM + 0.2pTM ≥ 0.75 in the AlphaFold2 multimer screening. Name, haplotype, and expression data courtesy of Reyes Caldas et al. (2022).

InterProScan does not predict any domains in HPE2 but does identify disordered regions throughout the protein. This is reflected in the predicted structure of the C14-HPE2 complex (Figure 4.6A). In this structural prediction, HPE2 appears to be largely disordered but contains one large alpha helix that directly interacts with the catalytic residues of C14. Each of the remaining 10 positive complexes also show direct interaction of the secreted CLso proteins with the catalytic pocket, suggesting that they may be directly interfering with the enzymatic activity of C14 (Figure 4.6B). Together, this analysis suggests that CLso encodes several candidate secreted proteins with potential C14-inhibiting capabilities.

It is of note that complex #56 features a CLso secreted protein that has an OmpA-like domain given that OmpA-like eight-stranded beta barrel OMPs were not identified in Liberibacters (Table 4.3, Figure 4.3). Structural alignment of this CLso protein with EcOmpA shows that it superimposes over its C-terminal peptidoglycan-binding domain with a strong RMSD value of 0.941 Å (Figure 4.7). In chapter 2, I demonstrated that EcOmpA is efficiently cleaved by C14 and papain, therefore it is unlikely that its C-terminal domain is a PLCP inhibitor. Indeed, the AlphaFold3 predicted complex of the mature EcOmpA with the C14 protease domain yields a poor interaction score of 0.218. This suggests that OmpA-like proteins that resemble the C-terminal OmpA-like peptidoglycan-binding domain may have neofunctionalized to become PLCP inhibitors and/or anchor the flagellar motor complex to peptidoglycan, as its domain analysis suggests (Table 4.3). Yet, as with any prediction, the AlphaFold multimer interactions analyzed here must be validated experimentally to draw further conclusions.

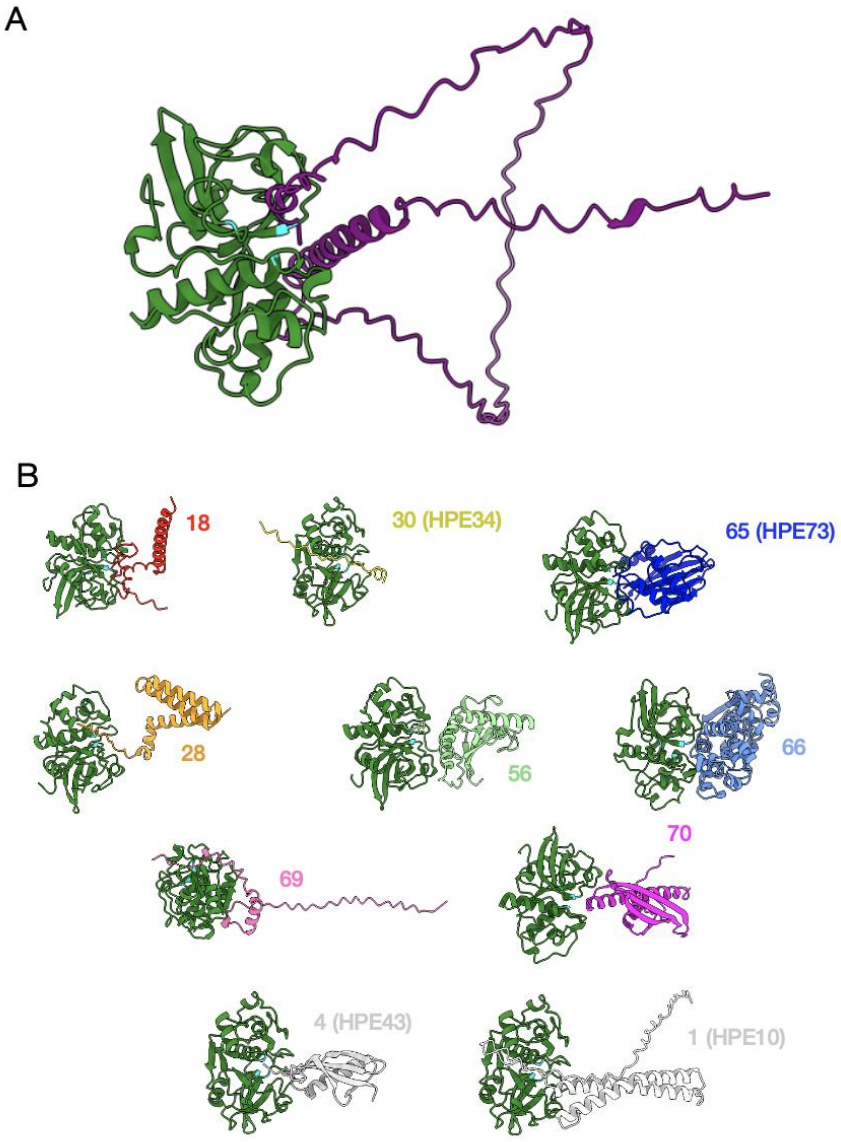

Figure 4.6. AlphaFold2 multimer predicts HPE2 as a putative tomato C14-inhibiting effector. A+B) The Alphafold2-predicted complexes of CLso secreted proteins and C14 were visualized using ChimeraX (Goddard et al., 2018, Meng et al., 2023, Pettersen et al., 2021). The protease domain of C14 is shown in green with its catalytic residues highlighted in cyan. HPE2 is shown in panel A in purple, and the remaining 10 complexes are shown in panel B in various colors with their complex numbers.

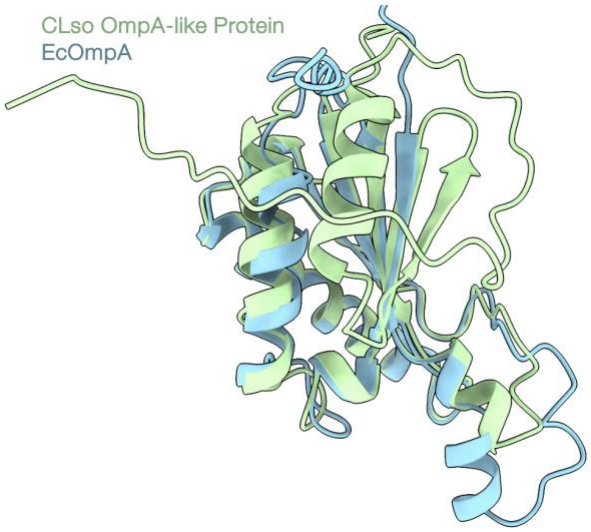

Figure 4.7. A CLso OmpA-like secreted protein structurally aligns with the C-terminal peptidoglycan-binding domain of *E. coli* OmpA. ChimeraX (Goddard et al., 2018, Meng et al., 2023, Pettersen et al., 2021) matchmaker structural alignment of the mature CLso OmpA-like protein (WP_013462162.1) with the mature *E. coli* OmpA protein (NP_415477.1) shown in mint green and light blue, respectively. The matchmaker RMSD score for this alignment is 0.941 Å, and the image is cropped to focus on the area of alignment only.

AY-WB Phytoplasma Encodes Six Candidate PLCP-Inhibiting SAPs

As discussed in Chapter 1, Phytoplasmas are devastating phloem-residing pathogens. However, unlike Gram-negative bacteria, they lack an outer membrane cell wall structure (Lee et al., 2000). While they do not encode OMPs, Phytoplasmas do have cell-surface exposed membrane proteins that may represent substrates of host proteases. These include three major classes of Phytoplasma membrane proteins: immunodominant membrane protein A (IdpA), antigenic membrane protein (Amp), and immunodominant membrane protein (Imp) (Ahmad et al., 2024, Konnerth et al., 2016). Not unlike the OMPs analyzed earlier in this chapter, many Phytoplasma membrane proteins are under selective pressure from their hosts (Fabre et al., 2011, Kakizawa et al., 2006b, Kakizawa et al., 2006a, Fernández and Conci, 2020). As such, I hypothesize that proteases may contribute to defense against Phytoplasmas in the phloem via membrane protein cleavage, and that Phytoplasmas may encode PLCP-inhibiting effectors as a counter-defense. Therefore, I set out to identify candidate protease-inhibiting effectors in AY-WB Phytoplasma.

Previously, 56 putative SAP effectors were predicted in AY-WB Phytoplasma (Bai et al., 2009). These SAPs have predicted N-terminal signal peptides and lack

predicted transmembrane domains. The latter step was not included in my analysis of putative C14-inhibiting secreted proteins, as I hypothesized that membrane-bound proteins on the cell surface may still inhibit host proteases. However, for this analysis, I decided to use the list of 56 predicted SAPs to screen for interaction with the protease domain of the Arabidopsis RD21a homolog, called here AtRD21a. Again, I utilized AlphaFold2 multimer for this purpose and used the same interaction score cut-off (0.8ipTM + 0.2pTM ≥ 0.75), which yielded a list of six putative AtRD21a-inhibiting SAPs (Table 4.4). The expression of five of the six SAPs were analyzed previously in infected *A. thaliana* and the leafhopper vector *Macrosteles quadrilineatus* (MacLean et al., 2011). SAP55 and SAP71 have similar or higher expression, respectively, in *A. thaliana* as compared to the leafhopper and may have a role in Phytoplasma infection of plants. Intriguingly, InterProScan predicted the presence of transmembrane domains in SAP71, SAP15, SAP72, and SAP74, suggesting that some of the SAPs analyzed by Bai et al. (2009) may actually contain transmembrane domains.

Protein ID (SAP name)	0.8ipTM + 0.2pTM =	InterProScan Domains	Expression
AYWB203 (SAP55)	0.85	FtsH protease domain-like, peptidase M41	insect ≈ plant
AYWB295 (SAP51)	0.89	-	insect > plant
AYWB568 (SAP71)	0.83	Transmembrane domain	insect < plant
AYWB624 (SAP15)	0.83	Nitrogenase molybdenum iron protein domain, high-affinity zinc uptake system protein ZnuA-related, transmembrane domain	insect > plant
AYWB667 (SAP72)	0.82	malE maltose-binding periplasmic protein, periplasmic binding protein-like II, transmembrane domain	insect > plant
AYWBpIII04 (SAP74)	0.78	Transmembrane domain	-

Table 4.4. Summary of putative AtRD21a-inhibiting AY-WB SAPs that scored 0.8ipTM + 0.2pTM ≥ 0.75 in the AlphaFold2 multimer screening. Protein IDs and SAP prediction courtesy of Bai et al. (2009). Expression data courtesy of MacLean et al. (2011).

Arabidopsis PLCPs have been identified and characterized previously by Richau et al. (2012). They identified 31 total Arabidopsis PLCPs, comprising nine total subfamilies. A good candidate PLCP-inhibiting SAP may target broadly target various subfamilies of PLCPs in Arabidopsis. Therefore, I decided to further screen the six SAPs that had a positive AlphaFold2 multimer interaction with AtRD21a against all 31 Arabidopsis PLCPs using the same interaction score cutoff. Overall, SAP71 was predicted to interact with the most (20/31) PLCPs and the most subfamilies of PLCPs (8/9) (Figure 4.8). SAP71, like SDE1, is expressed significantly higher in plants than insects, suggesting it is a promising virulence factor in plants (MacLean et al., 2011, Thapa et al., 2020, De Francesco et al., 2022, Pagliaccia et al., 2017). That it targets the most PLCP subfamilies also suggests it may have the broadest inhibition spectrum of any SAP tested here. SAP55 and SAP51 each target six PLCP subfamilies; SAP72 targets five subfamilies; and SAP15 and SAP74 target three subfamilies (Figure 4.8). Together, this suggests that AY-WB Phytoplasma may encode several PLCP-inhibiting enzymes, and these would be promising targets for further functional studies.

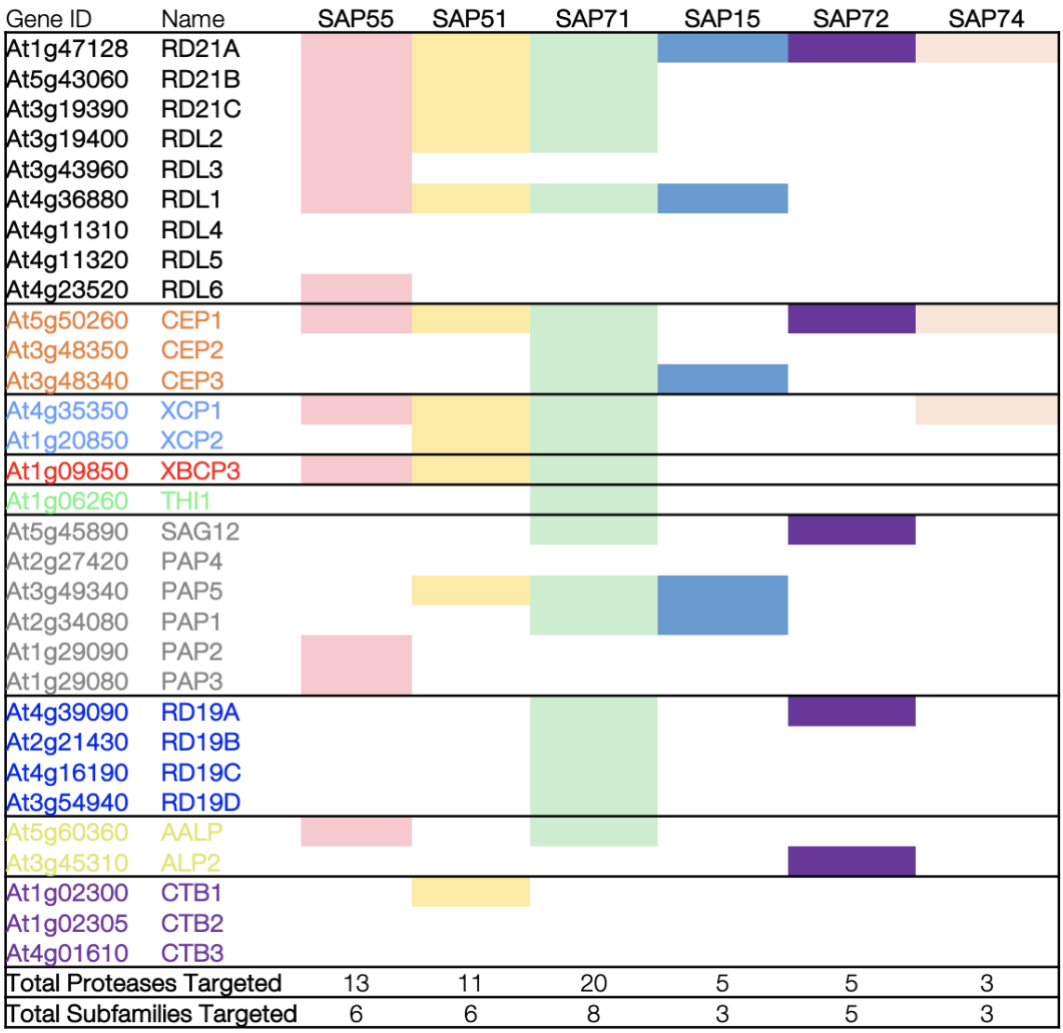

Figure 4.8. Summary of the AlphaFold2 multimer screening of six SAP effectors against 31 Arabidopsis PLCPs. Arabidopsis gene IDs and gene names are colored by PLCP subfamily as determined by Richau et al. (2012). Colored boxes (red, yellow, green, blue, purple, and pink) represent positive interactions for each SAP (SAP55, SAP51, SAP71, SAP15, SAP72, and SAP74, respectively) as determined by the interaction score (0.8ipTM + 0.2pTM ≥ 0.75) generated from AlphaFold2 multimer output.

Conclusions and Discussion

The work brought forth in this chapter aimed to use computational methods to understand the role of proteases, protease inhibitors, and OMPs in molecular plant-pathogen interactions. First, by generating a HMM to identify beta barrel OMPs and combining this with transmembrane domain HMM software, DeepTMHMM, I was able to create a dataset of 964 beta barrel OMPs in 20 Gram-negative bacteria. This list of bacteria includes pathogens of animals and plants, as well as a beneficial bacterium, and represents a large range of bacterial lifestyles across three major classes of bacteria. Each bacterium tested encodes beta barrel OMPs, ranging from five to 112 per bacterial proteome. Further, using topology information predicted by DeepTMHMM, I was able to break up the OMP dataset into smaller subsets based on the number of transmembrane domains present in each protein. I focused on eight-stranded beta barrel OMPs, finding that OMP1-like proteins appear to be specific to the order Hyphomicrobiales, specifically in the Rhizobiaceae family. Yet, a larger data set comprising more bacterial proteomes from different orders and families would further support this conclusion.

Intriguingly, OmpA proteins form two distinct clades among eight-stranded beta barrel OMPs. Both clades have extended C-terminal domains with presumptive peptidoglycan-binding functions, yet these proteins are absent in each of the Alphaproteobacteria and Betaproteobacteria tested. However, the C-terminal domain of OmpA, without the beta barrel domain, seems to have persisted in these bacteria, as demonstrated in this chapter by a putative PLCP-inhibiting CLso secreted protein. Moreover, InterPro has identified 33,530 OmpA-like family proteins across Alphaproteobacteria alone. Therefore, more work would have to be done to confidently conclude that OmpA proteins with both the transmembrane beta barrel domain and peptidoglycan-binding domain are completely absent outside of Gammaproteobacteria.

In Chapter 2, I demonstrated that OMP1 proteins exhibit sequence diversity in their extracellular domains. This is a phenomenon that has been observed previously in animal pathogen membrane proteins as well as Phytoplasma membrane proteins, likely as a result of selective pressure from their respective hosts (Padhi et al., 2009, Konnerth et al., 2016). Here, I demonstrate that this phenomenon is present in OmpA proteins found in plant pathogens *P. carotovorum*, *D. dadantii*, *E. amylovora,* and *Xanthomonas* spp.. I hypothesize that this may be due, in part, to the selective pressure applied by

plant-derived hydrolytic enzymes, such as proteases. Some of this selective pressure may pay off in reducing protease cleavage. For example, in Chapter 2, I demonstrated that LcrOMP1 is a weaker substrate of CsRD21a than CLasOMP1. This may be due to modifications of extracellular loops, but this needs to be further studied. By setting up a panel of OMPs predicted in this study, it could be possible to experimentally screen for their cleavage using proteases from representative families. Such an approach would begin to unravel how widespread OMP targeting by host proteases is across various pathosystems and how extracellular loop diversification may reduce protease cleavage.

Bacterial pathogens may partially overcome protease cleavage of OMPs by encoding functionally redundant OMPs. For example, *A. tumefaciens* appears to encode seven OMP1 proteins, *S. melitoti* encodes two, and Lcr encodes four. On the other hand, host protease cleavage can be overcome by deploying protease inhibitor effector proteins. Tomato C14 is active against CLas and Lcr OMP1 proteins and may have activity against CLsoOMP1. As CLso represents an increasingly emerging threat to carrots and solanaceous plants, namely potatoes and tomatoes (Trkulja et al., 2023), new strategies to combat this disease are in demand. Overexpression of C14 in these crops may result in lower CLso titers and reduced diseased symptoms, similar to CsRD21a against CLas in citrus. However, this needs to be functionally verified.

A major clue as to whether proteases contribute to defense against CLso would be the identification of protease-inhibiting effectors. Inspired by the AlphaFold2 multimer-based approach to identify novel protease inhibitor effectors used by Homma et al. (2023), I utilized a similar screening of 91 putative secreted proteins from CLso against tomato C14. The result was a list of 11 candidate C14-inhibiting proteins, of which at least one, HPE2, is more highly expressed in plants than insects and is present in four major CLso haplotypes. Future work should screen HPE2, along with the remaining candidates, for interaction with and enzymatic inhibition of C14. It is also possible that the candidates identified here represent cleaved substrates and not inhibitors. Therefore, purifying the proteins and treating them with PLCP-containing apoplastic fluid or purified papain may reveal their cleavage *in vitro*. Further, CLsoOMP1 cleavage by C14 should be tested *in vitro*. Together, this may provide molecular insight into the co-evolutionary mechanisms occurring between CLso and its hosts.

Phytoplasmas are devastating phloem-residing pathogens, but infection of AY-WB on Arabidopsis, for example, results in a very different outcome than CLas in citrus. AY-WB Phytoplasma induces “zombie-like” vegetative growth of Arabidopsis, maintaining the plant as a haven for feeding by its insect vector (Bendix and Lewis,

2018). CLas, on the other hand, reduces the overall growth of its citrus host, ultimately killing the plant by inducing phloem blockage (Achor et al., 2020, Kim et al., 2009). Despite these differing infection outcomes, both pathogens are successfully transmitted to new hosts with the help of their insect vectors and cause disease. Previous work on SDE1 and the current work presented in this thesis suggest that proteases may be important hubs of defense against phloem pathogens (Clark et al., 2018, Clark, 2019, Clark et al., 2020). While Phytoplasmas appear to encode several SAP effectors that alter the accumulation of host transcription factors to alter the plants development (Bertaccini et al., 2019, Correa Marrero et al., 2024), whether other Phytoplasma effectors also target and inhibit host proteases is unknown. Therefore, I applied the AlphaFold2 multimer-based screening strategy to identify SAPs that may inhibit Arabidopsis PLCPs. This yielded six SAPs that form predicted complexes with various subfamilies of Arabidopsis PLCPs. Therefore, I hypothesize that PLCPs contribute to defense against Phytoplasmas and that, as a counter-defense strategy, Phytoplasmas deploy PLCP-inhibiting SAP effectors. Yet, it should be noted that this screening system is biased to those SAPs that were initially found to have a positive interaction score with AtRD21a. Using the biased approach, a total of 236 protein complexes were predicted using AlphaFold2 multimer, where an all SAPs vs. all PLCPs screening would have included 1,736 protein pairs. Therefore, future work may identify more putative PLCP-inhibiting SAPs using an all vs. all multimer screen. Any such candidates should be then experimentally confirmed, as with the CLso secreted proteins discussed earlier.

Together, the approaches in this chapter lay out the computational groundwork for further contextualizing and uncovering OMP-protease-protease inhibitor dynamics in plant-pathogen interactions.

Chapter 5: General Discussion

Phloem-residing pathogens, such as *Ca.* Liberibacter spp. and *Ca.* Phytoplasma spp., represent major threats to the global agriculture industry. This thesis set out to investigate the roles of proteases in defense against these pathogens, particularly CLas, which causes citrus HLB. Our first clue that proteases contribute to defense against phloem pathogens was a previous finding that an effector protein, SDE1, from CLas inhibits citrus PLCPs and contributes to HLB disease progression (Clark et al., 2018, Clark, 2019, Clark et al., 2020). Our second clue was that PLCPs, along with serine, aspartic, and metalloproteases are largely induced in CLas-infected citrus, and many of these proteases were detected in an extract enriched for phloem tissues (Clark et al., 2018, Robledo et al., 2024, Franco et al., 2020). In this chapter, I will discuss the broader implications of our finding that an SDE1-inhibited PLCP cleaves a CLas OMP and contributes to defense against CLas.

The First Bacterial Substrate of a Plant PLCP

Despite ever-growing evidence that proteases regulate plant defense, few biologically relevant substrates have been characterized (Godson and van der Hoorn, 2021, Misas-Villamil et al., 2016). The functions of plant proteases in defense (discussed in Chapter 1) essentially boil down to three modes of action: cleavage of pathogen-derived substrates, cleavage of plant-derived substrates, and immune co-receptors (decoy guardees). While cleavage of pathogen proteins seems an obvious route for proteases to directly contribute to plant defense, few such substrates have been identified (Wang et al., 2019, Wang et al., 2021a). To my knowledge, only one pathogen-derived substrate, Pit2 of *Ustilago maydis*, is known to be cleaved by plant PLCPs. While the Pit2 effector from the fungus *Ustilago maydis* is cleaved by maize PLCPs, this cleavage actually results in PLCP inhibition and enhanced virulence (Misas Villamil et al., 2019). As such, there is much more to be uncovered regarding PLCP substrates in plant defense.

In this thesis, I found that two serine proteases and two PLCPs from citrus interact with a highly expressed, cell surface-exposed outer membrane protein of CLas, CLasOMP1, via yeast-two-hybrid assays. Of these proteases, I confirmed that the PLCP, CsRD21a, has proteolytic activity against CLasOMP1 in a semi-*in vitro* assay,

resulting in a cleaved product detected by Western blot. A CLasOMP1 cleaved peptide with a similar size was also observed in CLas-infected citrus, indicating that this cleavage may also happen during natural infection.

The fact that the interaction was detected between CLasOMP1 and CsRD21a via yeast-two-hybrid is admittedly surprising given the inherent instability of protease-substrate interactions. Despite this drawback, CsRD21a association with the N-terminus of CLasOMP1 is supported by both yeast-two-hybrid and the proteolytic cleavage that was observed in this region (Figure 2.5). This finding highlights CLasOMP1 as the first bacterial substrate of PLCPs identified to date. Further dissection of CLasOMP1-PLCP-SDE1 interaction dynamics may be better studied with the CsRD21a catalytic mutant and by testing these interactions with additional methods such as *in vitro* pulldown and co-immunoprecipitation.

Do Proteases Converge on CLasOMP1?

The challenges of studying proteases are clearly represented in Chapters 2 and 3 of this thesis. For example, simply finding an interacting partner of a protease alone is not sufficient to conclude it is a cleaved substrate. While CSPs 10909 and 8175 interact with CLasOMP1 at its N-terminus in an almost identical manner as CsRD21a, only CsRD21a cleavage of CLasOMP1 was observed using the semi-*in vitro* protease cleavage assay. This could be simply due to the fact that CLasOMP1 is not a substrate of CSPs or due to different requirements for the efficient activation of these proteases. Alternatively, as putative carboxypeptidases, these CSPs may remove a small number of C-terminal amino acids, thus not resulting in a change in the molecular weight of the substrates that is detectable via Western blotting. Another possibility is that CSPs may require the action of other proteases to produce neo-C-termini that can then be cleaved by CSPs. Yet combining apoplast fluid containing both CsRD21a and CSP10909 with CLasOMP1 or LcrOMP1 did not result in new cleavage products detected in the semi-*in vitro* cleavage assay in a preliminary experiment (data not included). Factors such as post-translational modifications, tissue specificity, and pH may account for a lack of sufficient CSP activation in this work. CSPs 10909 and 8175 may have adapted to the conditions of the phloem, where their activation and deployment have been finely tuned through evolution. For example, the pH of *Citrus sinensis* is reported to be slightly acidic at about 6.0 (Hijaz and Killiny, 2014), whereas the semi-*in vitro* cleavage assay includes sodium acetate buffer at pH 5.0 as used in a previous study of apoplastic proteases

(Paulus et al., 2020). These factors should be considered in establishing a modified proteolytic cleavage assay for phloem proteases. Therefore, CLasOMP1 may still be targeted by CSP(s) during infection.

Two lines of evidence suggest that CLasOMP1 may be subjected to cleavage by proteases other than CsRD21a. First, in Figure 2.5A, a small amount of the ~14 kDa CLasOMP1 cleavage product is detected when incubated with the apoplastic fluid containing the catalytic mutant of CsRD21a, regardless of E-64 concentration. Second, two smaller (~9-12 kDa) CLasOMP1-derived cleavage products were detected in infected Grapefruit samples. Interrogating the functions of these additional proteases, which may include CSPs, will reveal the extent to which CLasOMP1 is targeted by different classes of proteases and thus its importance as a defense target. This could be significant, for example, if PAMPs are released via a proteolytic cascade from CLasOMP1.

Engineering Defense to Combat HLB

Genetic modification has been proven to be a promising technique in combatting HLB, with increased tolerance from the overexpression of NPR1-like genes, an SA methyltransferase SAMT1, and a thionin antimicrobial peptide (Zou et al., 2021, Hao et al., 2016, Peng et al., 2021, Dutt et al., 2015, Soares et al., 2020, Sarkar et al., 2024). With the help of our collaborators at Huazhong Agricultural University, we were pleased to find that CsRD21a also reduces CLas titers in CsRD21a-overexpressing transgenic citrus. This confirmed that CsRD21a contributes to HLB disease tolerance, yet the mechanism remains elusive. We have observed cleaved CLasOMP1 in CLas-infected citrus seed coat vasculatures (Figure 2.5), but we were unable to detect CLasOMP1 using OMP1-specific antibodies in the midribs or leaf tissue of these transgenic plants. This is likely due to the low titer of bacteria in both wildtype and CsRD21a overexpression lines. Nonetheless, we cannot conclude that the transgenic lines have more CLasOMP1 cleavage than the wildtype lines. Even if this was observed, this would not justify the conclusion that CsRD21a defense functions are CLasOMP1-cleavage dependent. Ideally, CLasOMP1 would be knocked out in CLas to determine its requirement for CsRD21a defense functions. Perhaps this may one day be possible if CLas cultures can be maintained *in vitro*. As such, whether CsRD21a functions in a CLasOMP1-independent or -dependent manner remains unknown. N-terminal labeling of the proteome of infected CsRD21a-overexpressing transgenic plants may reveal the extent

to which it cleaves both citrus- and CLas-derived substrates and, thus, provide more context for its defense activities.

CsRD21a, CsSAG12, CSP10909, and CSP8175 are induced in the phloem of CLas-infected Washington navel citrus, a susceptible cultivar (Franco et al., 2020). However, proteases have not been extensively studied in both HLB susceptible and tolerant citrus cultivars. In one case, it was shown that PLCPs RD19 and AALP are induced during CLas infection of the tolerant cultivar Sugar Belle mandarin, where they are repressed in the susceptible Pineapple sweet orange (Robledo et al., 2024). Given the wide genetic diversity present in citrus and a range of tolerance reported in citrus relatives (Ramadugu et al., 2016), there is a lot to be explored in the genetic variation of both proteases and canonical resistance genes amongst these varieties. For example, HLB tolerant citrus varieties may exhibit expanded or diversified subfamilies of PLCPs that are able to overcome SDE1 inhibition or cleave CLas substrates with higher efficiency. Thus, introducing proteases from tolerant varieties into susceptible varieties may be an effective approach to combatting HLB. A thorough ABPP-based inhibition screening between SDE1 and citrus proteases would begin to address these questions.

Engineering known SDE1-targeted PLCPs to be SDE1-insensitive would also be a powerful strategy to combat HLB. An AlphaFold-based approach was previously employed in the generation of ePip1, an engineered version of the PLCP Pip1, which was made insensitive to the *Phytophthora infestans* effector EpiC2B (Schuster et al., 2024). However, through the work of this thesis, I found that SDE1 was not amenable to this sort of AlphaFold-based approach as it is likely intrinsically disordered. On the other hand, Rcr3 from tomato and wild potato were found to be insensitive to SDE1 inhibition (Clark et al., 2018). Structural and sequence-based comparisons of Rcr3 and SDE1-inhibited citrus PLCPs may facilitate the mutagenesis of a panel of PLCPs that could be tested for insensitivity to SDE1. Additionally, it is appealing to suggest that a catalytic mutant of CsRD21a may be able to function as a sponge to sequester SDE1 away from active PLCPs. While pretreating PLCPs with E-64 reduces their binding affinity to SDE1 (Clark et al., 2018), whether the CsRD21a mutant can still interact with SDE1 has not yet been experimentally determined.

Treating CLas-infected trees with chemicals that directly inhibit CLas growth in a targeted fashion is appealing to save trees that are currently infected in citrus groves. For example, two chemicals have been identified that inhibit a conserved *Ca.* Liberibacter phosphatase enzyme, thus reducing CLas and CLso growth in citrus and potato, respectively (Wang et al., 2024a). Identifying a chemical inhibitor of SDE1 may

provide further protection against CLas. A combination of such treatments would likely have less off-target effects compared to antibiotic treatments.

Together, this section highlights how fundamental, mechanistic research in plant pathology can reveal new opportunities to enhance disease resistance in crops.

Open Questions Concerning OMP1-SDE1-PLCP Dynamics

The reduced genome of CLas suggests that these bacteria requires many nutrients from citrus and its insect vector for survival (Fagen et al., 2014). As such, CLas OMPs may mediate this nutrient uptake. For example, the AlphaFold-predicted structure of CLasOMP1 reveals a small, hydrophilic, negatively charged channel that may allow the passage of ions in and/or out of the CLas cell (Figure 2.18). However, this was not experimentally verified in this work. Uncovering the biological functions of CLasOMP1 and the consequence of its cleavage is key to elucidating the mechanism of CsRD21a-mediated defense functions. That CLasOMP1 is one of the most highly expressed CLas genes *in planta* suggests that it has an important role in CLas survival and cleaving it may directly inhibit CLas growth or alter membrane stability. As CLas is unculturable, we decided to test whether CsRD21a or purified papain could inhibit Lcr growth *in vitro*. However, our collaborators at UF CREC in Lake Alfred, Florida, did not observe any growth defects of papain- or CsRD21a-treated Lcr cultures. This may be because CsRD21a and papain appear to cleave LcrOMP1 less efficiently than CLasOMP1 in semi-*in vitro* cleavage assays (Figure 2.5, 2.11, 2.12). Another possibility is that the three additional LcrOMP1 homologs (Table 2.1, Figure 2.9) function redundantly with LcrOMP1 and mask any PLCP-mediated growth inhibition. Due to the challenges of the microscopy- and CPRG-based membrane integrity assays in *E. coli* (Chapter 2), it would be worth looking for morphological changes in Lcr after the protease treatments.

The functions of CsRD21a, SDE1, and CLasOMP1 may be further elucidated with the generation of more transgenic lines. For example, generating transgenic citrus expressing the catalytic mutant of CsRD21a would serve as a better negative control to confirm that the function of CsRD21a in CLas resistance is due to its catalytic activity. Moreover, whether this function in defense is specific to citrus HLB remains unknown. To see if CsRD21a broadly contributes to phloem defense in citrus, the transgenic lines could be challenged with a citrus-infecting Phytoplasma strain. Alternatively, CsRD21a may regulate defense more broadly, against other pathogens in the apoplast, such as *Xanthomonas citri*. Additionally, expression of CsRD21a under a phloem-specific

promoter may showcase its potential tissue-specific defense function. Likewise, expression of SDE1 under a phloem-specific promoter would strengthen the claim that SDE1 functions by inhibiting PLCPs in the phloem. Further, if a cleaved CLasOMP1 product released by CsRD21a, for example, serves as a PAMP to induce immunity, then expressing full length or the cleaved CLasOMP1 alone under a phloem-specific promoter in citrus may enhance defense against CLas. Direct infiltration of CLasOMP1 cleavage products into the apoplast of citrus leaf disks was performed during the work of this thesis and inconsistently induced ROS bursts; this could be due to the requirement of other proteases, such as CSPs, to release a bioactive PAMP from CLasOMP1. Another possibility is that a CLasOMP1 PAMP may be detected intracellularly and not by a cell surface receptor. As such, direct study of a CLasOMP1 PAMP in the phloem through a transgenic-based approach may be more insightful.

The presumably disordered nature of SDE1 begs further questions into how this lack of secondary structure facilitates its virulence functions. For example, AtMC1, an Arabidopsis metacaspase family cysteine protease, has an intrinsically disordered domain that facilitates its localization to stress granules, which are membrane-less compartments formed by liquid-liquid phase separation (Ruiz-Solaní et al., 2023). This phase separation mediates AtMC1 regulation of senescence, allowing AtMC1 to clear toxic protein aggregates. Therefore, it may be of interest to experimentally determine if SDE1 undergoes phase separation in the phloem and whether this is important for its function. This could account for SDE1-induced senescence in transgenic plants (Clark et al., 2020). For example, SDE1 may inhibit other cysteine proteases with senescence regulatory functions in stress granules. As such, SDE1 phase separation in the phloem should first be determined using a cell biology approach by fusing it to a fluorescent reporter and expressing it under a phloem-specific promoter.

Proteases and OMPs in the Future of Molecular Plant-Microbe Interactions

CLasOMP1 represents just one bacterial pathogen-derived PLCP substrate identified to date. Yet it is likely that many pathogen-derived proteins from many phloem-residing pathogens are subjected to the activities of proteases in the phloem. As such, future work should investigate the role of PLCPs in defense against other phloem pathogens, including CLso and *Ca.* Phytoplasma spp. If these pathogens do have to overcome PLCP functions to colonize the phloem, they likely do so via the deployment of PLCP-inhibiting effectors, similar to SDE1. As such, I utilized an AlphaFold-based

pipeline (Homma et al., 2023) to identify putative PLCP-interacting effectors from these pathogens. If I were to continue this line of research, I would validate these interactors using yeast-two-hybrid and co-immunoprecipitation. The PLCPs and their interactors would then be expressed under phloem-specific promoters in their respective hosts, followed by infection assays to determine their role in defense and virulence, respectively. I would then test the effectors for inhibition of PLCPs. Together, this would provide further context for the role of PLCPs in a phloem-based immune response.

The work in this thesis has revealed that outer membrane proteins of pathogens may be important defense targets. As such, the principles of this defense strategy may apply to Gram-negative bacterial pathogens that infect other tissues of the plant, including the apoplast and xylem. For example, a tomato cultivar with tolerance against *Ralstonia solanacearum* exhibited higher PLCP and serine protease activities in the apoplast compared to a susceptible cultivar (Planas-Marquès et al., 2018). Indeed, given the transcriptional and protein-level induction of most defense proteases studied during infection to date, these genes may be considered PR genes (Godson and van der Hoorn, 2021). That OMP1 is the only identified bacterial substrate of a PLCP so far begs the question of the extent to which OMPs from Gram-negative bacteria are targeted by host defense proteases. That they are positioned on the surface of the bacterial cell makes them particularly attractive targets for defense. Thus, I have curated an OMP prediction pipeline using the proteomes of economically important pathogens. I also applied this pipeline to bacterial pathogens of animals, where one pathogen OMP substrate has already been identified (Belaaouaj, 2002, Belaaouaj et al., 1998, Belaaouaj et al., 2000). By studying their evolutionary signatures, we may gain further insight into how OMPs function as targets of both the adaptive and innate immune systems. For example, OMP1 and OmpA exhibit sequence diversification in their extracellular loops, potentially as a result of co-evolution to evade host defense or perhaps to alter their functions in ion uptake or cell-to-cell adhesion. Therefore, it will be interesting to apply this analysis to a wider range of bacterial species and to more families of OMPs.

Together, the findings in this thesis have contributed to a growing understanding of the co-evolutionary arms race between CLas and citrus and provides new insight into the fundamental role of host proteases and pathogen outer membrane proteins in plant-microbe interactions. Despite the inherent challenges of the system, our research on SDE1-CLasOMP1-PLCP dynamics represents one of the best characterized mechanistic studies in citrus HLB to date. I hope the advancements in our understanding

of plant proteases and outer membrane proteins brought forth by this thesis can inspire new lines of research and technologies to combat economically important pathogens in the field.

Chapter 6: Materials and Methods

Aphid Stylectomy

Black citrus aphid (*Toxoptera citricida*) colonies were obtained from Dr. Choaa El-Mohtar at UF CREC with the help of Dr. Victor Soria-Carrasco at the John Innes Centre Entomology and Insectary Facility. Colonies of aphids were maintained on Rough Lemon citrus by Dr. Soria-Carrasco's team. Aphids actively feeding on the phloem (as identified by the active production of honeydew) were targeted for stylet removal. Aphid stylets were cut under a light microscope as previously described (Pritchard, 1996) using electrolytically sharped tungsten wires attached to the HF Microcautery Unit CA-50 (Syntech). The microcautery machinery was provided by Dr. Jeremy Pritchard (University of Birmingham). Electrolysis of the tungsten wires was carried out by Martyn Hewitt (NBI Partnership Ltd).

Yeast Two Hybrid

Drs. Simon Schwizer and Kelley Clark cloned CSPs 10909 and 8175 and PLCPs (CsRD21a and CsSAG12) into the pGADT7 prey vector (Takara) and CLasOMP1 into the pGBKT7 bait vector (Takara). In the bait vector, I cloned truncations of CLasOMP1 from its original pGBKT7 construct (generated by Dr. Schwizer), LcrOMP1 from Lcr strain BT-1 liquid cultures, additional CLas OMPs from cDNA of HLB-infected citrus (courtesy of Dr. Amelia Lovelace), and all remaining OMP1 homologs from synthesized gene fragments (TWIST Bioscience). All plasmids were prepared using the Miraprep protocol (Pronobis et al., 2016).

The yeast strain AH109 (Takara) was maintained in YPAD medium prior to transformation. Briefly, overnight AH109 liquid cultures were sub-cultured until an OD_{600} between 0.5 and 0.8 was reached. The cells were then washed twice in sterile water followed by pelleting at 1,000 x g for 5 minutes prior to resuspension in transformation buffer, which comprised 50% PEG 3350, 1M LiAc pH 7.0 (pH adjusted with glacial acetic acid), and 10x TE buffer pH 8.0, at a ratio of 8:1:1. One part salmon sperm DNA was then added to six parts of the transformation mixture in addition to ~2,000 ng of both bait and prey vectors, and the cells were incubated at 42°C for 45 minutes. The cells were then pelleted and resuspended in 0.9% NaCl before being plated on YPAD

medium. Co-transformed colonies were resuspended in sterile water (and in some cases serially diluted after correcting the OD_{600}), and re-plated on SD/-Trp/-Leu and SD/-Trp/-Leu/-His/-Ade (Takara).

Backbone	Insert (protein/gene ID)	Primer 1	Primer 2	Source
pGADT7	CsRD21a (XM_006473212)	-	-	Clark et al. (2018)
pGADT7	CsSAG12-1 (XM_006495158)	-	-	Clark et al. (2018)
pGADT7	CSP10909 (orange1.1g010909m)	-	-	Dr. Simon Schwizer
pGADT7	CSP8175 (Ciclev10008175m)	-	-	Dr. Simon Schwizer
pGBKT7	CLas SDE1 (CLIBASIA_05315)	-	-	Clark et al. (2018)
pGBKT7	CLas OMP1 (CLIBASIA_02425)	-	-	Dr. Simon Schwizer
pGBKT7	CLasOMP1 – Truncation P1 (CLIBASIA_02425)	GGGAATTCGCTGATCCTGTGCGTCGTGC	CCGGATCCCTTATGCATACGGACCGTTAAAGT	This study
pGBKT7	CLasOMP1 – Truncation O1 (CLIBASIA_02425)	CCGGATCCCTTATGCATACGGACCGTTAAAGT	CCGGATCCCTTAAGATCCCCCAGCATTATGAT	This study
pGBKT7	CLasOMP1 – Truncation P2 (CLIBASIA_02425)	GGGAATTCATTTTCGCTGGATATAACGT	CCGGATCCCTTATCCCTCAACACCATACATTA	This study
pGBKT7	CLasOMP1 – Truncation O2 (CLIBASIA_02425)	GGGAATTCGATGTTCGCTATACTGTCCC	CCGGATCCCTTACAAAGAGCCTCCAATACCAT	This study

pGBKT7	CLasOMP1 – Truncation P3 (CLIBASIA_02425)	GGGAATTCC GTATCCGTGG AGGATATGA	CCGGATCCCTT AACCAACAGTA GCGTACAACA	This study
pGBKT7	CLasOMP1 – Truncation O3 (CLIBASIA_02425)	GGGAATTCCC AGATGTAGCT CAAAAATA	CCGGATCCCTT ATCCACCTATA GCAATAGGAG	This study
pGBKT7	CLasOMP1 – Truncation P4 (CLIBASIA_02425)	GGGAATTCAC TGCAGGTGTC GGTGTTGA	CCGGATCCCTT ATAAACGAGCT ACGAGACTTT	This study
pGBKT7	CLasOMP1 – Truncation O4-P5 (CLIBASIA_02425)	GGGAATTCGA GTACCGTGCA AGCAAATA	CCGGATCCCTT AAAACTTCATTC CTACACCCA	This study
pGBKT7	CLasOMP1 – Truncation 1 (CLIBASIA_02425)	GGGAATTCG GTCTGAGTGC ATTGTATAA	CCGGATCCCTT AAAACTTCATTC CTACACCCA	This study
pGBKT7	CLasOMP1 – Truncation 4 (CLIBASIA_02425)	GGGAATTCAT TTTCGCTGGA TATAACGT	CCGGATCCCTT AAAACTTCATTC CTACACCCA	This study
pGBKT7-**pAJM009**	CLasOMP1 – Truncation 2 (CLIBASIA_02425)	GGGAATTCTT TGGCGAAGA AGCCCATCAT	CCGGATCCCTT AAAACTTCATTC CTACACCCA	This study
pGBKT7-**pAJM010**	CLasOMP1 – Truncation 3 (CLIBASIA_02425)	GGGAATTCAA TGCTGGGGG ATCTATTTTC	CCGGATCCCTT AAAACTTCATTC CTACACCCA	This study
pGBKT7	LcrOMP1 (WP_015273568.1)	GGGAATTCG CAGATGCGG TACATGATAT	GGGGATCCTTA GAATTTTACAC CAATACCG	This study
pGBKT7-**pAJM023**	LcrOMP1-a (WP_244422703.1)	synthesized gene fragment (Twist Biosciences)		This study
pGBKT7-**pAJM024**	LcrOMP1-b (WP_015272991.1)	synthesized gene fragment (Twist Biosciences)		This study

pGBKT7-pAJM024	LcrOMP1-c (WP_015273041.1)	synthesized gene fragment (Twist Biosciences)		This study
pGBKT7	CLsoOMP1 (C0030_000230)	synthesized gene fragment (Twist Biosciences)		This study
pGBKT7	CLamOMP1 (G653_00275)	synthesized gene fragment (Twist Biosciences)		This study
pGBKT7	CLafOMP1 (G293_03405)	synthesized gene fragment (Twist Biosciences)		This study
pGBKT7	CLasOMP2 (CLIBASIA_04900)	GGGAATTCGT AGATCTTTAT CTGCCTAG	CCGGATCCCTT AGAAGTGCATA TTTATACCAA	This study
pGBKT7	CLasOMP3 (CLIBASIA_05150)	GGGAATTCGA CTATGGGTAT TCTCCCCA	CCGGATCCCTT AAAAGCGTAAA ACCACACCAG	This study
pGBKT7	CLasPorin (CLIBASIA_00995)	GGGAATTCTA TGTTCGTGGG AAAACGTC	CCGGATCCCTT AGAAAGATTTC TTTAAACCAA	This study
pGBKT7	CLasYajC (CLIBASIA_05090)	GGGAATTCGA TGCTCCTGCA ATTACTTC	CCGGATCCCTT ATACAGGTTCA GACTTTGATT	This study

Table 6.1. Yeast-two-hybrid vectors used in this study. Constructs generated in this study were PCR amplified with BamHI and EcoRI restriction cut sites in primers 1 and 2, respectively. Twist Biosciences gene fragments were synthesized with these cut sites added. The resulting amplicons or synthesized gene fragments were ligated into the pGBKT7 acceptor plasmid. Construct sequences were confirmed via Sanger sequencing and co-transformed into the yeast strain AH109.

Plant Material and Protein Expression Analyses

N. benthamiana plants used for Agrobacterium-mediated transient expression were grown in controlled conditions at 25ºC with a 16 hour light / 8 hour dark cycle at ~50% humidity with the help of the John Innes Horticultural Services support team. Transgenic CSP 10909 and 8175-expressing *A. thaliana* plants were generated by Dr. Morgan Halane and were maintained in long day conditions for transgenic line screening and seed collection or in short day conditions for phenotypic analyses, including protein

expression testing. To confirm CSP expression, protein was extracted from transgenic Arabidopsis via grinding up leaf disks in liquid nitrogen, adding loading dye to the ground samples, boiling the samples for 10 minutes, and centrifuging at 12,000 rpm at 4°C. The samples were then run on an SDS-PAGE gel and subjected to Western blotting using the anti-HA primary antibody (Roche) and goat anti-rat secondary antibody (Santa Cruz).

Apoplastic Fluid Extraction

The assays were performed as outlined in Figure 2.4. CsRD21a, C14, and CSP10909 (as well as their catalytic mutants) were cloned into the binary vector pJK268c (provided by Dr. Jiorgos Kourelis) which contains the RNA silencing suppressor P19 in the backbone. Expression was driven by a 2x35s CaMV promoter. CsRD21a and C14 were cloned in their full-length forms without a tag. These constructs were transformed into *A. tumefaciens* GV3101 competent cells and infiltrated in the leaves of four to six-week-old *N. benthamiana* plants. Three days post-inoculation, the leaves were removed, vacuum infiltrated with sterile water, and centrifuged in the barrel of a 20 mL syringe placed in a 50 mL Eppendorf tube. The flow-through apoplastic fluid from these leaves was then concentrated ~2X using 10 kDa concentrator columns (Thermo) and subjected directly to activity-based protein profiling or the semi-*in vitro* OMP cleavage assay.

Backbone	Insert (protein/gene ID)	Primer 1	Primer 2	Source
pICH41308 (Level 0)-**pAJM038**	CsRD21a-wildtype (XM_006473212)	CCGAAGACG GAATGGGTT TGTTTAGATC ACCA	CCGAAGACC AAAGCTCAAG CACTGCTACT TCCACC	This study
pICH41308 (Level 0)-**pAJM039**	CsRD21a-catalytic mutant (XM_006473212)	CCGAAGACG GAATGGGTT TGTTTAGATC ACCA	CCGAAGACG GGCACTCCC ACAGCTTCCT TGAT	This study
		CCGAAGACG GGTGCCTGG	CCGAAGACG GGCGTCCAG	

		GCATTTTCAACCAT	AGATGTCCCACATC	
		CCGAAGACGGACGCTGGTGTTACTGCTGTTGG	CCGAAGACGGGCCTTCACAATCCAGTAATCAG	
		CCGAAGACGGAGGCTTCATGGGGCAGTAGCTG	CCGAAGACCAAAGCTCAAGCACTGCTACTTCCACC	
pICH41308 (Level 0)- **pAJM040**	SlRD21a (C14)-wildtype (Solyc12g088670.2)	CCGAAGACGGAATGGCAGCTCACAGCTCAACTCTC	CCGAAGACGGAAGCTCAAGAACTGCTCT	This study
pICH41308 (Level 0) - **pAJM041**	SlRD21a (C14)-catalytic mutant (Solyc12g088670.2)	CCGAAGACGGAATGGCAGCTCACAGCTCAACTCTC	CCGAAGACGGATGCACTCCCACAGCTTCCTTG	This study
		CCGAAGACGGGCATGGGCATTCTCTGCTGTT	CCGAAGACGGAGCATCCACTGCAGTACCACA	
		CCGAAGACGGTGCTGGTGTAGTTATTGCTGG	CCGAAGACGGGGCCCTAACGATCCAATAATC	
		CCGAAGACGGGGCCTCATGGGGAGCTAACTG	CCGAAGACGGAAGCTCAAGAACTGCTCT	
pJK286c (Level 1)	pICH41308 (Level 0)- **pAJM038**	-	-	This study
pJK286c	pICH41308	-	-	This study

(Level 1)	(Level 0)- **pAJM039**			
pJK286c (Level 1)	pICH41308 (Level 0)- **pAJM040**	-	-	This study
pJK286c (Level 1)	pICH41308 (Level 0) - **pAJM041**	-	-	This study

Table 6.2. Tag-free vectors used for transient expression of PLCPs in *N. benthamiana*. Level 0 constructs were generated via the addition of BpiI restriction enzyme cut sites during PCR followed by a BpiI digestion-ligation reaction of the amplified fragment with the Level 0 acceptor pICH41308 (courtesy of TSL SynBio). Catalytic mutants were generated via domestication and thus four separate PCR amplicons were combined in the digestion-ligation reaction with pICH41308. Dr. Jiorgos Kourelis provided the Level 1 pJK268c acceptor which contains the P19 silencing suppressor in the backbone. The generated L0 constructs and pJK268c acceptor were combined with pICH51288::2x35s and pICH41414::35s-terminator modules (courtesy of TSL SynBio) in a BsaI digestion-ligation reaction to generate Level 1 GoldenGate constructs. These constructs were confirmed via Sanger sequencing and subsequently transformed into *A. tumefaciens* GV3101 pmp90 competent cells for agroinfiltration of *N. benthamiana*.

Membrane Isolation for Enrichment of OMPs

Tag-less, mature (lacking signal peptide) outer membrane proteins were N-terminally fused to the *E. coli* OmpA signal peptide and cloned into the pOPIN-F6-C vector under the control of a T7 promoter. These constructs were transformed into *E. coli* C41 competent cells and grown in liquid auto induction media at 30°C until OD_{600} of 0.5-0.7 was reached, at which point the cultures were moved to 18°C overnight. Pellets were collected via centrifugation at 5,500 rpm at 4°C and were resuspended in A1 buffer with cOMPLETE protease inhibitor tablets (Sigma). The cells were sonicated and centrifuged again at 5,000 rpm. The supernatant was then loaded into PA Ultracrimp tubes (Thermo) and ultracentrifuged at 27,500 rpm. The waxy pellet was then resuspended in A1 buffer with 1% DDM and incubated with rotation at 4°C overnight.

Backbone	Insert (protein/gene ID)	Source
pOPIN-F6-C	CLasOMP1 (CLIBASIA_02425)	This study
pOPIN-F6-C	LcrOMP1 (WP_015273568.1)	This study

Table 6.3. Tag-free vectors used for OMP isolation in *E. coli*. The CLas and Lcr OMP1 sequences were synthesized (Twist Biosciences) with their signal peptides replaced with

the EcOmpA signal peptide sequence. BsaI cut sites were added via PCR amplification using the above primer sequences. The amplicons were then combined with pOPIN-F6-C using a BsaI digestion-ligation reaction. Construct sequences were confirmed via Sanger sequencing and were subsequently transformed into *E. coli* C41 competent cells for membrane isolation.

Protease Cleavage Assays

E. coli membrane fractions containing OMP1 proteins were directly incubated with concentrated apoplastic fluid or purified papain enzyme (Sigma-Aldrich) for three hours at room temperature with final concentrations of 5 mM DTT and 50 mM sodium acetate (pH 5.0). Loading dye was added to the samples, which were then boiled. These samples were then run on SDS-PAGE gels and analyzed via Western blotting using custom monospecific OMP1 antibodies raised in rabbits (Pacific Immunology). CLasOMP1-specific antibody "ab1" was raised against the synthetic peptide GPDVAQKYETGKAGEIT, CLasOMP1-specific antibody "ab2" was raised against the synthetic peptide DPVRRAHHGGRGVVPTIATN, and LcrOMP1-specific antibody "ab3" was raised against the synthetic peptide RLEYRYTRLGKKDFTLRDA. Dr. Agustina de Francesco guided the design of the CLasOMP1-specific antibodies.

Activity-Based Protein Profiling

Concentrated apoplastic fluid was collected as mentioned above and was incubated for 30 minutes at room temperature with concentration gradients of E-64 (diluted with DMSO) or just DMSO at room temperature. DCG-04 was then added to a final concentration of 500 µM with 5 mM DTT and 50 mM sodium acetate (pH 5.0). After one hour incubation at room temperature, protein loading dye was added, and the samples were boiled prior to SDS-PAGE analysis. Western blotting was then performed, and active proteases were detected via chemiluminescence imaging using Streptavidin-HRP (Thermo).

OMP1 Expression in Citrus Seed Coat Vasculatures

Fruits from infected grapefruit and lemon trees were collected from groves at the UF CREC in Lake Alfred, Florida, USA. The seeds were isolated from the fruits, and the seed coats were carefully removed with forceps. The seed vasculatures were then also

removed with forceps and frozen in liquid nitrogen. These samples were then ground with a mortar and pestle and put on ice. After adding protein loading dye to the samples, they were boiled for 10 minutes and centrifuged at 12,000 rpm for 5 minutes. The supernatant was then subjected to SDS-PAGE and subsequent Western blot analyses using CLasOMP1-specific primary antibodies (Pacific Immunology—see "Protease Cleavage Assays" section above) and goat anti-rabbit secondary antibody (Invitrogen).

AlphaFold Structure Visualization

All protein structures were predicted using AlphaFold2 (Bryant et al., 2022) or AlphaFold3 (Abramson et al., 2024) as indicated. AlphaFold structural models were then visualized using ChimeraX (Goddard et al., 2018, Meng et al., 2023, Pettersen et al., 2021). Where indicated, protein structural models were colored by pLDDT scores imported from the AlphaFold output into ChimeraX. Structural alignments of the AlphaFold models using the matchmaker function.

Bioinformatic Analyses of OMPs

For OMP prediction, bacterial proteomes were downloaded from NCBI (https://www.ncbi.nlm.nih.gov/). PFAM alignments for the membrane beta barrel clan (CL0193) were downloaded, and hmmbuild was used to build the HMM (Potter et al., 2018). Next, hmmsearch (http://hmmer.org/) was used to scan each proteome for the presence of OMPs using the HMM. The resulting OMPs were screened using DeepTMHMM (Hallgren et al., 2022) and only proteins identified by both programs were subjected to further analyses. MUSCLE (Edgar, 2004) or MAFFT v7.490 (Katoh and Standley, 2013) alignments were generated, as indicated, of FASTA amino acid sequences. Subsequent maximum likelihood model FastTree v2.1.11-generated phylogenies (Price et al., 2010, Price et al., 2009) were made using Geneious Prime (https://www.geneious.com/). Where indicated, trees were further analyzed using ggtree (https://github.com/YuLab-SMU/ggtree), and trees were appended using beta-strand numbers derived from DeepTMHMM or NCBI annotations.

AlphaFold Multimer Screening

AlphaFold Multimer v2.3.2 (Bryant et al., 2022, Evans et al., 2021) was used to screen pathogen secreted protein interactions with host PLCPs. Positive interactors included multimer pairs that had an interaction score of at least 0.75, which was calculated as 0.8 ipTM + 0.2 pTM, which more heavily weighs the interaction accuracy (ipTM) over the intrinsic model accuracy (pTM) (Evans et al., 2021). 91 secreted proteins were identified from the CLso ZC1 proteome using SignalP 5.0 (Almagro Armenteros et al., 2019) and screened against the tomato RD21a (C14) (Solyc12g088670.2) protease domain. 56 AY-WB SAPs were identified previously (Bai et al., 2009). These were screened first against the *A. thaliana* RD21a (AT1G47128.1), and positive interactors were further screened against previously identified *A. thaliana* PLCPs (Richau et al., 2012).

Appendix

Appendix Table 1. 964 OMPs identified in Chapter IV via the HMM screening method. (Shown below) NCBI proteomes used for this analysis are outlined in Table 4.1. Annotations and protein IDs are from the NCBI reference genomes, while beta strand numbers were extracted from DeepTMHMM output.

Protein ID	Beta Strand #	Bacteria	NCBI Annotation
WP_162686251.1	8	*Agrobacterium tumefaciens*	hypothetical protein
WP_003502127.1	8	*Agrobacterium tumefaciens*	MULTISPECIES: porin family protein
WP_003505461.1	8	*Agrobacterium tumefaciens*	MULTISPECIES: porin family protein
WP_003506253.1	8	*Agrobacterium tumefaciens*	MULTISPECIES: porin family protein
WP_003523003.1	8	*Agrobacterium tumefaciens*	MULTISPECIES: porin family protein
WP_004430633.1	8	*Agrobacterium tumefaciens*	MULTISPECIES: porin family protein
WP_080868261.1	8	*Agrobacterium tumefaciens*	MULTISPECIES: porin family protein
WP_080866755.1	8	*Agrobacterium tumefaciens*	OmpW family protein
WP_080865871.1	8	*Agrobacterium tumefaciens*	outer membrane beta-barrel protein
WP_080866434.1	8	*Agrobacterium tumefaciens*	porin family protein
WP_060724049.1	10	*Agrobacterium tumefaciens*	omptin family outer membrane protease
WP_080866808.1	12	*Agrobacterium tumefaciens*	autotransporter domain-containing protein
WP_121668264.1	12	*Agrobacterium tumefaciens*	autotransporter outer membrane beta-barrel domain-containing protein
WP_233284506.1	12	*Agrobacterium tumefaciens*	autotransporter outer membrane beta-barrel domain-containing protein
WP_233284507.1	12	*Agrobacterium tumefaciens*	autotransporter outer membrane beta-barrel domain-containing protein
WP_035213545.1	12	*Agrobacterium tumefaciens*	MipA/OmpV family protein
WP_080866529.1	12	*Agrobacterium tumefaciens*	MipA/OmpV family protein
WP_003509739.1	14	*Agrobacterium tumefaciens*	MULTISPECIES: OmpP1/FadL family transporter

WP_080570252.1	16	*Agrobacterium tumefaciens*	autotransporter assembly complex protein TamA
WP_060724139.1	16	*Agrobacterium tumefaciens*	MULTISPECIES: outer membrane protein assembly factor BamA
WP_080866034.1	16	*Agrobacterium tumefaciens*	porin
WP_080866035.1	16	*Agrobacterium tumefaciens*	porin
WP_080867386.1	16	*Agrobacterium tumefaciens*	porin
WP_080867316.1	16	*Agrobacterium tumefaciens*	ShlB/FhaC/HecB family hemolysin secretion/activation protein
WP_121668145.1	16	*Agrobacterium tumefaciens*	ShlB/FhaC/HecB family hemolysin secretion/activation protein
WP_080867278.1	18	*Agrobacterium tumefaciens*	hypothetical protein
WP_080866995.1	18	*Agrobacterium tumefaciens*	outer membrane beta-barrel protein
WP_080866344.1	22	*Agrobacterium tumefaciens*	TonB-dependent hemoglobin/transferrin/lactoferrin family receptor
WP_080866882.1	22	*Agrobacterium tumefaciens*	TonB-dependent receptor
WP_080867245.1	22	*Agrobacterium tumefaciens*	TonB-dependent receptor
WP_233284511.1	22	*Agrobacterium tumefaciens*	TonB-dependent receptor
WP_003503591.1	22	*Agrobacterium tumefaciens*	TonB-dependent siderophore receptor
WP_003508455.1	22	*Agrobacterium tumefaciens*	TonB-dependent siderophore receptor
WP_035212943.1	22	*Agrobacterium tumefaciens*	TonB-dependent siderophore receptor
WP_080867310.1	22	*Agrobacterium tumefaciens*	TonB-dependent siderophore receptor
WP_080867349.1	22	*Agrobacterium tumefaciens*	TonB-dependent siderophore receptor
WP_080867369.1	22	*Agrobacterium tumefaciens*	TonB-dependent siderophore receptor
WP_080867400.1	24	*Agrobacterium tumefaciens*	fimbrial biogenesis outer membrane usher protein
WP_060726131.1	26	*Agrobacterium tumefaciens*	MULTISPECIES: LPS-assembly protein LptD
WP_047264568.1	8	*Ca.* Liberibacter africanus	hypothetical protein
WP_047264709.1	8	*Ca.* Liberibacter africanus	porin family protein

WP_047264148.1	16	*Ca.* Liberibacter africanus	outer membrane protein assembly factor BamA
WP_047263948.1	16	*Ca.* Liberibacter africanus	porin
WP_244464434.1	26	*Ca.* Liberibacter africanus	LPS assembly protein LptD
WP_007556586.1	8	*Ca.* Liberibacter americanus	outer membrane beta-barrel protein
WP_007557438.1	8	*Ca.* Liberibacter americanus	outer membrane beta-barrel protein
WP_007557366.1	10	*Ca.* Liberibacter americanus	outer membrane beta-barrel protein
WP_007556730.1	16	*Ca.* Liberibacter americanus	outer membrane protein assembly factor BamA
WP_007556998.1	16	*Ca.* Liberibacter americanus	porin
WP_007556927.1	26	*Ca.* Liberibacter americanus	LPS assembly protein LptD
WP_238556157.1	8	*Ca.* Liberibacter asiaticus	hypothetical protein
WP_015452561.1	8	*Ca.* Liberibacter asiaticus	outer membrane beta-barrel protein
WP_015452909.1	8	*Ca.* Liberibacter asiaticus	outer membrane beta-barrel protein
WP_015452389.1	16	*Ca.* Liberibacter asiaticus	outer membrane protein assembly factor BamA
WP_012778533.1	16	*Ca.* Liberibacter asiaticus	porin
WP_012778614.1	26	*Ca.* Liberibacter asiaticus	LPS assembly protein LptD
WP_013462180.1	8	*Ca.* Liberibacter solanacearum	hypothetical protein
WP_013461455.1	8	*Ca.* Liberibacter solanacearum	outer membrane beta-barrel protein
WP_013462120.1	8	*Ca.* Liberibacter solanacearum	outer membrane beta-barrel protein
WP_013461646.1	16	*Ca.* Liberibacter solanacearum	outer membrane protein assembly factor BamA
WP_013461918.1	16	*Ca.* Liberibacter solanacearum	porin
WP_244391984.1	26	*Ca.* Liberibacter solanacearum	LPS assembly protein LptD
WP_139348375.1	8	*Dickeya dadantii*	lipid IV(A) palmitoyltransferase PagP
WP_013317880.1	8	*Dickeya dadantii*	MULTISPECIES: outer membrane protein OmpW
WP_013317534.1	8	*Dickeya dadantii*	outer membrane protein OmpX
WP_013318906.1	8	*Dickeya dadantii*	porin OmpA
WP_033111697.1	10	*Dickeya dadantii*	YfaZ family outer membrane protein

WP_237703446.1	12	*Dickeya dadantii*	autotransporter domain-containing protein
WP_013318191.1	12	*Dickeya dadantii*	DUF481 domain-containing protein
WP_013316665.1	12	*Dickeya dadantii*	MipA/OmpV family protein
WP_013317841.1	12	*Dickeya dadantii*	MipA/OmpV family protein
WP_013319447.1	12	*Dickeya dadantii*	nucleoside-specific channel-forming protein Tsx
WP_013318071.1	12	*Dickeya dadantii*	oligogalacturonate-specific porin KdgM
WP_033112125.1	12	*Dickeya dadantii*	phospholipase A
WP_013317881.1	12	*Dickeya dadantii*	porin
WP_224063073.1	12	*Dickeya dadantii*	transporter
WP_013316670.1	14	*Dickeya dadantii*	conjugal transfer protein TraF
WP_013318769.1	14	*Dickeya dadantii*	long-chain fatty acid transporter FadL
WP_139348318.1	16	*Dickeya dadantii*	autotransporter assembly complex protein TamA
WP_013315818.1	16	*Dickeya dadantii*	cellulose biosynthesis protein BcsC
WP_013316758.1	16	*Dickeya dadantii*	outer membrane protein assembly factor BamA
WP_033111930.1	16	*Dickeya dadantii*	porin
WP_107768474.1	16	*Dickeya dadantii*	porin
WP_148226907.1	16	*Dickeya dadantii*	porin
WP_013318107.1	16	*Dickeya dadantii*	ShlB/FhaC/HecB family hemolysin secretion/activation protein
WP_013316070.1	18	*Dickeya dadantii*	carbohydrate porin
WP_013318351.1	18	*Dickeya dadantii*	carbohydrate porin
WP_013318830.1	18	*Dickeya dadantii*	maltoporin
WP_013316226.1	18	*Dickeya dadantii*	outer membrane beta-barrel protein
WP_013316596.1	22	*Dickeya dadantii*	TonB-dependent receptor
WP_013316926.1	22	*Dickeya dadantii*	TonB-dependent receptor
WP_013317107.1	22	*Dickeya dadantii*	TonB-dependent receptor
WP_013317291.1	22	*Dickeya dadantii*	TonB-dependent receptor
WP_033111759.1	22	*Dickeya dadantii*	TonB-dependent receptor
WP_013316406.1	22	*Dickeya dadantii*	TonB-dependent siderophore receptor
WP_013318789.1	22	*Dickeya dadantii*	TonB-dependent siderophore receptor
WP_013319435.1	22	*Dickeya dadantii*	TonB-dependent siderophore receptor

WP_237703431.1	22	*Dickeya dadantii*	TonB-dependent siderophore receptor
WP_013315912.1	22	*Dickeya dadantii*	TonB-dependent vitamin B12 receptor BtuB
WP_013317092.1	24	*Dickeya dadantii*	YjbH domain-containing protein
WP_077245922.1	26	*Dickeya dadantii*	LPS assembly protein LptD
WP_004155636.1	8	*Erwinia amylovora*	Ail/Lom family outer membrane beta-barrel protein
WP_004157755.1	8	*Erwinia amylovora*	outer membrane protein OmpW
WP_004156821.1	8	*Erwinia amylovora*	outer membrane protein OmpX
WP_004156983.1	8	*Erwinia amylovora*	porin OmpA
WP_013035937.1	10	*Erwinia amylovora*	lipid IV(A) palmitoyltransferase PagP
WP_004159658.1	10	*Erwinia amylovora*	omptin family outer membrane protease
WP_004159662.1	10	*Erwinia amylovora*	omptin family outer membrane protease
WP_004161755.1	10	*Erwinia amylovora*	omptin family outer membrane protease
WP_004160394.1	10	*Erwinia amylovora*	YfaZ family outer membrane protein
WP_004157369.1	12	*Erwinia amylovora*	DUF481 domain-containing protein
WP_004157818.1	12	*Erwinia amylovora*	MipA/OmpV family protein
WP_004159346.1	12	*Erwinia amylovora*	nucleoside-specific channel-forming protein Tsx
WP_004154940.1	12	*Erwinia amylovora*	phospholipase A
WP_004157336.1	12	*Erwinia amylovora*	YchO/YchP family invasin
WP_004160481.1	14	*Erwinia amylovora*	conjugal transfer protein TraF
WP_004160434.1	14	*Erwinia amylovora*	inverse autotransporter beta domain-containing protein
WP_004158735.1	14	*Erwinia amylovora*	long-chain fatty acid transporter FadL
WP_169799808.1	16	*Erwinia amylovora*	autotransporter assembly complex protein TamA
WP_004161057.1	16	*Erwinia amylovora*	cellulose biosynthesis protein BcsC
WP_004159456.1	16	*Erwinia amylovora*	outer membrane protein assembly factor BamA
WP_127133427.1	16	*Erwinia amylovora*	porin
WP_164877356.1	16	*Erwinia amylovora*	porin

WP_004158535.1	16	*Erwinia amylovora*	porin OmpC
WP_127133424.1	16	*Erwinia amylovora*	porin OmpC
WP_004155666.1	16	*Erwinia amylovora*	ShlB/FhaC/HecB family hemolysin secretion/activation protein
WP_004159813.1	16	*Erwinia amylovora*	ShlB/FhaC/HecB family hemolysin secretion/activation protein
WP_004160423.1	16	*Erwinia amylovora*	ShlB/FhaC/HecB family hemolysin secretion/activation protein
WP_004157323.1	18	*Erwinia amylovora*	carbohydrate porin
WP_004163947.1	22	*Erwinia amylovora*	fimbria/pilus outer membrane usher protein
WP_004157621.1	22	*Erwinia amylovora*	TonB-dependent copper receptor
WP_004157532.1	22	*Erwinia amylovora*	TonB-dependent receptor
WP_004160310.1	22	*Erwinia amylovora*	TonB-dependent siderophore receptor
WP_004154994.1	24	*Erwinia amylovora*	F4 (K88) fimbrial usher FaeD
WP_004157684.1	24	*Erwinia amylovora*	fimbria/pilus outer membrane usher protein
WP_004156570.1	24	*Erwinia amylovora*	TonB-dependent receptor
WP_004160506.1	24	*Erwinia amylovora*	YjbH domain-containing protein
WP_004159749.1	26	*Erwinia amylovora*	LPS assembly protein LptD
YP_009518782.1	4	*Escherichia coli*	putative uncharacterized protein YddL
NP_415155.1	8	*Escherichia coli*	Lipid A palmitoyltransferase
NP_415477.1	8	*Escherichia coli*	outer membrane protein A
NP_415772.1	8	*Escherichia coli*	outer membrane protein W
NP_415335.1	8	*Escherichia coli*	outer membrane protein X
NP_418004.4	8	*Escherichia coli*	putative outer membrane protein YhjY
NP_415097.1	10	*Escherichia coli*	omptin family outer membrane protease OmpT
NP_416753.4	10	*Escherichia coli*	putative porin YfaZ
NP_416236.1	12	*Escherichia coli*	acid-inducible putative outer membrane protein YdiY
NP_417134.2	12	*Escherichia coli*	adhesin-like autotransporter YpjA

NP_415100.1	12	*Escherichia coli*	exopolysaccharide secretion system outer membrane protein NfrA
YP_009518785.1	12	*Escherichia coli*	fimbrial usher domain-containing protein YdeT
NP_416485.4	12	*Escherichia coli*	inverse autotransporter adhesin
NP_416296.1	12	*Escherichia coli*	MltA-interacting protein
NP_418731.2	12	*Escherichia coli*	N-acetylneuraminate outer membrane channel
NP_414945.1	12	*Escherichia coli*	nucleoside-specific channel-forming protein Tsx
NP_418265.1	12	*Escherichia coli*	outer membrane phospholipase A
NP_418041.1	12	*Escherichia coli*	outer membrane protein YiaT
NP_415720.1	12	*Escherichia coli*	putative autotransporter adhesin YcgV
NP_416736.1	12	*Escherichia coli*	putative autotransporter adhesin YfaL
NP_415738.2	12	*Escherichia coli*	putative invasin YchO
NP_418311.1	12	*Escherichia coli*	putative outer membrane porin L
NP_416903.1	12	*Escherichia coli*	putative outer membrane porin YfeN
YP_026164.1	12	*Escherichia coli*	self recognizing antigen 43 (Ag43) autotransporter
NP_416846.2	14	*Escherichia coli*	long-chain fatty acid outer membrane channel/bacteriophage T2 receptor
NP_415835.1	14	*Escherichia coli*	outer membrane porin G
NP_414892.1	14	*Escherichia coli*	outer membrane protein YaiO
YP_026226.4	16	*Escherichia coli*	cellulose synthase outer membrane channel
NP_416719.1	16	*Escherichia coli*	outer membrane porin C
NP_415449.1	16	*Escherichia coli*	outer membrane porin F
NP_415895.1	16	*Escherichia coli*	outer membrane porin N
NP_414776.1	16	*Escherichia coli*	outer membrane porin PhoE
NP_414719.1	16	*Escherichia coli*	outer membrane protein assembly factor BamA
NP_418641.1	16	*Escherichia coli*	translocation and assembly module subunit TamA
NP_418176.1	18	*Escherichia coli*	carbohydrate-specific outer membrane porin, cryptic
NP_415207.1	18	*Escherichia coli*	chitooligosaccharide outer membrane channel
NP_418460.1	18	*Escherichia coli*	maltose outer membrane channel/phage lambda receptor protein
NP_416132.2	18	*Escherichia coli*	outer membrane porin family protein UidC

NP_418401.1	22	*Escherichia coli*	cobalamin outer membrane transporter
NP_418711.1	22	*Escherichia coli*	ferric citrate outer membrane transporter
NP_415620.1	22	*Escherichia coli*	ferric coprogen/ferric rhodotorulic acid outer membrane transporter
NP_415116.1	22	*Escherichia coli*	ferric enterobactin outer membrane transporter
NP_414692.1	22	*Escherichia coli*	ferrichrome outer membrane transporter/phage receptor
NP_415326.1	22	*Escherichia coli*	iron catecholate outer membrane transporter Fiu
NP_416660.1	22	*Escherichia coli*	iron-catecholate outer membrane transporter CirA
NP_415460.1	24	*Escherichia coli*	putative fimbrial usher protein ElfC
NP_414681.1	24	*Escherichia coli*	putative fimbrial usher protein HtrE
NP_415065.1	24	*Escherichia coli*	putative fimbrial usher protein SfmD
NP_415246.2	24	*Escherichia coli*	putative fimbrial usher protein YbgQ
NP_416612.1	24	*Escherichia coli*	putative fimbrial usher protein YehB
NP_417683.1	24	*Escherichia coli*	putative fimbrial usher protein YhcD
NP_417613.1	24	*Escherichia coli*	putative fimbrial usher protein YraJ
NP_415504.1	24	*Escherichia coli*	putative lipoprotein GfcD
NP_418453.1	24	*Escherichia coli*	putative lipoprotein YjbH
NP_415968.1	24	*Escherichia coli*	putative TonB-dependent outer membrane receptor
NP_418737.1	24	*Escherichia coli*	type I fimbriae usher protein
NP_414596.1	26	*Escherichia coli*	lipopolysaccharide assembly protein LptD
WP_015272991.1	8	*Liberibacter crescens*	outer membrane beta-barrel protein
WP_015273041.1	8	*Liberibacter crescens*	porin family protein
WP_015273568.1	8	*Liberibacter crescens*	porin family protein
WP_244422703.1	8	*Liberibacter crescens*	porin family protein
WP_172792750.1	16	*Liberibacter crescens*	autotransporter assembly complex protein TamA
WP_015272467.1	16	*Liberibacter crescens*	outer membrane protein assembly factor BamA
WP_015273477.1	16	*Liberibacter crescens*	porin

WP_015272661.1	26	*Liberibacter crescens*	LPS-assembly protein LptD
WP_161502089.1	6	*Pectobacterium carotovorum*	TolC family protein
WP_010298186.1	8	*Pectobacterium carotovorum*	Ail/Lom family outer membrane beta-barrel protein
WP_010300796.1	8	*Pectobacterium carotovorum*	MULTISPECIES: lipid IV(A) palmitoyltransferase PagP
WP_010295200.1	8	*Pectobacterium carotovorum*	MULTISPECIES: outer membrane protein OmpW
WP_010294853.1	8	*Pectobacterium carotovorum*	MULTISPECIES: outer membrane protein OmpX
WP_010305600.1	8	*Pectobacterium carotovorum*	porin OmpA
WP_010301323.1	10	*Pectobacterium carotovorum*	MULTISPECIES: YfaZ family outer membrane protein
WP_010295627.1	12	*Pectobacterium carotovorum*	autotransporter domain-containing protein
WP_010301614.1	12	*Pectobacterium carotovorum*	autotransporter domain-containing protein
WP_010310071.1	12	*Pectobacterium carotovorum*	DUF481 domain-containing protein
WP_010298973.1	12	*Pectobacterium carotovorum*	MipA/OmpV family protein
WP_039472997.1	12	*Pectobacterium carotovorum*	MULTISPECIES: MipA/OmpV family protein
WP_051982089.1	12	*Pectobacterium carotovorum*	MULTISPECIES: MipA/OmpV family protein
WP_010294533.1	12	*Pectobacterium carotovorum*	MULTISPECIES: phospholipase A
WP_010295566.1	12	*Pectobacterium carotovorum*	MULTISPECIES: porin
WP_010295568.1	12	*Pectobacterium carotovorum*	MULTISPECIES: porin
WP_010297950.1	12	*Pectobacterium carotovorum*	nucleoside-specific channel-forming protein Tsx
WP_010295199.1	12	*Pectobacterium carotovorum*	porin
WP_010299975.1	12	*Pectobacterium carotovorum*	porin
WP_010298583.1	14	*Pectobacterium carotovorum*	long-chain fatty acid transporter FadL
WP_235677737.1	16	*Pectobacterium carotovorum*	cellulose biosynthesis protein BcsC
WP_029368859.1	16	*Pectobacterium carotovorum*	MULTISPECIES: autotransporter assembly complex protein TamA
WP_010296417.1	16	*Pectobacterium carotovorum*	outer membrane protein assembly factor BamA
WP_117624693.1	16	*Pectobacterium carotovorum*	porin

WP_010295858.1	16	*Pectobacterium carotovorum*	ShlB/FhaC/HecB family hemolysin secretion/activation protein
WP_161502473.1	16	*Pectobacterium carotovorum*	ShlB/FhaC/HecB family hemolysin secretion/activation protein
WP_010297545.1	18	*Pectobacterium carotovorum*	carbohydrate porin
WP_010307908.1	18	*Pectobacterium carotovorum*	carbohydrate porin
WP_039532164.1	18	*Pectobacterium carotovorum*	carbohydrate porin
WP_010300985.1	18	*Pectobacterium carotovorum*	maltoporin
WP_010303439.1	18	*Pectobacterium carotovorum*	outer membrane beta-barrel protein
WP_161502823.1	22	*Pectobacterium carotovorum*	ferric-rhodotorulic acid/ferric-coprogen receptor FhuE
WP_161502284.1	22	*Pectobacterium carotovorum*	fimbrial biogenesis outer membrane usher protein
WP_010296513.1	22	*Pectobacterium carotovorum*	TonB-dependent hemoglobin/transferrin/lactoferri n family receptor
WP_010295343.1	22	*Pectobacterium carotovorum*	TonB-dependent receptor
WP_010297642.1	22	*Pectobacterium carotovorum*	TonB-dependent receptor
WP_010300047.1	22	*Pectobacterium carotovorum*	TonB-dependent receptor
WP_010301901.1	22	*Pectobacterium carotovorum*	TonB-dependent receptor
WP_010303068.1	22	*Pectobacterium carotovorum*	TonB-dependent receptor
WP_010309469.1	22	*Pectobacterium carotovorum*	TonB-dependent receptor
WP_029367294.1	22	*Pectobacterium carotovorum*	TonB-dependent receptor
WP_029369100.1	22	*Pectobacterium carotovorum*	TonB-dependent receptor
WP_161502944.1	22	*Pectobacterium carotovorum*	TonB-dependent receptor
WP_180890010.1	22	*Pectobacterium carotovorum*	TonB-dependent receptor
WP_010295756.1	22	*Pectobacterium carotovorum*	TonB-dependent siderophore receptor
WP_010298688.1	22	*Pectobacterium carotovorum*	TonB-dependent siderophore receptor
WP_010300453.1	22	*Pectobacterium carotovorum*	TonB-dependent siderophore receptor
WP_010305812.1	22	*Pectobacterium carotovorum*	TonB-dependent siderophore receptor

WP_010307464.1	22	*Pectobacterium carotovorum*	TonB-dependent siderophore receptor
WP_029368757.1	22	*Pectobacterium carotovorum*	TonB-dependent siderophore receptor
WP_180890091.1	22	*Pectobacterium carotovorum*	TonB-dependent siderophore receptor
WP_010308147.1	22	*Pectobacterium carotovorum*	TonB-dependent vitamin B12 receptor BtuB
WP_010301944.1	24	*Pectobacterium carotovorum*	fimbria/pilus outer membrane usher protein
WP_010296816.1	24	*Pectobacterium carotovorum*	YjbH domain-containing protein
WP_010299752.1	26	*Pectobacterium carotovorum*	LPS assembly protein LptD
NP_253350.1	8	*Pseudomonas aeruginosa*	lipid A 3-O-deacylase
NP_250468.1	8	*Pseudomonas aeruginosa*	outer membrane porin F
NP_252756.1	8	*Pseudomonas aeruginosa*	outer membrane protein OprG
NP_250754.1	12	*Pseudomonas aeruginosa*	copper resistance protein B
NP_253799.1	12	*Pseudomonas aeruginosa*	esterase
NP_248855.1	12	*Pseudomonas aeruginosa*	hypothetical protein PA0165
NP_249019.1	12	*Pseudomonas aeruginosa*	hypothetical protein PA0328
NP_249797.1	12	*Pseudomonas aeruginosa*	hypothetical protein PA1106
NP_250641.1	12	*Pseudomonas aeruginosa*	hypothetical protein PA1951
NP_251111.1	12	*Pseudomonas aeruginosa*	hypothetical protein PA2421
NP_251164.1	12	*Pseudomonas aeruginosa*	hypothetical protein PA2474
NP_252461.1	12	*Pseudomonas aeruginosa*	hypothetical protein PA3772
NP_253080.1	12	*Pseudomonas aeruginosa*	hypothetical protein PA4390
NP_253081.1	12	*Pseudomonas aeruginosa*	hypothetical protein PA4391
NP_254012.1	12	*Pseudomonas aeruginosa*	hypothetical protein PA5325
NP_252225.1	12	*Pseudomonas aeruginosa*	serine protease
NP_249979.1	14	*Pseudomonas aeruginosa*	hypothetical protein PA1288
NP_250455.1	14	*Pseudomonas aeruginosa*	hypothetical protein PA1764

NP_253279.1	14	*Pseudomonas aeruginosa*	hypothetical protein PA4589
NP_250981.1	16	*Pseudomonas aeruginosa*	glucose-sensitive porin
NP_248730.1	16	*Pseudomonas aeruginosa*	hypothetical protein PA0040
NP_249383.1	16	*Pseudomonas aeruginosa*	hypothetical protein PA0692
NP_249387.1	16	*Pseudomonas aeruginosa*	hypothetical protein PA0696
NP_250664.1	16	*Pseudomonas aeruginosa*	hypothetical protein PA1974
NP_251153.1	16	*Pseudomonas aeruginosa*	hypothetical protein PA2463
NP_251233.1	16	*Pseudomonas aeruginosa*	hypothetical protein PA2543
NP_252788.1	16	*Pseudomonas aeruginosa*	hypothetical protein PA4099
NP_253230.1	16	*Pseudomonas aeruginosa*	hypothetical protein PA4540
NP_253314.1	16	*Pseudomonas aeruginosa*	hypothetical protein PA4624
NP_252338.1	16	*Pseudomonas aeruginosa*	outer membrane protein Opr86
NP_251969.1	16	*Pseudomonas aeruginosa*	phosphate-specific outer membrane porin OprP
NP_251876.1	16	*Pseudomonas aeruginosa*	porin B
NP_251970.1	16	*Pseudomonas aeruginosa*	pyrophosphate-specific outer membrane porin OprO
NP_252234.1	18	*Pseudomonas aeruginosa*	alginate production protein AlgE
NP_248982.1	18	*Pseudomonas aeruginosa*	anaerobically-induced outer membrane porin OprE
NP_249446.1	18	*Pseudomonas aeruginosa*	cis-aconitate porin OpdH
NP_251772.1	18	*Pseudomonas aeruginosa*	glycine betaine transmethylase
NP_253191.1	18	*Pseudomonas aeruginosa*	glycine-glutamate dipeptide porin OpdP
NP_248852.1	18	*Pseudomonas aeruginosa*	histidine porin OpdC
NP_251450.1	18	*Pseudomonas aeruginosa*	hypothetical protein PA2760
NP_252112.1	18	*Pseudomonas aeruginosa*	hypothetical protein PA3422
NP_252612.1	18	*Pseudomonas aeruginosa*	hypothetical protein PA3923
NP_251390.1	18	*Pseudomonas aeruginosa*	OpdB proline porin

NP_252029.1	18	*Pseudomonas aeruginosa*	patatin-like protein
NP_248879.1	18	*Pseudomonas aeruginosa*	porin
NP_248931.1	18	*Pseudomonas aeruginosa*	porin
NP_249716.1	18	*Pseudomonas aeruginosa*	porin
NP_250903.1	18	*Pseudomonas aeruginosa*	porin
NP_251110.1	18	*Pseudomonas aeruginosa*	porin
NP_251728.1	18	*Pseudomonas aeruginosa*	porin
NP_252278.1	18	*Pseudomonas aeruginosa*	porin
NP_252826.1	18	*Pseudomonas aeruginosa*	porin
NP_252868.1	18	*Pseudomonas aeruginosa*	porin
NP_249649.1	18	*Pseudomonas aeruginosa*	porin D
NP_250803.1	18	*Pseudomonas aeruginosa*	pyroglutatmate porin OpdO
NP_251195.1	18	*Pseudomonas aeruginosa*	tyrosine porin OpdT
NP_253585.1	18	*Pseudomonas aeruginosa*	vanillate porin OpdK
NP_252479.1	22	*Pseudomonas aeruginosa*	copper transport outer membrane porin OprC
NP_252590.1	22	*Pseudomonas aeruginosa*	Fe(III) dicitrate transporter FecA
NP_252911.1	22	*Pseudomonas aeruginosa*	Fe(III)-pyochelin outer membrane receptor
NP_251378.1	22	*Pseudomonas aeruginosa*	ferric enterobactin receptor
NP_250600.1	22	*Pseudomonas aeruginosa*	ferric-mycobactin receptor FemA
NP_249161.1	22	*Pseudomonas aeruginosa*	ferrichrome receptor FiuA
NP_251156.1	22	*Pseudomonas aeruginosa*	ferrioxamine receptor FoxA
NP_251088.1	22	*Pseudomonas aeruginosa*	ferripyoverdine receptor
NP_252098.1	22	*Pseudomonas aeruginosa*	heme uptake outer membrane receptor HasR
NP_249993.1	22	*Pseudomonas aeruginosa*	heme utilization protein
NP_253398.1	22	*Pseudomonas aeruginosa*	heme/hemoglobin uptake outer membrane receptor PhuR

NP_249125.1	22	*Pseudomonas aeruginosa*	hypothetical protein PA0434
NP_249472.1	22	*Pseudomonas aeruginosa*	hypothetical protein PA0781
NP_250304.1	22	*Pseudomonas aeruginosa*	hypothetical protein PA1613
NP_250747.1	22	*Pseudomonas aeruginosa*	hypothetical protein PA2057
NP_250760.1	22	*Pseudomonas aeruginosa*	hypothetical protein PA2070
NP_250779.1	22	*Pseudomonas aeruginosa*	hypothetical protein PA2089
NP_250979.1	22	*Pseudomonas aeruginosa*	hypothetical protein PA2289
NP_251280.1	22	*Pseudomonas aeruginosa*	hypothetical protein PA2590
NP_253524.1	22	*Pseudomonas aeruginosa*	hypothetical protein PA4837
NP_253584.1	22	*Pseudomonas aeruginosa*	hypothetical protein PA4897
NP_253204.1	22	*Pseudomonas aeruginosa*	iron transport outer membrane receptor
NP_249622.1	22	*Pseudomonas aeruginosa*	outer membrane receptor FepA
NP_252857.1	22	*Pseudomonas aeruginosa*	second ferric pyoverdine receptor FpvB
NP_250056.1	22	*Pseudomonas aeruginosa*	siderophore receptor
NP_248841.1	22	*Pseudomonas aeruginosa*	TonB-dependent receptor
NP_248882.1	22	*Pseudomonas aeruginosa*	TonB-dependent receptor
NP_249962.1	22	*Pseudomonas aeruginosa*	tonB-dependent receptor
NP_250013.1	22	*Pseudomonas aeruginosa*	TonB-dependent receptor
NP_250612.1	22	*Pseudomonas aeruginosa*	TonB-dependent receptor
NP_251025.1	22	*Pseudomonas aeruginosa*	TonB-dependent receptor
NP_251601.1	22	*Pseudomonas aeruginosa*	TonB-dependent receptor
NP_251958.1	22	*Pseudomonas aeruginosa*	TonB-dependent receptor
NP_252845.1	22	*Pseudomonas aeruginosa*	TonB-dependent receptor
NP_253364.1	22	*Pseudomonas aeruginosa*	TonB-dependent receptor
NP_253341.1	24	*Pseudomonas aeruginosa*	hypothetical protein PA4652

NP_250820.1	24	*Pseudomonas aeruginosa*	usher CupA3
NP_252773.1	24	*Pseudomonas aeruginosa*	usher CupB3
NP_249685.1	24	*Pseudomonas aeruginosa*	usher CupC3
NP_249286.1	26	*Pseudomonas aeruginosa*	organic solvent tolerance protein OstA
WP_226992697.1	8	*Pseudomonas syringae*	MULTISPECIES: acyloxyacyl hydrolase
WP_003382460.1	8	*Pseudomonas syringae*	MULTISPECIES: OmpA family protein
WP_005768999.1	8	*Pseudomonas syringae*	MULTISPECIES: outer membrane beta-barrel protein
WP_005768209.1	8	*Pseudomonas syringae*	MULTISPECIES: transporter
WP_011104353.1	10	*Pseudomonas syringae*	carbohydrate porin
WP_046463799.1	12	*Pseudomonas syringae*	autotransporter domain-containing protein
WP_011103197.1	12	*Pseudomonas syringae*	autotransporter domain-containing SGNH/GDSL hydrolase family protein
WP_011103249.1	12	*Pseudomonas syringae*	autotransporter outer membrane beta-barrel domain-containing protein
WP_011103898.1	12	*Pseudomonas syringae*	autotransporter outer membrane beta-barrel domain-containing protein
WP_046463456.1	12	*Pseudomonas syringae*	autotransporter outer membrane beta-barrel domain-containing protein
WP_057443127.1	12	*Pseudomonas syringae*	autotransporter outer membrane beta-barrel domain-containing protein
WP_011103648.1	12	*Pseudomonas syringae*	autotransporter serine protease
WP_046463927.1	12	*Pseudomonas syringae*	autotransporter serine protease
WP_005764229.1	12	*Pseudomonas syringae*	MULTISPECIES: bacteriophage N4 adsorption protein A
WP_044392483.1	12	*Pseudomonas syringae*	MULTISPECIES: copper resistance protein B
WP_005764776.1	12	*Pseudomonas syringae*	MULTISPECIES: DUF3034 family protein
WP_005620274.1	12	*Pseudomonas syringae*	MULTISPECIES: DUF481 domain-containing protein
WP_005765329.1	12	*Pseudomonas syringae*	MULTISPECIES: membrane protein
WP_005762734.1	12	*Pseudomonas syringae*	MULTISPECIES: MipA/OmpV family protein

WP_005764915.1	12	*Pseudomonas syringae*	MULTISPECIES: nucleoside-specific channel-forming protein Tsx
WP_005770839.1	12	*Pseudomonas syringae*	MULTISPECIES: porin
WP_003382526.1	12	*Pseudomonas syringae*	MULTISPECIES: TorF family putative porin
WP_011105037.1	12	*Pseudomonas syringae*	MULTISPECIES: transporter
WP_046463880.1	14	*Pseudomonas syringae*	autotransporter domain-containing protein
WP_011103336.1	14	*Pseudomonas syringae*	MULTISPECIES: outer membrane protein transport protein
WP_046463934.1	14	*Pseudomonas syringae*	MULTISPECIES: outer membrane protein transport protein
WP_011104170.1	16	*Pseudomonas syringae*	autotransporter assembly complex protein TamA
WP_046463740.1	16	*Pseudomonas syringae*	cellulose biosynthesis protein BcsC
WP_005736419.1	16	*Pseudomonas syringae*	MULTISPECIES: carbohydrate porin
WP_007245414.1	16	*Pseudomonas syringae*	MULTISPECIES: outer membrane protein assembly factor BamA
WP_193383854.1	16	*Pseudomonas syringae*	ShlB/FhaC/HecB family hemolysin secretion/activation protein
WP_011103441.1	18	*Pseudomonas syringae*	DUF1302 domain-containing protein
WP_005615404.1	18	*Pseudomonas syringae*	MULTISPECIES: alginate export family protein
WP_032639929.1	18	*Pseudomonas syringae*	MULTISPECIES: carbohydrate porin
WP_011105421.1	18	*Pseudomonas syringae*	MULTISPECIES: OprD family outer membrane porin
WP_005763528.1	18	*Pseudomonas syringae*	MULTISPECIES: OprD family porin
WP_005769381.1	18	*Pseudomonas syringae*	MULTISPECIES: OprD family porin
WP_007244158.1	18	*Pseudomonas syringae*	MULTISPECIES: OprD family porin
WP_011105463.1	18	*Pseudomonas syringae*	MULTISPECIES: OprD family porin
WP_011103959.1	18	*Pseudomonas syringae*	OprD family porin
WP_011104277.1	18	*Pseudomonas syringae*	OprD family porin
WP_011104478.1	18	*Pseudomonas syringae*	OprD family porin

WP_011104816.1	18	*Pseudomonas syringae*	OprD family porin
WP_046463479.1	18	*Pseudomonas syringae*	OprD family porin
WP_005762818.1	22	*Pseudomonas syringae*	MULTISPECIES: TonB-dependent receptor
WP_005764059.1	22	*Pseudomonas syringae*	MULTISPECIES: TonB-dependent receptor
WP_005764409.1	22	*Pseudomonas syringae*	MULTISPECIES: TonB-dependent receptor
WP_005771478.1	22	*Pseudomonas syringae*	MULTISPECIES: TonB-dependent receptor
WP_007246690.1	22	*Pseudomonas syringae*	MULTISPECIES: TonB-dependent receptor
WP_005765172.1	22	*Pseudomonas syringae*	MULTISPECIES: TonB-dependent siderophore receptor
WP_005769699.1	22	*Pseudomonas syringae*	MULTISPECIES: TonB-dependent siderophore receptor
WP_005771258.1	22	*Pseudomonas syringae*	MULTISPECIES: TonB-dependent siderophore receptor
WP_011103229.1	22	*Pseudomonas syringae*	TonB-dependent receptor
WP_011103281.1	22	*Pseudomonas syringae*	TonB-dependent receptor
WP_011104229.1	22	*Pseudomonas syringae*	TonB-dependent receptor
WP_011104454.1	22	*Pseudomonas syringae*	TonB-dependent receptor
WP_011104482.1	22	*Pseudomonas syringae*	TonB-dependent receptor
WP_011104883.1	22	*Pseudomonas syringae*	TonB-dependent receptor
WP_044389891.1	22	*Pseudomonas syringae*	TonB-dependent receptor
WP_044392586.1	22	*Pseudomonas syringae*	TonB-dependent receptor
WP_046463781.1	22	*Pseudomonas syringae*	TonB-dependent receptor
WP_226992700.1	22	*Pseudomonas syringae*	TonB-dependent receptor
WP_011103467.1	22	*Pseudomonas syringae*	TonB-dependent siderophore receptor
WP_011103468.1	22	*Pseudomonas syringae*	TonB-dependent siderophore receptor
WP_011103628.1	22	*Pseudomonas syringae*	TonB-dependent siderophore receptor
WP_011104570.1	22	*Pseudomonas syringae*	TonB-dependent siderophore receptor
WP_011104677.1	22	*Pseudomonas syringae*	TonB-dependent siderophore receptor

WP_046463309.1	22	*Pseudomonas syringae*	TonB-dependent siderophore receptor
WP_226992672.1	22	*Pseudomonas syringae*	TonB-dependent siderophore receptor
WP_011103899.1	24	*Pseudomonas syringae*	fimbrial biogenesis outer membrane usher protein
WP_046463957.1	26	*Pseudomonas syringae*	LPS-assembly protein LptD
WP_003261236.1	8	*Ralstonia solanacearum*	acyloxyacyl hydrolase
WP_231408959.1	8	*Ralstonia solanacearum*	hypothetical protein
WP_013206924.1	8	*Ralstonia solanacearum*	OmpW family protein
WP_231408600.1	8	*Ralstonia solanacearum*	OmpW family protein
WP_231408691.1	8	*Ralstonia solanacearum*	OmpW family protein
WP_013207000.1	12	*Ralstonia solanacearum*	acetate kinase
WP_231408648.1	12	*Ralstonia solanacearum*	autotransporter domain-containing protein
WP_013206849.1	12	*Ralstonia solanacearum*	hypothetical protein
WP_064045134.1	12	*Ralstonia solanacearum*	MipA/OmpV family protein
WP_231408680.1	12	*Ralstonia solanacearum*	MipA/OmpV family protein
WP_231408522.1	12	*Ralstonia solanacearum*	putative Ig domain-containing protein
WP_231409783.1	12	*Ralstonia solanacearum*	tetratricopeptide repeat protein
WP_231408716.1	12	*Ralstonia solanacearum*	TonB-dependent receptor
WP_013207087.1	12	*Ralstonia solanacearum*	TorF family putative porin
WP_231408591.1	12	*Ralstonia solanacearum*	TorF family putative porin
WP_064299007.1	12	*Ralstonia solanacearum*	transporter
WP_231410117.1	12	*Ralstonia solanacearum*	transporter
WP_064297480.1	16	*Ralstonia solanacearum*	autotransporter assembly complex protein TamA
WP_013207399.1	16	*Ralstonia solanacearum*	carbohydrate porin
WP_231409156.1	16	*Ralstonia solanacearum*	carbohydrate porin
WP_231410014.1	16	*Ralstonia solanacearum*	carbohydrate porin

WP_003268143.1	16	*Ralstonia solanacearum*	outer membrane protein assembly factor BamA
WP_013204660.1	16	*Ralstonia solanacearum*	porin
WP_013204888.1	16	*Ralstonia solanacearum*	porin
WP_013205071.1	16	*Ralstonia solanacearum*	porin
WP_013206003.1	16	*Ralstonia solanacearum*	porin
WP_013208105.1	16	*Ralstonia solanacearum*	porin
WP_013208299.1	16	*Ralstonia solanacearum*	porin
WP_042590525.1	16	*Ralstonia solanacearum*	porin
WP_231408759.1	16	*Ralstonia solanacearum*	porin
WP_231408891.1	16	*Ralstonia solanacearum*	porin
WP_231409853.1	16	*Ralstonia solanacearum*	porin
WP_231410140.1	16	*Ralstonia solanacearum*	porin
WP_043944648.1	16	*Ralstonia solanacearum*	ShlB/FhaC/HecB family hemolysin secretion/activation protein
WP_231409384.1	16	*Ralstonia solanacearum*	ShlB/FhaC/HecB family hemolysin secretion/activation protein
WP_231409485.1	16	*Ralstonia solanacearum*	ShlB/FhaC/HecB family hemolysin secretion/activation protein
WP_231409747.1	16	*Ralstonia solanacearum*	ShlB/FhaC/HecB family hemolysin secretion/activation protein
WP_231409760.1	16	*Ralstonia solanacearum*	ShlB/FhaC/HecB family hemolysin secretion/activation protein
WP_231409503.1	18	*Ralstonia solanacearum*	carbohydrate porin
WP_231410041.1	22	*Ralstonia solanacearum*	fimbrial biogenesis outer membrane usher protein
WP_013208186.1	22	*Ralstonia solanacearum*	TonB-dependent receptor
WP_042589717.1	22	*Ralstonia solanacearum*	TonB-dependent receptor
WP_231408714.1	22	*Ralstonia solanacearum*	TonB-dependent receptor
WP_231409235.1	22	*Ralstonia solanacearum*	TonB-dependent receptor

WP_231409287.1	22	*Ralstonia solanacearum*	TonB-dependent receptor
WP_231409424.1	22	*Ralstonia solanacearum*	TonB-dependent receptor
WP_231409532.1	22	*Ralstonia solanacearum*	TonB-dependent receptor
WP_231410203.1	22	*Ralstonia solanacearum*	TonB-dependent receptor
WP_231410210.1	22	*Ralstonia solanacearum*	TonB-dependent receptor
WP_231408745.1	22	*Ralstonia solanacearum*	TonB-dependent siderophore receptor
WP_231409506.1	22	*Ralstonia solanacearum*	TonB-dependent siderophore receptor
WP_231409836.1	22	*Ralstonia solanacearum*	TonB-dependent siderophore receptor
WP_042591765.1	26	*Ralstonia solanacearum*	LPS-assembly protein LptD
NP_459304.1	8	*Salmonella enterica*	adhesin
NP_459897.1	8	*Salmonella enterica*	Fels-1 prophage attachment and invasion protein
NP_460018.1	8	*Salmonella enterica*	Gifsy-2 prophage attachment and invasion protein homolog
NP_459341.1	8	*Salmonella enterica*	hypothetical protein
NP_460215.1	8	*Salmonella enterica*	hypothetical protein
NP_461948.1	8	*Salmonella enterica*	hypothetical protein
NP_462542.1	8	*Salmonella enterica*	hypothetical protein
NP_460691.1	8	*Salmonella enterica*	outer membrane protein OmpW
NP_459810.1	8	*Salmonella enterica*	outer membrane protein OmpX
NP_459620.1	8	*Salmonella enterica*	PhoPQ-activated gene
NP_460044.1	8	*Salmonella enterica*	porin OmpA
NP_490524.1	8	*Salmonella enterica*	putative adhesin (plasmid)
NP_461188.1	8	*Salmonella enterica*	putative outer membrane protein
NP_490501.1	8	*Salmonella enterica*	resistance to complement killing (plasmid)
NP_462656.1	10	*Salmonella enterica*	autotransporter outer membrane beta-barrel domain-containing protein
NP_461336.1	10	*Salmonella enterica*	hypothetical protein

NP_461236.1	10	*Salmonella enterica*	putative inner membrane protein
NP_459368.1	12	*Salmonella enterica*	autotransporter outer membrane beta-barrel domain-containing protein
NP_459562.1	12	*Salmonella enterica*	autotransporter outer membrane beta-barrel domain-containing protein
NP_461448.1	12	*Salmonella enterica*	C-terminal region of AIDA-like protein
NP_459039.1	12	*Salmonella enterica*	hypothetical protein
NP_460103.1	12	*Salmonella enterica*	hypothetical protein
NP_460293.1	12	*Salmonella enterica*	hypothetical protein
NP_460294.1	12	*Salmonella enterica*	hypothetical protein
NP_461358.1	12	*Salmonella enterica*	hypothetical protein
NP_461968.1	12	*Salmonella enterica*	hypothetical protein
NP_461452.1	12	*Salmonella enterica*	intimin-like inverse autotransporter protein SinH
NP_460627.1	12	*Salmonella enterica*	invasin
NP_460252.1	12	*Salmonella enterica*	MltA-interacting protein MipA
NP_459408.1	12	*Salmonella enterica*	nucleoside-specific channel-forming protein Tsx
NP_462842.1	12	*Salmonella enterica*	phospholipase
NP_462896.1	12	*Salmonella enterica*	porin
NP_460724.3	12	*Salmonella enterica*	putative invasin
NP_462932.3	12	*Salmonella enterica*	putative outer membrane protein
NP_463107.1	14	*Salmonella enterica*	conjugal transfer protein
NP_461333.1	14	*Salmonella enterica*	transport of long-chain fatty acids
NP_462517.1	16	*Salmonella enterica*	cellulose biosynthesis protein BcsC
NP_460434.1	16	*Salmonella enterica*	hypothetical protein
NP_463270.1	16	*Salmonella enterica*	hypothetical protein
NP_459229.1	16	*Salmonella enterica*	outer membrane protein assembly factor BamA

NP_459317.1	16	*Salmonella enterica*	phosphoporin PhoE
NP_459974.1	16	*Salmonella enterica*	phosphoporin PhoE
NP_460490.1	16	*Salmonella enterica*	phosphoporin PhoE
NP_460531.1	16	*Salmonella enterica*	phosphoporin PhoE
NP_461742.1	16	*Salmonella enterica*	porin
NP_461210.1	16	*Salmonella enterica*	porin OmpC
NP_460946.1	16	*Salmonella enterica*	putative porin
NP_459672.1	18	*Salmonella enterica*	chitoporin
NP_463096.1	18	*Salmonella enterica*	maltoporin
NP_461144.1	22	*Salmonella enterica*	catecholate siderophore receptor CirA
NP_460174.1	22	*Salmonella enterica*	ferric-rhodotorulic acid/ferric-coprogen receptor FhuE
NP_459196.1	22	*Salmonella enterica*	ferrichrome porin FhuA
NP_459359.1	22	*Salmonella enterica*	ferrioxamine receptor
NP_459577.1	22	*Salmonella enterica*	outer membrane receptor protein
NP_461704.3	22	*Salmonella enterica*	TonB-dependent siderophore receptor protein
NP_463009.1	22	*Salmonella enterica*	TonB-dependent vitamin B12 receptor
NP_459180.1	24	*Salmonella enterica*	fimbrial assembly protein
NP_459333.1	24	*Salmonella enterica*	fimbrial assembly protein
NP_461094.1	24	*Salmonella enterica*	fimbrial assembly protein
NP_462539.1	24	*Salmonella enterica*	fimbrial assembly protein
NP_463428.1	24	*Salmonella enterica*	fimbrial assembly protein
NP_461945.1	24	*Salmonella enterica*	fimbrial protein
NP_463090.1	24	*Salmonella enterica*	hypothetical protein
NP_459028.1	24	*Salmonella enterica*	outer membrane usher protein
NP_459201.1	24	*Salmonella enterica*	outer membrane usher protein

NP_459541.1	24	*Salmonella enterica*	outer membrane usher protein
NP_459299.1	24	*Salmonella enterica*	pilin outer membrane usher protein SafC
NP_490509.1	24	*Salmonella enterica*	plasmid-encoded fimbriae; usher protein (plasmid)
NP_463449.1	24	*Salmonella enterica*	putative fimbrial usher protein
NP_460546.1	24	*Salmonella enterica*	TonB-dependent receptor
NP_459098.1	26	*Salmonella enterica*	LPS assembly protein LptD
WP_015456738.1	6	*Sinorhizobium meliloti*	autotransporter outer membrane beta-barrel domain-containing protein
WP_010969460.1	8	*Sinorhizobium meliloti*	acyloxyacyl hydrolase
WP_003527577.1	8	*Sinorhizobium meliloti*	porin family protein
WP_003530975.1	8	*Sinorhizobium meliloti*	porin family protein
WP_003531607.1	8	*Sinorhizobium meliloti*	porin family protein
WP_013844837.1	8	*Sinorhizobium meliloti*	porin family protein
WP_010967557.1	10	*Sinorhizobium meliloti*	hypothetical protein
WP_010968872.1	12	*Sinorhizobium meliloti*	MipA/OmpV family protein
WP_010976038.1	12	*Sinorhizobium meliloti*	transporter
WP_010969016.1	14	*Sinorhizobium meliloti*	autotransporter outer membrane beta-barrel domain-containing protein
WP_010969273.1	14	*Sinorhizobium meliloti*	OmpP1/FadL family transporter
WP_010970372.1	14	*Sinorhizobium meliloti*	surface lipoprotein assembly modifier
WP_013844890.1	16	*Sinorhizobium meliloti*	autotransporter assembly complex protein TamA
WP_010969258.1	16	*Sinorhizobium meliloti*	outer membrane protein assembly factor BamA
WP_003527304.1	16	*Sinorhizobium meliloti*	porin
WP_010969013.1	16	*Sinorhizobium meliloti*	porin
WP_010970203.1	18	*Sinorhizobium meliloti*	outer membrane beta-barrel protein
WP_010969901.1	22	*Sinorhizobium meliloti*	TonB-dependent hemoglobin/transferrin/lactoferrin family receptor

WP_010968208.1	22	*Sinorhizobium meliloti*	TonB-dependent receptor
WP_010968430.1	22	*Sinorhizobium meliloti*	TonB-dependent receptor
WP_010969653.1	22	*Sinorhizobium meliloti*	TonB-dependent receptor
WP_010969817.1	22	*Sinorhizobium meliloti*	TonB-dependent siderophore receptor
WP_041169987.1	22	*Sinorhizobium meliloti*	TonB-dependent siderophore receptor
WP_041170156.1	22	*Sinorhizobium meliloti*	TonB-dependent siderophore receptor
WP_010969074.1	26	*Sinorhizobium meliloti*	LPS-assembly protein LptD
WP_244953594.1	4	*Xanthomonas axonopodis*	YadA-like family protein
WP_042823933.1	8	*Xanthomonas axonopodis*	OmpA family protein
WP_042823503.1	8	*Xanthomonas axonopodis*	outer membrane beta-barrel protein
WP_042823504.1	8	*Xanthomonas axonopodis*	outer membrane beta-barrel protein
WP_042823799.1	8	*Xanthomonas axonopodis*	outer membrane beta-barrel protein
WP_042820984.1	10	*Xanthomonas axonopodis*	Ax21 family protein
WP_042823792.1	10	*Xanthomonas axonopodis*	hypothetical protein
WP_134984094.1	10	*Xanthomonas axonopodis*	hypothetical protein
WP_042823426.1	12	*Xanthomonas axonopodis*	autotransporter domain-containing esterase
WP_042823772.1	12	*Xanthomonas axonopodis*	copper resistance protein B
WP_042822936.1	12	*Xanthomonas axonopodis*	DUF3034 family protein
WP_042821242.1	12	*Xanthomonas axonopodis*	DUF481 domain-containing protein
WP_042823033.1	12	*Xanthomonas axonopodis*	MipA/OmpV family protein
WP_042821817.1	12	*Xanthomonas axonopodis*	phospholipase A
WP_134984070.1	12	*Xanthomonas axonopodis*	S8 family serine peptidase
WP_042823941.1	12	*Xanthomonas axonopodis*	TorF family putative porin
WP_042821526.1	12	*Xanthomonas axonopodis*	transporter
WP_042822272.1	12	*Xanthomonas axonopodis*	transporter

WP_134983912.1	12	*Xanthomonas axonopodis*	transporter
WP_042820905.1	14	*Xanthomonas axonopodis*	outer membrane protein transport protein
WP_042824346.1	16	*Xanthomonas axonopodis*	autotransporter assembly complex protein TamA
WP_042821115.1	16	*Xanthomonas axonopodis*	carbohydrate porin
WP_171890737.1	16	*Xanthomonas axonopodis*	DcaP family trimeric outer membrane transporter
WP_042824887.1	16	*Xanthomonas axonopodis*	OprO/OprP family phosphate-selective porin
WP_134983980.1	16	*Xanthomonas axonopodis*	OprO/OprP family phosphate-selective porin
WP_042821760.1	16	*Xanthomonas axonopodis*	outer membrane protein assembly factor BamA
WP_042823622.1	16	*Xanthomonas axonopodis*	porin
WP_042825292.1	16	*Xanthomonas axonopodis*	ShlB/FhaC/HecB family hemolysin secretion/activation protein
WP_042823517.1	22	*Xanthomonas axonopodis*	ferric-rhodotorulic acid/ferric-coprogen receptor FhuE
WP_134983883.1	22	*Xanthomonas axonopodis*	fimbria/pilus outer membrane usher protein
WP_042820885.1	22	*Xanthomonas axonopodis*	TonB-dependent receptor
WP_042820929.1	22	*Xanthomonas axonopodis*	TonB-dependent receptor
WP_042821334.1	22	*Xanthomonas axonopodis*	TonB-dependent receptor
WP_042821652.1	22	*Xanthomonas axonopodis*	TonB-dependent receptor
WP_042822473.1	22	*Xanthomonas axonopodis*	TonB-dependent receptor
WP_042822823.1	22	*Xanthomonas axonopodis*	TonB-dependent receptor
WP_042822968.1	22	*Xanthomonas axonopodis*	TonB-dependent receptor
WP_042823003.1	22	*Xanthomonas axonopodis*	TonB-dependent receptor
WP_042823060.1	22	*Xanthomonas axonopodis*	TonB-dependent receptor
WP_042823061.1	22	*Xanthomonas axonopodis*	TonB-dependent receptor
WP_042823239.1	22	*Xanthomonas axonopodis*	TonB-dependent receptor
WP_042823286.1	22	*Xanthomonas axonopodis*	TonB-dependent receptor
WP_042823358.1	22	*Xanthomonas axonopodis*	TonB-dependent receptor

WP_042823391.1	22	*Xanthomonas axonopodis*	TonB-dependent receptor
WP_042823398.1	22	*Xanthomonas axonopodis*	TonB-dependent receptor
WP_042823400.1	22	*Xanthomonas axonopodis*	TonB-dependent receptor
WP_042823401.1	22	*Xanthomonas axonopodis*	TonB-dependent receptor
WP_042823513.1	22	*Xanthomonas axonopodis*	TonB-dependent receptor
WP_042823594.1	22	*Xanthomonas axonopodis*	TonB-dependent receptor
WP_042823675.1	22	*Xanthomonas axonopodis*	TonB-dependent receptor
WP_042823923.1	22	*Xanthomonas axonopodis*	TonB-dependent receptor
WP_042824136.1	22	*Xanthomonas axonopodis*	TonB-dependent receptor
WP_042824388.1	22	*Xanthomonas axonopodis*	TonB-dependent receptor
WP_042824522.1	22	*Xanthomonas axonopodis*	TonB-dependent receptor
WP_042824615.1	22	*Xanthomonas axonopodis*	TonB-dependent receptor
WP_042824806.1	22	*Xanthomonas axonopodis*	TonB-dependent receptor
WP_042824851.1	22	*Xanthomonas axonopodis*	TonB-dependent receptor
WP_134812623.1	22	*Xanthomonas axonopodis*	TonB-dependent receptor
WP_171890733.1	22	*Xanthomonas axonopodis*	TonB-dependent receptor
WP_171890740.1	22	*Xanthomonas axonopodis*	TonB-dependent receptor
WP_171890754.1	22	*Xanthomonas axonopodis*	TonB-dependent receptor
WP_171890769.1	22	*Xanthomonas axonopodis*	TonB-dependent receptor
WP_171890904.1	22	*Xanthomonas axonopodis*	TonB-dependent receptor
WP_244953597.1	22	*Xanthomonas axonopodis*	TonB-dependent receptor
WP_244953601.1	22	*Xanthomonas axonopodis*	TonB-dependent receptor
WP_244953638.1	22	*Xanthomonas axonopodis*	TonB-dependent receptor
WP_042821217.1	22	*Xanthomonas axonopodis*	TonB-dependent siderophore receptor
WP_042821786.1	22	*Xanthomonas axonopodis*	TonB-dependent siderophore receptor

WP_134984078.1	22	*Xanthomonas axonopodis*	TonB-dependent siderophore receptor
WP_042821377.1	30	*Xanthomonas axonopodis*	LPS-assembly protein LptD
WP_076057120.1	8	*Xanthomonas campestris*	hypothetical protein
WP_011036149.1	8	*Xanthomonas campestris*	MULTISPECIES: OmpA family protein
WP_011035787.1	8	*Xanthomonas campestris*	outer membrane beta-barrel protein
WP_014508785.1	8	*Xanthomonas campestris*	outer membrane beta-barrel protein
WP_076054028.1	8	*Xanthomonas campestris*	outer membrane beta-barrel protein
WP_076057281.1	8	*Xanthomonas campestris*	outer membrane beta-barrel protein
WP_012437016.1	10	*Xanthomonas campestris*	Ax21 family protein
WP_011035933.1	10	*Xanthomonas campestris*	hypothetical protein
WP_162275447.1	10	*Xanthomonas campestris*	hypothetical protein
WP_076054510.1	10	*Xanthomonas campestris*	MipA/OmpV family protein
WP_076054090.1	12	*Xanthomonas campestris*	autotransporter domain-containing protein
WP_237385035.1	12	*Xanthomonas campestris*	autotransporter outer membrane beta-barrel domain-containing protein
WP_076055969.1	12	*Xanthomonas campestris*	autotransporter serine protease
WP_237385038.1	12	*Xanthomonas campestris*	copper resistance protein B
WP_162275512.1	12	*Xanthomonas campestris*	DUF2490 domain-containing protein
WP_040941043.1	12	*Xanthomonas campestris*	DUF3034 family protein
WP_012437324.1	12	*Xanthomonas campestris*	DUF481 domain-containing protein
WP_014509006.1	12	*Xanthomonas campestris*	lipid A deacylase LpxR family protein
WP_040941535.1	12	*Xanthomonas campestris*	phospholipase A
WP_076055300.1	12	*Xanthomonas campestris*	S8 family serine peptidase
WP_076056354.1	12	*Xanthomonas campestris*	TorF family putative porin
WP_076055747.1	12	*Xanthomonas campestris*	transporter
WP_076056168.1	12	*Xanthomonas campestris*	transporter

WP_081390758.1	12	*Xanthomonas campestris*	transporter
WP_011035275.1	14	*Xanthomonas campestris*	outer membrane protein transport protein
WP_019238119.1	16	*Xanthomonas campestris*	autotransporter assembly complex protein TamA
WP_162275343.1	16	*Xanthomonas campestris*	carbohydrate porin
WP_176994102.1	16	*Xanthomonas campestris*	cellulose biosynthesis protein BcsC
WP_042595882.1	16	*Xanthomonas campestris*	DcaP family trimeric outer membrane transporter
WP_076053292.1	16	*Xanthomonas campestris*	OprO/OprP family phosphate-selective porin
WP_076053869.1	16	*Xanthomonas campestris*	OprO/OprP family phosphate-selective porin
WP_076055720.1	16	*Xanthomonas campestris*	OprO/OprP family phosphate-selective porin
WP_019237827.1	16	*Xanthomonas campestris*	outer membrane protein assembly factor BamA
WP_076053880.1	16	*Xanthomonas campestris*	porin
WP_076055468.1	16	*Xanthomonas campestris*	ShlB/FhaC/HecB family hemolysin secretion/activation protein
WP_076057402.1	18	*Xanthomonas campestris*	alginate export family protein
WP_162275403.1	18	*Xanthomonas campestris*	alginate export family protein
WP_076053973.1	18	*Xanthomonas campestris*	OprD family porin
WP_076054006.1	22	*Xanthomonas campestris*	ferric-rhodotorulic acid/ferric-coprogen receptor FhuE
WP_076055869.1	22	*Xanthomonas campestris*	fimbria/pilus outer membrane usher protein
WP_076056497.1	22	*Xanthomonas campestris*	TonB-dependent hemoglobin/transferrin/lactoferrin family receptor
WP_016944144.1	22	*Xanthomonas campestris*	TonB-dependent receptor
WP_040941022.1	22	*Xanthomonas campestris*	TonB-dependent receptor
WP_043921542.1	22	*Xanthomonas campestris*	TonB-dependent receptor
WP_076035896.1	22	*Xanthomonas campestris*	TonB-dependent receptor
WP_076053020.1	22	*Xanthomonas campestris*	TonB-dependent receptor
WP_076053498.1	22	*Xanthomonas campestris*	TonB-dependent receptor

WP_076053740.1	22	*Xanthomonas campestris*	TonB-dependent receptor
WP_076053771.1	22	*Xanthomonas campestris*	TonB-dependent receptor
WP_076053796.1	22	*Xanthomonas campestris*	TonB-dependent receptor
WP_076054077.1	22	*Xanthomonas campestris*	TonB-dependent receptor
WP_076054245.1	22	*Xanthomonas campestris*	TonB-dependent receptor
WP_076054247.1	22	*Xanthomonas campestris*	TonB-dependent receptor
WP_076054250.1	22	*Xanthomonas campestris*	TonB-dependent receptor
WP_076054260.1	22	*Xanthomonas campestris*	TonB-dependent receptor
WP_076054300.1	22	*Xanthomonas campestris*	TonB-dependent receptor
WP_076054363.1	22	*Xanthomonas campestris*	TonB-dependent receptor
WP_076054576.1	22	*Xanthomonas campestris*	TonB-dependent receptor
WP_076054591.1	22	*Xanthomonas campestris*	TonB-dependent receptor
WP_076054627.1	22	*Xanthomonas campestris*	TonB-dependent receptor
WP_076054645.1	22	*Xanthomonas campestris*	TonB-dependent receptor
WP_076055096.1	22	*Xanthomonas campestris*	TonB-dependent receptor
WP_076055217.1	22	*Xanthomonas campestris*	TonB-dependent receptor
WP_076055233.1	22	*Xanthomonas campestris*	TonB-dependent receptor
WP_076055269.1	22	*Xanthomonas campestris*	TonB-dependent receptor
WP_076055512.1	22	*Xanthomonas campestris*	TonB-dependent receptor
WP_076055538.1	22	*Xanthomonas campestris*	TonB-dependent receptor
WP_076055853.1	22	*Xanthomonas campestris*	TonB-dependent receptor
WP_076055915.1	22	*Xanthomonas campestris*	TonB-dependent receptor
WP_076056029.1	22	*Xanthomonas campestris*	TonB-dependent receptor
WP_076056103.1	22	*Xanthomonas campestris*	TonB-dependent receptor
WP_076056259.1	22	*Xanthomonas campestris*	TonB-dependent receptor

WP_076056271.1	22	*Xanthomonas campestris*	TonB-dependent receptor
WP_076056352.1	22	*Xanthomonas campestris*	TonB-dependent receptor
WP_076056625.1	22	*Xanthomonas campestris*	TonB-dependent receptor
WP_076057005.1	22	*Xanthomonas campestris*	TonB-dependent receptor
WP_076057097.1	22	*Xanthomonas campestris*	TonB-dependent receptor
WP_076057098.1	22	*Xanthomonas campestris*	TonB-dependent receptor
WP_076057218.1	22	*Xanthomonas campestris*	TonB-dependent receptor
WP_162275121.1	22	*Xanthomonas campestris*	TonB-dependent receptor
WP_162275222.1	22	*Xanthomonas campestris*	TonB-dependent receptor
WP_162275273.1	22	*Xanthomonas campestris*	TonB-dependent receptor
WP_162275293.1	22	*Xanthomonas campestris*	TonB-dependent receptor
WP_162275312.1	22	*Xanthomonas campestris*	TonB-dependent receptor
WP_162275328.1	22	*Xanthomonas campestris*	TonB-dependent receptor
WP_162275339.1	22	*Xanthomonas campestris*	TonB-dependent receptor
WP_162275340.1	22	*Xanthomonas campestris*	TonB-dependent receptor
WP_162275368.1	22	*Xanthomonas campestris*	TonB-dependent receptor
WP_162275448.1	22	*Xanthomonas campestris*	TonB-dependent receptor
WP_162275463.1	22	*Xanthomonas campestris*	TonB-dependent receptor
WP_162275491.1	22	*Xanthomonas campestris*	TonB-dependent receptor
WP_176993935.1	22	*Xanthomonas campestris*	TonB-dependent receptor
WP_176993942.1	22	*Xanthomonas campestris*	TonB-dependent receptor
WP_176993966.1	22	*Xanthomonas campestris*	TonB-dependent receptor
WP_176993992.1	22	*Xanthomonas campestris*	TonB-dependent receptor
WP_176993999.1	22	*Xanthomonas campestris*	TonB-dependent receptor
WP_176994002.1	22	*Xanthomonas campestris*	TonB-dependent receptor

WP_176994097.1	22	*Xanthomonas campestris*	TonB-dependent receptor
WP_176994162.1	22	*Xanthomonas campestris*	TonB-dependent receptor
WP_176994214.1	22	*Xanthomonas campestris*	TonB-dependent receptor
WP_237384889.1	22	*Xanthomonas campestris*	TonB-dependent receptor
WP_070690331.1	22	*Xanthomonas campestris*	TonB-dependent siderophore receptor
WP_076053084.1	22	*Xanthomonas campestris*	TonB-dependent siderophore receptor
WP_076054237.1	22	*Xanthomonas campestris*	TonB-dependent siderophore receptor
WP_076056831.1	22	*Xanthomonas campestris*	TonB-dependent siderophore receptor
WP_162275481.1	22	*Xanthomonas campestris*	TonB-dependent siderophore receptor
WP_176993983.1	22	*Xanthomonas campestris*	TonB-dependent siderophore receptor
WP_162275301.1	22	*Xanthomonas campestris*	TonB-dependent vitamin B12 receptor
WP_076056475.1	30	*Xanthomonas campestris*	LPS-assembly protein LptD
WP_005915855.1	8	*Xanthomonas citri*	MULTISPECIES: OmpA family protein
WP_005911238.1	8	*Xanthomonas citri*	MULTISPECIES: outer membrane beta-barrel protein
WP_005927967.1	8	*Xanthomonas citri*	MULTISPECIES: outer membrane beta-barrel protein
WP_011052217.1	8	*Xanthomonas citri*	MULTISPECIES: outer membrane beta-barrel protein
WP_011052609.1	8	*Xanthomonas citri*	MULTISPECIES: outer membrane beta-barrel protein
WP_015463564.1	8	*Xanthomonas citri*	MULTISPECIES: outer membrane beta-barrel protein
WP_003488520.1	10	*Xanthomonas citri*	MULTISPECIES: Ax21 family protein
WP_005910986.1	10	*Xanthomonas citri*	MULTISPECIES: hypothetical protein
WP_011052426.1	10	*Xanthomonas citri*	MULTISPECIES: hypothetical protein
WP_011052178.1	12	*Xanthomonas citri*	MULTISPECIES: autotransporter domain-containing esterase
WP_011050862.1	12	*Xanthomonas citri*	MULTISPECIES: autotransporter serine protease
WP_011052413.1	12	*Xanthomonas citri*	MULTISPECIES: copper resistance protein B
WP_005928878.1	12	*Xanthomonas citri*	MULTISPECIES: DUF2490 domain-containing protein

WP_015463393.1	12	*Xanthomonas citri*	MULTISPECIES: DUF3034 family protein
WP_005916853.1	12	*Xanthomonas citri*	MULTISPECIES: DUF481 domain-containing protein
WP_015463777.1	12	*Xanthomonas citri*	MULTISPECIES: hypothetical protein
WP_005911164.1	12	*Xanthomonas citri*	MULTISPECIES: lipid A deacylase LpxR family protein
WP_015463417.1	12	*Xanthomonas citri*	MULTISPECIES: MipA/OmpV family protein
WP_040107595.1	12	*Xanthomonas citri*	MULTISPECIES: phospholipase A
WP_011051362.1	12	*Xanthomonas citri*	MULTISPECIES: S8 family serine peptidase
WP_003490453.1	12	*Xanthomonas citri*	MULTISPECIES: TorF family putative porin
WP_003485648.1	12	*Xanthomonas citri*	MULTISPECIES: transporter
WP_003490261.1	12	*Xanthomonas citri*	MULTISPECIES: transporter
WP_015462895.1	12	*Xanthomonas citri*	MULTISPECIES: transporter
WP_033482967.1	12	*Xanthomonas citri*	MULTISPECIES: transporter
WP_040107603.1	12	*Xanthomonas citri*	MULTISPECIES: transporter
WP_015462678.1	14	*Xanthomonas citri*	MULTISPECIES: outer membrane protein transport protein
WP_011052809.1	16	*Xanthomonas citri*	MULTISPECIES: autotransporter assembly complex protein TamA
WP_005933852.1	16	*Xanthomonas citri*	MULTISPECIES: carbohydrate porin
WP_011052327.1	16	*Xanthomonas citri*	MULTISPECIES: cellulose biosynthesis protein BcsC
WP_015463749.1	16	*Xanthomonas citri*	MULTISPECIES: DcaP family trimeric outer membrane transporter
WP_003487161.1	16	*Xanthomonas citri*	MULTISPECIES: OprO/OprP family phosphate-selective porin
WP_003488991.1	16	*Xanthomonas citri*	MULTISPECIES: OprO/OprP family phosphate-selective porin
WP_011052306.1	16	*Xanthomonas citri*	MULTISPECIES: OprO/OprP family phosphate-selective porin
WP_003485373.1	16	*Xanthomonas citri*	MULTISPECIES: outer membrane protein assembly factor BamA
WP_003483386.1	16	*Xanthomonas citri*	MULTISPECIES: porin
WP_040107696.1	16	*Xanthomonas citri*	MULTISPECIES: ShlB/FhaC/HecB family

			hemolysin secretion/activation protein
WP_045714571.1	16	*Xanthomonas citri*	ShlB/FhaC/HecB family hemolysin secretion/activation protein
WP_015462993.1	18	*Xanthomonas citri*	MULTISPECIES: alginate export family protein
WP_011052231.1	22	*Xanthomonas citri*	MULTISPECIES: ferric-rhodotorulic acid/ferric-coprogen receptor FhuE
WP_011050904.1	22	*Xanthomonas citri*	MULTISPECIES: fimbria/pilus outer membrane usher protein
WP_015462885.1	22	*Xanthomonas citri*	MULTISPECIES: TonB-dependent hemoglobin/transferrin/lactoferrin family receptor
WP_003483322.1	22	*Xanthomonas citri*	MULTISPECIES: TonB-dependent receptor
WP_003483908.1	22	*Xanthomonas citri*	MULTISPECIES: TonB-dependent receptor
WP_003486829.1	22	*Xanthomonas citri*	MULTISPECIES: TonB-dependent receptor
WP_003487035.1	22	*Xanthomonas citri*	MULTISPECIES: TonB-dependent receptor
WP_003488587.1	22	*Xanthomonas citri*	MULTISPECIES: TonB-dependent receptor
WP_005916938.1	22	*Xanthomonas citri*	MULTISPECIES: TonB-dependent receptor
WP_011050122.1	22	*Xanthomonas citri*	MULTISPECIES: TonB-dependent receptor
WP_011050222.1	22	*Xanthomonas citri*	MULTISPECIES: TonB-dependent receptor
WP_011050479.1	22	*Xanthomonas citri*	MULTISPECIES: TonB-dependent receptor
WP_011050481.1	22	*Xanthomonas citri*	MULTISPECIES: TonB-dependent receptor
WP_011050492.1	22	*Xanthomonas citri*	MULTISPECIES: TonB-dependent receptor
WP_011050551.1	22	*Xanthomonas citri*	MULTISPECIES: TonB-dependent receptor
WP_011050642.1	22	*Xanthomonas citri*	MULTISPECIES: TonB-dependent receptor
WP_011050656.1	22	*Xanthomonas citri*	MULTISPECIES: TonB-dependent receptor
WP_011050728.1	22	*Xanthomonas citri*	MULTISPECIES: TonB-dependent receptor
WP_011050812.1	22	*Xanthomonas citri*	MULTISPECIES: TonB-dependent receptor
WP_011050836.1	22	*Xanthomonas citri*	MULTISPECIES: TonB-dependent receptor

WP_011051126.1	22	*Xanthomonas citri*	MULTISPECIES: TonB-dependent receptor
WP_011051127.1	22	*Xanthomonas citri*	MULTISPECIES: TonB-dependent receptor
WP_011051653.1	22	*Xanthomonas citri*	MULTISPECIES: TonB-dependent receptor
WP_011051657.1	22	*Xanthomonas citri*	MULTISPECIES: TonB-dependent receptor
WP_011051796.1	22	*Xanthomonas citri*	MULTISPECIES: TonB-dependent receptor
WP_011051797.1	22	*Xanthomonas citri*	MULTISPECIES: TonB-dependent receptor
WP_011051858.1	22	*Xanthomonas citri*	MULTISPECIES: TonB-dependent receptor
WP_011052016.1	22	*Xanthomonas citri*	MULTISPECIES: TonB-dependent receptor
WP_011052021.1	22	*Xanthomonas citri*	MULTISPECIES: TonB-dependent receptor
WP_011052050.1	22	*Xanthomonas citri*	MULTISPECIES: TonB-dependent receptor
WP_011052072.1	22	*Xanthomonas citri*	MULTISPECIES: TonB-dependent receptor
WP_011052074.1	22	*Xanthomonas citri*	MULTISPECIES: TonB-dependent receptor
WP_011052075.1	22	*Xanthomonas citri*	MULTISPECIES: TonB-dependent receptor
WP_011052107.1	22	*Xanthomonas citri*	MULTISPECIES: TonB-dependent receptor
WP_011052184.1	22	*Xanthomonas citri*	MULTISPECIES: TonB-dependent receptor
WP_011052227.1	22	*Xanthomonas citri*	MULTISPECIES: TonB-dependent receptor
WP_011052358.1	22	*Xanthomonas citri*	MULTISPECIES: TonB-dependent receptor
WP_011052697.1	22	*Xanthomonas citri*	MULTISPECIES: TonB-dependent receptor
WP_011052707.1	22	*Xanthomonas citri*	MULTISPECIES: TonB-dependent receptor
WP_011052861.1	22	*Xanthomonas citri*	MULTISPECIES: TonB-dependent receptor
WP_011052924.1	22	*Xanthomonas citri*	MULTISPECIES: TonB-dependent receptor
WP_015462817.1	22	*Xanthomonas citri*	MULTISPECIES: TonB-dependent receptor
WP_015462848.1	22	*Xanthomonas citri*	MULTISPECIES: TonB-dependent receptor
WP_015463216.1	22	*Xanthomonas citri*	MULTISPECIES: TonB-dependent receptor
WP_015463452.1	22	*Xanthomonas citri*	MULTISPECIES: TonB-dependent receptor

WP_015463508.1	22	*Xanthomonas citri*	MULTISPECIES: TonB-dependent receptor
WP_015463573.1	22	*Xanthomonas citri*	MULTISPECIES: TonB-dependent receptor
WP_015463577.1	22	*Xanthomonas citri*	MULTISPECIES: TonB-dependent receptor
WP_015463587.1	22	*Xanthomonas citri*	MULTISPECIES: TonB-dependent receptor
WP_015463597.1	22	*Xanthomonas citri*	MULTISPECIES: TonB-dependent receptor
WP_015463733.1	22	*Xanthomonas citri*	MULTISPECIES: TonB-dependent receptor
WP_015463787.1	22	*Xanthomonas citri*	MULTISPECIES: TonB-dependent receptor
WP_015471522.1	22	*Xanthomonas citri*	MULTISPECIES: TonB-dependent receptor
WP_015471544.1	22	*Xanthomonas citri*	MULTISPECIES: TonB-dependent receptor
WP_015472635.1	22	*Xanthomonas citri*	MULTISPECIES: TonB-dependent receptor
WP_040107573.1	22	*Xanthomonas citri*	MULTISPECIES: TonB-dependent receptor
WP_040107639.1	22	*Xanthomonas citri*	MULTISPECIES: TonB-dependent receptor
WP_040107654.1	22	*Xanthomonas citri*	MULTISPECIES: TonB-dependent receptor
WP_040107707.1	22	*Xanthomonas citri*	MULTISPECIES: TonB-dependent receptor
WP_171843837.1	22	*Xanthomonas citri*	MULTISPECIES: TonB-dependent receptor
WP_223293140.1	22	*Xanthomonas citri*	MULTISPECIES: TonB-dependent receptor
WP_223293156.1	22	*Xanthomonas citri*	MULTISPECIES: TonB-dependent receptor
WP_011050145.1	22	*Xanthomonas citri*	MULTISPECIES: TonB-dependent siderophore receptor
WP_011050911.1	22	*Xanthomonas citri*	MULTISPECIES: TonB-dependent siderophore receptor
WP_011052081.1	22	*Xanthomonas citri*	MULTISPECIES: TonB-dependent siderophore receptor
WP_011052315.1	22	*Xanthomonas citri*	MULTISPECIES: TonB-dependent siderophore receptor
WP_011052402.1	22	*Xanthomonas citri*	MULTISPECIES: TonB-dependent siderophore receptor
WP_015463444.1	22	*Xanthomonas citri*	MULTISPECIES: TonB-dependent siderophore receptor
WP_015463504.1	22	*Xanthomonas citri*	MULTISPECIES: TonB-dependent vitamin B12 receptor
WP_230598899.1	22	*Xanthomonas citri*	TonB-dependent receptor

WP_230598900.1	22	*Xanthomonas citri*	TonB-dependent siderophore receptor
WP_234336746.1	22	*Xanthomonas citri*	TonB-dependent siderophore receptor
WP_011050583.1	30	*Xanthomonas citri*	MULTISPECIES: LPS-assembly protein LptD
WP_047340197.1	4	*Xanthomonas oryzae*	YadA-like family protein
WP_014502189.1	8	*Xanthomonas oryzae*	OmpA family protein
WP_014504710.1	8	*Xanthomonas oryzae*	outer membrane beta-barrel protein
WP_024712156.1	10	*Xanthomonas oryzae*	Ax21 family protein
WP_014501965.1	10	*Xanthomonas oryzae*	hypothetical protein
WP_024710517.1	10	*Xanthomonas oryzae*	hypothetical protein
WP_047340106.1	12	*Xanthomonas oryzae*	autotransporter domain-containing esterase
WP_047340017.1	12	*Xanthomonas oryzae*	autotransporter serine protease
WP_014503803.1	12	*Xanthomonas oryzae*	DUF3034 family protein
WP_024711084.1	12	*Xanthomonas oryzae*	DUF481 domain-containing protein
WP_011258340.1	12	*Xanthomonas oryzae*	MipA/OmpV family protein
WP_047339992.1	12	*Xanthomonas oryzae*	phospholipase A
WP_047339847.1	12	*Xanthomonas oryzae*	S8 family serine peptidase
WP_014502198.1	12	*Xanthomonas oryzae*	TorF family putative porin
WP_024711335.1	12	*Xanthomonas oryzae*	transporter
WP_047339618.1	12	*Xanthomonas oryzae*	transporter
WP_047339703.1	12	*Xanthomonas oryzae*	transporter
WP_047339405.1	14	*Xanthomonas oryzae*	outer membrane protein transport protein
WP_047340282.1	16	*Xanthomonas oryzae*	autotransporter assembly complex protein TamA
WP_047339743.1	16	*Xanthomonas oryzae*	carbohydrate porin
WP_024711808.1	16	*Xanthomonas oryzae*	DcaP family trimeric outer membrane transporter
WP_014502807.1	16	*Xanthomonas oryzae*	OprO/OprP family phosphate-selective porin

WP_024710600.1	16	*Xanthomonas oryzae*	OprO/OprP family phosphate-selective porin
WP_014503924.1	16	*Xanthomonas oryzae*	outer membrane protein assembly factor BamA
WP_047340142.1	16	*Xanthomonas oryzae*	porin
WP_047340213.1	16	*Xanthomonas oryzae*	ShlB/FhaC/HecB family hemolysin secretion/activation protein
WP_047340008.1	18	*Xanthomonas oryzae*	alginate export family protein
WP_076342570.1	18	*Xanthomonas oryzae*	TonB-dependent receptor
WP_014503913.1	22	*Xanthomonas oryzae*	fimbria/pilus outer membrane usher protein
WP_011258177.1	22	*Xanthomonas oryzae*	TonB-dependent receptor
WP_014502642.1	22	*Xanthomonas oryzae*	TonB-dependent receptor
WP_024710622.1	22	*Xanthomonas oryzae*	TonB-dependent receptor
WP_024710948.1	22	*Xanthomonas oryzae*	TonB-dependent receptor
WP_024711763.1	22	*Xanthomonas oryzae*	TonB-dependent receptor
WP_024712571.1	22	*Xanthomonas oryzae*	TonB-dependent receptor
WP_033005037.1	22	*Xanthomonas oryzae*	TonB-dependent receptor
WP_044749565.1	22	*Xanthomonas oryzae*	TonB-dependent receptor
WP_044750896.1	22	*Xanthomonas oryzae*	TonB-dependent receptor
WP_047339423.1	22	*Xanthomonas oryzae*	TonB-dependent receptor
WP_047339507.1	22	*Xanthomonas oryzae*	TonB-dependent receptor
WP_047339527.1	22	*Xanthomonas oryzae*	TonB-dependent receptor
WP_047339541.1	22	*Xanthomonas oryzae*	TonB-dependent receptor
WP_047339555.1	22	*Xanthomonas oryzae*	TonB-dependent receptor
WP_047339595.1	22	*Xanthomonas oryzae*	TonB-dependent receptor
WP_047339671.1	22	*Xanthomonas oryzae*	TonB-dependent receptor
WP_047339689.1	22	*Xanthomonas oryzae*	TonB-dependent receptor
WP_047339732.1	22	*Xanthomonas oryzae*	TonB-dependent receptor

WP_047339739.1	22	*Xanthomonas oryzae*	TonB-dependent receptor
WP_047339902.1	22	*Xanthomonas oryzae*	TonB-dependent receptor
WP_047340035.1	22	*Xanthomonas oryzae*	TonB-dependent receptor
WP_047340041.1	22	*Xanthomonas oryzae*	TonB-dependent receptor
WP_047340069.1	22	*Xanthomonas oryzae*	TonB-dependent receptor
WP_047340071.1	22	*Xanthomonas oryzae*	TonB-dependent receptor
WP_047340112.1	22	*Xanthomonas oryzae*	TonB-dependent receptor
WP_047340147.1	22	*Xanthomonas oryzae*	TonB-dependent receptor
WP_047340156.1	22	*Xanthomonas oryzae*	TonB-dependent receptor
WP_047340296.1	22	*Xanthomonas oryzae*	TonB-dependent receptor
WP_047340311.1	22	*Xanthomonas oryzae*	TonB-dependent receptor
WP_047340313.1	22	*Xanthomonas oryzae*	TonB-dependent receptor
WP_179208374.1	22	*Xanthomonas oryzae*	TonB-dependent receptor
WP_194928942.1	22	*Xanthomonas oryzae*	TonB-dependent receptor
WP_195765513.1	22	*Xanthomonas oryzae*	TonB-dependent receptor
WP_024711899.1	22	*Xanthomonas oryzae*	TonB-dependent receptor, partial
WP_014503900.1	22	*Xanthomonas oryzae*	TonB-dependent siderophore receptor
WP_047340074.1	22	*Xanthomonas oryzae*	TonB-dependent siderophore receptor
WP_047340206.1	22	*Xanthomonas oryzae*	TonB-dependent siderophore receptor
WP_228757530.1	22	*Xanthomonas oryzae*	TonB-dependent siderophore receptor
WP_024711330.1	28	*Xanthomonas oryzae*	LPS-assembly protein LptD
WP_011097760.1	4	*Xylella fastidiosa*	YadA-like family protein
WP_004089934.1	8	*Xylella fastidiosa*	OmpA family protein
WP_004088201.1	8	*Xylella fastidiosa*	outer membrane beta-barrel protein
WP_004572789.1	10	*Xylella fastidiosa*	Ax21 family protein
WP_004090465.1	12	*Xylella fastidiosa*	autotransporter domain-containing esterase

WP_011098080.1	12	*Xylella fastidiosa*	autotransporter domain-containing protein
WP_011097502.1	12	*Xylella fastidiosa*	copper resistance protein B
WP_004087308.1	12	*Xylella fastidiosa*	DUF481 domain-containing protein
WP_011097586.1	12	*Xylella fastidiosa*	S8 family serine peptidase
WP_012382579.1	12	*Xylella fastidiosa*	S8 family serine peptidase
WP_234552907.1	12	*Xylella fastidiosa*	S8 family serine peptidase
WP_004087368.1	14	*Xylella fastidiosa*	autotransporter domain-containing protein
WP_004089318.1	14	*Xylella fastidiosa*	outer membrane protein transport protein
WP_004087209.1	16	*Xylella fastidiosa*	autotransporter assembly complex protein TamA
WP_004087915.1	16	*Xylella fastidiosa*	OprO/OprP family phosphate-selective porin
WP_011097568.1	16	*Xylella fastidiosa*	OprO/OprP family phosphate-selective porin
WP_004089330.1	16	*Xylella fastidiosa*	outer membrane protein assembly factor BamA
WP_012382766.1	16	*Xylella fastidiosa*	ShlB/FhaC/HecB family hemolysin secretion/activation protein
WP_004088697.1	22	*Xylella fastidiosa*	catecholate siderophore receptor Fiu
WP_004087477.1	22	*Xylella fastidiosa*	TonB-dependent receptor
WP_004089020.1	22	*Xylella fastidiosa*	TonB-dependent receptor
WP_011097589.1	22	*Xylella fastidiosa*	TonB-dependent receptor
WP_011097995.1	22	*Xylella fastidiosa*	TonB-dependent receptor
WP_011097996.1	22	*Xylella fastidiosa*	TonB-dependent receptor
WP_011098035.1	22	*Xylella fastidiosa*	TonB-dependent receptor
WP_011098173.1	22	*Xylella fastidiosa*	TonB-dependent receptor
WP_011098206.1	22	*Xylella fastidiosa*	TonB-dependent receptor
WP_011098223.1	22	*Xylella fastidiosa*	TonB-dependent receptor
WP_004087687.1	24	*Xylella fastidiosa*	fimbrial biogenesis outer membrane usher protein
WP_011098274.1	28	*Xylella fastidiosa*	LPS-assembly protein LptD

References

ABRAMSON, J., ADLER, J., DUNGER, J., EVANS, R., GREEN, T., PRITZEL, A., RONNEBERGER, O., WILLMORE, L., BALLARD, A. J. & BAMBRICK, J. 2024. Accurate structure prediction of biomolecular interactions with AlphaFold 3. *Nature*, 1-3.

ACHOR, D., ETXEBERRIA, E., WANG, N., FOLIMONOVA, S., CHUNG, K. & ALBRIGO, L. 2010. Sequence of anatomical symptom observations in citrus affected with huanglongbing disease. *Plant Pathol. J,* 9, 56-64.

ACHOR, D., WELKER, S., BEN-MAHMOUD, S., WANG, C. X., FOLIMONOVA, S. Y., DUTT, M., GOWDA, S. & LEVY, A. 2020. Dynamics of Candidatus Liberibacter asiaticus Movement and Sieve-Pore Plugging in Citrus Sink Cells. *Plant Physiology,* 182, 882-891.

ADACHI, H., SAKAI, T., KOURELIS, J., PAI, H., GONZALEZ HERNANDEZ, J. L., UTSUMI, Y., SEKI, M., MAQBOOL, A. & KAMOUN, S. 2023. Jurassic NLR: conserved and dynamic evolutionary features of the atypically ancient immune receptor ZAR1. *The Plant Cell,* 35, 3662-3685.

ADE, J., DEYOUNG, B. J., GOLSTEIN, C. & INNES, R. W. 2007. Indirect activation of a plant nucleotide binding site–leucine-rich repeat protein by a bacterial protease. *Proceedings of the National Academy of Sciences,* 104, 2531-2536.

AHMAD, S., MALHOTRA, S., SAAD, S., KHAN, A. A. & SAJJAD, A. 2024. Molecular Characterization of Phytoplasma: An Overview. *Advanced Botany*, 77.

AL-SUBHI, A. M., AL-SADI, A. M., AL-YAHYAI, R., CHEN, Y., MATHERS, T., ORLOVSKIS, Z., MORO, G., MUGFORD, S., AL-HASHMI, K. & HOGENHOUT, S. 2021. Witches' broom disease of lime contributes to phytoplasma epidemics and attracts insect vectors. *Plant Disease,* 105, 2637-2648.

ALMAGRO ARMENTEROS, J. J., TSIRIGOS, K. D., SØNDERBY, C. K., PETERSEN, T. N., WINTHER, O., BRUNAK, S., VON HEIJNE, G. & NIELSEN, H. 2019. SignalP 5.0 improves signal peptide predictions using deep neural networks. *Nature biotechnology,* 37**,** 420-423.

ALQUÉZAR, B., CARMONA, L., BENNICI, S., MIRANDA, M. P., BASSANEZI, R. B. & PENA, L. 2022. Cultural Management of Huanglongbing: Current Status and Ongoing Research. *Phytopathology,* 112**,** 11-25.

ANDRADE, M. O., PANG, Z., ACHOR, D. S., WANG, H., YAO, T., SINGER, B. H. & WANG, N. 2020. The flagella of 'Candidatus Liberibacter asiaticus' and its movement in planta. *Molecular plant pathology,* 21**,** 109-123.

AXTELL, M. J., CHISHOLM, S. T., DAHLBECK, D. & STASKAWICZ, B. J. 2003. Genetic and molecular evidence that the Pseudomonas syringae type III effector protein AvrRpt2 is a cysteine protease. *Molecular microbiology,* 49**,** 1537-1546.

AXTELL, M. J. & STASKAWICZ, B. J. 2003. Initiation of RPS2-specified disease resistance in Arabidopsis is coupled to the AvrRpt2-directed elimination of RIN4. *Cell,* 112**,** 369-377.

BAI, X., CORREA, V. R., TORUÑO, T. Y., AMMAR, E.-D., KAMOUN, S. & HOGENHOUT, S. A. 2009. AY-WB phytoplasma secretes a protein that targets plant cell nuclei. *Molecular Plant-Microbe Interactions,* 22**,** 18-30.

BARDOEL, B. W., VAN DER ENT, S., PEL, M. J., TOMMASSEN, J., PIETERSE, C. M., VAN KESSEL, K. P. & VAN STRIJP, J. A. 2011. Pseudomonas evades immune recognition of flagellin in both mammals and plants. *PLoS pathogens,* 7**,** e1002206.

BARI, R. & JONES, J. D. 2009. Role of plant hormones in plant defence responses. *Plant molecular biology,* 69**,** 473-488.

BELAAOUAJ, A. 2002. Neutrophil elastase-mediated killing of bacteria: lessons from targeted mutagenesis. *Microbes and Infection,* 4**,** 1259-1264.

BELAAOUAJ, A., MCCARTHY, R., BAUMANN, M., GAO, Z. M., LEY, T. J., ABRAHAM, S. N. & SHAPIRO, S. D. 1998. Mice lacking neutrophil elastase reveal impaired host defense against gram negative bacterial sepsis. *Nature Medicine,* 4**,** 615-618.

BELAAOUAJ, A. A., KIM, K. S. & SHAPIRO, S. D. 2000. Degradation of outer membrane protein A in Escherichia coli killing by neutrophil elastase. *Science,* 289**,** 1185-1187.

BENDIX, C. & LEWIS, J. D. 2018. The enemy within: phloem-limited pathogens. *Molecular Plant Pathology,* 19**,** 238-254.

BENTHAM, A. R., YOULES, M., MENDEL, M. N., VARDEN, F. A., CONCEPCION, J. C. D. L. & BANFIELD, M. J. 2021. pOPIN-GG: a resource for modular assembly in protein expression vectors. *BioRxiv***,** 2021.08. 10.455798.

BERNARDINI, C., FRANCO, A., RUSSO, R., LIVINGSTON, T., GMITTER JR, F. G., LEVY, A. & VASHISTH, T. 2024. An efficient method for the extraction and the quantitative determination of callose from HLB-affected and healthy citrus. *Frontiers in Agronomy,* 6**,** 1307566.

BERTACCINI, A., OSHIMA, K., MAEJIMA, K. & NAMBA, S. 2019. Phytoplasma effectors and pathogenicity factors. *Phytoplasmas: Plant Pathogenic Bacteria-III: Genomics, Host Pathogen Interactions and Diagnosis***,** 17-34.

BREDDAM, K. 1986. Serine carboxypeptidases. A review. *Carlsberg Research Communications,* 51**,** 83-128.

BRYANT, P., POZZATI, G. & ELOFSSON, A. 2022. Improved prediction of protein-protein interactions using AlphaFold2. *Nature communications,* 13**,** 1265.

BUONO, R. A., HUDECEK, R. & NOWACK, M. K. 2019. Plant proteases during developmental programmed cell death. *Journal of Experimental Botany,* 70**,** 2097-2112.

BUSCAILL, P., CHANDRASEKAR, B., SANGUANKIATTICHAI, N., KOURELIS, J., KASCHANI, F., THOMAS, E. L., MORIMOTO, K., KAISER, M., PRESTON, G. M., ICHINOSE, Y. & VAN DER HOORN, R. A. L. 2019. Glycosidase and glycan polymorphism control hydrolytic release of immunogenic flagellin peptides. *Science,* 364**,** eaav0748.

BUSCAILL, P., SANGUANKIATTICHAI, N., KASCHANI, F., HUANG, J., LI, Y., LYU, J., SUELDO, D. J., KAISER, M. & VAN DER HOORN, R. A. 2024. Subtilase SBT5. 2 counterbalances flagellin immunogenicity in the plant apoplast. *bioRxiv***,** 2024.05. 23.595557.

CHANG, J. H., DESVEAUX, D. & CREASON, A. L. 2014. The ABCs and 123s of bacterial secretion systems in plant pathogenesis. *Annual review of phytopathology,* 52**,** 317-345.

CHAUDHARY, R., ATAMIAN, H. S., SHEN, Z., BRIGGS, S. P. & KALOSHIAN, I. 2014. GroEL from the endosymbiont Buchnera aphidicola betrays the aphid by triggering plant defense. *Proceedings of the National Academy of Sciences,* 111**,** 8919-8924.

CHEN, C., BUSCAILL, P., SANGUANKIATTICHAI, N., HUANG, J., KASCHANI, F., KAISER, M. & VAN DER HOORN, R. A. 2024. Extracellular plant subtilases dampen cold shock peptide elicitor levels. *bioRxiv***,** 2024.06. 14.599038.

CHEN, D., HAO, F., MU, H., AHSAN, N., THELEN, J. J. & STACEY, G. 2021. S-acylation of P2K1 mediates extracellular ATP-induced immune signaling in Arabidopsis. *Nature Communications,* 12**,** 2750.

CHEN, Y.-C., HOLMES, E. C., RAJNIAK, J., KIM, J.-G., TANG, S., FISCHER, C. R., MUDGETT, M. B. & SATTELY, E. S. 2018. N-hydroxy-pipecolic acid is a mobile metabolite that induces systemic disease resistance in Arabidopsis. *Proceedings of the National Academy of Sciences,* 115**,** E4920-E4929.

CHIA, K.-S., KOURELIS, J., TEULET, A., VICKERS, M., SAKAI, T., WALKER, J. F., SCHORNACK, S., KAMOUN, S. & CARELLA, P. 2024. The N-terminal domains of NLR immune receptors exhibit structural and functional similarities across divergent plant lineages. *The Plant Cell***,** koae113.

CHOI, U. & LEE, C.-R. 2019. Distinct roles of outer membrane porins in antibiotic resistance and membrane integrity in Escherichia coli. *Frontiers in microbiology,* 10**,** 953.

CLARK, K., FRANCO, J. Y., SCHWIZER, S., PANG, Z., HAWARA, E., LIEBRAND, T. W., PAGLIACCIA, D., ZENG, L., GURUNG, F. B. & WANG, P. 2018. An effector from the Huanglongbing-associated pathogen targets citrus proteases. *Nature communications,* 9**,** 1718.

CLARK, K. J. 2019. *An Effector of the Citrus Huanglongbing-Associated Pathogen Provides Mechanistic Insight to Pathogenesis and Potential Strategies to Enhance Disease Management*, University of California, Riverside.

CLARK, K. J., PANG, Z., TRINH, J., WANG, N. & MA, W. 2020. Sec-delivered effector 1 (SDE1) of 'Candidatus Liberibacter asiaticus' promotes citrus huanglongbing. *Molecular Plant-Microbe Interactions,* 33**,** 1394-1404.

COAKER, G., FALICK, A. & STASKAWICZ, B. 2005. Activation of a phytopathogenic bacterial effector protein by a eukaryotic cyclophilin. *Science,* 308**,** 548-550.

COLL, N. S., VERCAMMEN, D., SMIDLER, A., CLOVER, C., VAN BREUSEGEM, F., DANGL, J. L. & EPPLE, P. 2010. Arabidopsis type I metacaspases control cell death. *Science,* 330**,** 1393-1397.

CONFER, A. W. & AYALEW, S. 2013. The OmpA family of proteins: roles in bacterial pathogenesis and immunity. *Veterinary microbiology,* 163**,** 207-222.

CONTRERAS, M. P., LÜDKE, D., PAI, H., TOGHANI, A. & KAMOUN, S. 2023. NLR receptors in plant immunity: making sense of the alphabet soup. *EMBO reports,* 24**,** e57495.

CORREA MARRERO, M., CAPDEVIELLE, S., HUANG, W., AL-SUBHI, A. M., BUSSCHER, M., BUSSCHER-LANGE, J., VAN DER WAL, F., DE RIDDER, D., VAN DIJK, A. D. J., HOGENHOUT, S. A. & IMMINK, R. G. H. 2024. Protein interaction mapping reveals widespread targeting of development-related host transcription factors by phytoplasma effectors. *The Plant Journal,* 117**,** 1281-1297.

COURT, C. D., HODGES, A.W., RAHMANI, M., SPREEN, T.H. 2017. *Economic Contributions of the Florida Citrus Industry in 2015/16* [Online]. Food and Resource Economics Department, UF/IFAS Extension. Available: http://edis.ifas.ufl.edu/ [Accessed 2024].

CURTOLO, M., DE SOUZA PACHECO, I., BOAVA, L. P., TAKITA, M. A., GRANATO, L. M., GALDEANO, D. M., DE SOUZA, A. A., CRISTOFANI-YALY, M. & MACHADO, M. A. 2020. Wide-ranging transcriptomic analysis of Poncirus trifoliata, Citrus sunki, Citrus sinensis and contrasting hybrids reveals HLB tolerance mechanisms. *Scientific Reports,* 10**,** 20865.

DAVIS, M. J., MONDAL, S. N., CHEN, H. Q., ROGERS, M. E. & BRIANSKY, R. H. 2008. Co-cultivation of 'Candidatus Liberibacter asiaticus' with Actinobacteria from Citrus with Huanglongbing. *Plant Disease,* 92**,** 1547-1550.

DE FRANCESCO, A., LOVELACE, A. H., SHAW, D., QIU, M., WANG, Y., GURUNG, F., ANCONA, V., WANG, C., LEVY, A. & JIANG, T. 2022. Transcriptome profiling of 'Candidatus Liberibacter asiaticus' in citrus and psyllids. *Phytopathology®,* 112**,** 116-130.

DEMIR, F., NIEDERMAIER, S., VILLAMOR, J. G. & HUESGEN, P. F. 2018. Quantitative proteomics in plant protease substrate identification. *New Phytologist,* 218**,** 936-943.

DENG, H., ACHOR, D., EXTEBERRIA, E., YU, Q., DU, D., STANTON, D., LIANG, G. & GMITTER JR, F. G. 2019. Phloem regeneration is a mechanism for Huanglongbing-tolerance of "Bearss" lemon and "LB8-9" Sugar Belle® mandarin. *Frontiers in Plant Science,* 10**,** 277.

DI MATTEO, A., BONIVENTO, D., TSERNOGLOU, D., FEDERICI, L. & CERVONE, F. 2006. Polygalacturonase-inhibiting protein (PGIP) in plant defence: a structural view. *Phytochemistry,* 67**,** 528-533.

DIXON, M. S., GOLSTEIN, C., THOMAS, C. M., VAN DER BIEZEN, E. A. & JONES, J. D. 2000. Genetic complexity of pathogen perception by plants: the example of Rcr3, a tomato gene required specifically by Cf-2. *Proceedings of the National Academy of Sciences,* 97**,** 8807-8814.

DODDS, P. N., CHEN, J. & OUTRAM, M. A. 2024. Pathogen perception and signaling in plant immunity. *The Plant Cell,* 36**,** 1465-1481.

DOMÍNGUEZ, F., GONZÁLEZ, M. & CEJUDO, F. J. 2002. A germination-related gene encoding a serine carboxypeptidase is expressed during the differentiation of the vascular tissue in wheat grains and seedlings. *Planta,* 215**,** 727-734.

DUTT, M., BARTHE, G., IREY, M. & GROSSER, J. 2015. Transgenic citrus expressing an Arabidopsis NPR1 gene exhibit enhanced resistance against Huanglongbing (HLB; Citrus Greening). *PloS one,* 10**,** e0137134.

DYER, R. P. & WEISS, G. A. 2022. Making the cut with protease engineering. *Cell chemical biology,* 29**,** 177-190.

EASTMAN, S., JIANG, T., FICCO, K., LIAO, C., JONES, B., WEN, S., OLIVAS BIDDLE, Y., EYCEOZ, A., YATSISHIN, I. & NAUMANN, T. A. 2024. A type II secreted subtilase from commensal rhizobacteria disarms the immune elicitor peptide flg22. *bioRxiv*, 2024.05. 07.592856.

EDGAR, R. C. 2004. MUSCLE: multiple sequence alignment with high accuracy and high throughput. *Nucleic acids research,* 32, 1792-1797.

ERDŐS, G. & DOSZTÁNYI, Z. 2020. Analyzing protein disorder with IUPred2A. *Current protocols in bioinformatics,* 70, e99.

EVANS, R., O'NEILL, M., PRITZEL, A., ANTROPOVA, N., SENIOR, A., GREEN, T., ŽÍDEK, A., BATES, R., BLACKWELL, S. & YIM, J. 2021. Protein complex prediction with AlphaFold-Multimer. *biorxiv*, 2021.10. 04.463034.

FABRE, A., DANET, J.-L. & FOISSAC, X. 2011. The stolbur phytoplasma antigenic membrane protein gene stamp is submitted to diversifying positive selection. *Gene,* 472, 37-41.

FAGEN, J. R., LEONARD, M. T., MCCULLOUGH, C. M., EDIRISINGHE, J. N., HENRY, C. S., DAVIS, M. J. & TRIPLETT, E. W. 2014. Comparative genomics of cultured and uncultured strains suggests genes essential for free-living growth of Liberibacter. *PLoS One,* 9, e84469.

FAIRMAN, J. W., NOINAJ, N. & BUCHANAN, S. K. 2011. The structural biology of β-barrel membrane proteins: a summary of recent reports. *Current opinion in structural biology,* 21, 523-531.

FEDERICI, L., DI MATTEO, A., FERNANDEZ-RECIO, J., TSERNOGLOU, D. & CERVONE, F. 2006. Polygalacturonase inhibiting proteins: players in plant innate immunity? *Trends in Plant Science,* 11, 65-70.

FERNÁNDEZ, F. D. & CONCI, L. R. 2020. Diversity analysis of amp gene sequences in the 'Candidatus Phytoplasma meliae'. *bioRxiv*, 2020.06. 01.128413.

FLOR, H. H. 1971. Current status of the gene-for-gene concept. *Annual review of phytopathology,* 9, 275-296.

FRANCO, J. Y., THAPA, S. P., PANG, Z., GURUNG, F. B., LIEBRAND, T. W., STEVENS, D. M., ANCONA, V., WANG, N. & COAKER, G. 2020. Citrus vascular proteomics highlights the role of peroxidases and serine proteases during Huanglongbing disease progression. *Molecular & Cellular Proteomics,* 19, 1936-1952.

FRASER, C. M., RIDER, L. W. & CHAPPLE, C. 2005. An expression and bioinformatics analysis of the Arabidopsis serine carboxypeptidase-like gene family. *Plant physiology,* 138, 1136-1148.

GODDARD, T. D., HUANG, C. C., MENG, E. C., PETTERSEN, E. F., COUCH, G. S., MORRIS, J. H. & FERRIN, T. E. 2018. UCSF ChimeraX: Meeting modern challenges in visualization and analysis. *Protein science,* 27, 14-25.

GODSON, A. & VAN DER HOORN, R. A. 2021. The front line of defence: a meta-analysis of apoplastic proteases in plant immunity. *Journal of Experimental Botany,* 72, 3381-3394.

GU, C., SHABAB, M., STRASSER, R., WOLTERS, P. J., SHINDO, T., NIEMER, M., KASCHANI, F., MACH, L. & VAN DER HOORN, R. A. L. 2012. Post-Translational Regulation and Trafficking of the Granulin-Containing Protease RD21 of Arabidopsis thaliana. *Plos One,* 7.

GUO, H., ZHANG, Y., TONG, J., GE, P., WANG, Q., ZHAO, Z., ZHU-SALZMAN, K., HOGENHOUT, S. A., GE, F. & SUN, Y. 2020. An aphid-secreted salivary protease activates plant defense in phloem. *Current Biology,* 30, 4826-4836. e7.

GUST, A. A., PRUITT, R. & NÜRNBERGER, T. 2017. Sensing danger: key to activating plant immunity. *Trends in plant science,* 22**,** 779-791.

HALLGREN, J., TSIRIGOS, K. D., PEDERSEN, M. D., ALMAGRO ARMENTEROS, J. J., MARCATILI, P., NIELSEN, H., KROGH, A. & WINTHER, O. 2022. DeepTMHMM predicts alpha and beta transmembrane proteins using deep neural networks. *BioRxiv***,** 2022.04. 08.487609.

HAO, G., STOVER, E. & GUPTA, G. 2016. Overexpression of a modified plant thionin enhances disease resistance to citrus canker and huanglongbing (HLB). *Frontiers in plant science,* 7**,** 1078.

HE, J., YE, W., CHOI, D. S., WU, B., ZHAI, Y., GUO, B., DUAN, S., WANG, Y., GAN, J. & MA, W. 2019. Structural analysis of Phytophthora suppressor of RNA silencing 2 (PSR2) reveals a conserved modular fold contributing to virulence. *Proceedings of the National Academy of Sciences,* 116**,** 8054-8059.

HIJAZ, F. & KILLINY, N. 2014. Collection and chemical composition of phloem sap from Citrus sinensis L. Osbeck (sweet orange). *PloS one,* 9**,** e101830.

HOGENHOUT, S. A., VAN DER HOORN, R. A., TERAUCHI, R. & KAMOUN, S. 2009. Emerging concepts in effector biology of plant-associated organisms. *Molecular plant-microbe interactions,* 22**,** 115-122.

HOMMA, F., HUANG, J. & VAN DER HOORN, R. A. 2023. AlphaFold-Multimer predicts cross-kingdom interactions at the plant-pathogen interface. *Nature Communications,* 14**,** 6040.

HOSHI, A., OSHIMA, K., KAKIZAWA, S., ISHII, Y., OZEKI, J., HASHIMOTO, M., KOMATSU, K., KAGIWADA, S., YAMAJI, Y. & NAMBA, S. 2009. A unique virulence factor for proliferation and dwarfism in plants identified from a phytopathogenic bacterium. *Proceedings of the National Academy of Sciences,* 106**,** 6416-6421.

HOU, Y., ZHAI, Y., FENG, L., KARIMI, H. Z., RUTTER, B. D., ZENG, L., CHOI, D. S., ZHANG, B., GU, W. & CHEN, X. 2019. A Phytophthora effector suppresses trans-kingdom RNAi to promote disease susceptibility. *Cell host & microbe,* 25**,** 153-165. e5.

HU, J., JIANG, J. & WANG, N. 2018. Control of citrus Huanglongbing via trunk injection of plant defense activators and antibiotics. *Phytopathology,* 108**,** 186-195.

HU, X., DONG, Q., YANG, J. & ZHANG, Y. 2016. Recognizing metal and acid radical ion-binding sites by integrating ab initio modeling with template-based transferals. *Bioinformatics,* 32**,** 3260-3269.

HUANG, C.-Y., ARAUJO, K., SÁNCHEZ, J. N., KUND, G., TRUMBLE, J., ROPER, C., GODFREY, K. E. & JIN, H. 2021a. A stable antimicrobial peptide with dual functions of treating and preventing citrus Huanglongbing. *Proceedings of the National Academy of Sciences,* 118**,** e2019628118.

HUANG, W. & HOGENHOUT, S. A. 2022. Interfering with plant developmental timing promotes susceptibility to insect vectors of a bacterial parasite. *Biorxiv***,** 2022.03.30.486463.

HUANG, W., MACLEAN, A. M., SUGIO, A., MAQBOOL, A., BUSSCHER, M., CHO, S.-T., KAMOUN, S., KUO, C.-H., IMMINK, R. G. & HOGENHOUT, S. A. 2021b. Parasitic modulation of host development by ubiquitin-independent protein degradation. *Cell,* 184**,** 5201-5214. e12.

HULIN, M. T., HILL, L., JONES, J. D. G. & MA, W. 2023. Pangenomic analysis reveals plant NAD⁺ manipulation as an important virulence activity of bacterial pathogen effectors. *Proceedings of the National Academy of Sciences,* 120**,** e2217114120.

HURST, C. H., TURNBULL, D., XHELILAJ, K., MYLES, S., PFLUGHAUPT, R. L., KOPISCHKE, M., DAVIES, P., JONES, S., ROBATZEK, S. & ZIPFEL, C. 2023. S-

acylation stabilizes ligand-induced receptor kinase complex formation during plant pattern-triggered immune signaling. *Current Biology,* 33**,** 1588-1596. e6.

IZORÉ, T., JOB, V. & DESSEN, A. 2011. Biogenesis, regulation, and targeting of the type III secretion system. *Structure,* 19**,** 603-612.

JAIN, M., FLEITES, L. A. & GABRIEL, D. W. 2015. Prophage-encoded peroxidase in 'Candidatus Liberibacter asiaticus' is a secreted effector that suppresses plant defenses. *Molecular Plant-Microbe Interactions,* 28**,** 1330-1337.

JAIN, M., MUNOZ-BODNAR, A., ZHANG, S. & GABRIEL, D. W. 2018. A secreted 'Candidatus Liberibacter asiaticus' peroxiredoxin simultaneously suppresses both localized and systemic innate immune responses in planta. *Molecular Plant-Microbe Interactions,* 31**,** 1312-1322.

JONES, J. D. & DANGL, J. L. 2006. The plant immune system. *nature,* 444**,** 323-329.

JONES, J. D., STASKAWICZ, B. J. & DANGL, J. L. 2024. The plant immune system: From discovery to deployment. *Cell,* 187**,** 2095-2116.

JONES, P., BINNS, D., CHANG, H.-Y., FRASER, M., LI, W., MCANULLA, C., MCWILLIAM, H., MASLEN, J., MITCHELL, A. & NUKA, G. 2014. InterProScan 5: genome-scale protein function classification. *Bioinformatics,* 30**,** 1236-1240.

JUGE, N. 2006. Plant protein inhibitors of cell wall degrading enzymes. *Trends in plant science,* 11**,** 359-367.

JUMPER, J., EVANS, R., PRITZEL, A., GREEN, T., FIGURNOV, M., RONNEBERGER, O., TUNYASUVUNAKOOL, K., BATES, R., ŽÍDEK, A. & POTAPENKO, A. 2021. Highly accurate protein structure prediction with AlphaFold. *nature,* 596**,** 583-589.

KAKIZAWA, S., OSHIMA, K., JUNG, H.-Y., SUZUKI, S., NISHIGAWA, H., ARASHIDA, R., MIYATA, S.-I., UGAKI, M., KISHINO, H. & NAMBA, S. 2006a. Positive selection acting on a surface membrane protein of the plant-pathogenic phytoplasmas. *Journal of Bacteriology,* 188**,** 3424-3428.

KAKIZAWA, S., OSHIMA, K. & NAMBA, S. 2006b. Diversity and functional importance of phytoplasma membrane proteins. *Trends in microbiology,* 14**,** 254-256.

KALUNKE, R. M., TUNDO, S., BENEDETTI, M., CERVONE, F., DE LORENZO, G. & D'OVIDIO, R. 2015. An update on polygalacturonase-inhibiting protein (PGIP), a leucine-rich repeat protein that protects crop plants against pathogens. *Frontiers in plant science,* 6**,** 146.

KAN, C.-C., MENDOZA-HERRERA, A., LEVY, J., HULL, J. J., FABRICK, J. A. & TAMBORINDEGUY, C. 2021. HPE1, an effector from zebra chip pathogen interacts with tomato proteins and perturbs ubiquitinated protein accumulation. *International Journal of Molecular Sciences,* 22**,** 9003.

KASCHANI, F., SHABAB, M., BOZKURT, T., SHINDO, T., SCHORNACK, S., GU, C., ILYAS, M., WIN, J., KAMOUN, S. & VAN DER HOORN, R. A. 2010. An effector-targeted protease contributes to defense against Phytophthora infestans and is under diversifying selection in natural hosts. *Plant physiology,* 154**,** 1794-1804.

KATOH, K. & STANDLEY, D. M. 2013. MAFFT multiple sequence alignment software version 7: improvements in performance and usability. *Molecular biology and evolution,* 30**,** 772-780.

KILLINY, N. & HIJAZ, F. 2016. Amino acids implicated in plant defense are higher in Candidatus Liberibacter asiaticus-tolerant citrus varieties. *Plant signaling & behavior,* 11**,** e1171449.

KIM, J.-S., SAGARAM, U. S., BURNS, J. K., LI, J.-L. & WANG, N. 2009. Response of sweet orange (Citrus sinensis) to 'Candidatus Liberibacter asiaticus' infection: microscopy and microarray analyses. *Phytopathology,* 99**,** 50-57.

KNOBLAUCH, M., PETERS, W. S., BELL, K., ROSS-ELLIOTT, T. J. & OPARKA, K. J. 2018. Sieve-element differentiation and phloem sap contamination. *Current opinion in plant biology,* 43**,** 43-49.

KONNERTH, A., KRCZAL, G. & BOONROD, K. 2016. Immunodominant membrane proteins of phytoplasmas. *Microbiology,* 162**,** 1267-1273.

KOSTAKIOTI, M., NEWMAN, C. L., THANASSI, D. G. & STATHOPOULOS, C. 2005. Mechanisms of protein export across the bacterial outer membrane. *Journal of bacteriology,* 187**,** 4306-4314.

KOURELIS, J., MALIK, S., MATTINSON, O., KRAUTER, S., KAHLON, P. S., PAULUS, J. K. & VAN DER HOORN, R. A. 2020. Evolution of a guarded decoy protease and its receptor in solanaceous plants. *Nature Communications,* 11**,** 4393.

KOURELIS, J., SAKAI, T., ADACHI, H. & KAMOUN, S. 2021. RefPlantNLR is a comprehensive collection of experimentally validated plant disease resistance proteins from the NLR family. *PLoS Biology,* 19**,** e3001124.

KOURELIS, J., SCHUSTER, M., DEMIR, F., MATTINSON, O., KRAUTER, S., KAHLON, P. S., O'GRADY, R., ROYSTON, S., BRAVO-CAZAR, A. L. & MOONEY, B. C. 2024. Bioengineering secreted proteases converts divergent Rcr3 orthologs and paralogs into extracellular immune co-receptors. *bioRxiv***,** 2024.02. 14.580413.

KOURELIS, J. & VAN DER HOORN, R. A. 2018. Defended to the nines: 25 years of resistance gene cloning identifies nine mechanisms for R protein function. *The Plant Cell,* 30**,** 285-299.

KRUGER, J., THOMAS, C. M., GOLSTEIN, C., DIXON, M. S., SMOKER, M., TANG, S., MULDER, L. & JONES, J. D. 2002. A tomato cysteine protease required for Cf-2-dependent disease resistance and suppression of autonecrosis. *Science,* 296**,** 744-747.

LAGAERT, S., BELIËN, T. & VOLCKAERT, G. Plant cell walls: Protecting the barrier from degradation by microbial enzymes. Seminars in cell & developmental biology, 2009. Elsevier, 1064-1073.

LEE, I.-M., DAVIS, R. E. & GUNDERSEN-RINDAL, D. E. 2000. Phytoplasma: phytopathogenic mollicutes. *Annual Reviews in Microbiology,* 54**,** 221-255.

LEWIS, J. D., KNOBLAUCH, M. & TURGEON, R. 2022. The phloem as an arena for plant pathogens. *Annual Review of Phytopathology,* 60**,** 77-96.

LI, H., WANG, J., KUAN, T. A., TANG, B., FENG, L., WANG, J., CHENG, Z., SKŁENAR, J., DERBYSHIRE, P. & HULIN, M. 2023. Pathogen protein modularity enables elaborate mimicry of a host phosphatase. *Cell,* 186**,** 3196–3207.

LI, J., LEASE, K. A., TAX, F. E. & WALKER, J. C. 2001. BRS1, a serine carboxypeptidase, regulates BRI1 signaling in Arabidopsis thaliana. *Proceedings of the National Academy of Sciences,* 98**,** 5916-5921.

LI, J., PANG, Z., DUAN, S., LEE, D., KOLBASOV, V. G. & WANG, N. 2019. The in planta effective concentration of oxytetracycline against 'Candidatus Liberibacter asiaticus' for suppression of citrus Huanglongbing. *Phytopathology,* 109**,** 2046-2054.

LI, J., PANG, Z., TRIVEDI, P., ZHOU, X., YING, X., JIA, H. & WANG, N. 2017. 'Candidatus Liberibacter asiaticus' encodes a functional salicylic acid (SA) hydroxylase that degrades SA to suppress plant defenses. *Molecular Plant-Microbe Interactions,* 30**,** 620-630.

LI, L., KIM, P., YU, L., CAI, G., CHEN, S., ALFANO, J. R. & ZHOU, J.-M. 2016. Activation-dependent destruction of a co-receptor by a Pseudomonas syringae effector dampens plant immunity. *Cell host & microbe,* 20**,** 504-514.

LI, W., YE, T., YE, W., LIANG, J., WANG, W., HAN, D., LIU, X., HUANG, L., OUYANG, Y. & LIAO, J. 2024. S-acylation of a non-secreted peptide controls plant immunity via secreted-peptide signal activation. *EMBO reports,* 25**,** 489-505.

LIU, H., WANG, X., ZHANG, H., YANG, Y., GE, X. & SONG, F. 2008. A rice serine carboxypeptidase-like gene OsBISCPL1 is involved in regulation of defense responses against biotic and oxidative stress. *Gene,* 420**,** 57-65.

LIU, J., ELMORE, J. M., LIN, Z.-J. D. & COAKER, G. 2011. A receptor-like cytoplasmic kinase phosphorylates the host target RIN4, leading to the activation of a plant innate immune receptor. *Cell host & microbe,* 9**,** 137-146.

LIU, Q., MAQBOOL, A., MIRKIN, F. G., SINGH, Y., STEVENSON, C. E., LAWSON, D. M., KAMOUN, S., HUANG, W. & HOGENHOUT, S. A. 2023. Bimodular architecture of bacterial effector SAP05 that drives ubiquitin-independent targeted protein degradation. *Proceedings of the National Academy of Sciences,* 120**,** e2310664120.

LIU, X., FAN, Y., ZHANG, C., DAI, M., WANG, X. & LI, W. 2019. Nuclear import of a secreted "Candidatus Liberibacter asiaticus" protein is temperature dependent and contributes to pathogenicity in Nicotiana benthamiana. *Frontiers in Microbiology,* 10**,** 1684.

LOVELACE, A. H., DORHMI, S., HULIN, M. T., LI, Y., MANSFIELD, J. W. & MA, W. 2023. Effector identification in plant pathogens. *Phytopathology®,* 113**,** 637-650.

LOVELACE, A. H., WANG, C., LEVY, A. & MA, W. 2024. Transcriptomic profiling of Candidatus Liberibacter asiaticus in different citrus tissues reveals novel insights into Huanglongbing pathogenesis. *bioRxiv***,** 2024.09. 02.610751.

LYCKLAMA A NIJEHOLT, J. A. & DRIESSEN, A. J. 2012. The bacterial Sec-translocase: structure and mechanism. *Philosophical Transactions of the Royal Society B: Biological Sciences,* 367**,** 1016-1028.

MA, W. X., PANG, Z. Q., HUANG, X. E., XU, J., PANDEY, S. S., LI, J. Y., ACHOR, D. S., VASCONCELOS, F. N. C., HENDRICH, C., HUANG, Y. X., WANG, W. T., LEE, D., STANTON, D. & WANG, N. 2022. Citrus Huanglongbing is a pathogen-triggered immune disease that can be mitigated with antioxidants and gibberellin. *Nature Communications,* 13.

MACKEY, D., BELKHADIR, Y., ALONSO, J. M., ECKER, J. R. & DANGL, J. L. 2003. Arabidopsis RIN4 is a target of the type III virulence effector AvrRpt2 and modulates RPS2-mediated resistance. *Cell,* 112**,** 379-389.

MACKEY, D., HOLT, B. F., WIIG, A. & DANGL, J. L. 2002. RIN4 interacts with Pseudomonas syringae type III effector molecules and is required for RPM1-mediated resistance in Arabidopsis. *Cell,* 108**,** 743-754.

MACLEAN, A. M., ORLOVSKIS, Z., KOWITWANICH, K., ZDZIARSKA, A. M., ANGENENT, G. C., IMMINK, R. G. & HOGENHOUT, S. A. 2014. Phytoplasma effector SAP54 hijacks plant reproduction by degrading MADS-box proteins and promotes insect colonization in a RAD23-dependent manner. *PLoS biology,* 12**,** e1001835.

MACLEAN, A. M., SUGIO, A., MAKAROVA, O. V., FINDLAY, K. C., GRIEVE, V. M., TÓTH, R., NICOLAISEN, M. & HOGENHOUT, S. A. 2011. Phytoplasma effector SAP54 induces indeterminate leaf-like flower development in Arabidopsis plants. *Plant Physiology,* 157**,** 831-841.

MANSFIELD, J., GENIN, S., MAGORI, S., CITOVSKY, V., SRIARIYANUM, M., RONALD, P., DOW, M., VERDIER, V., BEER, S. V. & MACHADO, M. A. 2012. Top 10 plant pathogenic bacteria in molecular plant pathology. *Molecular plant pathology,* 13**,** 614-629.

MARCEC, M. J., GILROY, S., POOVAIAH, B. & TANAKA, K. 2019. Mutual interplay of Ca2+ and ROS signaling in plant immune response. *Plant Science,* 283**,** 343-354.

MARCHAL, C., MICHALOPOULOU, V. A., ZOU, Z., CEVIK, V. & SARRIS, P. F. 2022. Show me your ID: NLR immune receptors with integrated domains in plants. *Essays in biochemistry,* 66**,** 527-539.

MARGETS, A., FOSTER, J., KUMAR, A., MAIER, T., MASONBRINK, R. E., MEJIAS, J., BAUM, T. J. & INNES, R. W. 2024. The Soybean Cyst Nematode Effector Cysteine Protease 1 (CPR1) Targets a Mitochondrial Soybean Branched-Chain Amino Acid Aminotransferase (GmBCAT1) for Degradation. *bioRxiv***,** 2024.07.01.601533.

MCCLEAN, S. 2012. Eight stranded β -barrel and related outer membrane proteins: role in bacterial pathogenesis. *Protein and peptide letters,* 19**,** 1013-1025.

MCCLELLAND, A. J. & MA, W. 2024. Zig, Zag, and'Zyme: leveraging structural biology to engineer disease resistance. *aBIOTECH***,** 1-5.

MCILWAIN, B. C. & KERMANI, A. A. 2020. Membrane protein production in Escherichia coli. *Expression, Purification, and Structural Biology of Membrane Proteins***,** 13-27.

MCLELLAN, H., GILROY, E. M., YUN, B. W., BIRCH, P. R. & LOAKE, G. J. 2009. Functional redundancy in the Arabidopsis Cathepsin B gene family contributes to basal defence, the hypersensitive response and senescence. *New Phytologist,* 183**,** 408-418.

MEHTA, R. A., WARMBARDT, R. D. & MATTOO, A. K. 1996. Tomato (Lycopersicon esculentum cv. Pik-Red) leaf carboxypeptidase: identification, N-terminal sequence, stress-regulation, and specific localization in the paraveinal mesophyll vacuoles. *Plant and cell physiology,* 37**,** 806-815.

MENG, E. C., GODDARD, T. D., PETTERSEN, E. F., COUCH, G. S., PEARSON, Z. J., MORRIS, J. H. & FERRIN, T. E. 2023. UCSF ChimeraX: Tools for structure building and analysis. *Protein Science,* 32**,** e4792.

MÉSZÁROS, B., ERDŐS, G. & DOSZTÁNYI, Z. 2018. IUPred2A: context-dependent prediction of protein disorder as a function of redox state and protein binding. *Nucleic acids research,* 46**,** W329-W337.

MILKOWSKI, C. & STRACK, D. 2004. Serine carboxypeptidase-like acyltransferases. *Phytochemistry,* 65**,** 517-524.

MILNES, L., YOULES, M. & MAIDMENT, J. H. 2023. pOPARA: Vectors for Golden Gate assembly of expression constructs containing the araBAD promoter. *bioRxiv***,** 2023.05. 31.543011.

MINATO, N., HIMENO, M., HOSHI, A., MAEJIMA, K., KOMATSU, K., TAKEBAYASHI, Y., KASAHARA, H., YUSA, A., YAMAJI, Y. & OSHIMA, K. 2014. The phytoplasmal virulence factor TENGU causes plant sterility by downregulating of the jasmonic acid and auxin pathways. *Scientific reports,* 4**,** 7399.

MISAS VILLAMIL, J. C., MUELLER, A. N., DEMIR, F., MEYER, U., ÖKMEN, B., SCHULZE HÜYNCK, J., BREUER, M., DAUBEN, H., WIN, J. & HUESGEN, P. F. 2019. A fungal substrate mimicking molecule suppresses plant immunity via an inter-kingdom conserved motif. *Nature communications,* 10**,** 1576.

MISAS-VILLAMIL, J. C., VAN DER HOORN, R. A. L. & DOEHLEMANN, G. 2016. Papain-like cysteine proteases as hubs in plant immunity. *New Phytologist,* 212**,** 902-907.

MOURA, D. S., BERGEY, D. R. & RYAN, C. A. 2001. Characterization and localization of a wound-inducible type I serine-carboxypeptidase from leaves of tomato plants (Lycopersicon esculentum Mill.). *Planta,* 212**,** 222-230.

MUGFORD, S. T. & MILKOWSKI, C. 2012. Serine carboxypeptidase-like acyltransferases from plants. *Methods in enzymology.* Elsevier.

MUGFORD, S. T., QI, X., BAKHT, S., HILL, L., WEGEL, E., HUGHES, R. K., PAPADOPOULOU, K., MELTON, R., PHILO, M. & SAINSBURY, F. 2009. A serine carboxypeptidase-like acyltransferase is required for synthesis of antimicrobial compounds and disease resistance in oats. *The Plant Cell,* 21**,** 2473-2484.

NEUPANE, A., SHAHZAD, F., BERNARDINI, C., LEVY, A. & VASHISTH, T. 2023. Poor shoot and leaf growth in Huanglongbing-affected sweet orange is associated with increased investment in defenses. *Frontiers in Plant Science,* 14**,** 1305815.

NGOU, B. P. M., AHN, H.-K., DING, P. & JONES, J. D. 2021. Mutual potentiation of plant immunity by cell-surface and intracellular receptors. *Nature,* 592**,** 110-115.

NGOU, B. P. M., DING, P. & JONES, J. D. 2022a. Thirty years of resistance: Zig-zag through the plant immune system. *The Plant Cell,* 34**,** 1447-1478.

NGOU, B. P. M., JONES, J. D. & DING, P. 2022b. Plant immune networks. *Trends in plant science,* 27**,** 255-273.

NGUYEN, Q. M., ISWANTO, A. B. B., KANG, H., MOON, J., PHAN, K. A. T., SON, G. H., SUH, M. C., CHUNG, E. H., GASSMANN, W. & KIM, S. H. 2024. The processed C-terminus of AvrRps4 effector suppresses plant immunity via targeting multiple WRKYs. *Journal of Integrative Plant Biology*.

NOVINEC, M., BEMBIČ, P., JANKOVIĆ, M., KISILAK, M., KLJUN, J. & TUREL, I. 2022. Kinetic characterization of cerium and gallium ions as inhibitors of cysteine cathepsins L, K, and S. *International Journal of Molecular Sciences,* 23**,** 8993.

OH, J., LEVY, J. G., KAN, C.-C., IBANEZ-CARRASCO, F. & TAMBORINDEGUY, C. 2022. CLIBASIA_00460 disrupts hypersensitive response and interacts with citrus Rad23 proteins. *International Journal of Molecular Sciences,* 23**,** 7846.

ORLOVSKIS, Z., SINGH, A., KLIOT, A., HUANG, W. & HOGENHOUT, S. A. 2024. Phytoplasma Targeting of MADS-Box Factor SVP Suppresses Leaf Responses to Insect Vector Males, Promoting Female Attraction and Colonization. *bioRxiv***,** 2024.05. 09.593434.

PADHI, A., VERGHESE, B. & OTTA, S. K. 2009. Detecting the form of selection in the outer membrane protein C of Enterobacter aerogenes strains and Salmonella species. *Microbiological Research,* 164**,** 282-289.

PAGLIACCIA, D., SHI, J., PANG, Z., HAWARA, E., CLARK, K., THAPA, S. P., DE FRANCESCO, A. D., LIU, J., TRAN, T.-T. & BODAGHI, S. 2017. A pathogen secreted protein as a detection marker for citrus huanglongbing. *Frontiers in microbiology,* 8**,** 2041.

PANG, Z., ZHANG, L., COAKER, G., MA, W., HE, S.-Y. & WANG, N. 2020. Citrus CsACD2 is a target of Candidatus Liberibacter asiaticus in Huanglongbing disease. *Plant physiology,* 184**,** 792-805.

PARADIS-BLEAU, C., KRITIKOS, G., ORLOVA, K., TYPAS, A. & BERNHARDT, T. G. 2014. A genome-wide screen for bacterial envelope biogenesis mutants identifies a novel factor involved in cell wall precursor metabolism. *PLoS genetics,* 10**,** e1004056.

PAULUS, J. K., KOURELIS, J., RAMASUBRAMANIAN, S., HOMMA, F., GODSON, A., HÖRGER, A. C., HONG, T. N., KRAHN, D., OSSORIO CARBALLO, L. & WANG, S. 2020. Extracellular proteolytic cascade in tomato activates immune protease Rcr3. *Proceedings of the National Academy of Sciences,* 117**,** 17409-17417.

PEL, M. J., VAN DIJKEN, A. J., BARDOEL, B. W., SEIDL, M. F., VAN DER ENT, S., VAN STRIJP, J. A. & PIETERSE, C. M. 2014. Pseudomonas syringae evades host immunity by degrading flagellin monomers with alkaline protease AprA. *Molecular Plant-Microbe Interactions,* 27**,** 603-610.

PENG, A., ZOU, X., HE, Y., CHEN, S., LIU, X., ZHANG, J., ZHANG, Q., XIE, Z., LONG, J. & ZHAO, X. 2021. Overexpressing a NPR1-like gene from Citrus paradisi enhanced Huanglongbing resistance in C. sinensis. *Plant cell reports,* 40**,** 529-541.

PETTERSEN, E. F., GODDARD, T. D., HUANG, C. C., MENG, E. C., COUCH, G. S., CROLL, T. I., MORRIS, J. H. & FERRIN, T. E. 2021. UCSF ChimeraX: Structure visualization for researchers, educators, and developers. *Protein science,* 30**,** 70-82.

PITINO, M., ALLEN, V. & DUAN, Y. 2018. Las Δ5315 effector induces extreme starch accumulation and chlorosis as Ca. Liberibacter asiaticus infection in Nicotiana benthamiana. *Frontiers in Plant Science,* 9**,** 338821.

PITINO, M., ARMSTRONG, C. M., CANO, L. M. & DUAN, Y. 2016. Transient expression of Candidatus Liberibacter asiaticus effector induces cell death in Nicotiana benthamiana. *Frontiers in Plant Science,* 7**,** 204775.

PLANAS-MARQUÈS, M., BERNARDO-FAURA, M., PAULUS, J., KASCHANI, F., KAISER, M., VALLS, M., VAN DER HOORN, R. A. L. & COLL, N. S. 2018. Protease Activities Triggered by Ralstonia solanacearum Infection in Susceptible and Tolerant Tomato Lines *. *Molecular & Cellular Proteomics,* 17**,** 1112-1125.

POTTER, S. C., LUCIANI, A., EDDY, S. R., PARK, Y., LOPEZ, R. & FINN, R. D. 2018. HMMER web server: 2018 update. *Nucleic Acids Research,* 46**,** W200-W204.

POTTINGER, S. E. & INNES, R. W. 2020. RPS5-mediated disease resistance: fundamental insights and translational applications. *Annual review of phytopathology,* 58**,** 139-160.

PRICE, M. N., DEHAL, P. S. & ARKIN, A. P. 2009. FastTree: computing large minimum evolution trees with profiles instead of a distance matrix. *Molecular biology and evolution,* 26**,** 1641-1650.

PRICE, M. N., DEHAL, P. S. & ARKIN, A. P. 2010. FastTree 2–approximately maximum-likelihood trees for large alignments. *PloS one,* 5**,** e9490.

PRITCHARD, J. 1996. Aphid stylectomy reveals an osmotic step between sieve tube and cortical cells in barley roots. *Journal of Experimental Botany,* 47**,** 1519-1524.

PRONOBIS, M. I., DEUITCH, N. & PEIFER, M. 2016. The Miraprep: A protocol that uses a Miniprep kit and provides Maxiprep yields. *PLoS One,* 11**,** e0160509.

QIAO, Y., LIU, L., XIONG, Q., FLORES, C., WONG, J., SHI, J., WANG, X., LIU, X., XIANG, Q. & JIANG, S. 2013. Oomycete pathogens encode RNA silencing suppressors. *Nature genetics,* 45**,** 330-333.

RAMADUGU, C., KEREMANE, M. L., HALBERT, S. E., DUAN, Y. P., ROOSE, M. L., STOVER, E. & LEE, R. F. 2016. Long-term field evaluation reveals Huanglongbing resistance in Citrus relatives. *Plant Disease,* 100**,** 1858-1869.

REYES CALDAS, P. A., ZHU, J., BREAKSPEAR, A., THAPA, S. P., TORUÑO, T. Y., PERILLA-HENAO, L. M., CASTEEL, C., FAULKNER, C. R. & COAKER, G. 2022. Effectors from a bacterial vector-borne pathogen exhibit diverse subcellular localization, expression profiles, and manipulation of plant defense. *Molecular Plant-Microbe Interactions,* 35**,** 1067-1080.

RICHAU, K. H., KASCHANI, F., VERDOES, M., PANSURIYA, T. C., NIESSEN, S., STÜBER, K., COLBY, T., OVERKLEEFT, H. S., BOGYO, M. & VAN DER

HOORN, R. A. 2012. Subclassification and biochemical analysis of plant papain-like cysteine proteases displays subfamily-specific characteristics. *Plant physiology,* 158**,** 1583-1599.

ROBLEDO, J., WELKER, S., SHTEIN, I., BERNARDINI, C., VINCENT, C. & LEVY, A. 2024. Phloem and Xylem Responses Are Both Implicated in Huanglongbing Tolerance of Sugar Belle. *Phytopathology®,* 114**,** 441-453.

ROLLAUER, S. E., SOORESHJANI, M. A., NOINAJ, N. & BUCHANAN, S. K. 2015. Outer membrane protein biogenesis in Gram-negative bacteria. *Philosophical Transactions of the Royal Society B: Biological Sciences,* 370**,** 20150023.

ROONEY, H. C., VAN'T KLOOSTER, J. W., VAN DER HOORN, R. A., JOOSTEN, M. H., JONES, J. D. & DE WIT, P. J. 2005. Cladosporium Avr2 inhibits tomato Rcr3 protease required for Cf-2-dependent disease resistance. *Science,* 308**,** 1783-1786.

ROUMIA, A. F., TSIRIGOS, K. D., THEODOROPOULOU, M. C., TAMPOSIS, I. A., HAMODRAKAS, S. J. & BAGOS, P. G. 2021. OMPdb: a global hub of beta-barrel outer membrane proteins. *Frontiers in Bioinformatics,* 1**,** 646581.

ROUSSIN-LÉVEILLÉE, C., ROSSI, C. A., CASTROVERDE, C. D. M. & MOFFETT, P. 2024. The plant disease triangle facing climate change: A molecular perspective. *Trends in Plant Science*.

RUIZ-SOLANÍ, N., SALGUERO-LINARES, J., ARMENGOT, L., SANTOS, J., PALLARÈS, I., VAN MIDDEN, K. P., PHUKKAN, U. J., KOYUNCU, S., BORRÀS-BISA, J. & LI, L. 2023. Arabidopsis metacaspase MC1 localizes in stress granules, clears protein aggregates, and delays senescence. *The Plant Cell,* 35**,** 3325-3344.

SALGUERO-LINARES, J. & COLL, N. S. 2019. Plant proteases in the control of the hypersensitive response. *Journal of experimental botany,* 70**,** 2087-2095.

SAMSUDIN, F., ORTIZ-SUAREZ, M. L., PIGGOT, T. J., BOND, P. J. & KHALID, S. 2016. OmpA: a flexible clamp for bacterial cell wall attachment. *Structure,* 24**,** 2227-2235.

SANGUANKIATTICHAI, N., BUSCAILL, P. & PRESTON, G. M. 2022. How bacteria overcome flagellin pattern recognition in plants. *Current Opinion in Plant Biology,* 67**,** 102224.

SARKAR, P., EL-MOHTAR, C., TURNER, D., WELKER, S., ROBERTSON, C. J., ORBOVIC, V., MOU, Z. & LEVY, A. 2024. NONEXPRESSOR OF PATHOGENESIS-RELATED GENES control Huanglongbing tolerance by regulating immune balance in citrus plants. *bioRxiv***,** 2024.03. 18.585579.

SARKAR, P., LIN, C.-Y., BURITICA, J. R., KILLINY, N. & LEVY, A. 2023. Crossing the Gateless Barriers: Factors Involved in the Movement of Circulative Bacteria Within Their Insect Vectors. *Phytopathology®,* 113**,** 1805-1816.

SARRIS, P. F., DUXBURY, Z., HUH, S. U., MA, Y., SEGONZAC, C., SKLENAR, J., DERBYSHIRE, P., CEVIK, V., RALLAPALLI, G. & SAUCET, S. B. 2015. A plant immune receptor detects pathogen effectors that target WRKY transcription factors. *Cell,* 161**,** 1089-1100.

SCHORNACK, S., MOSCOU, M. J., WARD, E. R. & HORVATH, D. M. 2013. Engineering plant disease resistance based on TAL effectors. *Annual review of phytopathology,* 51**,** 383-406.

SCHUSTER, M., EISELE, S., ARMAS-EGAS, L., KESSENBROCK, T., KOURELIS, J., KAISER, M. & VAN DER HOORN, R. A. 2024. Enhanced late blight resistance by engineering an EpiC2B-insensitive immune protease. *Plant Biotechnology Journal,* 22**,** 284.

SHI, J., GONG, Y., SHI, H., MA, X., ZHU, Y., YANG, F., WANG, D., FU, Y., LIN, Y. & YANG, N. 2023. 'Candidatus Liberibacter asiaticus' secretory protein SDE3

inhibits host autophagy to promote Huanglongbing disease in citrus. *Autophagy,* 19**,** 2558-2574.

SINGH, B. K., DELGADO-BAQUERIZO, M., EGIDI, E., GUIRADO, E., LEACH, J. E., LIU, H. & TRIVEDI, P. 2023. Climate change impacts on plant pathogens, food security and paths forward. *Nature Reviews Microbiology,* 21**,** 640-656.

SINGH, S., GIRI, M. K., SINGH, P. K., SIDDIQUI, A. & NANDI, A. K. 2013. Down-regulation of OsSAG12-1 results in enhanced senescence and pathogen-induced cell death in transgenic rice plants. *Journal of biosciences,* 38**,** 583-592.

SOARES, J. M., TANWIR, S. E., GROSSER, J. W. & DUTT, M. 2020. Development of genetically modified citrus plants for the control of citrus canker and huanglongbing. *Tropical Plant Pathology,* 45**,** 237-250.

STEHLE, F., BRANDT, W., STUBBS, M. T., MILKOWSKI, C. & STRACK, D. 2009. Sinapoyltransferases in the light of molecular evolution. *Phytochemistry,* 70**,** 1652-1662.

SUELDO, D. J., GODSON, A., KASCHANI, F., KRAHN, D., KESSENBROCK, T., BUSCAILL, P., SCHOFIELD, C. J., KAISER, M. & VAN DER HOORN, R. A. 2024. Activity-based proteomics uncovers suppressed hydrolases and a neo-functionalised antibacterial enzyme at the plant–pathogen interface. *New Phytologist,* 241**,** 394-408.

SUGIO, A., KINGDOM, H. N., MACLEAN, A. M., GRIEVE, V. M. & HOGENHOUT, S. A. 2011a. Phytoplasma protein effector SAP11 enhances insect vector reproduction by manipulating plant development and defense hormone biosynthesis. *Proceedings of the National Academy of Sciences,* 108**,** E1254-E1263.

SUGIO, A., MACLEAN, A. M. & HOGENHOUT, S. A. 2014. The small phytoplasma virulence effector SAP 11 contains distinct domains required for nuclear targeting and CIN-TCP binding and destabilization. *New Phytologist,* 202**,** 838-848.

SUGIO, A., MACLEAN, A. M., KINGDOM, H. N., GRIEVE, V. M., MANIMEKALAI, R. & HOGENHOUT, S. A. 2011b. Diverse targets of phytoplasma effectors: from plant development to defense against insects. *Annual review of phytopathology,* 49**,** 175-195.

SUN, Y., WANG, Y., ZHANG, X., CHEN, Z., XIA, Y., WANG, L., SUN, Y., ZHANG, M., XIAO, Y. & HAN, Z. 2022. Plant receptor-like protein activation by a microbial glycoside hydrolase. *Nature,* 610**,** 335-342.

TAN, C. M., LI, C.-H., TSAO, N.-W., SU, L.-W., LU, Y.-T., CHANG, S. H., LIN, Y. Y., LIOU, J.-C., HSIEH, L.-C., YU, J.-Z., SHEUE, C.-R., WANG, S.-Y., LEE, C.-F. & YANG, J.-Y. 2016. Phytoplasma SAP11 alters 3-isobutyl-2-methoxypyrazine biosynthesis in Nicotiana benthamiana by suppressing NbOMT1. *Journal of Experimental Botany,* 67**,** 4415-4425.

TANAKA, K. & HEIL, M. 2021. Damage-associated molecular patterns (DAMPs) in plant innate immunity: applying the danger model and evolutionary perspectives. *Annual review of phytopathology,* 59**,** 53-75.

THAPA, S. P., DE FRANCESCO, A., TRINH, J., GURUNG, F. B., PANG, Z., VIDALAKIS, G., WANG, N., ANCONA, V., MA, W. & COAKER, G. 2020. Genome-wide analyses of Liberibacter species provides insights into evolution, phylogenetic relationships, and virulence factors. *Molecular plant pathology,* 21**,** 716-731.

TRAN, T.-T., CLARK, K., MA, W. & MULCHANDANI, A. 2020. Detection of a secreted protein biomarker for citrus Huanglongbing using a single-walled carbon nanotubes-based chemiresistive biosensor. *Biosensors and Bioelectronics,* 147**,** 111766.

TRINH, J., LI, T., FRANCO, J. Y., TORUÑO, T. Y., STEVENS, D. M., THAPA, S. P., WONG, J., PINEDA, R., DE DIOS, E. Á. & KAHN, T. L. 2023. Variation in microbial feature perception in the Rutaceae family with immune receptor conservation in citrus. *Plant Physiology,* 193**,** 689-707.

TRKULJA, V., TOMIĆ, A., MATIĆ, S., TRKULJA, N., ILIČIĆ, R. & POPOVIĆ MILOVANOVIĆ, T. 2023. An Overview of the Emergence of Plant Pathogen 'Candidatus Liberibacter solanacearum'in Europe. *Microorganisms,* 11**,** 1699.

TURGEON, R. & WOLF, S. 2009. Phloem transport: cellular pathways and molecular trafficking. *Annual review of plant biology,* 60**,** 207-221.

USDA-ERS. 2024. *Natural disasters, disease cut Florida orange production an estimated 92 percent since 2003/04* [Online]. Available: https://www.ers.usda.gov/data-products/chart-gallery/gallery/chart-detail/?chartId=109051 [Accessed 10/2024].

VAN BEL, A. J. E., EHLERS, K. & KNOBLAUCH, M. 2002. Sieve elements caught in the act. *Trends in Plant Science,* 7**,** 126-132.

VAN DER HOORN, R. A., LEEUWENBURGH, M. A., BOGYO, M., JOOSTEN, M. H. & PECK, S. C. 2004. Activity profiling of papain-like cysteine proteases in plants. *Plant physiology,* 135**,** 1170-1178.

VAN WERSCH, R., LI, X. & ZHANG, Y. 2016. Mighty dwarfs: Arabidopsis autoimmune mutants and their usages in genetic dissection of plant immunity. *Frontiers in plant science,* 7**,** 1717.

WAN, W.-L., FROEHLICH, K., PRUITT, R. N., NUERNBERGER, T. & ZHANG, L. 2019. Plant cell surface immune receptor complex signaling. *Current opinion in plant biology,* 50**,** 18-28.

WANG, H., IRIGOYEN, S., LIU, J., RAMASAMY, M., PADILLA, C., BEDRE, R., YANG, C., THAPA, S. P., MULGAONKAR, N. & ANCONA, V. 2024a. Inhibition of a

conserved bacterial dual-specificity phosphatase confers plant tolerance to Candidatus Liberibacter spp. *Iscience,* 27.

WANG, N., PIERSON, E. A., SETUBAL, J. C., XU, J., LEVY, J. G., ZHANG, Y., LI, J., RANGEL, L. T. & MARTINS JR, J. 2017. The Candidatus Liberibacter–host interface: insights into pathogenesis mechanisms and disease control. *Annual review of phytopathology,* 55**,** 451-482.

WANG, R., BAI, B., LI, D., WANG, J., HUANG, W., WU, Y. & ZHAO, L. 2024b. Phytoplasma: A plant pathogen that cannot be ignored in agricultural production—Research progress and outlook. *Molecular Plant Pathology,* 25**,** e13437.

WANG, R., WANG, Z. & LU, H. 2023. Separation methods for system-wide profiling of protein terminome. *Proteomics,* 23**,** 2100374.

WANG, S., XING, R., WANG, Y., SHU, H., FU, S., HUANG, J., PAULUS, J. K., SCHUSTER, M., SAUNDERS, D. G. & WIN, J. 2021a. Cleavage of a pathogen apoplastic protein by plant subtilases activates host immunity. *New Phytologist,* 229**,** 3424-3439.

WANG, Y., GARRIDO-OTER, R., WU, J., WINKELMÜLLER, T. M., AGLER, M., COLBY, T., NOBORI, T., KEMEN, E. & TSUDA, K. 2019. Site-specific cleavage of bacterial MucD by secreted proteases mediates antibacterial resistance in Arabidopsis. *Nature communications,* 10**,** 2853.

WANG, Y., LI, X., FAN, B., ZHU, C. & CHEN, Z. 2021b. Regulation and function of defense-related callose deposition in plants. *International Journal of Molecular Sciences,* 22**,** 2393.

WANG, Y., PRUITT, R. N., NUERNBERGER, T. & WANG, Y. 2022. Evasion of plant immunity by microbial pathogens. *Nature Reviews Microbiology,* 20**,** 449-464.

WANG, Y., WANG, Y. & WANG, Y. 2020. Apoplastic proteases: powerful weapons against pathogen infection in plants. *Plant Communications,* 1.

WEI, W., XU, L., PENG, H., ZHU, W., TANAKA, K., CHENG, J., SANGUINET, K. A., VANDEMARK, G. & CHEN, W. 2022. A fungal extracellular effector inactivates plant polygalacturonase-inhibiting protein. *Nature Communications,* 13**,** 2213.

XIAO, Y., SUN, G., YU, Q., GAO, T., ZHU, Q., WANG, R., HUANG, S., HAN, Z., CERVONE, F. & YIN, H. 2024. A plant mechanism of hijacking pathogen virulence factors to trigger innate immunity. *Science,* 383**,** 732-739.

XIONG, Q., YE, W., CHOI, D., WONG, J., QIAO, Y., TAO, K., WANG, Y. & MA, W. 2014. Phytophthora suppressor of RNA silencing 2 is a conserved RxLR effector that promotes infection in soybean and Arabidopsis thaliana. *Molecular Plant-Microbe Interactions,* 27**,** 1379-1389.

YU, G. 2020. Using ggtree to visualize data on tree-like structures. *Current protocols in bioinformatics,* 69**,** e96.

YU, H., XU, W., CHEN, S., WU, X., RAO, W., LIU, X., XU, X., CHEN, J., NISHIMURA, M. T., ZHANG, Y. & WAN, L. 2024. Activation of a helper NLR by plant and bacterial TIR immune signaling. *Science*.

ZHANG, C. & TURGEON, R. 2018. Mechanisms of phloem loading. *Current Opinion in Plant Biology,* 43**,** 71-75.

ZHANG, D., ZHAO, Y., WANG, J., ZHAO, P. & XU, S. 2021. BRS1 mediates plant redox regulation and cold responses. *BMC Plant Biology,* 21**,** 1-10.

ZHANG, J., SUN, L., WANG, Y., LI, B., LI, X., YE, Z. & ZHANG, J. 2024a. A calcium-dependent protein kinase regulates the defense response in Citrus sinensis. *Molecular Plant-Microbe Interactions,* 37**,** 459-466.

ZHANG, L., DU, Y., QU, Q. & ZHENG, Q. 2024b. Structure basis for recognition of plant Rpn10 by phytoplasma SAP05 in ubiquitin-independent protein degradation. *Iscience,* 27.

ZHENG, K., LYU, J. C., THOMAS, E. L., SCHUSTER, M., SANGUANKIATTICHAI, N., NINCK, S., KASCHANI, F., KAISER, M. & VAN DER HOORN, R. A. 2024. The proteome of Nicotiana benthamiana is shaped by extensive protein processing. *New Phytologist*.

ZHOU, A. & LI, J. 2005. Arabidopsis BRS1 is a secreted and active serine carboxypeptidase. *Journal of Biological Chemistry,* 280**,** 35554-35561.

ZHOU, J.-M. & CHAI, J. 2008. Plant pathogenic bacterial type III effectors subdue host responses. *Current opinion in microbiology,* 11**,** 179-185.

ZIEMANN, S., VAN DER LINDE, K., LAHRMANN, U., ACAR, B., KASCHANI, F., COLBY, T., KAISER, M., DING, Y. Z., SCHMELZ, E., HUFFAKER, A., HOLTON, N., ZIPFEL, C. & DOEHLEMANN, G. 2018. An apoplastic peptide activates salicylic acid signalling in maize. *Nature Plants,* 4**,** 172-180.

ZOU, X., ZHAO, K., LIU, Y., DU, M., ZHENG, L., WANG, S., XU, L., PENG, A., HE, Y. & LONG, Q. 2021. Overexpression of salicylic acid carboxyl methyltransferase (CsSAMT1) enhances tolerance to Huanglongbing disease in Wanjincheng orange (Citrus sinensis (L.) Osbeck). *International Journal of Molecular Sciences,* 22**,** 2803.